

Table 4.
 GFZ pole solution (from June 21 to October 29, 1992)

| | | | |
|----------|----------|---------|---------|
| 48794.50 | -0015045 | 0.35879 | 0.00000 |
| 48795.50 | -0.15066 | 0.36070 | 0.00000 |
| 48796.50 | -0.14993 | 0.36168 | 0.00000 |
| 48797.50 | -0.14817 | 0.36510 | 0.00000 |
| 48798.50 | -0.14777 | 0.36836 | 0.00000 |
| 48799.50 | -0.14623 | 0.37023 | 0.00000 |
| 48800.50 | -0.14496 | 0.37264 | 0.00000 |
| 48801.50 | -0.14291 | 0.37618 | 0.00000 |
| 48802.50 | -0.14137 | 0.37862 | 0.00000 |
| 48803.50 | -0.14043 | 0.38009 | 0.00000 |
| 48804.50 | -0.13952 | 0.38310 | 0.00000 |
| 48805.50 | -0.13794 | 0.38538 | 0.00000 |
| 48806.50 | -0.13538 | 0.38672 | 0.00000 |
| 48807.50 | -0.13470 | 0.38889 | 0.00000 |
| 48808.50 | -0.13435 | 0.39207 | 0.00000 |
| 48809.50 | -0.13365 | 0.39331 | 0.00000 |
| 48810.50 | -0.13126 | 0.39483 | 0.00000 |
| 48811.50 | -0.12935 | 0.39767 | 0.00000 |
| 48812.50 | -0.12888 | 0.39968 | 0.00000 |
| 48813.50 | -0.12724 | 0.40233 | 0.00000 |
| 48814.50 | -0.12701 | 0.40509 | 0.00000 |
| 48815.50 | -0.12620 | 0.40760 | 0.00000 |
| 48816.50 | -0.12544 | 0.40949 | 0.00000 |
| 48817.50 | -0.12469 | 0.41078 | 0.00000 |
| 48818.50 | -0.12305 | 0.41236 | 0.00000 |
| 48819.50 | -0.12130 | 0.41406 | 0.00000 |
| 48820.50 | -0.11827 | 0.41628 | 0.00000 |
| 48821.50 | -0.11607 | 0.41898 | 0.00000 |
| 48822.50 | -0.11327 | 0.42131 | 0.00000 |
| 48823.50 | -0.11074 | 0.42408 | 0.00000 |
| 48824.50 | -0.10823 | 0.42716 | 0.00000 |
| 48825.50 | -0.10619 | 0.42878 | 0.00000 |
| 48826.50 | -0.10464 | 0.43014 | 0.00000 |
| 48827.50 | -0.10198 | 0.43225 | 0.00000 |
| 48828.50 | -0.10000 | 0.43447 | 0.00000 |
| 48829.50 | -0.09812 | 0.43709 | 0.00000 |
| 48830.50 | -0.09656 | 0.43859 | 0.00000 |
| 48831.50 | -0.09537 | 0.44007 | 0.00000 |
| 48832.50 | -0.09342 | 0.44252 | 0.00000 |
| 48833.50 | -0.09058 | 0.44460 | 0.00000 |
| 48834.50 | -0.08805 | 0.44680 | 0.00000 |
| 48835.50 | -0.08602 | 0.44920 | 0.00000 |
| 48836.50 | -0.08400 | 0.45161 | 0.00000 |
| 48837.50 | -0.08194 | 0.45388 | 0.00000 |
| 48838.50 | -0.08002 | 0.45545 | 0.00000 |
| 48839.50 | -0.07820 | 0.45703 | 0.00000 |
| 48840.50 | -0.07655 | 0.45913 | 0.00000 |
| 48841.50 | -0.07480 | 0.46158 | 0.00000 |
| 48842.50 | -0.07267 | 0.46438 | 0.00000 |
| 48843.50 | -0.07054 | 0.46718 | 0.00000 |
| 48844.50 | -0.06897 | 0.46984 | 0.00000 |
| 48845.50 | -0.06716 | 0.47224 | 0.00000 |
| 48846.50 | -0.06491 | 0.47396 | 0.00000 |
| 48847.50 | -0.06344 | 0.47614 | 0.00000 |
| 48848.50 | -0.06152 | 0.47840 | 0.00000 |
| 48849.50 | -0.05872 | 0.47971 | 0.00000 |
| 48850.50 | -0.05553 | 0.48106 | 0.00000 |
| 48851.50 | -0.05247 | 0.48304 | 0.00000 |
| 48852.50 | -0.04974 | 0.48472 | 0.00000 |
| 48853.50 | -0.04646 | 0.48589 | 0.00000 |
| 48854.50 | -0.04286 | 0.48737 | 0.00000 |
| 48855.50 | -0.03962 | 0.48873 | 0.00000 |
| 48856.50 | -0.03675 | 0.49001 | 0.00000 |
| 48857.50 | -0.03351 | 0.49116 | 0.00000 |
| 48858.50 | -0.03139 | 0.49269 | 0.00000 |
| 48859.50 | -0.02933 | 0.49365 | 0.00000 |

| | | | |
|----------|----------|---------|---------|
| 48860.50 | -0.02558 | 0.49499 | 0400000 |
| 48861.50 | -0.02220 | 0.49705 | 0,00000 |
| 48862.50 | -0.01895 | 0.49885 | 0,00000 |
| 48863.50 | -0.01590 | 0.50007 | 0.00000 |
| 48864.50 | -0.01340 | 0.50177 | 0.00000 |
| 48865.50 | -0.01133 | 0.50276 | 0.00000 |
| 48866.50 | -0.00942 | 0.50225 | 0.00000 |
| 48867.50 | -0.00678 | 0.50179 | 0.00000 |
| 48868.50 | -0.00485 | 0.50128 | 0.00000 |
| 48869.50 | -0.00297 | 0.50170 | 0.00000 |
| 48870.50 | -0.00059 | 0.50231 | 0.00000 |
| 48871.50 | 0.00221 | 0.50375 | 0.00000 |
| 48872.50 | 0.00479 | 0.50505 | 0.00000 |
| 48873.50 | 0.00720 | 0.50531 | 0000000 |
| 48874.50 | 0.00998 | 0.50558 | 0.00000 |
| 48875.50 | 0.01225 | 0.50590 | 0.00000 |
| 48876.50 | 0.01452 | 0.50621 | 0.00000 |
| 48877.50 | 0.01680 | 0.50653 | 0.00000 |
| 48878.50 | 0.01907 | 0.50685 | 0.00000 |
| 48879.50 | 0.02143 | 0.50738 | 0.00000 |
| 48880.50 | 0.02387 | 0.50855 | 0.00000 |
| 48881.50 | 0.02654 | 0.50779 | 0.00000 |
| 48882.50 | 0.02790 | 0.50707 | 0.00000 |
| 48883.50 | 0.02936 | 0.50779 | 0.00000 |
| 48884.50 | 0.03247 | 0.50754 | 0.00000 |
| 48885.50 | 0,03557 | 0,50728 | 0.00000 |
| 48886.50 | 0.03740 | 0.50725 | 0.00000 |
| 48887.50 | 0.03916 | 0.50696 | 0.00000 |
| 48888.50 | 0.04178 | 0.50735 | 0.00000 |
| 48889.50 | 0.04461 | 0.50801 | 0.00000 |
| 48890.50 | 0.04709 | 0.50780 | 0.00000 |
| 48891.50 | 0.04866 | 0.50766 | 0.00000 |
| 48892.50 | 0.05024 | 0.50752 | 0.00000 |
| 48893.50 | 0.05229 | 0.50594 | 0.00000 |
| 48894.50 | 0.05523 | 0.50423 | 0.00000 |
| 48895.50 | 0.05766 | 0.50359 | 0.00000 |
| 48896.50 | 0.05952 | 0.50305 | 0.00000 |
| 48897.50 | 0.06218 | 0.50290 | 0.00000 |
| 48898.50 | 0.06524 | 0.50278 | 0.00000 |
| 48899.50 | 0.06832 | 0.50266 | 0.00000 |
| 48900.50 | 0.07170 | 0.50272 | 0.00000 |
| 48901.50 | 0.07432 | 0.50276 | 0.00000 |
| 48902.50 | 0.07734 | 0.50260 | 0.00000 |
| 48903.50 | 0.08059 | 0.50192 | 0.00000 |
| 48904.50 | 0.08257 | 0.50072 | 0.00000 |
| 48905.50 | 0.08454 | 0.49953 | 0.00000 |
| 48906.50 | 0,08652 | 0.49833 | 0.00000 |
| 48907.50 | 0.08866 | 0.49750 | 0.00000 |
| 48908.50 | 0.09205 | 0.49663 | 0.00000 |
| 48909.50 | 0.09547 | 0.49593 | 0.00000 |
| 48910.50 | 0.09781 | 0.49562 | 0.00000 |
| 48911.50 | 0.10013 | 0.49512 | 0.00000 |
| 48912.50 | 0.10246 | 0.49463 | 0.00000 |
| 48913.50 | 0.10478 | 0.49413 | 0.00000 |
| 48914.50 | 0.10545 | 0.49335 | 0.00000 |
| 48915.50 | 0.10687 | 0.49160 | 0.00000 |
| 48916.50 | 0.10979 | 0.49062 | 0.00000 |
| 48917.50 | 0.11213 | 0.48886 | 0.00000 |
| 48918.50 | 0.11436 | 0.48683 | 0.00000 |
| 48919.50 | 0.11609 | 0.48678 | 0.00000 |
| 48920.50 | 0.11782 | 0.48673 | 0.00000 |
| 48921.50 | 0.12045 | 0.48581 | 0.00000 |
| 48922.50 | 0.12256 | 0.48435 | 0.00000 |
| 48923.50 | 0.12381 | 0.48348 | 0.00000 |
| 48924.50 | 0.12526 | 0.48269 | 0.00000 |

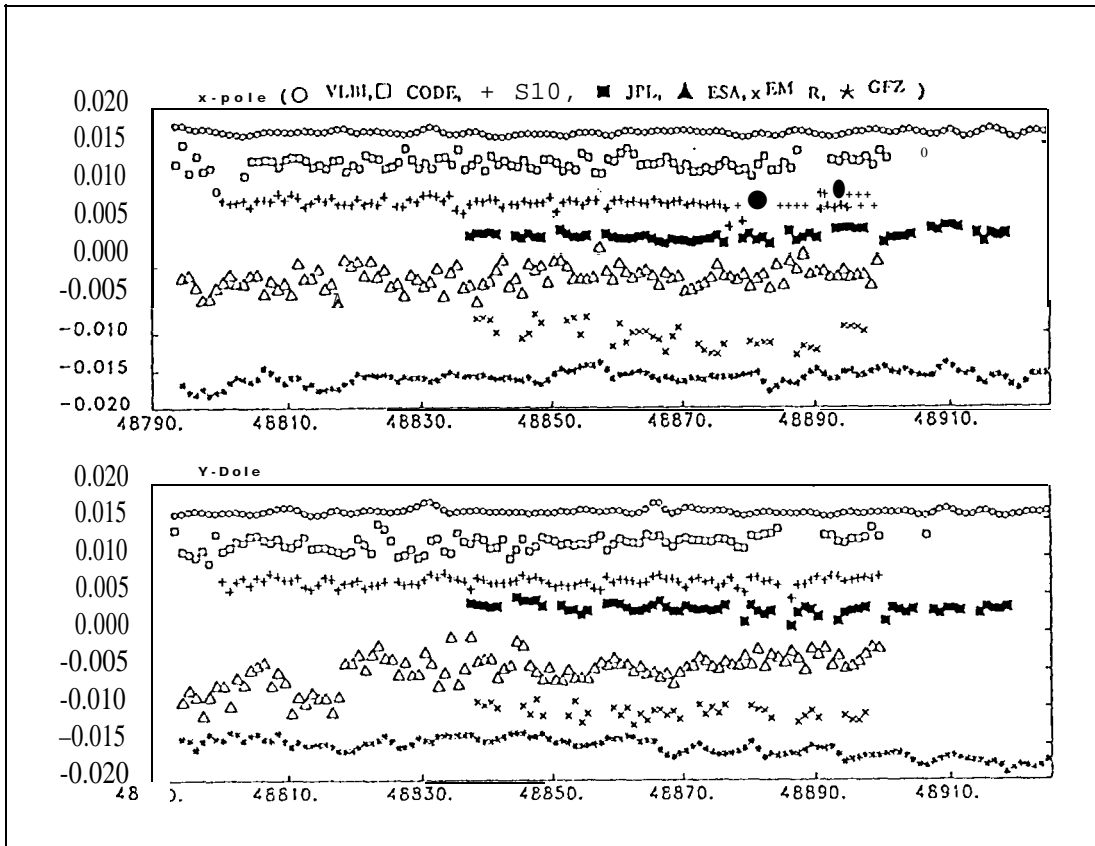


Fig. 1 Comparison of pole solution

JET PROPULSION LABORATORY IGS ANALYSIS CENTER REPORT, 1992

James F. Zumberge[†], David C. Jefferson* ,
Geoffrey Blewitt[†], Michael B. Hefflin[†], Frank H. Webb[†]

Beginning in 1992 June and continuing indefinitely as part of our contribution to FLINN (Fiducial Laboratories for an International Natural Science Network), DOSE (NASA's Dynamics of the Solid Earth Program), and the International GPS Geodynamics Service (IGS), analysts at the Jet Propulsion Laboratory (JPL) have routinely reduced data from a globally-distributed network of Rogue Global Positioning System (GPS) receivers.

Three products are produced and distributed weekly: (i) precise GPS ephemerides, providing satellite positions with one to two orders of magnitude improvement over the broadcast ephemerides, (ii) estimates of polar motion and length-of-day, and (iii) a descriptive narrative of the analysis for the week. These are typically made available to the public approximately two weeks following the data recording.

Based on comparisons of our earth orientation parameters with independent techniques, we estimate pole positions accuracies (1σ) of ± 0.6 milliarseconds, and length-of-day accuracies of ± 0.13 msec.

Based on separate estimates of GPS ephemerides using nearly-independent data sets, we estimate their accuracy to be approximately ± 40 cm (3-dimensional root-sum-squared) in an earth-fixed reference frame. A comparison of JPL-produced ephemerides with those from other IGS Analysis centers shows similar agreement.

Ongoing work at JPL is aimed at continuing the trend of producing more and higher-quality results at lower cost.

INTRODUCTION

The first GPS experiment for the IERS and Geodynamics (GIG '91), a two-week campaign in early 1991, saw the first globally-distributed deployment of precise Global Positioning System receivers, and demonstrated few-parts-per-billion precision [1] in estimates of terrestrial site locations. Largely as a result of the success of GIG '91, the International GPS Geodynamics Service (IGS) began informally in 1992 June. JPL has contributed to the IGS since it began and, in conjunction with its ongoing support of NASA's Dynamics of the Solid Earth (DOSE) program, will continue to contribute.

Shown in Figure 1 is the distribution of terrestrial GPS P-code receivers as of 1993 February. Global coverage is currently very good, with only a few noticeable "holes". Within the next two years it is anticipated that these holes will be plugged with new receivers at strategic locations.

[†]Satellite Geodesy and Geodynamics Systems Group, Jet Propulsion Laboratory, California Institute of Technology, Mail Stop 238-600, 4800 Oak Grove Drive, Pasadena, CA 91109.

● Earth Orbiter Systems Group, Jet Propulsion Laboratory, California Institute of Technology, Mail Stop 238-600, 4800 Oak Grove Drive, Pasadena, CA 91109.

Figure 2 summarizes the steadily increasing number of stations and satellites beginning in early 1992 and continuing to the present. One can speculate on whether the trend will continue, but currently the data volume, as measured by stations \times satellites, doubles in just over a year!

Described in this paper are the analysis procedures used at JPL, the resulting products, and their estimated accuracies. We conclude with a brief look at **JPL's** plans for improving the efficiency and quality of its analyses.

PROCEDURE AND PRODUCTS

Figure 3 gives a simplified overview of the routine procedure. JPL's GPS Networks Operations (**GNO**) Group retrieves data from the **global** network, organizes them by time and site, converts them to the Rinex format, and makes them available for analysts.

Once it is determined that sufficient data are available for a given day, a file like that shown in Figure 4 is created. Such a file specifies what data are to be used in the day's analysis, as well as specific sites or GPS satellites from which data should be deleted or deweighted, due to known problems.

Based on input from this file, a daily script that runs several programs is launched, requiring a total of approximately **19 hours** of cpu time on a **17-Mflop** Unix workstation when data from 30 stations and 20 satellites are included. When completed, the daily analysis results in estimates for earth orientation, GPS satellite ephemerides, and location of terrestrial sites.

Each day is processed separately using the 24 hours of the UTC day plus the last 3 hours of the previous day and first 3 hours of the following day. Normal points are formed every 10 minutes. The data types are the **undifferenced** ionosphere-free phase and pseudorange, with assumed noise of 5 mm and 50 cm, respectively.

The GPS satellite motion is modeled as a 9-parameter epoch state vector which includes three-dimensional position, velocity, and solar radiation pressure. Additional parameters allow the solar radiation pressure to vary in a stochastic way about its average value. The noise model for this variation is Gauss-Markov with a 4-hour time constant and 10% standard deviation. Especially during periods when a satellite is in the Earth's shadow, the extra variation allows significantly better modeling of its motion.

The nominal value of the Earth's pole position is that of the IERS Bulletin B predicts, and its deviation from that nominal is modeled as a linear function of time. The deviation of **UT1R-UTC** from the nominal (again, IERS Bulletin B predicts) is also assumed to be linear with time, but in this case only the rate is estimated. This rate is the negative of length of day (**LODR**).

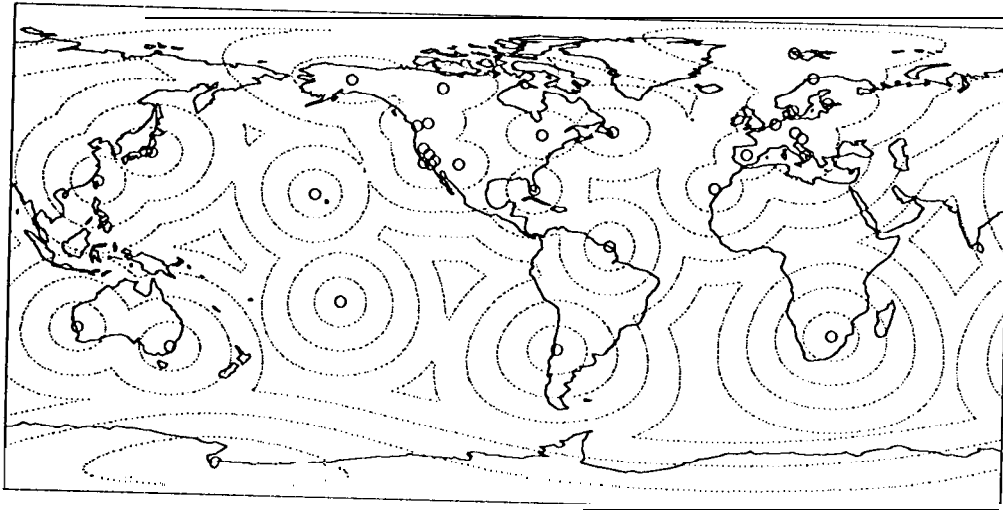


Figure 1 Distribution of terrestrial GPS receivers used in the daily analyses. The dotted lines represent contours of the distance-to-nearest-site function. The contour interval is 1000 km.

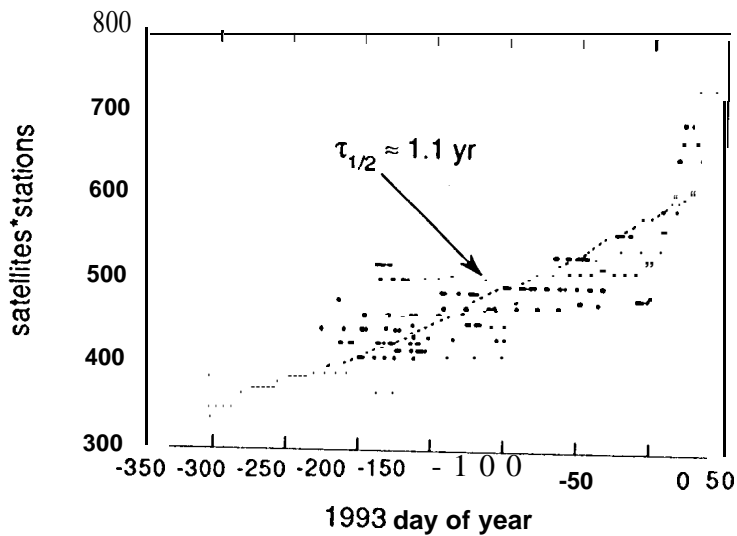


Figure 2 The number of satellites times the number of stations used in daily analyses beginning early 1992. At the current rate, the data volume doubles in a little over 1 year.

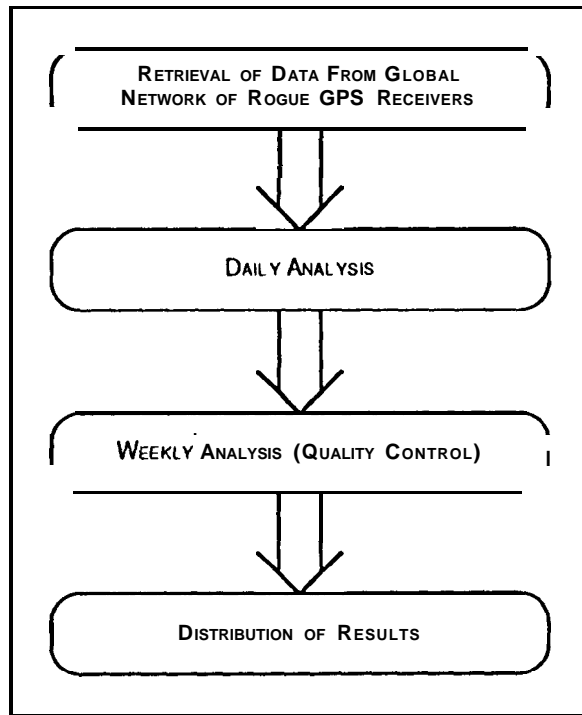


Figure 3 Simplified Flow Chart of FLINN Analysis

```

setenv RUNDIR /usr3/djeff # run directory
setenv TEMPLATES ~jfz/Flinn # template directory
set SRCE = ( /net/logos/rinex /net/apu/usr1/djeff/xrinex )
setenv DEST /net/apu/usr3/jfz/hold # output files
setenv YYYYMMDD 93febl 4 # day of analysis
setenv YYYYMMDDa 13-FEB-1993 # for tp_nml start
setenv YYYYMMDDb 15-FEB-1993 # for tp_nml end
setenv YES 044_ # yesterday
setenv DOY 045_ # today
setenv TOM 046_ # tomorrow
setenv OI_START '13-FEB-1993 11:00:00' # oi file start
setenv OI_END '15-FEB-1993 13:00:00' # oi file end
setenv DT_START '13-FEB-1993 21:00:00' #.rnx file start
setenv DT_END '15-FEB-1993 03:00:00' #.rnx file end
setenv INTERVAL 600 # 10-minute data interval
set DELQMs = ( ) # delete transmitters
set DELQMs = ( JPL1 JPLL MCMU WEST ) # delete receivers
set DEWGTs = ( GPS08 ) # deweight transmitters
set DEWGTg = ( CASA ) # deweight receivers
set SCLNOs = 100.0 # dwgt xmtr scale factor
setenv MAP_START '13-FEB-1993 11:59:52.0000' # mapping interval, start.
setenv MAP_END '15-FEB-1993 11:44:52.0000' # mapping interval, end
setenv RATEPOCH '14-FEB-1993 11:59:52.0000' # epoch for rate estimate
setenv SITEPOCH '1993 02' # epoch for site locations
  
```

Figure4 Example of file used to control analysis of a given day.

The terrestrial sites include eight which are assumed to be at known locations. These are Algonquin Park, Ontario, Canada; Fairbanks, Alaska, U. S.; Hartebeesthoek, South Africa; Kokee Park, Hawaii, U. S.; Madrid, Spain; Santiago, Chile; Tromso, Norway, and Yaragadee, Australia. The fixed values are updated at the beginning of each month to allow site velocities from ITRF91(IGS mail message 90).

Location of other terrestrial sites are solved for every day.

The operational cycle is one week, during which seven daily analyses are completed. Together with the result from Saturday of the previous week and Sunday of the following week, these are used in quality control.

The three dimensional root-sum square orbit overlap Q for a given satellite and day is defined as

$$Q^2 \equiv \sum_t |X(t) - X_{-}(t)|^2 + \sum_t |X(t) - X_{+}(t)|^2 , \quad [1]$$

where $X(t)$, $X_{-}(t)$, and $X_{+}(t)$ are, respectively, the vector estimates of the satellite's position at time t using data from the current, previous, and subsequent days. In the first sum, t covers the first three hours of the current day, while in the second sum it covers the last three hours, for a six-hour total overlap with adjacent days.

Four files are produced and distributed weekly, with naming convention `jp10www7`, where `www` is the GPS week and `7` indicates the results are for the entire week. The files are distinguished by their extension, `.sum` for a narrative summary, `.sp1` or `.sp3` for GPS ephemerides [2,3], and `.erp` for Earth orientation.

RESULTS

Earth Orientation

Shown in Figure 5 are the Earth orientation results. A discontinuity at 1992 days 200-201 (July 18- 19) is a consequence of the change in fiducial strategy which went from three (Fairbanks, Algonquin, and Madrid) fixed sites to the eight described earlier. From July 19 through the end of 1992, excluding some days during which anti-spoofing was in effect, the average difference between JPL's pole position measurements and those from the IERS Bulletin B Final values is about 0.8 mas for X and 1.2 mas for Y, with standard deviations of about 0.6 mas for both X and Y.

Although GPS measurements are almost completely insensitive to UT1 R-UTC, they are sensitive to its time derivative, essentially the Earth's spin rate. With $T \equiv 1$ day, the quantity

$$\text{LODR} \equiv -T \frac{d}{dt}(\text{UT1R}-\text{UTC}), \quad [2]$$

is the conventional measure of this spin rate. We began including daily estimates of LODR beginning with GPS week 660 (1992 August 30). Shown at the bottom of Figure 5 are our daily estimates of LODR and a smooth curve which represents the negative derivative of the IERS Bulletin B Final values of UT1 R-UTC. Excluding a few 3σ outliers, the agreement is approximately 0.13 msec, 10, with a negligible bias.

Because the daily estimates of LODR are independent, an integration of them to recover UT1 R-UTC (given some initial starting value) would exhibit random-walk behavior, so some method is required to prevent the walk from wandering too far away. We are currently investigating the forward-running filter

$$UT1R-UTC(t+T) = (\alpha A + (1 - \alpha) [UT1 R-UTC(t) + LODR(t+T/2)]), \quad [3]$$

where A is a separate estimate of $UT1 R-UTC(t+T)$ and α is a free parameter. (We continue to use $T \equiv 1$ day.) The parameter α should be small enough so that the resulting $UT1 R-UTC$ series will exhibit a time variation consistent with the daily GPS-measured LODR values, and only just large enough to suppress large random-walk excursions. A reasonable choice for A is the most-recent IERS Bulletin B *Final value* of $UT1R-UTC$ (typically 30- to 60-days old), incremented to the present by the daily GPS measurements of $LODR$. In the near future we intend to include the results of such a procedure in our .erp files. We expect the resulting series to be consistent with the IERS Bulletin B Final values to within a few msec or better, and will be available several weeks earlier.

GPS Satellite Ephemerides

Shown in Figure 6 is a histogram of the quantity Q defined in [1] above, for all satellites and days from GPS week 666 through 684 (1992 Oct 11 – 1993 Feb 20; we began 30-hour daily arcs with stochastic solar radiation pressure on Oct 11). The median value is 40 cm. Using this as a measure of orbit accuracy, the precise ephemerides are more than an order or magnitude better than the broadcast ones.

Another indication of orbit quality is shown in Figure 7. Based on “Orbit Comparison” results published in IGS Reports and covering GPS weeks 660 through 682 (1992 August 30 – 1993 Feb 06), we show the comparison between JPL-produced ephemerides and those produced by the Center for Orbit Determination in Europe (CODE). Histograms for the rotation, translation, and scale indicate how much these need to be adjusted to bring into alignment the JPL and CODE coordinate systems. Once this is done, the satellite position estimates differ by amounts indicated in the 3drss histogram. The median value is 39 cm, remarkably consistent with the distribution of Q .

EPOCH '92

The Epoch '92 period, 1992 July 26 – August 8, occurred when our estimation strategy had not matured to its current state. These days were reprocessed in early 1993 with the current estimation strategy. The results are on JPL's *sboh* distribution computer, and will be available also on the Crystal Dynamics Data Information System at Goddard Space Flight Center.

Figure 8 shows histograms similar to Figure 6. The dotted line is the original result for the Epoch '92 period, while the solid line is a histogram of the same quantity after reprocessing. The improvement is clear.

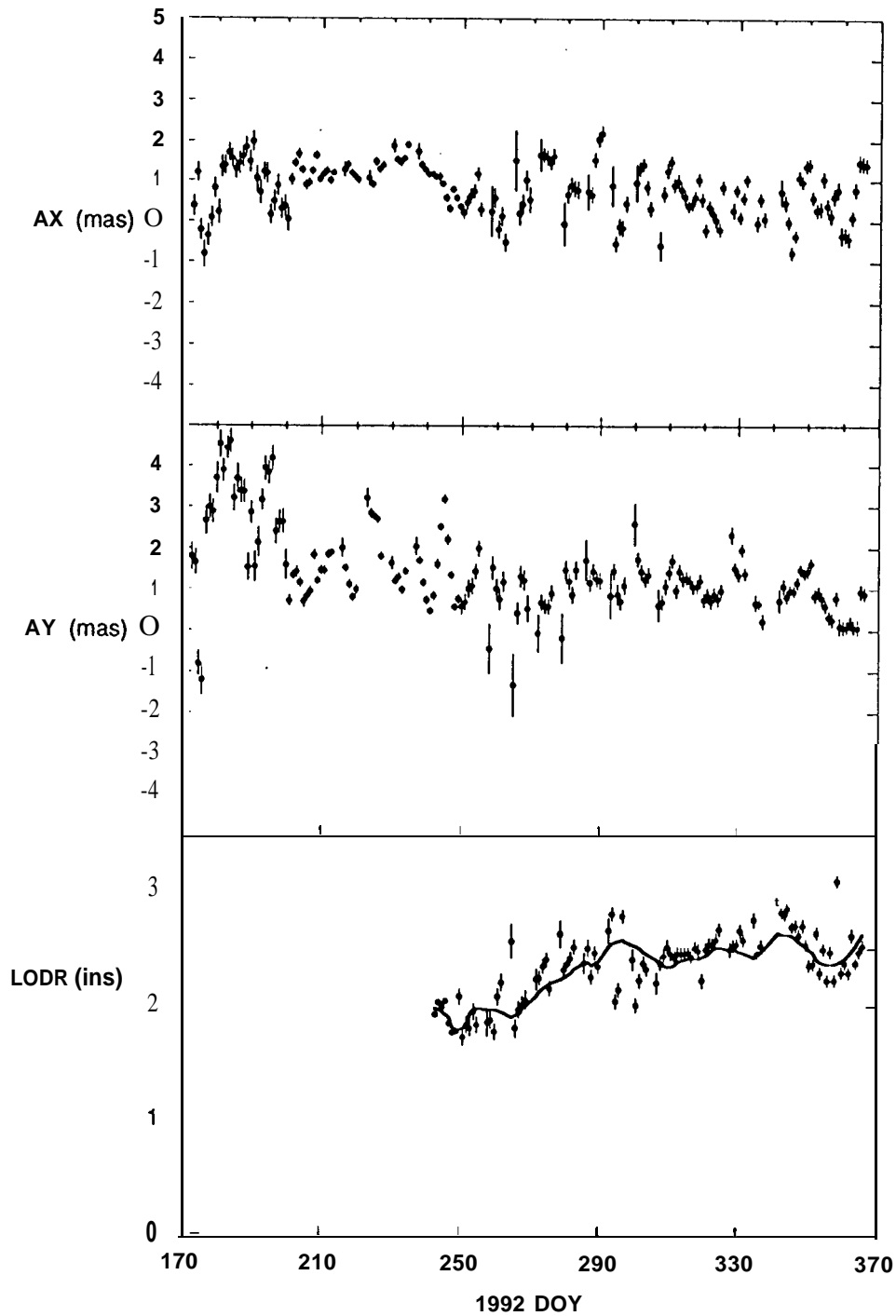


Figure 5 GPS estimates of Earth orientation parameters compared with IERS Bulletin B Final Values. For pole position, the values shown (AX and AY) are the GPS measurements minus the IERS values, and the error bars reflect the formal uncertainty in the GPS measurements. For LODR, the solid line indicates the negative time derivative of the IERS value of UT1R-UTC, and the points indicate the GPS measurements and formal uncertainties.

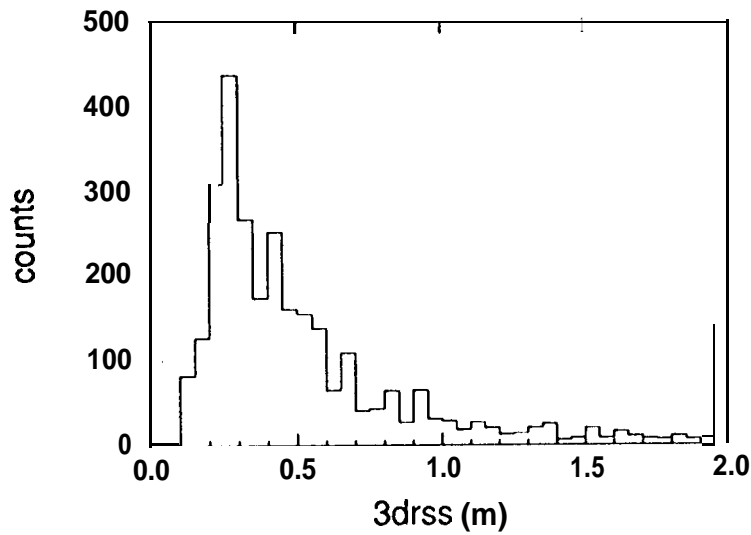


Figure 6 Quality of GPS ephemerides based on the degree to which ephemerides from adjacent days agree near midnight. The median value is 40 cm.

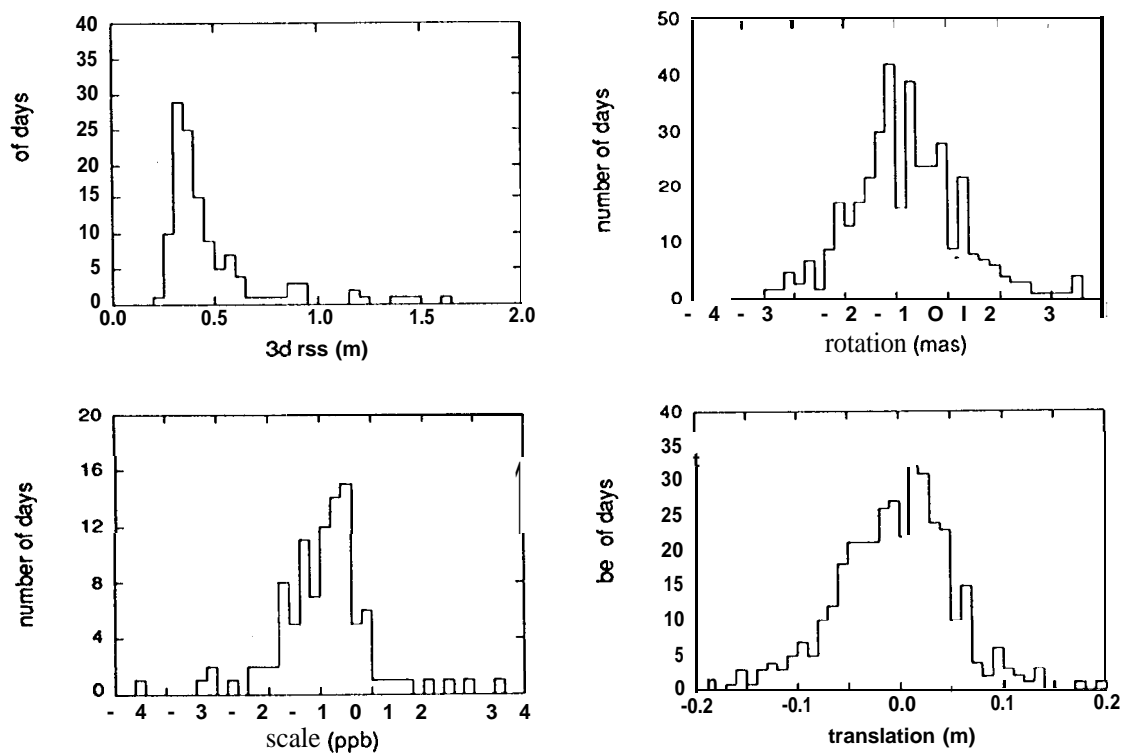


Figure 7 Comparison of JPL-produced GPS ephemerides with those from the Center for Orbit Determination in Europe.

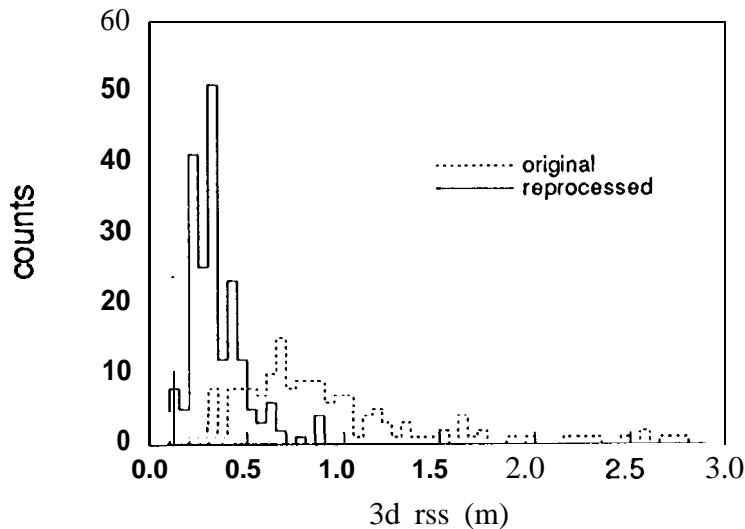


Figure 8 Improvement in orbit repeatability for the **Epoch '92** period (1992 July 26 – August 8). The **dotted** line indicates the original result, and the **solid** line indicates the result after re-processing with the current estimation strategy.

CONCLUSIONS AND FUTURE PROSPECTS

Since the first half of 1992, JPL has made regular contributions to the IGS, consisting of precise GPS orbits and Earth orientation results. We expect to continue these contributions.

Accuracies are currently estimated to be a few tens of cm for GPS orbits, about half a milliarcsec for pole position, and a bit over 0.1 msec for LODR.

Accuracies of all quantities may improve significantly once we start resolving carrier phase bias ambiguities [4], which should begin sometime this calendar year (the current limit is computing resources). Quality control will be enhanced by daily monitoring of several regional baselines.

A number of weekends during 1992 saw implementation of Anti-spoofing (AS). Only recently has the Rogue receiver software been upgraded to handle AS data. Since the upgrade, AS has been processed successfully, although with somewhat degraded accuracies. Analysts at JPL will be investigating modifications of the nominal strategy to better accommodate AS data.

As was shown earlier in Figure 2, the quantity of data has steadily increased, and will probably continue to increase in the near future, because of both more satellites and more receivers. So that the computational burden remains tractable, we may need to process a select number of stations to fix orbits, and then use fixed orbits for the remaining stations.

In addition to the current offerings, new products to be distributed soon will be satellite and station clock solutions. If a demand exists, troposphere estimates and stochastic solar radiation pressure estimates could also be made available.

Finally, additional automation in the routine processing may reduce the manpower required to keep up to date with the analyses. The current turnaround of approximately two weeks could conceivably be **reduced** to a few days, or even less.

ACKNOWLEDGMENT

The work described in this paper was carried out by the Jet Propulsion Laboratory, California Institute of Technology, under contract with the National Aeronautics and Space Administration.

REFERENCES

- [1] Blewitt, G., M. B. Heflin, F. H. Webb, U. J. Lindqwister, and R. P. Malla, Global coordinates with centimeter accuracy in the International Terrestrial Reference Frame using the Global Positioning System, *Geophys. Res. Lett.*, 19, pp. 853-856, 1992.
- [2] Remondi, B. W., NOAA Technical Report NOS 133 NGS 46, *Extending the National Geodetic Survey Standard GPS Orbits Format*, November, 1989
- [3] Remondi, B. W., *NGS Second Generation ASCII and Binary Orbit Formats and Associated Interpolation Studies*, presented at the Twentieth General Assembly of the International Union of Geodesy and Geophysics, Vienna, Austria, Aug 11-24, 1991.
- [4] Blewitt, G., and S. M. Lichten, Carrier phase ambiguity resolution up to 12000 km: Results from the GIG '91 experiment, in *Proc. of the Sixth Int. Symp. on Satellite Positioning*, Columbus, Ohio State University, 1992.

Chapter 4

**Comparisons (Orbits, Earth Rotation
Parameters) and**

Reference Frame Aspects

THE EARTH VIEWED AS A DEFORMING POLYHEDRON: METHOD AND RESULTS

Geoffrey Blewitt,^{*} Michael B. Hefflin, Yvonne Vigue,
James F. Zumberge, David Jefferson,
and Frank H. Webb

As geodesists, it is natural for us to think of the Earth's surface as approximated by a network of points. We extend this concept to one of a rotating, braced polyhedron whose origin is at the Earth's center of mass, and whose vertices are defined by GPS stations. The realization of a terrestrial reference frame with estimated site velocities requires the specification of 3 Euler angles and their first time derivatives to align site coordinates with convention. We illustrate practical aspects of such reference frame alignment with examples from global GPS data acquired from June 1992 to March 1993. Finally, we describe the JPL GPS coordinate solution, JGC9301, which has also been submitted to the IERS Annual Report.

INTRODUCTION

GPS is quite unlike any other geodetic technique, because we can use it to look at the Earth with high spatial and temporal resolution. For example, the GPS global network provides us with a daily snapshot of the Earth, allowing us to look with high temporal resolution at the motion of sites before, during, and after a large earthquake. At the other extreme of the spatial and temporal scale, GPS has great potential for mapping post-glacial rebound of the Earth's crust.

Currently, the GPS global network has over 30 simultaneously operating receivers. Given that the current "core" network will double within the next few years, and that the total number of permanent receivers will possibly reach 200 within 5 years (most of them in regional arrays), we are faced with the rather daunting and exciting task of reducing all these data into a consistent picture of the Earth.

This paper does not address the technical issues of communication, storage, and data processing for such a vast data rate, suffice it to say that regional data reduction, least-squares partitioning, and collaborative exchange of subnetwork solutions, will all play a role. This requires international collaboration, and the IGS already provides the cohesiveness, organization, standards, and goodwill that is necessary to make this work.

The main focus of this paper is to view the Earth as an evolving polyhedron, whose vertices are defined by the GPS sites. We review the prime estimable parameters of the free-network approach [1, 2], and then go on to describe how a time-series of coordinates can be derived without imposing external constraints on any particular site coordinate or velocity. We show examples of time-histories of site latitude, longitude, and height, taken from a 13-week time period in 1992, including the effects of the Landers earthquake of 28

June, 1992 in California. Finally, we present Cartesian coordinates for 38 stations at epoch 1992.5, with 3 rotation angles applied so that the polyhedron is oriented to ITRF91 [3,4]. We compare the scale, geocenter, and individual station coordinates of our solution with ITRF91.

ESTIMABLE PARAMETERS OF THE POLYHEDRON

Figure 1 illustrates parameters which are well-constrained by the GPS data, even when all station coordinates and satellite orbits are freely estimated without a priori constraints. Certain functions of these parameters may be even better determined (for example, the angle between a long baseline and the spin axis, or the differential geocentric distance between two nearby stations).

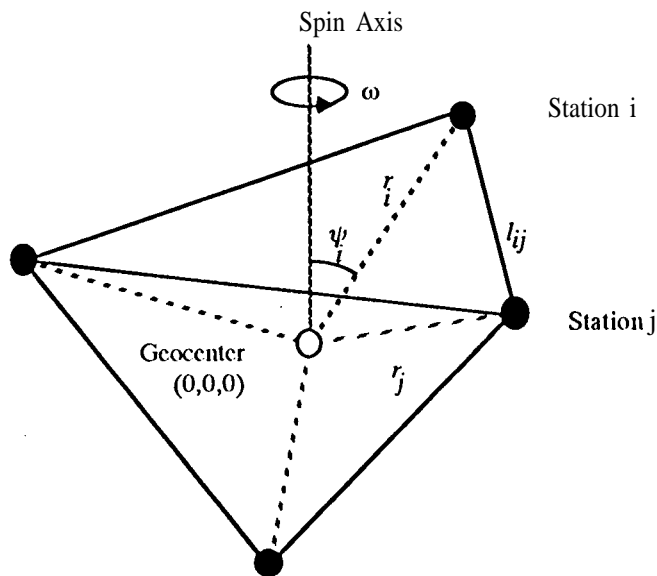


Fig 1. This figure illustrates estimable parameters, that is, those parameters which are well-constrained by the GPS data, and do not require external constraints. The parameters include baseline length between station *i* and station *j*, l_{ij} , geocentric distance of station *i*, r_i , colatitude of station *i* to the instantaneous spin axis, ψ_i , and the rate of rotation, ω .

This type of parameterization is inconvenient for least squares estimation and for reporting results. Quite simply, the polyhedron is over specified. (For example, we could actually compute r_j given all other parameters.)

It is much more convenient to represent the station coordinates as **cartesian** coordinates. However, cartesian coordinates themselves are not estimable! Even if we define the spin axis lie on the z-axis at a certain time, the azimuthal angle of the polyhedron is not defined. If we also choose to explicitly estimate the spin axis direction, then a total of 3 Euler angles are undefined. Note that, if we estimate station velocities, these 3 Euler angles are also free to drift at a constant rate, hence we would need to specify 3 Euler angles and their 3 first time derivatives (or, equivalently, 3 Euler angles at two epochs).

We must keep in mind that we are choosing the Cartesian coordinate representation (or the equivalent representation of latitude, longitude and height for a specified ellipsoid) for

convenience only, and that the coordinates themselves are not necessary for interpretation (a notion crucial to the development of relativity theory).

SITE COORDINATES

We have chosen to estimate all cartesian coordinates and a daily pole direction, all with very loose constraints. As a final step, the free-network GPS solution is oriented to ITRF91 [3, 4] at epoch 1992.5. When deriving the rotational angles between two reference frames, it is essential to simultaneously estimate the 3 angles, and also 3 translational components and a scale parameter. The reason for this is that the angles are correlated with the translations, so if the GPS solution's location of the "geocenter" (Earth's center of mass) disagrees with the reference solution, the estimate of 3 angles alone will absorb some of the translational offset, thus giving an erroneous orientation. Having estimated all 7 parameters, only the 3 angles are then used to transform the GPS solution.

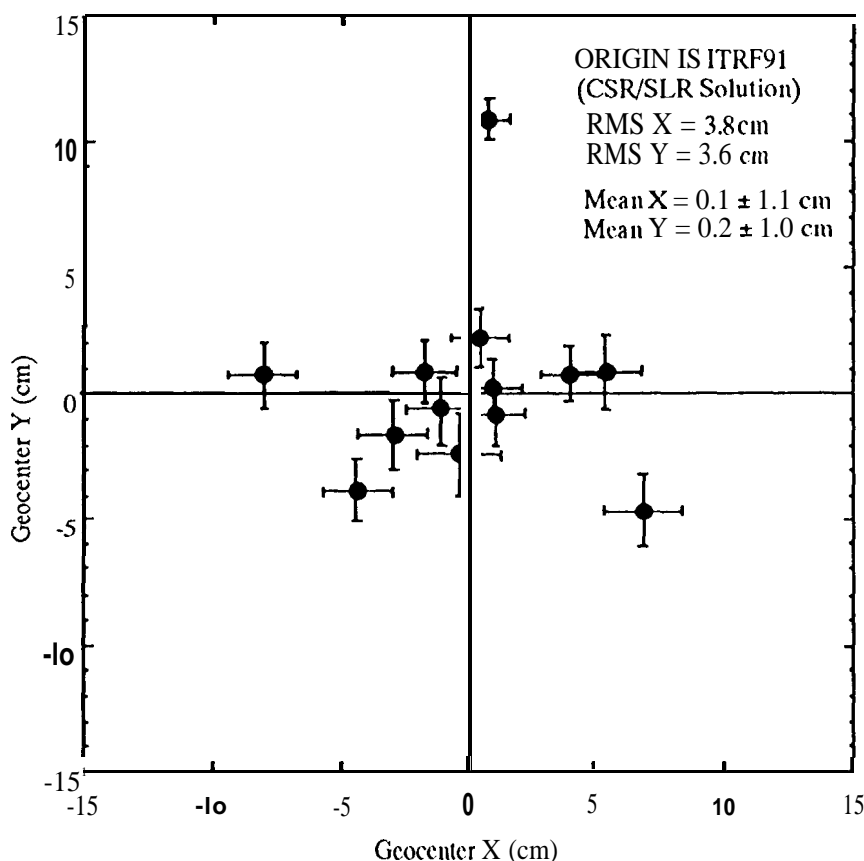


Fig 2. Weekly GPS solution for the geocenter (Earth center of mass), as compared with the origin of ITRF91, which is based on a satellite later ranging solution by CSR.

In the following examples, we use data from a 13 week period from June-August, 1992. For this purpose, we simply assumed a zero-velocity mode] for station coordinates, and formed a fully weighted average solution for the free-network polyhedron, which was then oriented to ITRF91 using the above procedure. We then took each weekly solution, and estimated a 7-parameter transformation into the 13-week combined solution.

Fig. 2 shows the translational offset of each week's solution. These translations can be interpreted as the discrepancy between the GPS determination of the geocenter and the origin of ITRF91. Since we know of no mechanism which can induce few-cm level variations in the Earth's center of mass (relative to the crust) over such a short period, we must interpret Fig. 2 as a measure of the stability of the GPS origin, which is implicitly defined through orbital dynamics. Hence, Fig. 2 illustrates one aspect of orbital mismodeling. There is no evidence of a bias between GPS and ITRF. The z-component is not as precisely constrained by the GPS data, but nevertheless agrees on average to better than 10 cm with ITRF. (Our most recent solution, described below, agrees with the ITRF origin to within 2 cm in all 3 components).

After removing each week's geocenter, scale, and orientation so that it is transformed into the 13-week reference frame, we obtain weekly estimates of station coordinates. Fig. 3 shows a representative examples of time-series of coordinates for Wettzell, Germany. Wettzell is typical of all northern hemisphere sites. The average RMS for geocentric coordinates are summarized in Table 1 below.

Fig. 4 shows the motion of Pinyon Flat Observatory (PIN1), California, due to the Landers earthquake of 28 June, 1992. It is important to realize that this plot is showing the latitude of the station (not baseline estimates, such as those shown in [5] and [6]). This illustrates the power of this technique to observe absolute co-seismic displacement, without reference to any particular fixed station. In fact, the geocentric coordinates are generally better determined than baseline coordinates for long baselines. Baseline precision is at the level of 2 parts per billion, which exceeds 4 mm for baselines longer than 2000 km.

Table 1
RMS OF WEEKLY GPS GEOCENTRIC COORDINATES

| Coordinate | Northern Hem. (m m) | Southern Hem. (m m) |
|-------------------|---------------------------------|---------------------------------|
| Latitude | 4.0 | 11 |
| Longitude | 4.4 | 14 |
| Height | 7.5 | 23 |

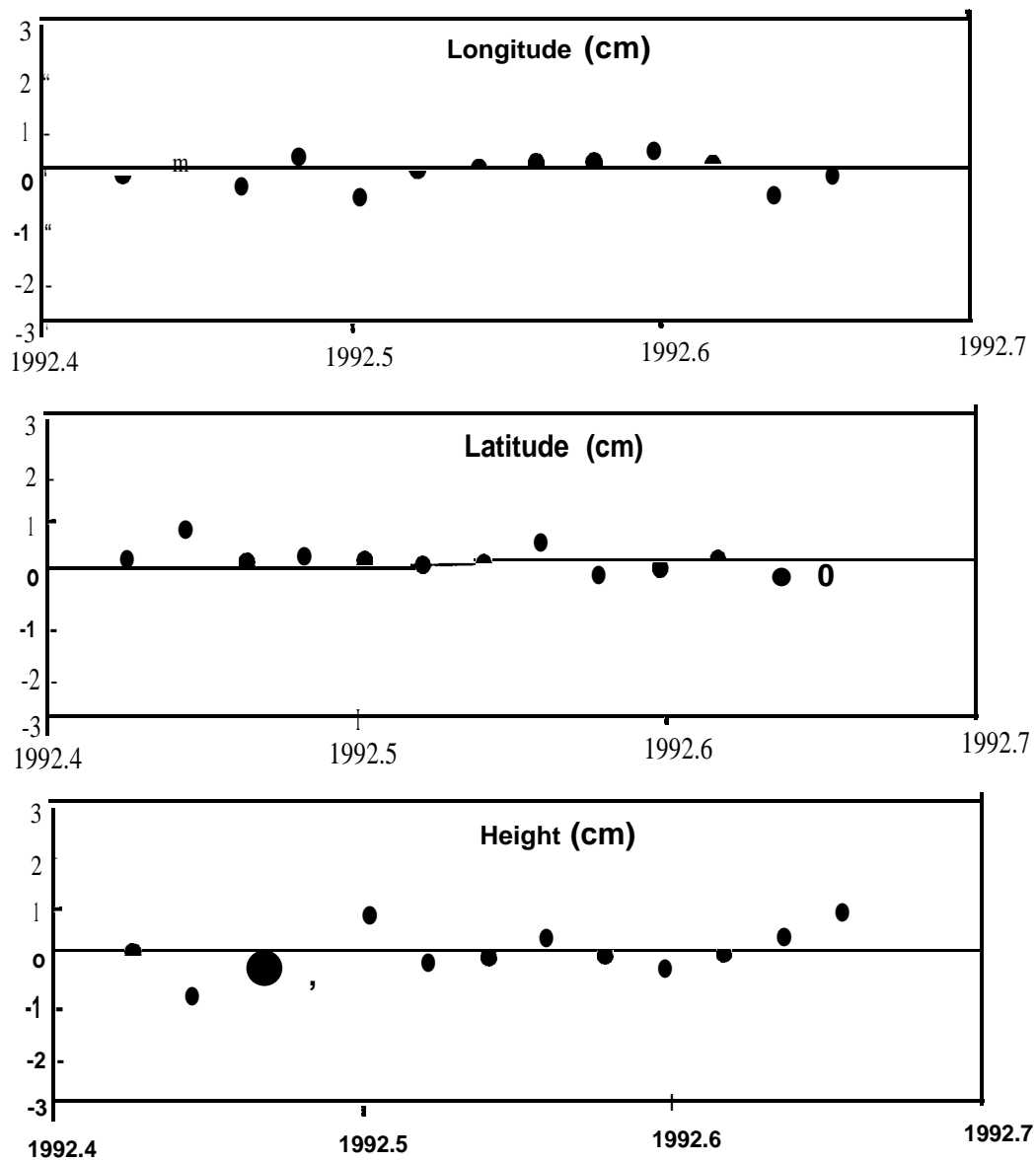


Fig 3. Weekly GPS solution for the geocentric coordinates of Wettzell, Germany. The 13-week average solution has been subtracted out. RMS in lat. and long. is 3 mm, and 7 mm for height.

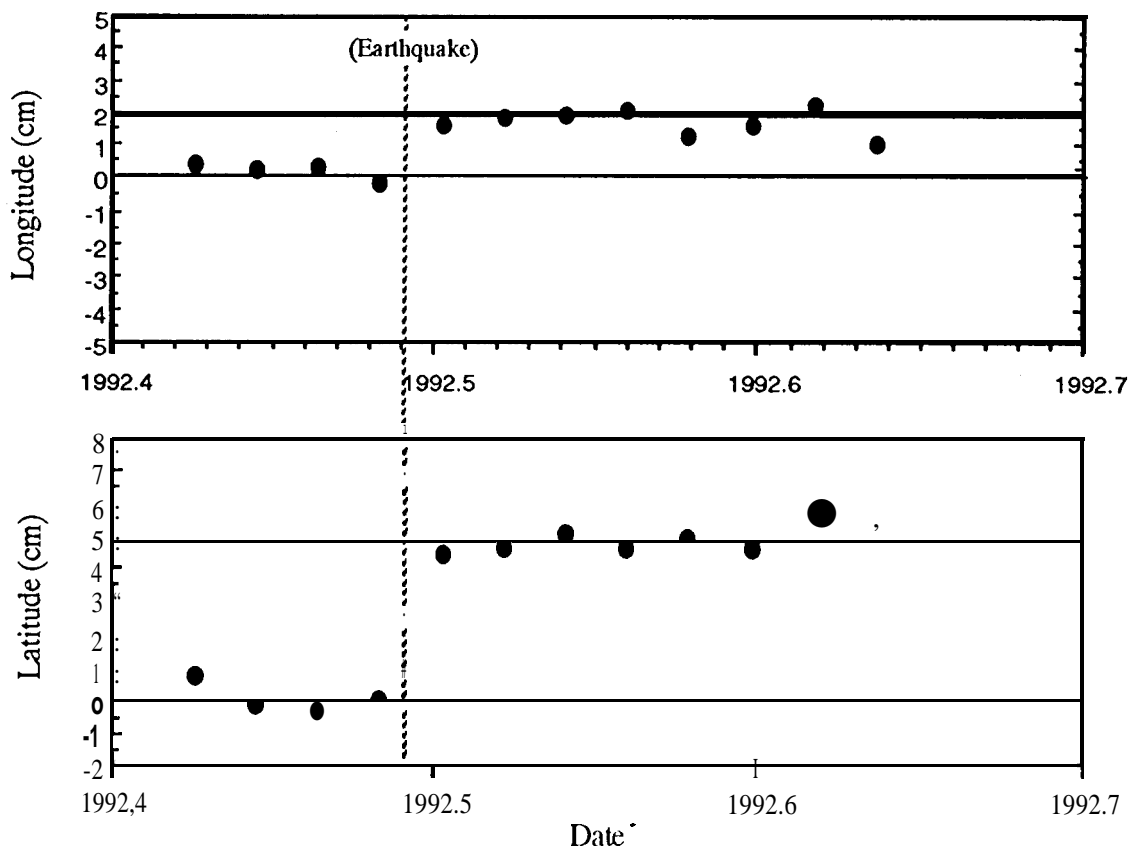


Fig 4. Weekly GPS solutions for the geocentric coordinates of Pinyon Flat Observatory, California. The step-functon is due to co-seismic displacement associated with the Landers earthquake of 28 June, 1992.

SITE VELOCITIES

We mentioned above the additional complexity in reference frame definition when station coordinates are estimated as an epoch position plus a velocity: Euler angle rates must be specified, otherwise the polyhedron is free to rotate about some arbitrary pole. For example, velocities in the longitudinal direction would be perfectly correlated with the Earth spin rate. Fixing the Euler angle rates will affect the apparent drift of the coordinates of the Earth's spin axis ("apparent," because it does not affect the estimable parameter, which are the colatitudes of all stations with respect to the instantaneous spin axis!). Conversely, the Euler angles and their rates may be arbitrarily fixed by defining the direction of Earth's pole on 2 days, and fixing the longitude and longitudinal velocity of one station. The choice we suggest here, is to apply a rate constraint such that the station velocities are aligned in some average sense with conventional geological plate motion models, such as NUVEL NNR-1 ("NNR" means "no net rotation") [7].

One way to achieve this is to expand the notion of a 7-parameter transformation into a 14-parameter transformation (the original 7-parameters plus their rates). We could then solve for the Euler angles and rates and directly apply it to our free network solution. The

advantage of such a technique is that no station (or station velocity) has special treatment in the reference frame definition, and no coordinate (or velocity) has zero formal error.

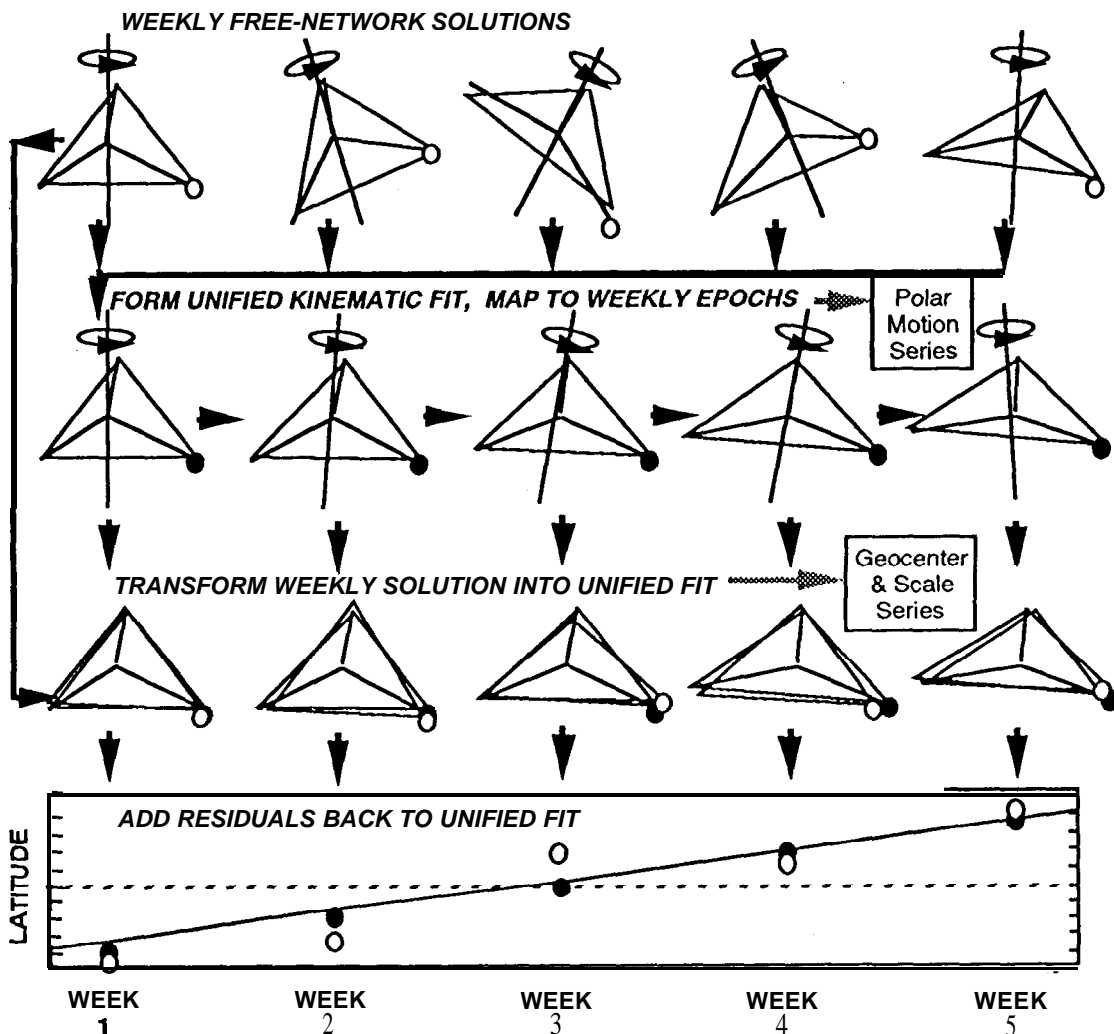


Fig. 5. A schematic description of how to derive a time-series of geocentric station coordinates. In this example, we obtain weekly station coordinates, pole positions, **geocenter** location, and scale parameter. in **practice**, the pole position is estimated every day.

Figure 5 illustrates how station coordinates at, for example, weekly epochs can be derived by mapping weekly solutions into a unified kinematic solution (with station velocities estimated). To avoid complication, the alignment to ITRF is not explicitly shown in this figure. Note that this is similar to method used to derive Figs. 3 and 4, (except that station velocities were not estimated, and pole positions were actually estimated daily).

JPL GLOBAL COORDINATE SOLUTION JGC9301

JPL solution **JGC9301** has been submitted to IERS for inclusion in the Annual Report. The solution is listed in the Appendix. We describe it here to illustrate how the above techniques can be applied.

The inputs to JGC9301 are daily free-network solutions from (approximately) June, July, August, 1992, plus January and February 1993. (We do not yet have free-network solutions for the missing months). These daily solutions were first combined into weekly solutions, and a few (about 5%) suspected problem days were removed by checking baseline length repeatability. Using these weekly solutions, station velocities and coordinates were estimated at a specified epoch (in this case, 1992.5). At this point, the solution was very ill-determined for the reasons given above. Since the period spanned by the data is a fraction of a year, this solution's was constrained to the ITRF91 velocity field [3, 4]. We solved for a 7-parameter transformation into ITRF91 [3] at epoch 1992.5, and then applied only the 3 rotational angles to the GPS solution. The solution JGC9301, augmented with the NUVEL NNR-1 velocity field (at designated primary sites on stable plate interiors) can now be used to define the orientation for all future GPS solutions.

The geocenter and scale for JGC9301 were not fixed to ITRF91. The differences in geocenter and scale are given in Table 2. Removing the geocenter and scale, the RMS coordinate difference is 16 mm (for 66 coordinates, 59 degrees of freedom).

Table 2
TRANSFORMATION JGC9301-ITRF91
Standard errors are given for JGC9301 only

| Parameter | JGC9301-ITRF91 |
|------------------|----------------------------|
| Geocenter X | 8.9 ±11 mm |
| Geocenter Y | 0.6 ±10 mm |
| Geocenter Z | 17.7 ±15 mm |
| Scale | -2.4 ±0.2×10 ⁻⁹ |

CONCLUSIONS

In conclusion, we suggest that GPS can provide a very strong reference frame, capable of providing geocentric coordinates with sub centimeter accuracy. The terrestrial reference frame will be deficient in 6 quantities which must be specified in order for station coordinates and their velocities to be consistent with convention. These quantities are 3 Euler angles and their first time derivatives. We suggest orienting free-network GPS solution at a specific epoch with ITRF (for example, by solving for a 7-parameter transformation, then applying the solution for the 3 rotation angles). The 3 Euler angle rates can be fixed by applying a global rotation rate to minimize the RMS difference in station velocity with NUVEL NNR-1 for sites on stable plate interiors.

ACKNOWLEDGEMENTS

The work described in this paper was carried out by the Jet Propulsion Laboratory, California Institute of Technology, under contract with the National Aeronautical and Space Administration

REFERENCES

- [1] Heflin, M. B., W.I. Bertiger, G. Blewitt, A.P. Freedman, K.J. Hurst, S.M. Lichten, U.J. Lindqwister, Y. Vigue, F.H. Webb, T.P. Yunck, and J.F. Zumberge, Global geodesy using GPS without fiducial sites, *Geophys. Res. Lett.*, 19, 131-134, 1992.
- [2] Blewitt, G., M.B. Heflin, F.H. Webb, U. J. Lindqwister, and R.P. Malla, Global coordinates with centimeter accuracy in the International Terrestrial Reference Frame using the Global Positioning System, *Geophys. Res. Lett.*, 19, 853-856, 1992
- [3] Boucher, C. and Z. Altamimi, IGS electronic mail message #90, 1992.
- [4] Boucher, C., Z. Altamimi, and L. Duhem, ITRF 91 and its associated velocity field, *IERS technical note 12*, Observatoire de Paris, 1992.
- [5] Blewitt, G., M.B. Heflin, K.J. Hurst, D.C. Jefferson, F.H. Webb, and J.F. Zumberge, Absolute far-field displacements from the 28 June 1992 Landers earthquake sequence, *Nature*, 361, 340-342, 1993.
- [6] Bock, Y., D.C. Agnew, P. Fang, J.F. Genrich, B.H. Hager, T.A. Herring, R.W. King, S. Larsen, J.B. Minster, K. Stark, S. Wdowinski, and F.K. Wyatt, Detection of crustal deformation from the Landers earthquake sequence using continuous geodetic measurements, *Nature*, 361, 338-340, 1993.
- [7] DeMets, C., R.G. Gordon, D.F. Argus, and S. Stein, Current plate motions, *Geophys. J. Int.*, 101, 425-478, 1990.

APPENDIX

JPL GPS Coordinate Solution: JGC9301

** EPOCH OF ADJUSTMENT IS 1992.5; ALL VELOCITIES CONSTRAINED TO ITRF91

** GPS DATA SPAN: 1-JUN-1992 to 30-AUG-1992, and 1-JAN-1993 to 1-MAR-1993.

- (1) **with the following exceptions**, antenna heights are as reported in IGS Mail#90. Note that **PN1Q**, **GOLQ**, and **JPIQ** refer to post-seismic positions.
- (2) All "s"-type points are to the top of the choke ring, hence they should more properly be designated a new **DOMES** number, located 7 cm above the current S point.
- (3) Unknown or unassigned **DOMES** sites are given the number 99999.
- (4) Unknown or unassigned **DOMES** points are assigned the number 999.
- (5) Station character ID's follow IGS **Mail#90**, except for the **following**:
 - (a) **CASA** is an uncatalogued point near Mammoth Lakes, California.
 - (b) **HARV** is an off-shore oil platform near Vandenberg, Calif.
 - (c) **KOUR** is the new global tracking site at **Kourou**, S. America.
 - (d) **NYA*** is "post explosives" (referring to the accident of late 1992), but should in principle be equivalent to **NYAL**. A separate solution was obtained to assess the new antenna height provided by Statens Kartverk. Assumed antenna heights to top of ring were: **NYAL=5.286 m**, **NYA*=5.273 m**
 - (e) **PAM*** is to the top of the choke ring (for June-August, 1992).
 - (f) **PIE1** is a new point at Pie Town, New Mexico. According the H. Bryant, **GSFC**, the tie from the ref. point of CDP 7234 to JPL 4009 S is **DX= 36.9162 m**, **DY= 34.8267 m**, **DZ= 35.2550 m**
 - (g) **USU2** (until Aug 9, 1992) and **USU3** (since Aug 9, 1992) are both different points than **USUD** (which was valid only for **Jan'91 expt.**)
 - (h) **VNDP** is a new Rogue monument at Vandenberg, Calif.

JPL GPS Coordinate Solution: JGC9301 (continued)

| DOMES # | Station | X(m) | Y(m) | Z(m) | SX(m) | SY(m) | SZ(m) |
|------------------|----------------|----------------------|----------------------|---------------|--------------|--------------|---------------|
| 40129MO03 | ALBH | -2341332.8188 | -3539049.5063 | 4745791.3986 | 0.0027 | 0.0036 | 0.0032 |
| 40104MO02 | ALGO | 918129.6062 | -4346071.2190 | 4561977.7926 | 0.0032 | 0.0036 | 0.0036 |
| 50103S017 | CANB | -4460996.1118 | 2682557.1741 | -3674443.9985 | 0.0063 | 0.0063 | 0.0050 |
| 40437M999 | CASA | -2444430.1146 | -4428687.6998 | 3875747.4434 | 0.0239 | 0.0338 | 0.0270 |
| 40105MO02 | DRAO | -2059164.5868 | -3621108.3908 | 4814432.4129 | 0.0027 | 0.0036 | 0.0032 |
| 40408M001 | FAIR | -2281621.3153 | -1453595.7717 | 5756961.9615 | 0.0027 | 0.0032 | 0.0040 |
| 40405S028 | GOLD | -2353614.1045 | -4641385.4774 | 3676976.5198 | 0.0036 | 0.0045 | 0.0036 |
| 40405S031 | GOLQ | -2353614.0916 | -4641385.4647 | 3676976.5243 | 0.0054 | 0.0076 | 0.0058 |
| 11001MO02 | GRAZ | 4194424.0635 | 1162702.4962 | 4647245.2583 | 0.0045 | 0.0036 | 0.0045 |
| 40400MO06 | JPL1 | -2493304.0622 | -4655215.5740 | 3565497.3586 | 0.0036 | 0.0040 | 0.0036 |
| 40400M007 | JPIQ | -2493304.0487 | -4655215.5673 | 3565497.3406 | 0.0050 | 0.0072 | 0.0054 |
| 99999S001 | HARV | -2686069.1359 | -4527084.4727 | 3589502.2322 | 0.0040 | 0.0054 | 0.0040 |
| 30302MO02 | HART | 5084625.4517 | 2670366.5648 | -2768494.0472 | 0.0104 | 0.0090 | 0.0054 |
| 13212M007 | HERS | 4033470.3093 | 23672.7011 | 4924301.1537 | 0.0045 | 0.0036 | 0.0045 |
| 40424MO04 | KOKB | -5543838.0765 | -2054587.5465 | 2387809.5811 | 0.0054 | 0.0050 | 0.0036 |
| 13504MO03 | KOSG | 3899225.3394 | 396731.7611 | 5015078.2819 | 0.0032 | 0.0027 | 0.0032 |
| 99999S999 | KOUR | 3839591.5927 | -5059567.6757 | 579956.8479 | 0.0076 | 0.0086 | 0.0036 |
| 13407S012 | MADR | 4849202.5739 | -360329.1847 | 4114913.0528 | 0.0036 | 0.0032 | 0.0032 |
| 31303M001 | MASP | 5439189.2326 | -1522054.8584 | 2953464.2000 | 0.0054 | 0.0040 | 0.0036 |
| 12734M008 | MATE | 4641949.8225 | 1393045.2204 | 4133287.2514 | 0.0040 | 0.0032 | 0.0032 |
| 66001M001 | MCMU | -1310695.2319 | 310468.8975 | -6213363.4752 | 0.0054 | 0.0063 | 0.0081 |
| 10503S011 | METS | 2892571.0552 | 1311843.3063 | 5512634.0591 | 0.0027 | 0.0027 | 0.0036 |
| 10317MO01 | NYAL | 1202430.7419 | 252626.6293 | 6237767.4903 | 0.0027 | 0.0027 | 0.0063 |
| 10317MO01 | NYA* | 1202430.7483 | 252626.6281 | 6237767.5077 | 0.0036 | 0.0032 | 0.0094 |
| 10402M004 | ONSA | 3370658.7584 | 711876.9849 | 5349786.8156 | 0.0027 | 0.0027 | 0.0032 |
| 92201S999 | PAM* | -5245202.1159 | -3080476.4838 | -1912828.0770 | 0.0099 | 0.0086 | 0.0045 |
| 92201MO03 | PAMA | -5245195.1164 | -3080472.3882 | -1912825.5272 | 0.0121 | 0.0108 | 0.0050 |
| 40129MO02 | PGC1 | -2327188.0475 | -3522529.0014 | 4764832.3874 | 0.0040 | 0.0050 | 0.0050 |
| 40456M999 | PIE1 | -1640916.6978 | -5014781.1876 | 3575447.1450 | 0.0040 | 0.0054 | 0.0045 |
| 40407MO02 | PIN1 | -2369510.3526 | -4761207.2139 | 3511396.1471 | 0.0040 | 0.0054 | 0.0040 |
| 40407MO03 | PNIQ | -2369510.3751 | -4761207.2145 | 3511396.0951 | 0.0050 | 0.0072 | 0.0054 |
| 40433MO04 | QUIN | -2517230.9574 | -4198595.2959 | 4076531.3450 | 0.0036 | 0.0050 | 0.0040 |
| 40499MO02 | RCM2 | 961318.9938 | -5674090.9670 | 2740489.5737 | 0.0045 | 0.0068 | 0.0040 |
| 41705MO03 | SANT | 1769693.2841 | -5044574.1095 | -3468321.1600 | 0.0068 | 0.0086 | 0.0058 |
| 40460M001 | sl01 | -2455521.6655 | -4767213.4340 | 3441654.9141 | 0.0086 | 0.0139 | 0.0099 |
| 40101MO01 | STJO | 2612631.3467 | -3426807.0053 | 4686757.7401 | 0.0032 | 0.0032 | 0.0032 |
| 23601M001 | TAIW | -3024781.8690 | 4928936.9104 | 2681234.5286 | 0.0063 | 0.0072 | 0.0050 |
| 10302MO03 | TROM | 2102940.4466 | 721569.3569 | 5958192.0724 | 0.0027 | 0.0027 | 0.0036 |
| 21729S999 | USU2 | -3855262.6529 | 3427432.2180 | 3741020.9954 | 0.0076 | 0.0072 | 0.0063 |
| 21729S999 | USU3 | -3855263.0376 | 3427432.5738 | 3741020.4726 | 0.0063 | 0.0063 | 0.0050 |
| 40420M999 | VNDP | -2678090.4952 | -4525439.0423 | 3597432.4703 | 0.0423 | 0.0625 | 0.0437 |
| 14201S020 | WETT | 4075578.7195 | 931852.6398 | 4801570.0361 | 0.0036 | 0.0032 | 0.0036 |
| 14201M999 | WET* | 4075577.6580 | 931852.3942 | 4801568.7689 | 0.0040 | 0.0032 | 0.0045 |
| 50107MO04 | YAR1 | -2389025.3445 | 5043316.8547 | -3078530.9517 | 0.0063 | 0.0076 | 0.0050 |
| 40127M003 | YELL | -1224452.3754 | -2689216.0862 | 5633638.2826 | 0.0027 | 0.0032 | 0.0036 |

CONTRIBUTION OF IGS 92 TO THE TERRESTRIAL REFERENCE FRAME

Claude Botcher*, Zuheir Altamimi*

As a sub-product of the IGS 92 campaign of the Core Network, several sets of station coordinates are now available. These sets were analysed in order to assess their accuracy as well as their contribution to the establishment of a worldwide terrestrial reference frame. In a first step, these sets have been combined together, leading to a global GPS combined solution. This has allowed to assess the mutual consistency of the different solutions. The GPS combined solution was then compared to the IERS Terrestrial Reference Frame (ITRF91), showing an agreement of about 1 cm RMS level. Then, a common set of station coordinates has been obtained by combining the ITRF91 and the global GPS combined solution. This common set was performed in order to be used by the IGS analysis centers in their orbit computations.

DESCRIPTION OF THE INDIVIDUAL GPS SOLUTIONS

5 GPS solutions based on IGS92 campaign are available, coming from 5 different analysis centers. Table 1 summarizes these solutions.

**Table 1
GLOBAL GPS IGS 92 SOLUTIONS**

| Label | DESIGNATION | Number of stations | COMMENTS |
|-------|-------------------|--------------------|-----------------------------------------------------------------------------|
| PJ | SSC(JPL) 92P 02 | 36 | based on a 3 month period 01-jun / 01-sep-1992 |
| PR | SSC(SIO) 93P 01 | 48 | based on 16 months of PGAA analysis. coordinates referred to epoch 1992.836 |
| PC | SSC(CSR) 92P 03 | 24 | free network solution based on about 50 days centred on 1992.6 |
| PB | SSC(CODE) 92 P 01 | 13 | contains european stations only based on the period 19-jun / 11-oct-1992 |
| PE | SSC(EMR) 92P 01 | 17 | based on the period 04-aug / 17-oct-1992 |

*Institut Géographique National, B.P. 68,2 Avenue Pasteur, 94160 Saint-Mandé, France

THE GPS COMBINED SOLUTION

A global GPS combined solution has been performed including the 5 solutions described in Table 1 with the following assumptions:

- the original formal errors of the individual sets were modified in order to obtain statistically realistic combined solution. This was done using the formula:

$$\sigma = \sqrt{A^2 + B^2\sigma_f^2} \quad (1)$$

where σ is the input error and σ_f is the original formal error as provided in the individual sets. A and B are determined by an empirical estimation. The adopted values for A and B are given in Table 2.

Table 2
WEIGHTING SCHEME OF THE
GPS COMBINED SOLUTION

| SOLUTION | A(cm) | B | COMMENTS |
|----------|------------|------------|---------------------------|
| PJ | 0.0 | 8.0 | |
| PR | 1.5 | | formal error not provided |
| PC | 0.0 | 8.0 | |
| PB | 0.8 | | formal error not provided |
| PE | 0.0 | 4.0 | |

- due to inconsistency between some solutions, some stations were deweighted in the individual solutions. This is described in Table 3.

Table 3
DEWEIGHTED STATIONS IN THE
GPS COMBINED SOLUTION

| SOLUTION | INPUT ERROR (m) | STATIONS |
|----------|-----------------|------------------------|
| PR | 0.200 | SANT, PAMA, HART |
| PR | 0.100 | MCMU, CANB, YAR1 |
| PR | 0.050 | STJO, ALGO, FAIR, NYAL |
| P c | 0.200 | HART, SANT |
| P c | 0.100 | USUD, TAIW |
| P c | 0.030 | GOLD |
| PE | 0.100 | SANT |

- the reference epoch of the GPS combined solution is selected to be 1992.6 (MJD 48840) which correspond to the central epoch of the IGS 92 campaign (21-jun-23 to sep-1992).

As results of the GPS combined solution, Table 4 gives the transformation parameters from SSC(JPL) 92 P 02 to the other solutions. On the other hand, Table 5 summarizes the global statistic issued from the combination. This Table gives for each solution the following numbers:

- N : number of points common to other solutions,
- SP : unweighed 2-D horizontal RMS
- Su : unweighed vertical RMS
- WSX : weighted 3-D (X, Y, Z) RMS
- NSX : 3-D normalized RMS
- A and B : the two weighting parameters of the equation 1

Table 4
TRANSFORMATION PARAMETERS FROM SSC(JPL) 92 P 02
TO OTHER SOLUTIONS

| SOLUTION | T1 cm | T2 cm | T3 cm | D 10 ⁻⁸ | R1 0.001" | 0.%1 " | R3 0.001" |
|-------------------|--------------|--------------|---------------|-----------------------|----------------|---------------|-----------------|
| SSC(SIO) 93 P 01 | -2.2 ±0.5 | 2.1 ±0.5 | 8.6 ±0.4 | 0.04 ±0.07 | -1.62 ±0.20 | 3.24 ±0.18 | -5.91 ±0.15 |
| SSC(CSR) 92 P 03 | -6.3 ±0.5 | 20.7 ±0.6 | -57.8 ±0.4 | 0.51 ±0.06 | -3.87 ±0.24 | 1.12 ±0.15 | -67.42 ±0.15 |
| SSC(CODE) 92 P 01 | -2.9 ±1.2 | -4.9 ±2.4 | 11.6 ±1.2 | 0.05 ±0.17 | -4.56 ±0.66 | 3.72 ±0.45 | -6.92 ±0.55 |
| SSC(EMR) 92 P 01 | 1.3 ±0.7 | 0.5 ±0.8 | 11.0 ±0.7 | 0.17 ±0.09 | -1.63 ±0.30 | 2.39 ±0.26 | -5.88 ±0.22 |

COMPARISON BETWEEN THE GPS COMBINED SOLUTION AND ITRF91

The above described GPS combined solution has been compared to the ITRF91. This latter was moved from its reference epoch (1988.0) to 1992.6 using its associated velocity field. For a full description of the ITRF91, see the 1991 IERS Annual Report and the IERS Technical Note 12. The results of this comparison are given in Tables 6 and 7.

Table 5
STATISTIC OF THE GPS COMBINED SOLUTION

| SOLUTION | N | SP cm | S _u cm | WSX cm | NSX | A cm | B |
|-------------------|----|----------|----------------------|-----------|------|---------|-----|
| SSC(JPL) 92P 02 | 34 | 0.4 | 0.9 | 0.5 | 0.94 | 0.0 | 8.0 |
| SSC(SIO) 93P 01 | 34 | 5.9 | 6.9 | 1.4 | 1.26 | 1.5 | |
| SSC(CSR) 92 P 03 | 21 | 3.7 | 4.5 | 0.7 | 1.02 | 0.0 | 8.0 |
| SSC(CODE) 92 P 01 | 11 | 0.3 | 1.0 | 0.6 | 1.18 | 0.8 | |
| SSC(EMR) 92 P 01 | 15 | 1.2 | 4.3 | 0.7 | 0.78 | 0.0 | 4.0 |

Table. 6
TRANSFORMATION PARAMETERS FROM THE ITRF91
TO THE GPS COMBINED SOLUTION

| T1 cm | T2 cm | T3 cm | D 10 ⁻⁸ | R1 0.001" | R2 0.001" | R3 0.001" |
|-------------|-------------|--------------|-----------------------|---------------|----------------|---------------|
| 0.2 ±0.5 | 1.6 ±0.5 | -8.3 ±0.4 | -0.17 ±0.06 | 2.83 ±0.20 | -2.54 ±0.18 | 6.41 ±0.15 |

Table 7
STATISTIC OF THE COMPARISON BETWEEN THE ITRF91
AND THE GPS COMBINED SOLUTION

| SOLUTION | N | SP cm | S _u cm | WSX cm | NSX | A cm | B |
|--------------------------|----|----------|----------------------|-----------|------|---------|-----|
| ITRF91 | 36 | 4.5 | 2.4 | 0.9 | 1.20 | 0.0 | 1.0 |
| GPS Combined Solution | 33 | 0.8 | 1.1 | 0.7 | 1.00 | 0.0 | 2.0 |

CONTRIBUTION OF GPS TO THE ESTABLISHMENT OF THE TERRESTRIAL REFERENCE FRAME

Until the 1990 realization of the IERS Terrestrial Reference System (ITRS), namely the ITRF90, the contributed space-geodetic techniques were VLBI, LLR and SLR. In ITRF91, in addition to VLBI, LLR and SLR solutions a unique global GPS solution was incorporated, provided by JPL and issued from GIG'91 campaign.

The future ITRS realization, namely the ITRF92 which will be available in mid 93, will contain several GPS solutions based on the observations coming from IGS 92 campaign. In order to assess the contribution of GPS solutions to this oncoming realization, two test combinations have been performed. The first combination included one VLBI and one SLR solution. These two are respectively, a GSFC VLBI solution (SSC(GSFC) 92 R 03) and a CSR SLR solution (SSC(CSR) 92 L 01). The second combination included in addition to the two previous VLBI and SLR solutions, **the global** GPS combined solution described above. Tables 8 to 11 give the results of these two combinations

**Table 8
COMPARISON VLBI - SLR
TRANSFORMATION PARAMETERS
FROM SSC(CSR) 92 L 01 TO SSC(GSFC) 92 R 03**

| T1 cm | T2 cm | T3 cm | D 10 ⁻⁸ | R1 0.001" | R2 0.001" | R3 0.001" |
|-------------|---------------------|---------------------|-----------------------|---------------|----------------------|-----------------------|
| 1.7 ±1.1 | -0.1 ±1.2 | -1.5 ±1.2 | -0.23 ±0.15 | 2.17 ±0.48 | 0.95 ±0.42 | -2.58 ±0.32 |

**Table 9
COMPARISON VLBI - SLR - GPS
TRANSFORMATION PARAMETERS
FROM SSC(CSR) 92 L 01 TO SSC(GSFC) 92 R 03
AND THE GPS COMBINED SOLUTION**

| SOLUTION | T1 cm | T2 cm | T3 cm | D 10 ⁻⁸ | R1 0.001" | 0.%" " | R3 0.001" |
|-----------------------|---------------------|---------------------|--------------|------------------------------|---------------|-----------------------|----------------|
| SSC(GSFC) 92 R 03 | 1.5 ±0.9 | -0.2 ±1.0 | -1.8 ±0.9 | -0.20 fo.13 | 2.08 ±0.38 | 1.02 ±0.36 | -2.55 ±0.27 |
| GPS Combined Solution | -0.6 ±1.0 | 2.3 ±1.0 | -7.9 ±0.8 | -0.22 ±0.14 | 3.98 ±0.38 | -2.52 ±0.37 | 7.35 ±0.30 |

Table 10
STATISTICS OF THE COMPARISON VLBI - SLR

| SOLUTION | N | SP cm | S u cm | WSX cm | NSX | A cm | B |
|-------------------|----|----------|-----------|-----------|------|---------|-----|
| SSC(GSFC) 92 R 03 | 31 | 0.9 | 2.5 | 0.7 | 1.14 | 0.5 | 1.5 |
| SSC(CSR) 92 L 01 | 46 | 10.3 | 11.9 | 2.4 | 1.46 | 1.0 | 1.0 |

Table 11
STATISTICS OF THE COMPARISON VLBI - SLR - GPS

| SOLUTION | N | SP cm | S u cm | WSX cm | NSX | A cm | B |
|-----------------------|----|----------|-----------|-----------|------|---------|------------|
| SSC(GSFC) 92 R 03 | 40 | 1.1 | 3.1 | 0.8 | 1.33 | 0.5 | 1.5 |
| SSC(CSR) 92 L 01 | 50 | 9.9 | 12.2 | 2.1 | 1.31 | 1.0 | 1.0 |
| GPS Combined Solution | 22 | 1.3 | 2.7 | 1.1 | 1.30 | 0.0 | 2.0 |

COMBINATION OF THE ITRF91 AND THE GPS COMBINED SOLUTION

This combination was performed in order to produce a common set of station coordinates to be used by the IGS analysis centers in their orbit computations. It has been elaborated by fixing to zero the origin, scale and orientation of the ITRF91 at epoch 1992.6. Table 12 lists the coordinates obtained from this combination. These coordinates supersedes those published earlier via IGS mail.

CONCLUSION

The quality of the analysed GPS solutions could be evaluated from the statistics given in tables 5, 7 and 11. Among the different RMS values given in these Tables, the most significant one is the weighted 3-D RMS (WSX) which is an indicator of the quality of the analysed sets. From Table 5 we see that the WSX is varying from 5 to 14 mm for the 5 GPS solutions compared to each other. Meanwhile, in Table 7, this value is 7 mm for the combined GPS solution and 9 mm for the ITRF91. Moreover, when comparing the combined GPS solution to others coming from the two "classical" techniques; VLBI and SLR, the values of the WSX become 8,21 and 1 lmm, respectively for VLBI, SLR and GPS.

The analysis presented in this paper of the GPS solutions derived from the IGS 92 campaign, shows the success of this campaign in producing a high quality site positions of a global network. This success is also due to the effort of the observing and processing IGS centers.

In order to minimize differences in origin, scale and orientation of the terrestrial reference frames used by the analysis centers in their orbit computations, we recommend that they use the common set of coordinates presented here in Table 12.

Finally, with 1 cm level accuracy, GPS technique has now its place within other space-geodetic techniques, mainly VLBI and SLR, for establishing a global terrestrial reference frame. This will contribute greatly to the future realization of the IERS Terrestrial Reference System.

Table 12
IGS/IERS STATION COORDINATES IN THE ITRF91 AT 1992.6

| DOMES | SITE | CDP | x | Y | z | Sx | SY | Sz | Vx | VY | Vz | SVX | SVY | SVZ | * |
|------------|-----------------|------|--------------|--------------|--------------|-------|-------|-------|--------|--------|--------|-------|-------|-------|----|
| NVMBER | | IGS | m | m | m | m | m | m | m | m | m | m | m | m | |
| 103 02M002 | TROMSO | 7602 | 2102904.160 | 721602.485 | 5958201.291 | 0.007 | 0.007 | 0.008 | -0.017 | 0.013 | 0.004 | 0.003 | 0.003 | 0.003 | N |
| 10302MOO3 | TROMSO | TROM | 2102940.446 | 721569.369 | 5958192.076 | 0.007 | 0.007 | 0.008 | -0.017 | 0.013 | 0.004 | 0.003 | 0.003 | 0.003 | N |
| 10317MOO1 | NY-ALESUND | NYAL | 1202430.741 | 252626.641 | 6237767.500 | 0.009 | 0.009 | 0.010 | -0.016 | 0.010 | 0.003 | 0.003 | 0.003 | 0.003 | N |
| 10325MOO1 | HONEFOSS | HONE | 3132539.011 | 566401.731 | 5508609.875 | 0.026 | 0.026 | 0.026 | -0.016 | 0.016 | 0.007 | 0.003 | 0.003 | 0.003 | N |
| 10402NOO4 | ONSALA | ONSA | 3370658.758 | 711876.987 | 5349786.823 | 0.008 | 0.008 | 0.008 | -0.015 | 0.016 | 0.006 | 0.001 | 0.002 | 0.002 | CN |
| 10402s002 | ONSALA | 7213 | 3370505.126 | 711917.453 | 5349830.683 | 0.006 | 0.006 | 0.007 | -0.015 | 0.016 | 0.006 | 0.001 | 0.002 | 0.002 | CN |
| 10503MOO2 | METSAHOVI | 7601 | 2890652.844 | 1310295.299 | 5513958.657 | 0.009 | 0.008 | 0.011 | -0.018 | 0.015 | 0.006 | 0.003 | 0.003 | 0.003 | N |
| 10503S011 | METSAHOVI | METS | 2892571.038 | 1311843.300 | 5512634.036 | 0.010 | 0.010 | 0.010 | -0.018 | 0.015 | 0.006 | 0.003 | 0.003 | 0.003 | N |
| 11001MOO2 | GRAZ | GRAZ | 4194424.064 | 1162702.502 | 4647245.274 | 0.013 | 0.013 | 0.015 | -0.017 | 0.017 | 0.009 | 0.002 | 0.002 | 0.003 | CN |
| 11001S002 | GRAZ | 7839 | 4194426.626 | 1162693.971 | 4647245.591 | 0.009 | 0.009 | 0.009 | -0.017 | 0.017 | 0.009 | 0.002 | 0.002 | 0.003 | CN |
| 12734M008 | MATERA | MATE | 4641949.815 | 1393045.211 | 4133287.265 | 9.007 | 0.007 | 0.007 | -0.020 | 0.019 | 0.014 | 0.002 | 0.002 | 0.002 | CN |
| 12734s001 | MATERA | 7939 | 4541964.990 | 1393070.038 | 4133262.300 | 0.007 | 0.006 | 0.007 | -0.020 | 0.019 | 0.014 | 0.002 | 0.002 | 0.002 | CN |
| 13212M007 | HERSTMONCEUX | HERS | 4033470.300 | 23672.699 | 4924301.154 | 0.010 | 0.010 | 0.010 | -0.014 | 0.016 | 0.008 | 0.002 | 0.002 | 0.003 | CN |
| 13212s001 | HERSTMONCEUX | 7840 | 4033463.788 | 23662.414 | 4924305.097 | 0.007 | 0.007 | 0.007 | -0.014 | 0.016 | 0.008 | 0.002 | 0.002 | 0.003 | CN |
| 13407S010 | MADRID | 1565 | 4849336.760 | -360488.845 | 4114748.730 | 0.007 | 0.007 | 0.008 | -0.011 | 0.022 | 0.007 | 0.004 | 0.003 | 0.003 | CN |
| 13407s012 | MADRID | MADR | 4849202.516 | -360329.182 | 4114913.006 | 0.006 | 0.006 | 0.007 | -0.011 | 0.022 | 0.007 | 0.004 | 0.003 | 0.003 | CN |
| 13504M002 | KOOTWIJK | 8833 | 3899237.799 | 396769.262 | 5015055.263 | 0.008 | 0.008 | 0.008 | -0.016 | 0.017 | 0.006 | 0.005 | 0.004 | 0.005 | CN |
| 13504M003 | KOOTWIJK | KOSG | 3899225.338 | 396731.759 | 5015078.287 | 0.007 | 0.007 | 0.007 | -0.016 | 0.017 | 0.006 | 0.005 | 0.004 | 0.005 | CN |
| 14001S001 | ZIMMERWALD | 7810 | 4331283.599 | 567549.663 | 4633140.034 | 0.009 | 0.009 | 0.009 | -0.008 | 0.020 | 0.016 | 0.004 | 0.002 | 0.004 | CN |
| 14201s004 | WETTZELL | 7224 | 4075539.981 | 931735.215 | 4801629.304 | 0.006 | 0.006 | 0.006 | -0.019 | 0.017 | 0.004 | 0.001 | 0.002 | 0.002 | CN |
| 14201S020 | WETTZELL | WETT | 4075578.676 | 931852.530 | 4801559.982 | 0.006 | 0.006 | 0.006 | -0.019 | 0.017 | 0.004 | 0.001 | 0.002 | 0.002 | CN |
| 20702M002 | BAR GIYYORA | BARG | 4443959.362 | 3121953.102 | 3334710.334 | 0.023 | 0.019 | 0.024 | -0.024 | 0.015 | 0.017 | 0.011 | 0.008 | 0.009 | CN |
| 21729s001 | USUDA | 7246 | -3855355.402 | 3427427.607 | 3740971.310 | 0.035 | 0.032 | 0.038 | -0.021 | -0.009 | -0.013 | 0.003 | 0.003 | 0.003 | N |
| 21729s003 | USUDA ORIGINAL | USUD | -3855262.628 | 3427432.203 | 3741020.952 | 0.019 | 0.019 | 0.013 | -0.021 | -0.009 | -0.013 | 0.003 | 0.003 | 0.003 | N |
| 21729S005 | USUDA DISPLACED | USJ2 | -3855263.055 | 3427432.575 | 3741020.469 | 0.019 | 0.019 | 0.020 | -0.021 | -0.009 | -0.013 | 0.003 | 0.003 | 0.003 | N |
| 21729S007 | USUDA CURRENT | USU3 | -3855263.049 | 3427.432.526 | 3741020.437 | 0.026 | 0.026 | 0.029 | -0.021 | -0.009 | -0.013 | 0.003 | 0.003 | 0.003 | N |
| 21730s001 | TSUKUBA | 7311 | -3957172.864 | 3310237.879 | 3737708.914 | 0.025 | 0.021 | 0.027 | 0.004 | -0.012 | -0.024 | 0.003 | 0.003 | 0.004 | CN |
| 23601M001 | TAIPEI | TAIW | -3024781.867 | 4928936.916 | 2681234.520 | 0.019 | 0.019 | 0.014 | -0.023 | -0.007 | -0.013 | 0.003 | 0.003 | 0.003 | N |
| 30302M002 | HARTEBEESTHOEK | HART | 5084625.425 | 2670366.519 | -2768494.036 | 0.013 | 0.012 | 0.011 | -0.005 | 0.021 | 0.013 | 0.004 | 0.004 | 0.003 | CN |
| 30302s001 | HARTEBEESTHOEK | 7232 | 5085442.795 | 2668263.474 | -2768697.160 | 0.013 | 0.012 | 0.011 | -0.006 | 0.021 | 0.013 | 0.004 | 0.004 | 0.003 | CN |
| 31303M001 | MASPALOMAS | MASP | 5439189.186 | -1522054.848 | 2953464.161 | 0.014 | 0.010 | 0.010 | -0.003 | 0.020 | 0.016 | 0.003 | 0.003 | 0.003 | N |
| 40101MOO1 | ST. JOHNS | STJO | 2512631.340 | -3426807.001 | 4686757.745 | 0.010 | 0.010 | 0.010 | -0.018 | -0.002 | 0.009 | 0.003 | 0.003 | 0.003 | N |
| 40103MOO1 | PRINCE ALBERT | PRAL | -1050708.054 | -3680995.831 | 5085127.915 | 0.010 | 0.021 | 0.028 | -0.020 | -0.001 | -0.005 | 0.003 | 0.003 | 0.003 | N |
| 40104M002 | ALGONQUIN | ALGO | 918129.508 | -4346071.220 | 4561977.778 | 0.006 | 0.005 | 0.007 | -0.016 | -0.004 | -0.001 | 0.001 | 0.002 | 0.002 | CN |
| 40104S001 | ALGONQUIN | 7282 | 918034.852 | -4345132.243 | 4561971.132 | 0.006 | 0.007 | 0.007 | -0.016 | -0.004 | -0.001 | 0.001 | 0.002 | 0.002 | CN |
| 40105MOO1 | PENTICTON | 7283 | -2058840.417 | -3621285.445 | 4814420.790 | 0.009 | 0.011 | 0.012 | -0.024 | -0.016 | 0.010 | 0.001 | 0.001 | 0.002 | CN |
| 40105MOO2 | PENTICTON | DRAO | -2059164.597 | -3621109.392 | 4814432.425 | 0.009 | 0.011 | 0.011 | -0.024 | -0.016 | 0.010 | 0.001 | 0.001 | 0.002 | CN |
| 40124MOO1 | CALGARY | PRDS | -1659602.748 | -3676725.741 | 4925493.632 | 0.078 | 0.098 | 0.142 | -0.019 | -0.001 | -0.007 | 0.003 | 0.003 | 0.003 | N |
| 40127M001 | YELLOWKNIFE | 7285 | -1224124.523 | -2689530.646 | 5633555.403 | 0.012 | 0.016 | 0.018 | -0.022 | -0.001 | -0.005 | 0.003 | 0.003 | 0.003 | N |
| 40127MOO3 | YELLOWKNIFE | YELL | -1224452.378 | -2689216.072 | 5633638.284 | 0.008 | 0.009 | 0.009 | -0.022 | -0.001 | -0.005 | 0.003 | 0.003 | 0.003 | N |

| | | | | | | | | | | | | | | |
|-----------|------------------|------|--------------|--------------|---------------|-------|-------|-------|--------|--------|--------|-------|--------|----------|
| 40129M001 | VICTORIA | 7289 | -2341310.090 | -3539083.864 | 4745768.349 | 0.024 | 0.037 | 0.045 | -0.018 | -0.001 | -0.010 | 0.003 | 0.0030 | 0.003N |
| 40129M002 | VICTORIA | PGC1 | -2327188.048 | -3522528.980 | 4764832.376 | 0.011 | 0.011 | 0.011 | -0.018 | -0.001 | -0.010 | 0.003 | 0.003 | 0.003 N |
| 40129M003 | ALBERT HEAD | ALBH | -2341332.823 | -3539049.499 | 4745791.397 | 0.010 | 0.012 | 0.012 | -0.018 | -0.001 | -0.010 | 0.003 | 0.003 | 0.003 N |
| 40400M003 | PASADENA | 7263 | -2493306.039 | -4655197.549 | 3565519.412 | 0.011 | 0.013 | 0.013 | -0.032 | 0.019 | 0.006 | 0.001 | 0.001 | 0.002 CN |
| 40400M006 | PASADENA | JPL1 | -2493304.054 | -4655215.583 | 3565497.349 | 0.008 | 0.009 | 0.009 | -0.032 | 0.019 | 0.006 | 0.001 | 0.001 | 0.002 CN |
| 40400M007 | PASADENA PEQ | JPIQ | -2493304.061 | -4655215.548 | 3565497.345 | 0.012 | 0.012 | 0.012 | -0.032 | 0.019 | 0.006 | 0.001 | 0.001 | 0.002 CN |
| 40405M013 | GOLDSTONE | 7288 | -2356494.088 | -4646607.650 | 3668426.621 | 0.008 | 0.009 | 0.009 | -0.014 | 0.007 | -0.008 | 0.001 | 0.001 | 0.001 CN |
| 40405s028 | GOLDSTONE | GOLD | -2353614.071 | -4641385.390 | 3676976.487 | 0.009 | 0.010 | 0.009 | -0.014 | 0.007 | -0.008 | 0.001 | 0.001 | 0.001 CN |
| 40405S031 | GOLDSTONE PEQ | GOLQ | -2353614.083 | -4641385.417 | 3676976.478 | 0.012 | 0.012 | 0.012 | -0.014 | 0.007 | -0.008 | 0.001 | 0.001 | 0.001 CN |
| 40405S009 | MOJAVE | 7222 | -2356170.966 | -4646755.85? | 3668470.592 | 0.006 | 0.007 | 0.007 | -0.014 | 0.007 | -0.008 | 0.001 | 0.001 | 0.001 CN |
| 40407M001 | PINYON FLATS | 7256 | -2369635.962 | -4761324.889 | 3511116.171 | 0.011 | 0.014 | 0.015 | -0.024 | 0.015 | 0.002 | 0.001 | 0.001 | 0.002 CN |
| 40407M002 | PINYON FLATS | PIN1 | -2369510.378 | -4761207.226 | 3511396.090 | 0.008 | 0.011 | 0.009 | -0.024 | 0.015 | 0.002 | 0.001 | 0.001 | 0.002 CN |
| 40407M003 | PINYON FLATS PEQ | PNIQ | -2369510.363 | -4761207.199 | 3511396.140 | 0.010 | 0.011 | 0.012 | -0.024 | 0.015 | 0.002 | 0.001 | 0.001 | 0.002 CN |
| 40408M001 | FAIRBANKS | FAIR | -2281621.322 | -1453595.773 | 5756961.966 | 0.006 | 0.007 | 0.007 | -0.024 | -0.005 | -0.008 | 0.001 | 0.001 | 0.002 CN |
| 40408s002 | FAIRBANKS | 7225 | -2281547.189 | -1453645.057 | 5756993.207 | 0.007 | 0.007 | 0.008 | -0.024 | -0.005 | -0.008 | 0.001 | 0.001 | 0.002 CN |
| 40420M006 | VANDENBERG | VAND | -2678089.798 | -4525437.027 | 3597431.510 | 0.026 | 0.026 | 0.026 | -0.030 | 0.029 | 0.018 | 0.001 | 0.002 | 0.002 CN |
| 40420M007 | VANDENBERG ?EQ | VANQ | -2678089.789 | -4525437.803 | 3597431.506 | 0.026 | 0.026 | 0.026 | -0.030 | 0.029 | 0.018 | 0.001 | 0.002 | 0.002 CN |
| 40424M004 | KAUAI | KOKB | -5543838.081 | -2054587.527 | 2387809.575 | 0.007 | 0.007 | 0.008 | -0.011 | 0.062 | 0.030 | 0.001 | 0.002 | 0.002 CN |
| 40424S001 | KAUAI | 1311 | -5543846.021 | -2054563.899 | 2387813.980 | 0.009 | 0.008 | 0.009 | -0.011 | 0.062 | 0.030 | 0.001 | 0.002 | 0.002 CN |
| 40433M004 | QUINCY | 7221 | -2517230.899 | -4198595.190 | 4076531.281 | 0.026 | 0.026 | 0.026 | -0.019 | 0.009 | -0.010 | 0.001 | 0.001 | 0.001 CN |
| 40440S003 | WESTFORD | 7209 | 1492206.700 | -4458130.500 | 4296015.503 | 0.006 | 0.006 | 0.007 | -0.015 | -0.002 | 0.000 | 0.001 | 0.001 | 0.001 CN |
| 40460M001 | SCRIPPS 1 | S101 | -2455521.657 | -4767213.456 | 3441654.913 | 0.014 | 0.013 | 0.015 | -0.014 | 0.000 | -0.011 | 0.003 | 0.003 | 0.003 N |
| 40460M002 | SCRIPPS 2 | s102 | -2455539.225 | -4767224.123 | 3441628.878 | 0.026 | 0.026 | 0.026 | -0.014 | 0.000 | -0.011 | 0.003 | 0.003 | 0.003 N |
| 40460M003 | SCRIPPS 2 PEQ | S02Q | -2455539.213 | -4767224.108 | 3441628.896 | 0.026 | 0.026 | 0.026 | -0.014 | 0.000 | -0.011 | 0.003 | 0.003 | 0.003 N |
| 40464M001 | CARP. HILL | CARR | -2620447.020 | -4460941.698 | 3718442.667 | 0.026 | 0.026 | 0.026 | -0.015 | -0.001 | -0.011 | 0.003 | 0.003 | 0.003 N |
| 40499S001 | RICHMOND | 7219 | 961258.126 | -5674090.035 | 2740533.758 | 0.006 | 0.006 | 0.008 | -0.009 | -0.001 | -0.003 | 0.001 | 0.001 | 0.002 CN |
| 41705M003 | SANTIAGO | SANT | 1769693.251 | -5044574.115 | -3468321.155 | 0.016 | 0.017 | 0.015 | 0.001 | -0.005 | 0.008 | 0.003 | 0.003 | 0.003 N |
| 41705s006 | SANTIAGO | 1404 | 1769693.020 | -5044504.505 | -3468435.082 | 0.016 | 0.017 | 0.015 | 0.001 | -0.005 | 0.008 | 0.003 | 0.003 | 0.003 N |
| 50103S007 | ORRORAL | 7843 | -4446476.914 | 2678127.018 | -3696251.445 | 0.013 | 0.013 | 0.013 | -0.037 | -0.003 | 0.046 | 0.004 | 0.003 | 0.003 CN |
| 50103S010 | CANBERRA | 1545 | -4460935.239 | 2682765.593 | -3674381.376 | 0.016 | 0.012 | 0.012 | -0.037 | -0.003 | 0.046 | 0.004 | 0.003 | 0.003 CN |
| 50103S017 | CANBERRA CURRENT | CANB | -4460996.083 | 2682557.150 | -3674443.957 | 0.016 | 0.012 | 0.012 | -0.037 | -0.003 | 0.046 | 0.004 | 0.003 | 0.003 CN |
| 50103s020 | CANBERRA 1 | DS40 | -4460987.939 | 2692362.746 | -3674626.615 | 0.031 | 0.031 | 0.031 | -0.037 | -0.003 | 0.046 | 0.004 | 0.003 | 0.003 CN |
| 50103s021 | CANBERRA 2 | DS41 | -4460979.465 | 2682381.151 | -3674624.212 | 0.031 | 0.031 | 0.031 | -0.037 | -0.003 | 0.046 | 0.004 | 0.003 | 0.003 CN |
| 50107M001 | YARRAGADEE | 7090 | -2389006.732 | 5043329.301 | -3078525.084 | 0.011 | 0.011 | 0.012 | -0.050 | 0.005 | 0.053 | 0.003 | 0.003 | 0.003 N |
| 50107MOO4 | YARRAGADEE | YAR1 | -2389025.339 | 5043315.833 | -3078530.933 | 0.011 | 0.010 | 0.010 | -0.050 | 0.005 | 0.053 | 0.003 | 0.003 | 0.003 N |
| 50116s002 | HOBART | 7242 | -3950236.543 | 2522347.521 | -4311562.687 | 0.047 | 0.055 | 0.039 | -0.046 | 0.012 | 0.035 | 0.005 | 0.004 | 0.005 CN |
| 50116s004 | HOBART | HOBA | -3950184.053 | 2522364.507 | -4311588.493 | 0.047 | 0.055 | 0.039 | -0.046 | 0.012 | 0.035 | 0.005 | 0.004 | 0.005 CN |
| 50126s004 | TOWNSVILLE | TOWN | -5041024.918 | 3296980.267 | -2090553.318 | 0.057 | 0.056 | 0.043 | -0.033 | -0.016 | 0.054 | 0.003 | 0.003 | 0.003 N |
| 50134M001 | DARWIN | DARW | -4091358.641 | 4684606.918 | -1408580.973 | 0.031 | 0.029 | 0.031 | -0.038 | -0.015 | 0.060 | 0.003 | 0.003 | 0.003 N |
| 50208s002 | WELLINGTON | WELL | -4780648.819 | 436507.116 | -4185440.401 | 0.054 | 0.069 | 0.031 | -0.025 | 0.003 | 0.029 | 0.003 | 0.003 | 0.003 N |
| 66001M001 | MC MURDO | MCMU | -1310695.242 | 310468.883 | -6213363.477 | 0.016 | 0.017 | 0.023 | 0.010 | -0.010 | -0.003 | 0.003 | 0.003 | 0.003 N |
| 92201M003 | PAMATAI | PAMA | -5245195.204 | -30S0472.425 | -1'212825.530 | 0.025 | 0.025 | 0.013 | -0.042 | 0.052 | 0.031 | 0.003 | 0.003 | 0.003 N |

* N : NNR-NUVEL1 velocity

CN : ITRF91 velocity field (combined solution from SLR and VLBI estimates)

DETERMINATION OF EARTH ROTATION PARAMETERS USING GPS: EXPERIMENTS USING TWO WEEKS OF DATA FROM THE 1992 IGS TEST CAMPAIGN

S. Fankhauser, G. Beutler, M. Rothacher¹

Two weeks of AS-free data of the 1992 IGS Test Campaign were processed using different strategies. The goal was to learn more about the determination of earth rotation parameters (ERPs) under different conditions and influences. The following questions were addressed:

- . What is the impact of the orbit arc length on the ERP determination? (We used 1-day, 2-days and 3-days arcs).
- What is the influence of different troposphere models on the ERP determination?
- . What is the impact of the ERP model itself on the ERPs.

INTRODUCTION

For our investigations we chose the time interval from 25-Aug-92 to 9-Sep-92, which seemed suitable since AS (Anti Spoofing) was not turned on. Typically data from more than 20 stations were processed for each day. The baselines were formed maximizing the number of observations.

Figure 2 shows the net for 27-Aug-92 (DOY 240). On every day we produced a 3-day solution that was shifted with respect to the previous day by one day (overlapping solution). The orbits and the ERPs of the middle day were always extracted and treated as our results (Figure 1).

Three consecutive one-day result files were then modeled by one three-days arc. The statistical information (RMS of fit for each satellite) was used as 'an indicator of the orbit consistency (Figure 1).

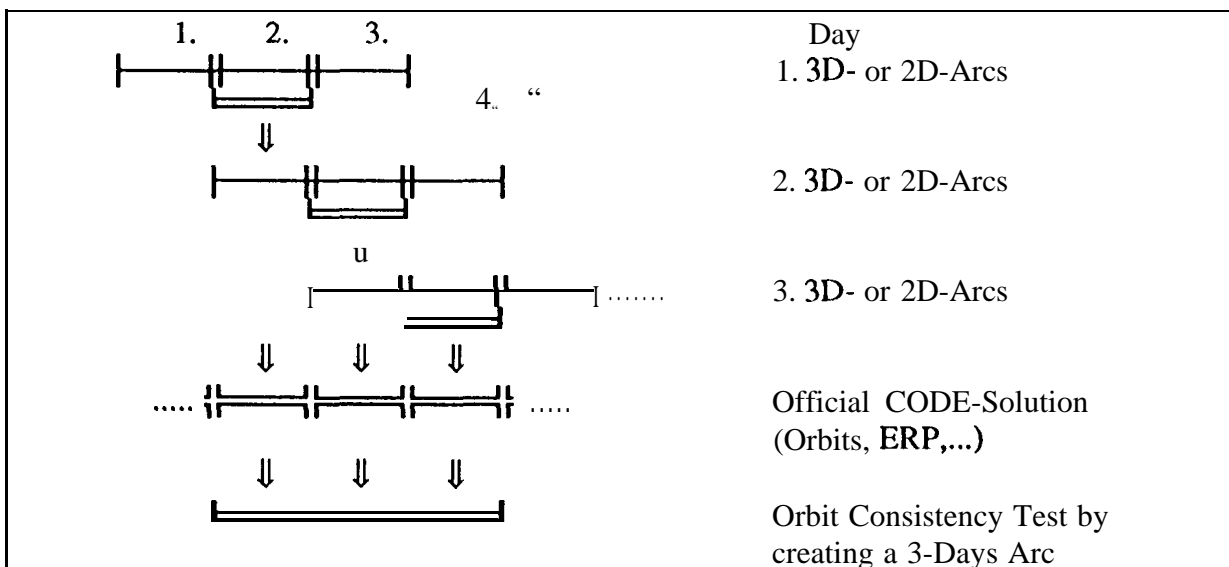


Figure 1

Overlapping 3 days arcs and orbit consistency test.

¹ Astronomical Institute University of Bern, Sidlerstrasse 5, 3012 Bern, Switzerland

BASELINES FOR 27-AUG-1992 (DOY 240)

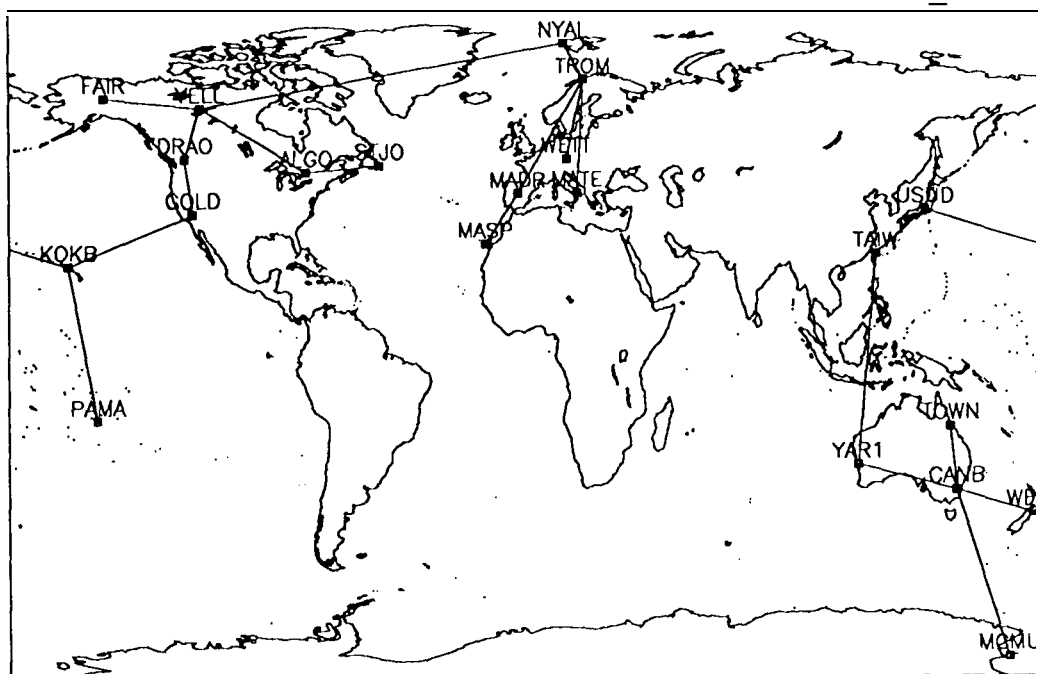


Figure 2
 Example for baselines formed (27-Aug- 1992).
 List of the station names:

| | | |
|-------------------|------------------|------------------|
| KOKB: Kokee Park | FAIR: Fairbanks | PAMA: Pama |
| YELL: Yellowknife | DRAO: Penticton | GOLD: Goldstone |
| ALGO: Algonquin | STJO: St, Jones | NYAL: Ny Alesund |
| TROM: Tromso | MADR: Madrid | MATE: Matera |
| WETT: Wettzell | MASP: Maspalomas | USUD: Usuda |
| TAIW: Taiwan | TOWN: Townswille | YAR1: Yaragadee |
| CANB: Canberra | WELL: Wellington | MCMU: Mac Murdo |

ERPs using 3-Days, 2-Days and 1-Day Arcs

The entire 2 weeks dataset was processed using 1 day, 2 days and 3 days of observations and the corresponding arc lengths for the orbits.

Parameters estimated:

- Troposphere: 4 parameters per station and day
- Station Coordinates: 10 ITRF stations fixed, additional stations estimated
- ERP: 1 set of parameter per day (X, Y, UT1-UTC)
- 3-days, 2-days solution: 8 orbit parameters per satellite (6 osculating elements, two radiation pressure parameters)
- 1-day solution: 7 orbit parameters (no y-bias estimated)

The main results may be summarized as follows:

The 1-day solution is much less consistent than the 2-days and the 3-days solutions. The quality difference of the 2-days and 3-days solutions is small.

The following Table shows the advantages and the disadvantages of the two multi-day solutions:

| 2-days solution | 3-days solution |
|------------------------------------------------|-----------------------------------------------------------------------------------------------------|
| smaller RMS error in X and Y-pole | smaller RMS error of the drift in UT1-UTC |
| same quality of X and Y-pole as 3-day solution | slightly smaller Drift in UT1 -UTC relative to the official IERS pole (derived from VLBI, C04-pole) |
| | better consistency of the orbits |

Note:

- It is not possible to solve for UT1 -UTC using only GPS observations. Therefore, in our 2-days and 3-days solutions we always held the UT1-UTC value of the first day fixed. In Figure 4 we summed up our estimates of the drift in UT 1 -UTC before subtracting the corresponding values of the IERS pole.

. Eclipsing satellites caused some problems (see Figure 5, marked by asterisk).

Figure 3 shows the X-component of the pole, Figure 4 UT1-UTC. The differences (CODE estimates - C04 pole) for X, Y, UT1 -UTC are given as a function of time. C04 is the IERS solution from bulletin B. Figure 5 shows the orbit consistency test.

ERP with 3D-, 2D-, 1 D-Arcs X-Component

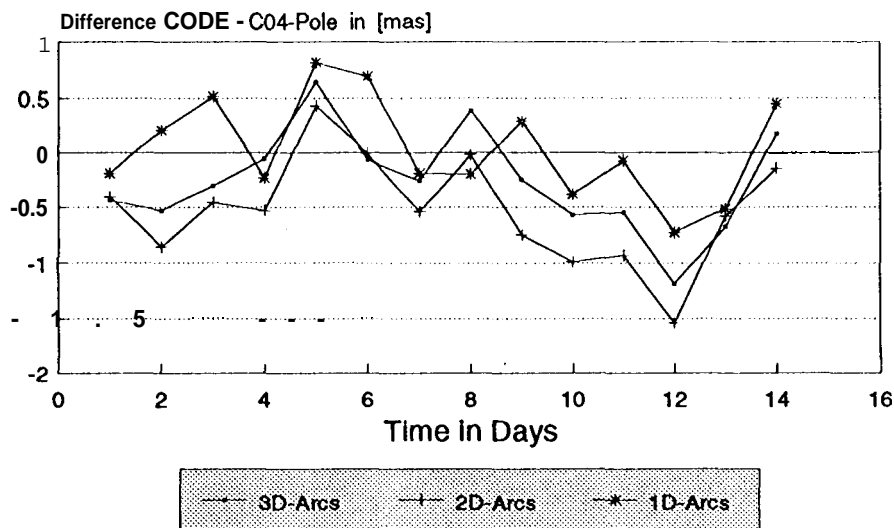


Figure 3

Differences of the ERP determination between 1-day, 2-days and 3-days solution.

ERP using 3D- and 2D-Arcs Drift in UT1 -UTC

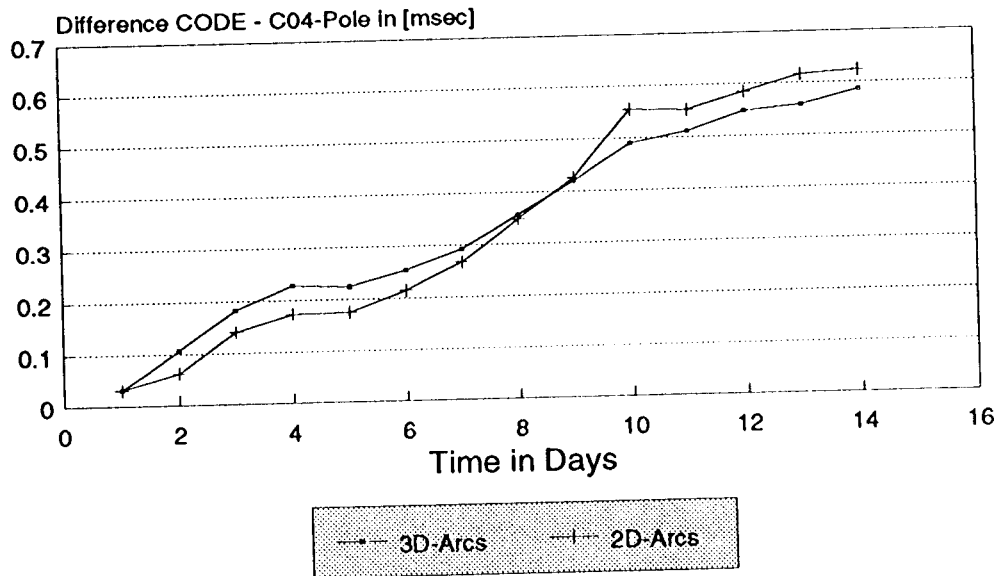
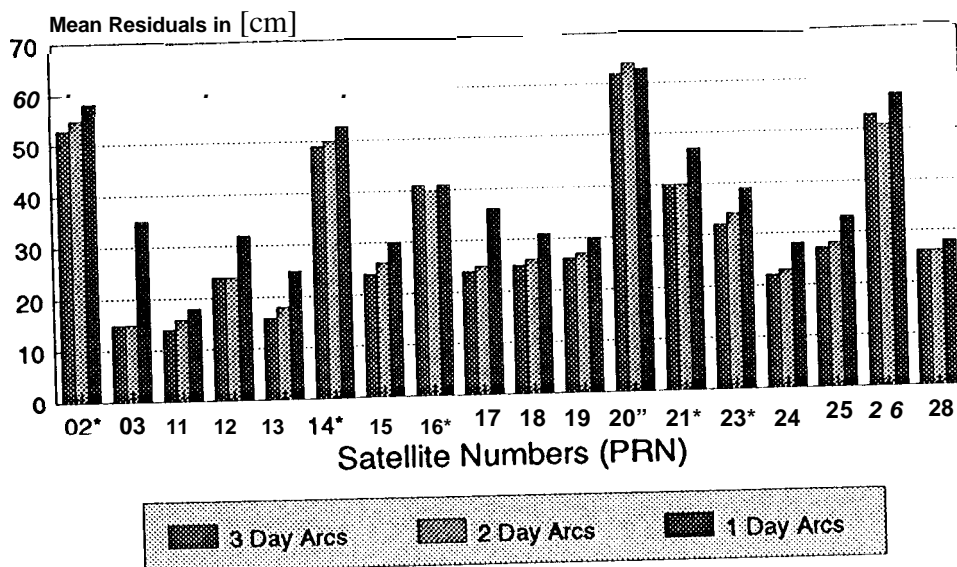


Figure 4

Difference of the determination of UT1 -UTC using 2-days and 3-days solutions.

Orbit Consistency 3D-, 2D- and 1 D-Arcs



*: Eclipsing Satellites

Figure 5

Test of the orbit consistency by modelling three one-day arcs by a three-days arc.

Influence of troposphere modelling on the ERP determination

Four solutions are discussed below. In each solution we estimated a different number of zenith delay parameters per day and station. A priori constraints of 0.04 m were used for each parameter. No constraints were applied between subsequent parameter sets.

In the first solution no troposphere parameters were estimated. In the second solution we estimated 2, in the third solution 4, and in the fourth solution 8 parameters per station and day.

Other estimated parameters:

- . Processing type: 3-days overlapping arcs
- Troposphere: 0, 2, 4 and 8 parameters per day and station
- . Station coordinates: 10 ITRF stations fixed, additional stations estimated
- ERP: 1 set of parameters per day

The results in Figures 6, 7, and 8 may be summarized as follows:

It is important that troposphere parameters were estimated. The precise number of parameters per day seems not to be critical as long as we do not consider constraints between subsequent parameters.

**Impact of Troposphere on ERP
Y-Component**

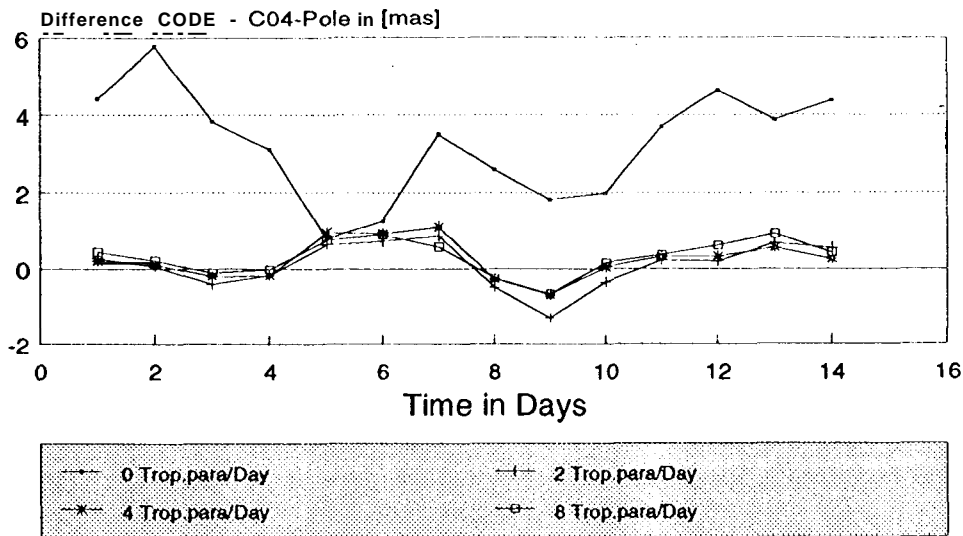


Figure 6
Difference of ERP determination using different troposphere models.
Y-component of pole used as example.

Impact of Troposphere on ERP RMS Error of Y-Component

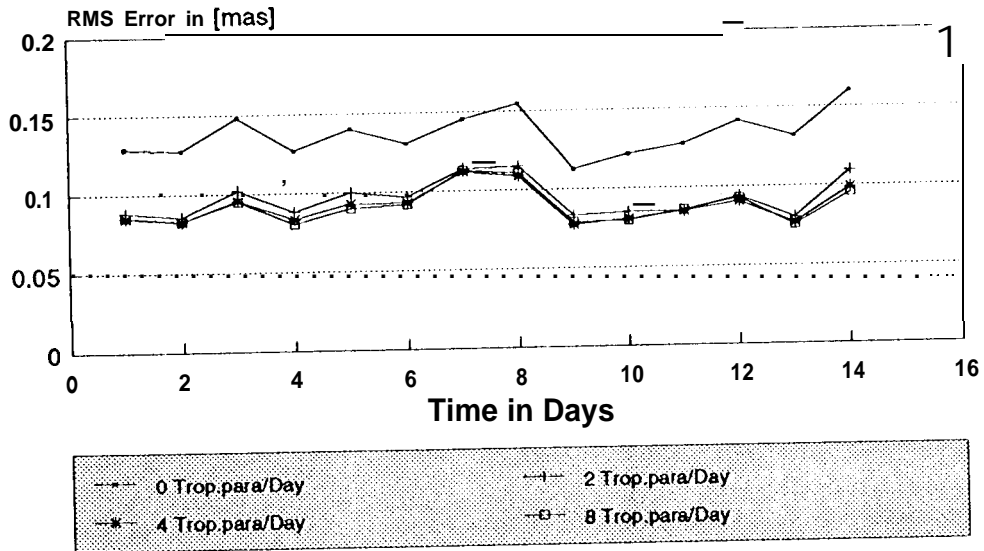


Figure 7

Influence of troposphere modelling on the determination of ERPs.
As example: RMS error of Y-component of pole, corresponding to Figure 6.

Orbit Consistency Troposphere

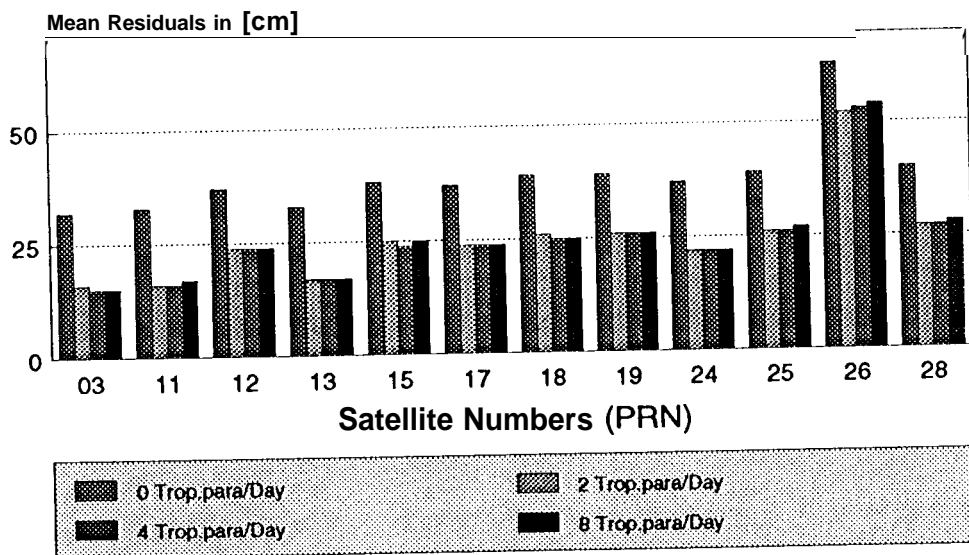


Figure 8

Test of orbit consistency by modelling three one-day arcs by one three-days arc.
(Eclipsing satellites were removed)

Impact of the ERP Model on the Determination of ERPs

The ERPs are assumed to be polynomials. When processing an arc of n days, we may divide the interval into m subintervals and solve for one set of polynomial coefficients in each subinterval. We even may ask for continuity at the interval boundaries (we did not use this option in this investigation).

We used the following three different models:

- . 1 set of ERPs per day
- . polynomial of degree 1 for 3 days
- . 12 sets of ERPs per day

Other solution characteristics:

- . Processing type: 3-days overlapping
- . Troposphere: 4 parameters per day and station
- . Station coordinates: 10 ITRF stations fixed, additional stations estimated
- ERP: as mentioned above

Figures 9 to 11 show the results:

Figure 9 shows the X-component of pole and Figure 10 the corresponding RMS error. Figure 11 shows the result of the orbit consistency test.

The results can be summarized as follows:

| ERP model | Advantages | Disadvantages |
|-----------------------------------|-----------------------------------------------------------------------------------------------------------------------------------------------------------------------------------|---------------------------------------------------------------------------------------------------------------------------------------------------------|
| 1 set of ERPs per day | <ul style="list-style-type: none"> • Use of only one day of observations. ◦ Relatively small RMS error • Smallest drift in UT1-UTC | <ul style="list-style-type: none"> • Drift of the a priori Pole file will be used (cannot be improved). |
| Polynomial of degree 1 for 3 days | <ul style="list-style-type: none"> • Relatively smooth pole coordinates as a function of time | <ul style="list-style-type: none"> • Short periodic terms will not be modelled sufficiently |
| 12 sets of ERPs per day | <ul style="list-style-type: none"> • High temporal resolution possible | <ul style="list-style-type: none"> • Reason for the daily period not yet clear. • RMS errors of some estimations are very high. |

Impact of ERP-Model X-Component

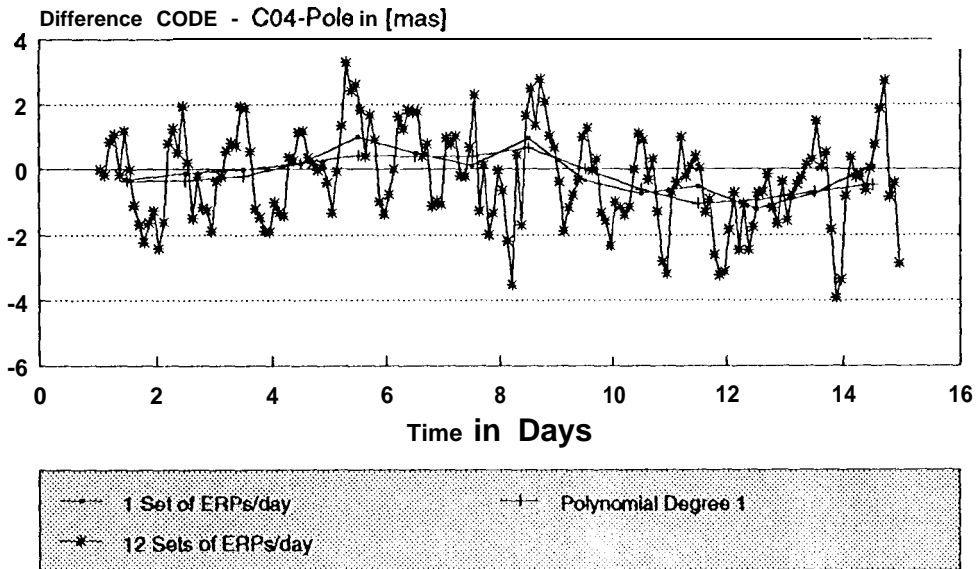


Figure 9
 Influence on ERP determination using different ERP models.
 X-component of **the** pole used as an example.

Impact of ERP-Model RMS Error of X-Component

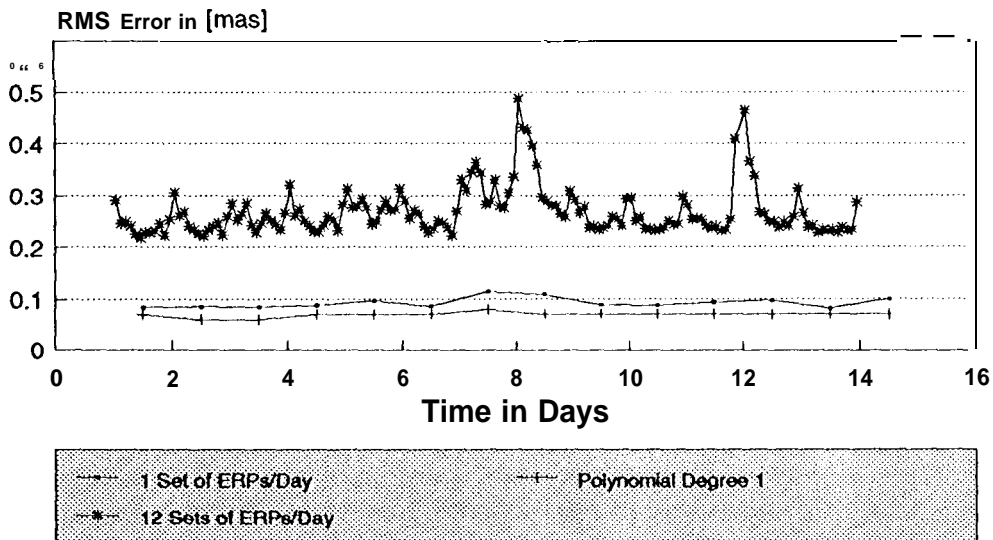


Figure 10
 Influence on ERP determination using different ERP models.
 RMS error of X-component of the pole used as an example.

Orbit Consistency ERP Model

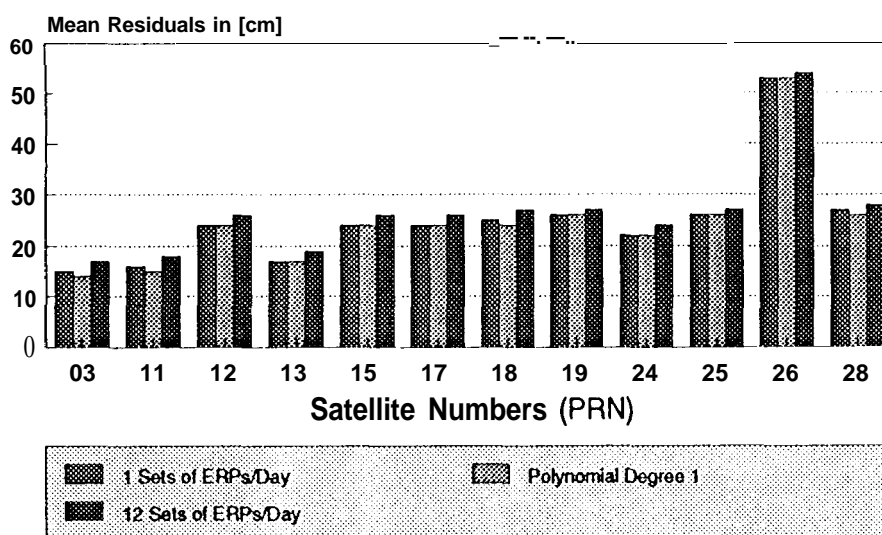


Figure 11
Orbit consistency when fitting three one-day arcs by one three-days arc.
(Eclipsing satellites removed)

conclusions:

Influences like the arc length of the orbits, the number of troposphere parameters, the model for the polar movement and the changes in the net of the reference stations play an important role in the determination of ERPs. Our results can be summarized as follows:

- The troposphere is one of the most important influences on the ERP determination. The differences between the solutions where troposphere parameters have been determined and the solution where the troposphere was not modelled may be of the order of 3 to 6 mas.
- The difference of the arc length causes differences in the ERP determination in the order of 0.5 mas to 1.5 mas. Major differences are found between the 1-day and the 2-days and the 1-day and 3-days solution. The differences between the 2-days and the 3-days solutions are marginal. A similar statement holds for the orbit consistency.
- Different ERP models can be used for different purposes. The polynomials give a relatively smooth pole as a function of time. The estimated RMS error of the model with one set of ERPs per day is small and the orbit consistency check is slightly better than the one for the polynomial of degree 1 for 3 days. Quite different results are produced by the model with 12 sets of ERPs per day. With this model we found a daily period with an amplitude of about 1.1 mas. We have doubts whether this phenomenon is real.
- This paper is a summary of the "Diplom Arbeit" of the first author. (Fankhauser, 1993)

References

- Beutler G. (1992). "The 1992 Activities of the International GPS Geodynamics Service (IGS)", Proceedings, Geodesy and Physics of the Earth, IAG-Symposium No. 112, October 1992.
- Fankhauser S., (1993), "Die Bestimmung von Erdrotationsparametern mit Hilfe von GPS-Beobachtungen, Mitteilungen der Satelliten Beobachtungsstation Zimmerwald Nr. 29, Druckerei der University Bern.
- International Earth Rotation Service (IERS) (1990). "Annual Report for 1989", July 1990, Observatoire de Paris.



**INTERNATIONAL EARTH ROTATION SERVICE (IERS)
SERVICE INTERNATIONAL DE LA ROTATION TERRESTRE**

BUREAU CENTRAL DE L'IERS
OBSERVATOIRE DE PARIS
61, Av. de l'Observatoire 75014 PARIS (France)
Tél. (33) 1-4051 2226 Téléx : 270776 OBS
Internet : icrs @iap.fr
Span : IAPOBS::IERS
FAX : (33) 1 -4051 2232

9 November 1992

IGS'92 CAMPAIGN
COMPARISONS OF GPS, SLR, AND VLBI
EARTH ORIENTATION DETERMINATIONS

(Final report)

Starting with IERS Bulletin B58, issued early December 1992 and covering October 1992, the GPS Earth Orientation Parameters will be introduced in the computation of the Central Bureau of IERS. Section 6 of Bulletin B will include statistics on the VLBI, LLR, GPS and SLR solutions received. The present Earth Orientation Bulletin is the last one issued in support to the IGS'92 campaign.

GPS: TERRESTRIAL FRAME ORIENTATION FIXING

Various strategies are tested by the GPS Processing Centres for maintaining the terrestrial frame orientation. The choices concern the nominal orientation (ITRF90 or ITRF91), the site motion model used to transfer the coordinates at the reference epoch, the number of fiducial stations that are fixed, and the source from which the fixed coordinates are taken. We summarize in Table 1 our understanding of the terrestrial frame definitions according to the Centres and to the time periods.

Table 1
GPS SOLUTIONS: TERRESTRIAL FRAME ORIENTATION

| Series (IERS label) | MJD from to | GPS weeks | Nominal refrnce | Source |
|------------------------|----------------|--------------|--------------------|------------------------|
| EOP (CODE) 92 P 04 | 48792-48923 | 650-668 | ITRF91 | IERS (IGSMail 33) |
| EOP (CSR) 92 P 01 | 48794-48870 | 650-660 | | CSR+GSFC (IGSMail 62) |
| EOP (EMR) 92 P 01 | 48838-48904 | 655-665 | ITRF91 | IERS (IGSMail 90) |
| EOP (EMR) 92 P 02 | 48901-48911 | 655-666 | ITRF91 | IERS (IGSMail 90) |
| EOP (ESOC) 92 P 01 | 48794-48912 | 650-666 | ITRF91 | IERS (IGSMail 90) |
| EOP (GFZ) 92 P 01 | 48794-48821 | 650-653 | ITRF90 | S10 (01/91-05/92) |
| EOP (GFZ) 92 P 02 | 48822-48918 | 654-667 | ITRF90 | S10 (IGSMail 56) |
| EOP (JPL) 92 P 01 | 48794-48821 | 650-653 | ITRF90 | JPL (GIG'91+VLBI vel.) |
| EOP (JPL) 92 P 02 | 48820-48918 | 654-667 | ITRF91 | IERS (IGSMail 90) |
| EOP (SIO) 92 P 03 | 48780-48918 | 648-66-1 | ITRF90 | S10 (51 IGS'92 days) |

VLBI, LLR, SLR, GPS EOP DETERMINATIONS: AGREEMENT WITH THE IERS SYSTEM

In this section, the VLBI, LLR, SLR, and GPS observations available over the time period of the IGS'92 Campaign and its continuation (MJD 48779-48923) are compared to the IERS series EOP(IERS) 90 C 04, which is a combination of the series of Table 2.

Table 2
IERS OPERATIONAL SERIES OF EOP

| Techn. | Series | Time span | Time interv. | EOP determined |
|--------|---------------------|--------------|-----------------|-----------------------|
| VLBI | EOP (NOAA) 92 R 01 | 24 h | 3/4 d | x, y, UT1, dPsi, dEps |
| VLBI | EOP (NOAA) 92 R 02 | 1 h | 1/2 d | UT1 |
| VLBI | EOP (USNO) 92 R 03 | 24 h | 7 d | x, y, UT1, dPsi, dEps |
| LLR | EOP (UTXMO) 92 M 02 | 1 h | 0.1/30d | UT1 |
| SLR | EOP (CSR) 91 L 01 | 72 h | 3 d | x, y, "UT1 " |
| SLR | EOP (DUT) 91 L 02 | 120 h | 5 d | x, y, "UT1 " |

The GPS series are those listed in Table 1. They give the x,y coordinates of the pole, except CODE, which gives a series of UT1 that is tied at the beginning of the complete series to an apriori value, and the new EMR series, which UT1 tied to an a priori value at the beginning of each week. The "UT1" determinations obtained by the SLR Analysis Centre at DUT is left free, whereas in the CSR SLR solution, it is tied to a VLBI solution for periods longer than about 60 days.

The GPS results are obtained from one-day observations of 16 to 18 satellites in a network of 11 to 29 stations: 14-19 for CODE, 14-20 for CSR, 17-18 for EMR, 11-18 for ESOC, 22-27 for JPL, and 17-29 for S10.

Most of the centres treat independently the successive daily arcs, the exceptions being CODE (three-day overlapping arcs) and GFZ (two-day overlapping arcs). The centres estimate the EOP at 12h UT.

Table 3 gives the differences of the VLBI, SLR, and GPS series with EOP(IERS) 90 C 04 under the form of a constant bias, corrected for the predicted value of the systematic difference. In the case of the GPS results, which are referred directly to ITRF, the predicted bias and its uncertainty are derived from Table I-3, p.II- 13 of the 1991 IERS Annual Report. It reflects the slight misalignment of the IERS EOP relative to the IERS terrestrial frame. In the case of the SLR and VLBI results, the expected values are derived from analyses of previous years results.

Table 3
SYSTEMATIC DIFFERENCES OF EOP RESULTS WITH IERS

| Techn | Series | x (0.001") | y (0.001") | UT1 (0.0001s) | Nines |
|-------|---------------------|--------------|--------------|-------------------|-------|
| VLBI | EOP (NOAA) 92 R 01 | -0.15 ± 0.08 | -0.03 ± 0.09 | 0.00 ± 0.06 | 39 |
| VLBI | EOP (NOAA) 92 R 02 | | | 0.11 ± 0.05 | 90 |
| VLBI | EOP (USNO) 92 R 03 | -0.43 ± 0.06 | -0.12 ± 0.08 | 0.03 ± 0.06 | 27 |
| LLR | EOP (UTXMO) 92 M 02 | | | -0.91 ± 0.29 | 17 |
| SLR | EOP (CSR) 91 L 01 | 0.09 ± 0.07 | 0.17 ± 0.05 | 0.10 ± 0.09 | 48 |
| SLR | EOP (DUT) 91 L 02 | 0.98 ± 0.18 | -0.84 ± 0.21 | | 29 |
| GPS | EOP (CODE) 92 P 04 | -0.31 ± 0.36 | -0.07 ± 0.45 | | 122 |
| GPS | EOP (CSR) 92 P 01 | -0.18 ± 0.37 | 2.46 ± 0.48 | | 69 |
| GPS | EOP (EMR) 92 P 01 | -0.44 ± 0.45 | 1.08 ± 0.46 | | 44 |
| GPS | EOP (EMR) 92 P 02 | 0.71 ± 0.39 | -0.22 ± 0.46 | | 8 |
| GPS | EOP (ESOC) 92 P 01 | 1.01 ± 0.38 | 0.01 ± 0.48 | | 112 |
| GPS | EOP (GFZ) 92 P 01 | -2.68 ± 0.43 | -3.29 ± 0.56 | | 27 |
| GPS | EOP (GFZ) 92 P 02 | +1.68 ± 0.36 | 1.92 ± 0.45 | | 68 |
| GPS | EOP (JPL) 92 P 01 | -0.19 ± 0.38 | 1.51 ± 0.50 | | 28 |
| GPS | EOP (JPL) 92 P 02 | 0.09 ± 0.35 | 0.14 ± 0.45 | | 79 |
| | | | | LOD : 0.16 ± 0.15 | 43 |
| GPS | EOP (S10) 92 P 03 | 0.35 ± 0.35 | 1.68 ± 0.44 | | 137 |

GPS: FORMAL AND ESTIMATED UNCERTAINTIES

The correlation of high frequency variations in the GPS polar motion results was estimated on the basis of the residuals of each series of daily values relative to its own smoothing (frequency cutoff 1 cycle/10 days). The common time intervals between two series cover 17 to 109 days. No significant correlation was found.

Using the days which are common to pairs of series without change of reference system, we estimate the true uncertainty of the daily EOP values by the Allan variance (or pair variance) based on the 15 series of differences two by two (see the 1991 IERS Annual Report, p.II-52). Table 4 shows the uncertainties thus estimated for every GPS series, together with the corresponding rms formal uncertainty provided by the Processing Centre.

Table 4
ESTIMATED AND FORMAL UNCERTAINTY OF DAILY GPS
POLAR MOTION VALUES

| Techn | Series | x (0.001") | | y (0.001") | | Nmes |
|-------|--------------------|-------------|-------------|-------------|-------------|-----------|
| | | est. im. | formal | estim. | formal | |
| GPS | EOP (CODE) 92 P 04 | 0.50 | 0.13 | 0.58 | 0.13 | 66 |
| GPS | EOP (CSR) 92 P 01 | 0.59 | 0.20 | 0.69 | 0.20 | 75 |
| GPS | EOP (EMR) 92 P 01 | 0.69 | 0.55 | 0.49 | 0.37 | 66 |
| GPS | EOP (EMR) 92 P 02 | 0.48 | 0.23 | 0.39 | 0.20 | 8 |
| GPS | EOP (ESOC) 92 P 01 | 1.02 | 0.39 | 1.14 | 0.42 | 82 |
| GPS | EOP (GFZ) 92 P 01 | 1.11 | 0.86 | 1.11 | 0.89 | 26 |
| GPS | EOP (GFZ) 92 P 02 | 0.75 | 0.47 | 0.40 | 0.52 | 66 |
| GPS | EOP (JPL) 92 P 01 | 0.37 | 0.25 | 0.47 | 0.30 | 26 |
| GPS | EOP (JPL) 92 P 02 | 0.10 | 0.21 | 0.42 | 0.23 | 66 |
| GPS | EOP (SIO) 92 P 03 | 0.38 | 0.33 | 0.22 | 0.30 | 82 |

VLBI, LLR, SLR, GPS EOP DETERMINATIONS: DAY-TO-DAY AGREEMENT WITH IERS

The series of EOP obtained by VLBI, LLR, SLR and GPS already considered in Table 3 are considered now under the form of the weighted rms residual to EOP(IERS) 90 C 04, after the biases of Table 2 are taken out. The statistics are listed in Table 5.

Table 5
WEIGHTED RMS DIFFERENCES OF EOP RESULTS WITH EOP(IERS) 90 C 04
The biases of Table 3 are taken out.

| Techn Nmes | Series | x (0.001") | y(0.001") | UT1 (0.0001s) | |
|---------------|----------------------------|-------------|-------------|-------------------|------------|
| VLBI | EOP (NOAA) 92 R 01 | 0.47 | 0.58 | 0.36 | 39 |
| VLBI | EOP (NOAA) 92 R 02 | | | 0.48 | 90 |
| VLBI | EOP (USNO) 92 R 03 | 0.30 | 0.42 | 0.29 | 27 |
| LLR | EOP (UTXMO) 92 M 02 | | | 1.18 | 17 |
| SLR | EOP (CSR) 91 L 01 | 0.47 | 0.37 | 0.62 (1) | 48 |
| S LR | EOP (DUT) 91 L 02 | 0.90 | 1.08 | 3.41 (2) | 29 |
| GPS | EOP (CODE) 92 P 04 | 0.83 | 0.89 | 0.89 (3) | 132 |
| GPS | EOP (CSR) 92 P 01 | 0.90 | 1.57 | 2.73 | 69 |
| GPS | EOP (EMR) 92 P 01 | 1.45 | 0.80 | | 44 |
| GPS | EOP (EMR) 92 P 02 | 0.49 | 0.39 | | 8 |
| GPS | EOP (ESOC) 92 P 01 | 1.29 | 1.73 | | 112 |
| GPS | EOP (GFZ) 92 P 01 | 1.35 | 1.83 | | 27 |
| GPS | EOP (GFZ) 92 P 01 | 1.04 | 0.72 | | 76 |
| GPS | EOP (JPL) 92 P 01 | 0.72 | 1.31 | | 28 |
| GPS | EOP (JPL) 92. P 02 | 0.42 | 0.48 | | 78 |
| | | | | LOD : 0.99 | 43 |
| GPS | EOP (SIO) 92 P 03 | 0.67 | 0.62 | | 137 |

Notes: 1 - CSR - Referred to VLBI in the long term (p > 60 d).
2- DUT - With a drift of +0.027 ms/d and a quadratic term taken out.
3-CODE - With a drift of +0.045 ms/d, a quadratic term and a 92d
periodic term taken out.

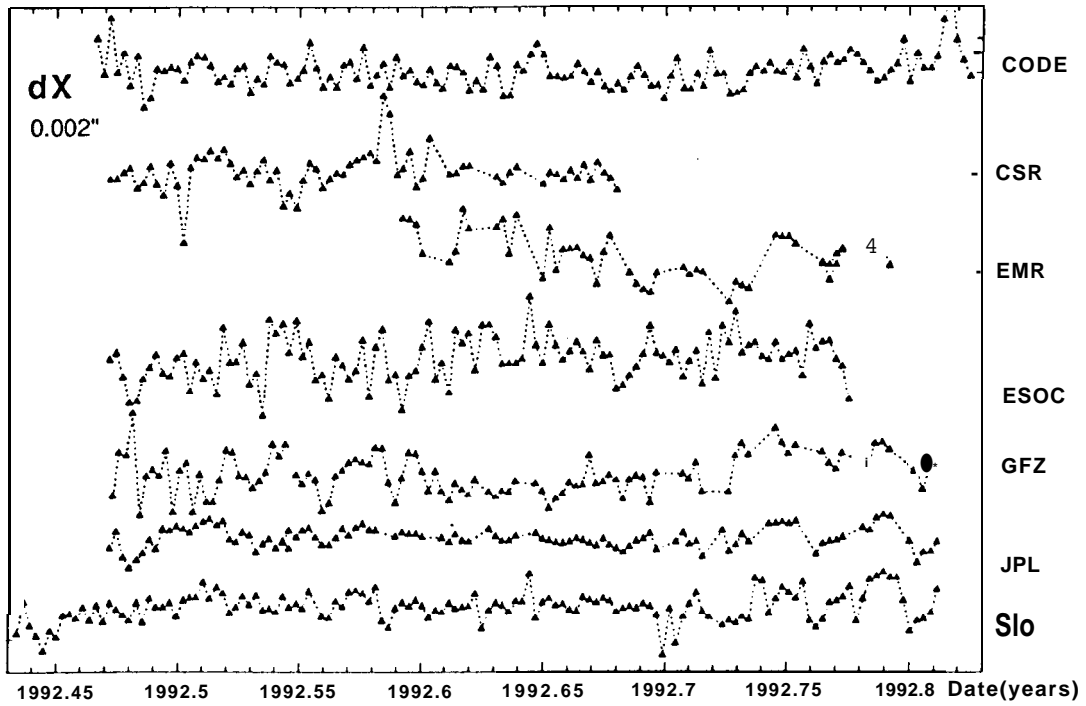


Fig. 1 Differences of the GPS series of the x coordinate of the pole with EOP(IERS)90 C 04

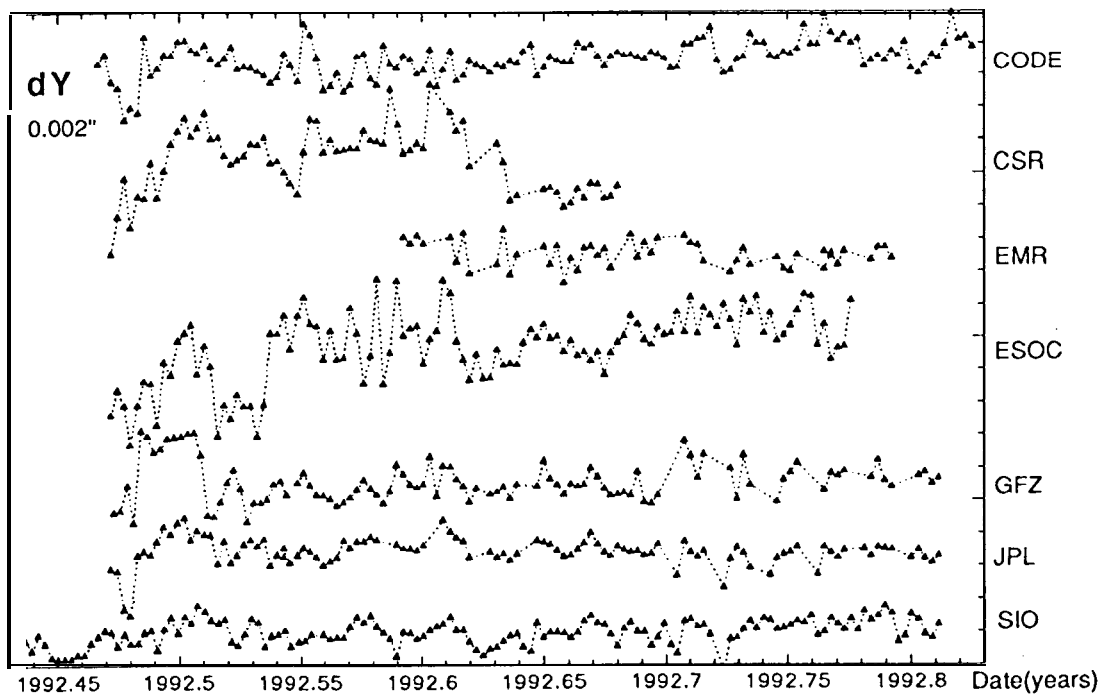


Fig. 2 Differences of the GPS series of the y coordinate of the pole with EOP(IERS)90 C 04

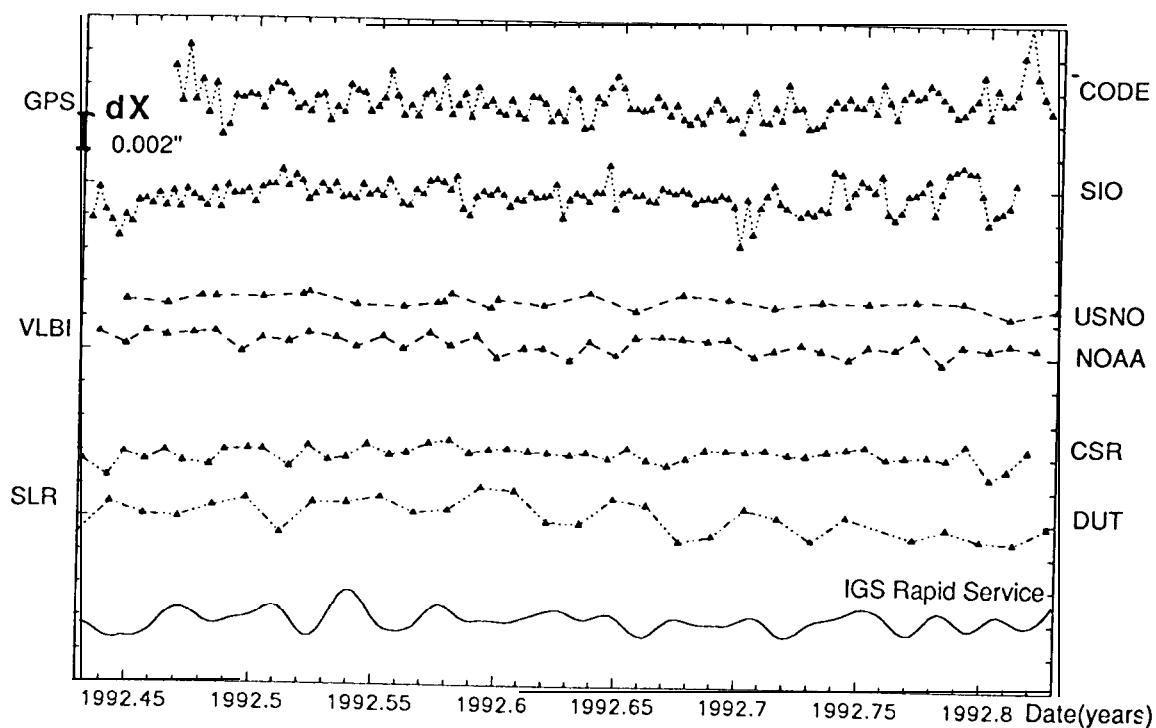


Fig. 3 Differences of GPS, SLR, VLBI, and Rapid Service series of the x coordinate of the pole with EOP(IERS) 90 C 04

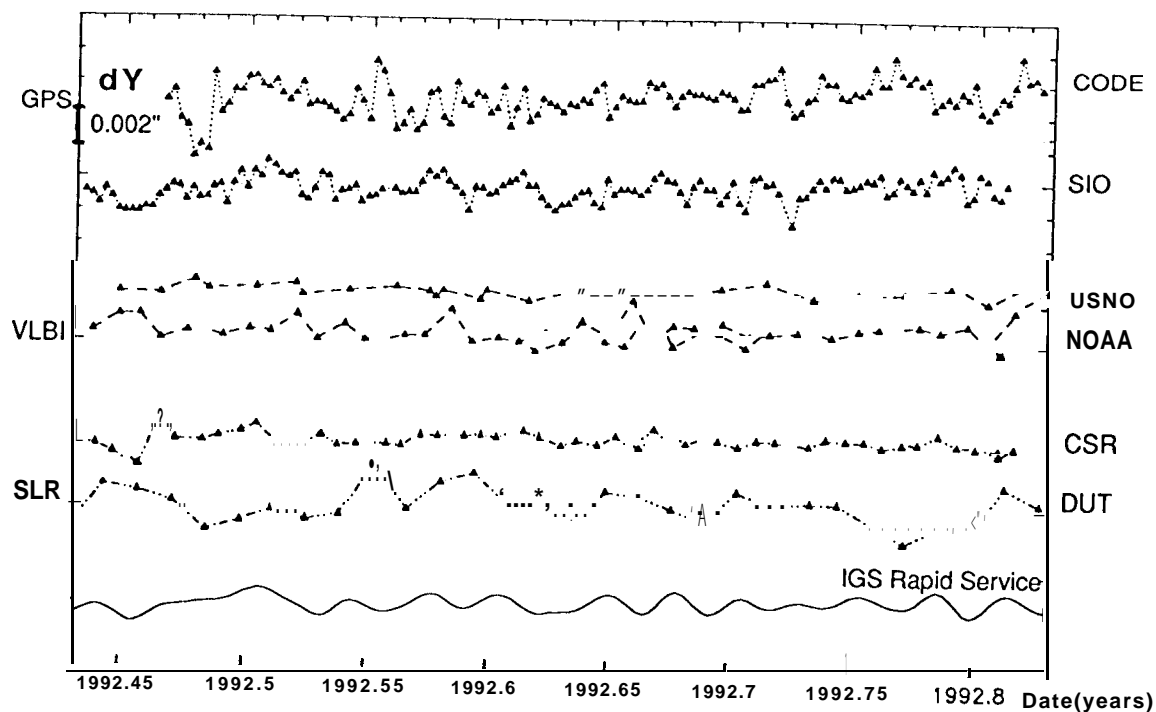


Fig. 4 Differences of GPS, SLR, VLBI, and Rapid Service series of the y coordinate of the pole with EOP(IERS) 90 C 04

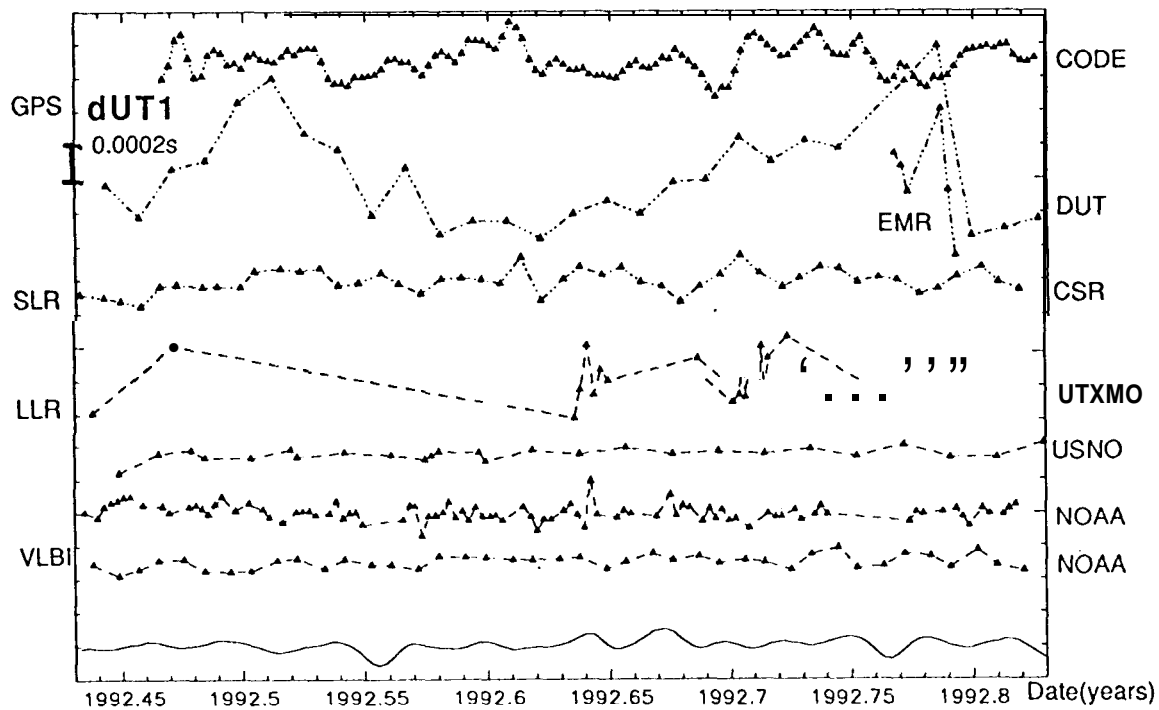


Fig. 5 Differences of GPS, SLR, VLBI, and Rapid Service series of Universal time with EOP(IERS) 90 C 04

- Notes :
- 1- CSR - Referred to VLBI in the long term ($p > 60$ d).
 - 2- DUT - With a drift of +0.027 ins/d and a quadratic term taken out.
 - 3- CODE - With a drift of +0.045 ms/d, a quadratic term and a 92d periodic term taken out.

SUB-DAILY EARTH ROTATION DURING EPOCH '92

A. P. Freedman*, R. Ibanez-Meier*, J. O. Dickey*, S. M. Lichten*, T. A. Herring†

Earth rotation data were obtained with GPS during the Epoch '92 campaign in the summer of 1992. About 10 days of data were acquired from 25 globally distributed stations and a constellation of 17 GPS satellites. These data were processed to estimate UT1 corrections every 30-minutes, then smoothed to form a UT1 series with 3-hour spacing. Earth orientation data during Epoch '92 were also obtained by several VLBI groups, and were processed together to yield VLBI estimates of UT1 with 3-hour time resolution. The high frequency behavior of both data sets is similar, although drifts between the two series of -0.1 ms over 2-5 days are evident. Tidally induced UT1 both from theoretical ocean models and empirically determined were compared with the GPS and VLBI series. Estimates of atmospheric angular momentum (AAM) at 6-hour intervals generated by several meteorological centers were also compared with the geodetic data. These comparisons indicate that most of the GPS signal in the diurnal and semidiurnal bands can be attributed to tidal processes? and that UT1 variations over a few days are mostly atmospheric in origin.

INTRODUCTION

Variations in the rate of rotation of the solid Earth result both from torques applied to the Earth from the exterior or interior and from mass redistribution within the Earth. For high-frequency Earth rotation variations, defined here as rotation rate changes occurring over time scales of a week or less, the principal forces on the solid Earth are thought to come from the atmosphere and oceans. In particular, tidal forcing of the oceans is expected to dominate the rotational variations at periods of one day and less.

A variety of techniques have historically been used to monitor the rotation of the Earth, but only over the past few years has the capability for daily and even sub-daily monitoring of Earth rotation with the requisite precision become available. Current high-precision techniques include very long baseline interferometry (VLBI), satellite laser ranging (SLR), lunar laser ranging (LLR), and, most recently, the Global Positioning System (GPS). VLBI estimates of Earth's rotation angle (UT1-UTC) at daily intervals and SLR estimates at roughly 3-day intervals have been made for several years. Over the past three years, measurements of UT1 variations with hourly or so time resolution have been made sporadically by both VLBI and GPS techniques [1, 2].

In association with the International GPS Geodynamics Service's (IGS) proof of concept campaign for the summer of 1992, an additional campaign known as SEARCH '92

* Tracking Systems and Applications Section, Jet Propulsion Laboratory, California Institute of Technology, Pasadena, California 91109

† Department of Earth, Atmospheric, and Planetary Sciences, Massachusetts Institute of Technology, Cambridge, Massachusetts 02139

(Study of Earth-Atmosphere Rapid Changes) was held to monitor high-frequency Earth orientation variations utilizing all space geodetic techniques and to advocate for and facilitate the collection of the best available related geophysical data [3]. Data from a variety of complementary techniques providing a good level of redundancy were acquired, in particular, during the intensive two-week period known as Epoch '92. In this paper, we present GPS estimates of sub-daily variations in UT1 during Epoch '92 and compare these results with a number of these other related data sets. This intercomparison should provide a robust estimate of Earth's true rotational variations at time scales as short as a few hours, and should help as well to improve strategies for processing GPS data.

DATA SETS

GPS

The GPS data processing strategy is a version of that discussed elsewhere using the JPL GIPSY/OASIS II software [4, 5] and is summarized in Table 1. Data from a network of 25 stations using a GPS constellation of 17 satellites were acquired over more than 10 days during the last week of July and first week of August, 1992. Due to the use of anti-spoofing (AS) signal encryption over the weekend, these data are not continuous but are divided into two groups from which two multi-day GPS orbit arcs were created. Corrections to a nominal UTPM series (derived from the IERS Bulletin B) were obtained from the data, with UT1 estimated every 30 minutes and polar motion every two hours. UT1 was modeled as a Gauss-Markov (AR 1) process with a steady-state sigma of 0.06 ms and a time constant of 4 hours. Thus, over 30 minutes, 0.028 ms of process noise was added.

Table 1
GPS ESTIMATION STRATEGY

| | |
|--------------------------------------------------------------------|--------------------------------------|
| Estimated parameters | |
| Station locations | Wet zenith troposphere (random walk) |
| Satellite states | Clock biases (white-noise) |
| Solar radiation pressure | Carrier phase biases |
| UT1 (AR1) | Polar motion (white noise) |
| Eight fiducial sites | |
| Standard models | |
| Solid Earth tides and equilibrium ocean tides from Yoder et al.[7] | |
| Gravity field coefficients: GEMT3, 8x8 truncation | |
| Nutation model: 1980 IAU model | |
| A priori and fiducial site locations ITRF 91 | |
| Nominal UTPM from IERS Bulletin B | |
| Rogue receivers | |
| Pseudo range (1-meter) and Carrier Phase (1 cm) | |
| 6-minute data interval (obtained by decimation) | |

We generated UT1 time series using a variety of orbit modeling strategies [6]. Our preferred strategy employed multi-day orbit arcs wherein one set of satellite states (positions and velocities) was estimated for each satellite. Three stochastic solar radiation parameters for each satellite were modeled as AR1 processes and estimated every hour. Alternative estimation strategies yield UT1 series that differ, but the results and conclusions described below do not significantly change if these other UT1 series are used.

For comparison with the VLBI data, we constructed a smoothed GPS UT1 data set. This time series uses the 30-minute solution and applies a Gaussian filter with a half-width of about one-half hour to smooth and interpolate the data to the epochs of the VLBI data. It

contains GPS-derived UT1 measurements every 3 hours. Note that this data set will not be identical to a 3-hour GPS solution, since the latter solution would contain UT1 values averaged over a 3-hour window, whereas the solution used below is effectively smoothed over a 1- to 2-hour window.

VLBI

VLBI data were acquired from the three networks described in Table 2. Note that on certain days, UT1 was measured by more than one VLBI network, providing an estimate of the quality of the VLBI data. The correlated VLBI data were combined using the MIT Kalman filter programs CALC/SOLVK. UT], polar motion, nutation corrections, and station troposphere parameters were estimated over 24 hour time spans, with UT 1, polar motion, and the troposphere parameters modeled as random walks.

Several solutions were generated in which UT1 was estimated either every 30 minutes or every 3 hours [6]. The 30-minute solutions are rather noisy, so the 3-hour solutions were used in this study. For this data set, UT1 was estimated every 3 hours with 0.04 ms sigma resets after a diurnal and semidiurnal a priori tide model had been applied. A final smoothed VLBI solution was generated in which the 24-hour data sets from all the networks were combined using a mild Gaussian filter. Since data from different networks for the same day sometimes differ significantly, and there are no VLBI data sets from any one network continuous over more than three days, the smoothed 3-hour VLBI UT1 solution will be used in the following comparisons.

**Table 2
VLBI DATA**

| |
|---------------------------------------------------------------------------------------------------|
| NASA's Goddard Space Flight Center (GSFC) - NASA R&D |
| 8 experiments |
| 5-6 sites in N. America, Hawaii, and Europe |
| National Oceanic and Atmospheric Administration's (NOAA) Laboratory for Geosciences – IRIS |
| 4 experiments (one mobile, three IRISA) |
| 5 sites in N. America and Europe |
| United States Naval Observatory (USNO) - NAVNET |
| 6 experiments |
| 4-6 sites, located around globe |
| Data from July 26 through August 11 |
| Four days have double sets of measurements from NAVNET and NASA R&D |
| NOTE: Each experiment can have significantly different formal errors |

Tide models

A variety of additional data sets were used in evaluating the GPS and VLBI time series. Two models for tidally-induced diurnal and semidiurnal UT1 variations were compared, one based on theoretical ocean models [8] and one determined from many years of measured UT variations [9]. The theoretical series, referred to as the Gross tide model, is based on the oceanic angular momentum model of Seiler [10]. This formulation also contains corrections to the standard tide model [7] for non-equilibrium ocean tides at fortnightly and monthly periods. The empirical model, referred to as the Herring tide model, is based on 8 years of VLBI data. It contains estimates of the diurnal and semidiurnal tidal terms only. Note that this empirical tide series may contain additional diurnal signals other than those due to the non-equilibrium ocean tides, such as the effects of atmospheric tides. Both tidal UT1 series may be compared directly to geodetic UT1 estimates.

AAM 6-hourly data

If angular momentum were exchanged solely between the atmosphere and the solid Earth, atmospheric angular momentum (AAM) variations would result in corresponding changes in the length of the day (LOD), the time derivative of UT1. Several sets of AAM were computed every 6 hours as part of the SEARCH/IGS effort by three meteorological centers: the U. S. National Meteorological Center (NMC), the **European** Center for Medium-Range Weather Forecasts (ECMWF), and the Japanese Meteorological Agency (JMA). For each center, the AAM quantity that we use consists of the χ_3 AAM wind term integrated to the top of the model atmosphere (either 51 mbar or 10 mbar, depending on center) plus the full pressure (not inverted-barometer) term. Gaps in the AAM series were filled by linear interpolation.

We used these data sets to estimate atmospherically induced variations in UT1. Since AAM is a substitute LOD, the AAM series must be integrated to be compared to a UT1 series. However, two arbitrary constants, a bias in LOD and a bias in UT1, enter into this integration. For the comparisons shown below, linear models are removed from the AAM and geodetic UT1 series to account for these constants.

Smoothed Reference Series

A reference series, based on the IERS Bulletin B nominal values used for the GPS analysis, was used to remove long-period UT1 variations. Note that all the geodetic series shown have the shorter-period (<35 day) tides explicitly removed according to the standard Yoder et al. [7] model, while subtracting the nominal UT1R series from VLBI, for example, effectively removes the longer period terms of [7].

RESULTS

GPS vs. VLBI

We have compared the GPS-derived UT1 with VLBI estimates of UT1 -TA1 for each network-day of data. UT1 was estimated every 30 minutes in both sets of data. Typical formal errors of the various time series are summarized in Table 3. For reasons mentioned above, and due to space limitations, we will present here only results for the smoothed and interpolated sets of VLBI and GPS data. These two data sets are shown in Figure 1. For display purposes, the UT1 values have been differenced with a nominal smoothed UT1 time series derived from the IERS Bulletin B. The offset between GPS and VLBI is due to slightly different terrestrial reference frames in the two solutions. Note the gap in GPS data due to the presence of AS during the weekend of August 1-2 which precludes the construction of a continuous two-week long GPS time series. The 6-day time span at **the end of July** where data exist from both techniques is referred to below as period A, while the 4.5-day time span in August is referred to as period B.

Although there appears to be a drift between the two series over several days, their diurnal variability is similar. If the two series are difference, linear trends can be fit separately to periods A and B to quantify both the drift and residual scatter in GPS minus VLBI. These values are given in Table 3. Over 4 to 6 day time spans, the GPS shows a fairly linear drift with respect to VLBI, with drift rates of ± 20 -40 $\mu\text{sec/day}$. After removing these drifts, the total RMS scatter of GPS minus VLBI UT1 is 0.023 tns.

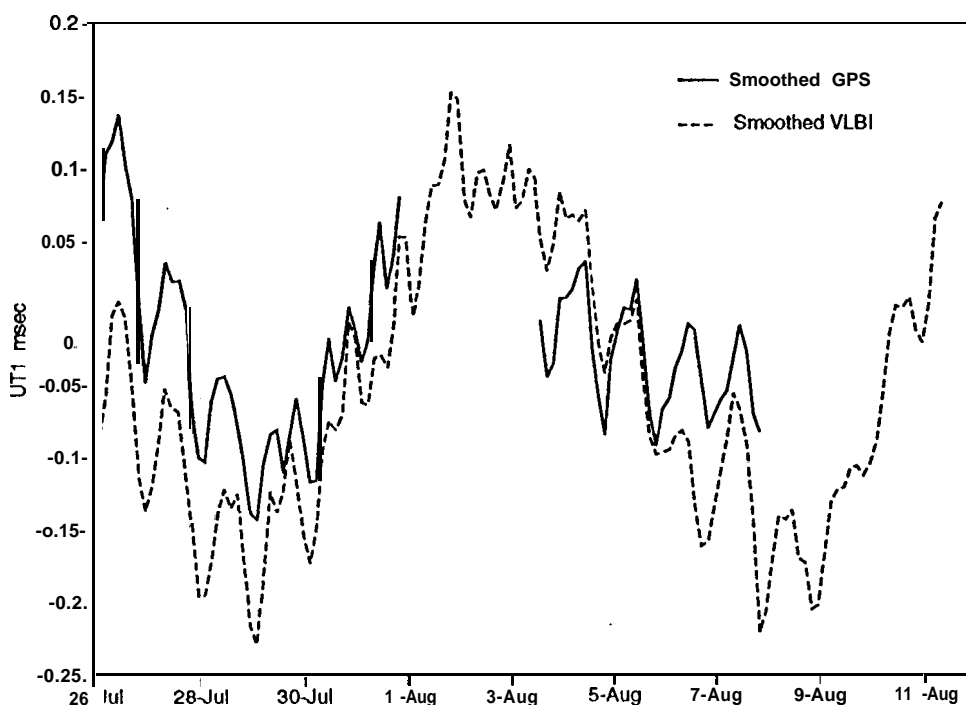


Fig. 1 UT1 from GPS and VLBI evaluated every 3 hours.

The relationship between GPS and VLBI may be further explored by computing power spectra of the GPS and VLBI UT1 and their difference (Fig. 2). Power spectra were obtained separately for the two periods A and B and averaged together. A 3-point spectral smoothing was used (corresponding to a bin width of 0.375 cycles per day). Both the VLBI and GPS series show similar power in the diurnal and semidiurnal bands. Differencing the two removes the peaks in power at both frequencies, suggesting that there is a true geodetic signal in these bands that is accurately sensed by both techniques. This signal is for the most part tidal in origin, as shown below. The drift between GPS and VLBI is probably a result of drift in the GPS time series due to systematic effects such as orbit mismodeling.

Table 3
STATISTICS

| Typical 30-Minute UT1 Formal Errors | | | |
|-------------------------------------|---------------------|--------------------------|-------------------------|
| GPS | IRIS VLBI | NAVNET | NASA R&D |
| 0.02-0.03 ms | 0.02-0.04 ms | 0.015-0.04 ms | 0.01-0.025 ms |
| GPS Minus VLBI | | | |
| | Period A | Period B | Entire time span |
| Slope | -0.018 ms/day | 0.041 ins/day | -- |
| RMS scatter | 0.022 ms | 0.026 ms | 0.023 ms |
| GPS Minus AAM | | | |
| | GPS UT1 only | GPS minus Herring | GPS minus Gross |
| RMS Scatter | 0.032 ms | 0.018 ms | 0.035 ms |
| GPS Minus AAM+Tides | | | |
| | NMC | ECMWF | JMA |
| RMS of difference | 0.021 ms | 0.022 ms | 0.019 ms |
| GPS | 0.027 ms | 0.022 ms | 0.022 ms |
| VLBI | | | |

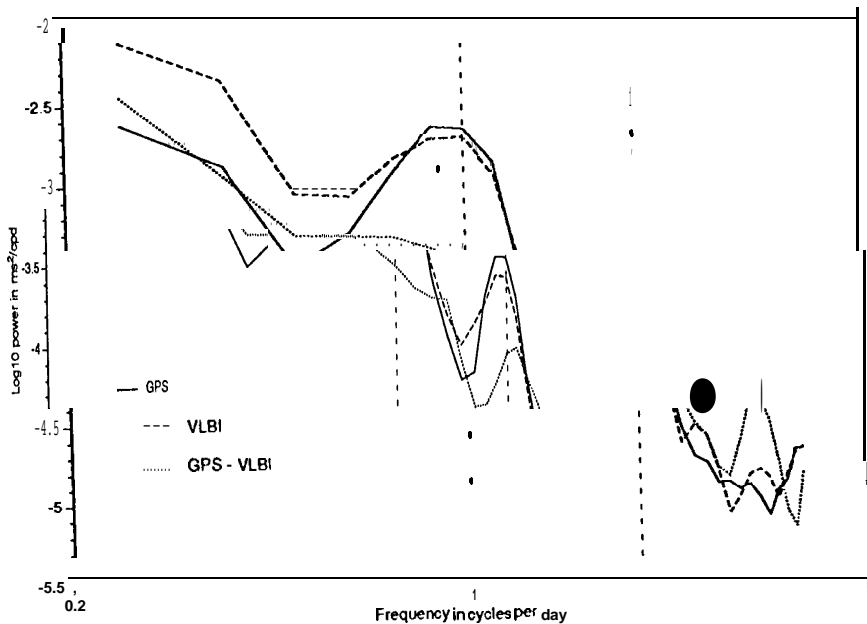
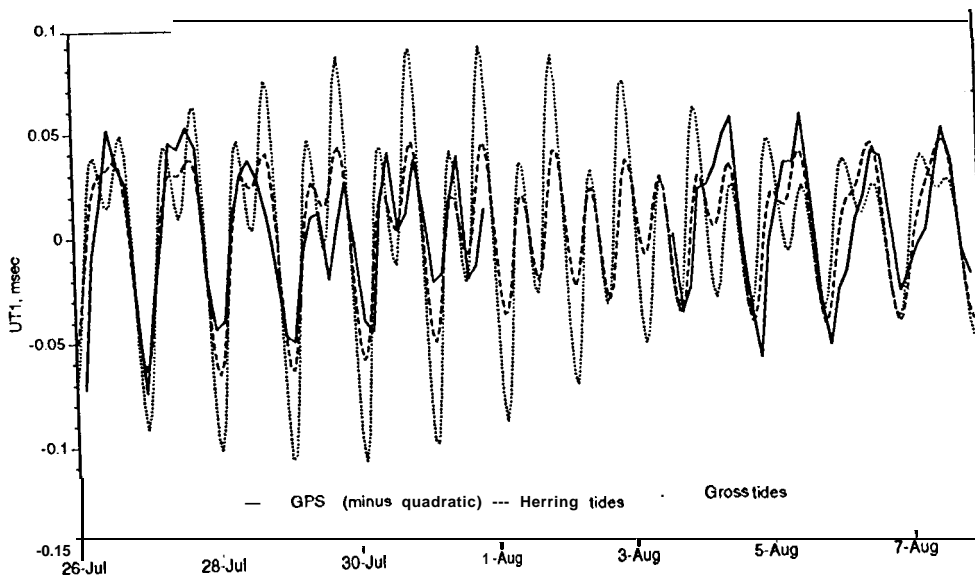


Fig. 2 Comparative power spectra of the GPS and VLBI UT1 series and their difference.

GPS vs. Tides

In Figure 3, we compare the smoothed GPS UT1 to the two models of tidally-induced UT1 variations. The GPS series for each period (A and B) has had a best-fitting quadratic subtracted to remove longer-period fluctuations, thus making the residual series easy to compare with the tides. Note that the Herring, empirical model more accurately reflects the observed UT 1 variability than does the Gross, theoretical model.



“Fig. 3 GPS UT1 compared to two models of tidally induced UT1 variations.

These differences can again be described through the use of power spectra. Power spectra (computed as before) of the GPS UT1 series and the GPS series minus the two tide models are shown in Fig. 4. The Herring model removes most of the excess power in the diurnal and semidiurnal bands, with a hint of signal remaining at 2 cycles per day (cpd). The Gross model removes some power at diurnal frequencies, but adds substantial power at semidiurnal frequencies (consistent with the large amplitudes seen in Fig. 3). These differences are quantified in Table 3, which shows the RMS scatter of the three time series whose power spectra are plotted in Fig. 4. The Herring model appears to more accurately reflect the actual UT1 variations at diurnal and semidiurnal frequencies. Reasons for this may include inaccuracies in the theoretical ocean models and additional non-oceanic signal at these frequencies.

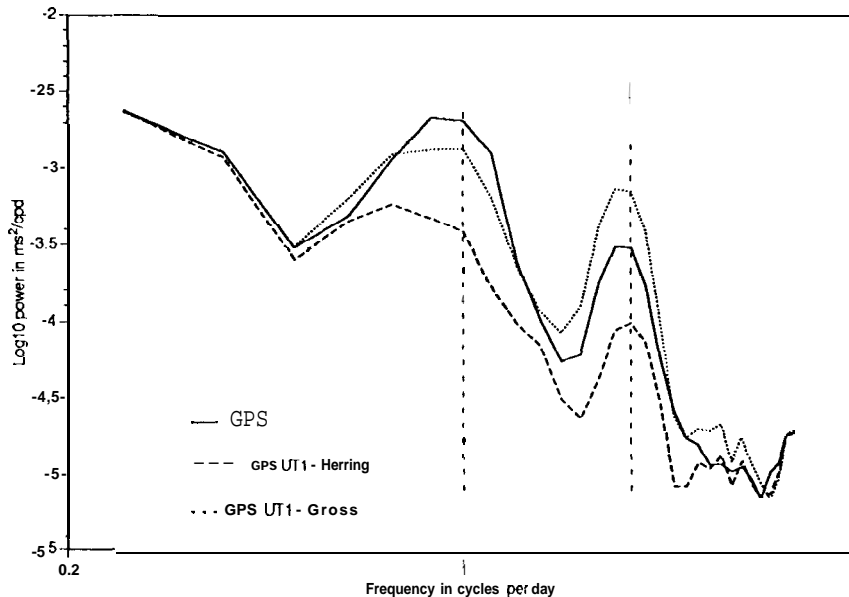


Fig. 4 Power spectra of the GPS UT1 series and the GPS series differenced with each of the two tide models.

GPS vs. AAM

The three series of atmospheric angular momentum (AAM) values evaluated every 6 hours provided by the NMC, the ECMWF, and the JMA are shown in Fig. 5. The variations in each series over periods greater than 1 to 2 days are similar, but the higher frequency fluctuations do not appear to be common among the three. The biases between the series are real, and come from differences in the meteorological models of the centers.

Since AAM represents a form of LOD, the curves in Fig. 5 must be numerically integrated to generate UT1 series whose variations are implied by the AAM. These series are shown in Figure 6. Also shown are UT1 variations expected from the longer-period (14 and 30-day) non-equilibrium ocean tides emerging from the numerical ocean model [8], and a GPS UT 1 series computed by adding the GPS residual estimates to the nominal values used in the GPS estimation procedure. Adding back this nominal restores its multi-day variability to the GPS UT 1 solution. Each series for each of periods A and B has had a best-fitting linear bias and trend removed. Since the ECMWF series for period A starts on July 27 and thus is one day shorter, it has had a trend removed which minimizes the differences between the ECMWF curve and the other two AAM curves. The

three integrated AAM curves show similar behavior for period A, with more contrasting forms for period B. All the AAM curves appear consistent with the overall shape of the GPS UT1 curve. The longer-period tide corrections do not add substantial signal at these few-day periods.

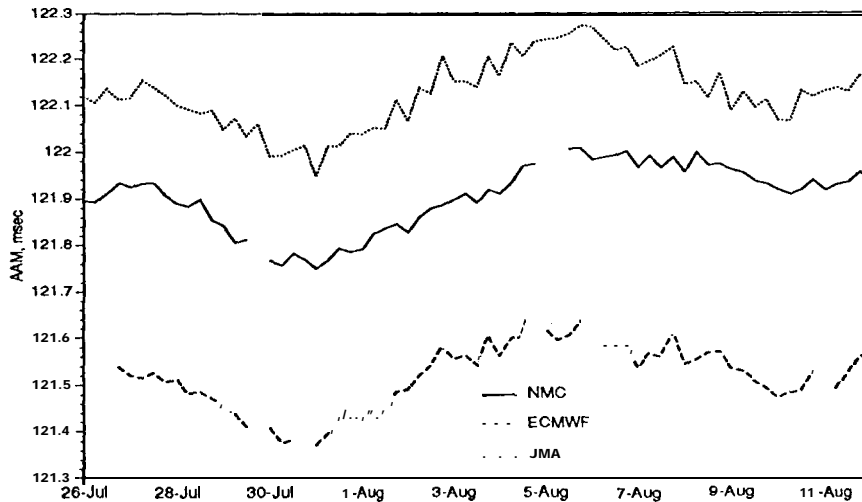


Fig. 5 Three series of atmospheric angular momentum (AAM) values.

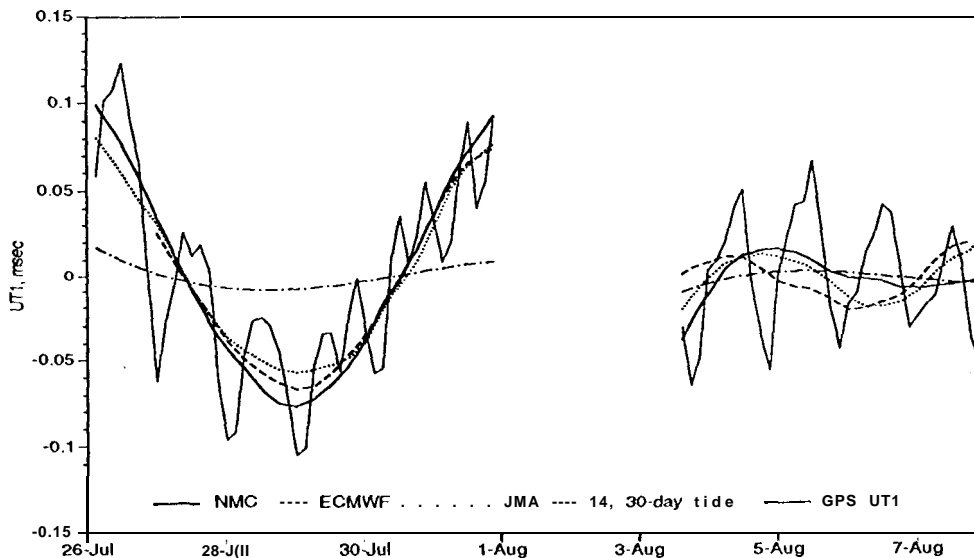


Fig. 6 Comparison of integrated AAM with geodetic UT1 variations.

The sum total of the integrated AAM, diurnal and semidiurnal tides (from Herring) and longer-period tides (from Gross) are shown in Figure 7, together with the observed UT1 variations from GPS and VLBI. Linear trends were removed from each series for each period. Most of the geodetic signal can be described by the sum of AAM variations and tidally induced UT1, with the tides acting at periods of one day and less and AAM acting at periods greater than a day. The differences between GPS and VLBI are at least as large as those between the AAM series themselves and the AAM and geodetic series. Thus, no center or technique stands out as superior. The RMS of the differences between the geodetic and AAM+tides series are shown in Table 3; all are consistent with the typical GPS and VLBI formal errors of **0.02-0.03 ms**.

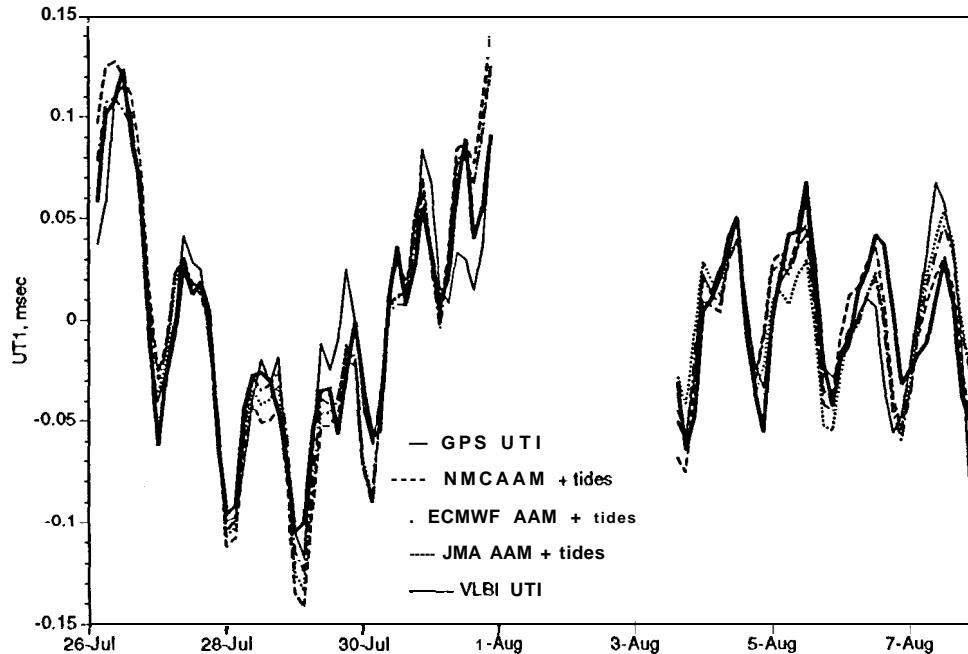


Fig. 7 The sum of the integrated AAM, diurnal and semidiurnal tides and longer-period tides, compared with the observed UT1 variations from GPS and VLBI.

CONCLUSIONS

Differences between the various series considered here tend to be at the level of 0.02 to 0.03 ms. These RMS differences are consistent “with the formal uncertainties of the data themselves. The main exception is the theoretical tide model, which simply does not yield the signal seen geodetically. There is also a drift in the GPS data relative to VLBI which, over time spans of 6 days or so, appears to be linear but with a non-unique drift rate.

Both GPS and VLBI exhibit nearly identical variability in the diurnal and semidiurnal bands, attributable to tidal variations whose values are well derived from many years of geodetic VLBI data. There is no residual signal in these frequency bands that exceeds the level of formal error of the data, although residual signals with amplitudes smaller than 0.02 ms could certainly be present. Although the theoretical tide model does not agree with observations in either band, the disagreement is largest in the semidiurnal frequency band.

The multi-day variability of AAM from all the meteorological centers is similar, and yields AAM-derived UT1 curves that are consistent with the variability of the geodetic UT1 at periods longer than one day. At diurnal and shorter periods, however, the AAM centers generate inconsistent estimates. Moreover, the sub-daily variability of the AAM is quite small and cannot, at this point, be disentangled from oceanic tidal effects and noise in the geodetic data. However, limits can be placed on the size of any residual AAM signal.

Thus the signal seen in the GPS time series can be represented by the sum of four effects: tides at diurnal and semi-diurnal periods, AAM fluctuations at periods of one to at least several days, a linear drift in UT1 due possibly to orbit mismodeling, and a high-fre-

quency noise component. To accurately solve for UT1 with GPS at these frequencies, the tidal variations in UT1 must certainly be modeled, either by explicit use of the Herring tide model, or by allowing adequate variability in the estimated UT1. AAM-induced variations are slow enough that if UT 1 (or LOD) is estimated at least daily, this variability need not be explicitly modeled. Further research is necessary to investigate and reduce both the drift in UT 1 of -0.1 ms over 2-5 days, and the level of high-frequency noise present in the data.

ACKNOWLEDGMENT

The authors thank and acknowledge the cast of literally thousands who were involved in collecting and processing the vast quantities of data from both GPS and VLBI, as well as the people and institutions involved in generating the AAM data sets. The work described in this paper was carried out by the Jet Propulsion Laboratory, California Institute of Technology, under contract with the National Aeronautics and Space Administration.

REFERENCES

- [1] Herring, T. A., and D. Dong, "Current and Future Accuracy of Earth Rotation Measurements," in Proceedings of the AGU Chapman Conference on Geodetic VLBI: Monitoring Global Change (Washington DC, April 22-26, 1991) pp. 306-324, NOAA Tech. Rep. NOS 137 NGS 49, NOS/NOAA, Rockville, MD, 1991.
- [2] Lichten, S. M., S. L. Marcus, and J. O. Dickey, "Sub-Daily Resolution of Earth Rotation Variations With Global Positioning System Measurements," *Geophys. Res. Lett.*, 19,537-540, 1992.
- [3] Dickey, J. O., M. Feissel, W. G. Melbourne, J. Ray, D. A. Salstein, B. E. Schutz, and C. Veillet, "SEARCH'92 Campaign (abstract)," *EOS, Trans. AGU*, 73 (43), Fall Meeting Suppl., 134, 1992.
- [4] Lichten, S. M., and J. S. Border, "Strategies for High-Precision Global Positioning System Orbit Determination," *J. Geophys. Res.*, 92, 12751-12762, 1987.
- [5] Lichten, S. M., "Estimation and Filtering for High-Precision GPS Positioning Applications," *Man. Geod.*, 15, 159-176, 1990.
- [6] Freedman, A. P., R. Ibanez-Meier, J. O. Dickey, S. M. Lichten, and T. A. Herring, "Sub-Daily Earth Rotation Determined With GPS: Recent Results (abstract)," *EOS, Trans. A.G.U.*, 73 (43), Fall Meeting Suppl., 135, 1992.
- [7] Yoder, C. F., J. G. Williams, and M. E. Parke, "Tidal Variations of Earth Rotation," *J. Geophys. Res.*, 86,881-891, 1981.
- [8] Gross, R. S., "The Effect of Ocean Tides on the Earth's Rotation as Predicted by the Results of an Ocean Tide Model," *Geophys. Res. Lett.*, 20,293-296, 1993.
- [9] Herring, T. A., "Diurnal and Semidiurnal Variations in Earth Rotation," in *Advances in Space Research*, in press, 1993.
- [10] Seiler, U., "Periodic Changes of the Angular Momentum Budget Due to the Tides of the World Ocean," *J. Geophys. Res.*, 96, 10,287-10,300, 1991.

UNIVERSAL TIME DERIVED FROM VLBI, SLR AND GPS

D.Gambis, N. Essaffi, E. Elsop and M. Feissel

Universal Time solution combined by IERS from individual series is mainly based on VLBI inertial techniques. Although satellite methods like SLR or GPS have reached a remarkable precision, they do not give access to a highly accurate non-rotating reference frame, which restricts the possibility of determining directly UT1 from their data processing. This is mainly due to uncertainties in the even zonal harmonics of the gravity field and in various models (ocean tides). We show here that it is still possible to combine the high-frequency fluctuations contained in GPS "UT1" series with the long-term variations in the VLBI solution to derive a mixed UT1 (VLBI+GPS) solution of great interest for its accuracy, time resolution but also for its economic advantage.

INTRODUCTION

By 1988, GPS had shown its ability to monitor polar motion. As a result IERS decided to include this technique as a part of its activities. After IGS'92 campaign extending from June through September 1992, five analysis centers continued their work on a routine basis. IERS has recently begun to incorporate these data in its regular analyses. In addition to the pole components estimation some analysis centers, CODE, JPL, ESOC and EMR [1,2] are also computing an internal "UT1" series or a derived quantity (*e.g* the excess to 86400 s of the length of the day, LOD). Due to the fact that satellite methods are not inertial the celestial reference system they define is not stable over long periods of time; this prevents the satellite technique to accurately determine long-term UT1 variations. We show in the present paper that their high-frequency signal is still valuable when associated to the long-term variations of UT1 VLBI series.

IERS/BC, URA1125/CNRS, Paris Observatory
61, avenue de l'Observatoire F-75014 Paris

DATA USED IN THE ANALYSES.

Four GPS analysis centers currently derive UT1 -UTC (or LOD values). The present study is only concerned by UT1 for Earth orientation purposes, consequently, LOD series given by JPL and ESOC have been integrated to give a "UT1" series. Because of missing values or gaps in some series, interpolation was required to derive continuous and homogeneous "UT1" series. Due to large jumps in the data, the analysis was made on a restricted interval for EMR. The characteristics of each series are listed on table 1. Other operational series used in the analyses and/or in the comparisons are also listed.

| | | | | 1992 | | 1993 | |
|-------------------|---|------|--------|------|-------|------|-------|
| | | | | June | Sept. | Jan. | March |
| | | int. | sampl. | | | | |
| | | (d) | (dj) | | | | |
| GPS | | | | | | | |
| EOP(CODE) 92 P 04 | 1 | 1 | | | | | |
| EOP(JPL) 92 P 02 | 1 | 1 | | | | | |
| EOP(JPL) 92 P 03 | 1 | 1 | | | | | |
| EOP(ESOC) 92 P 02 | 1 | 1 | | | | | |
| EOP(EMR) 92 P 04 | 1 | 1 | | | | | |
| VLBI | | | | | | | |
| EOP(NOAA) 93 R 01 | 3 | 1 | | | | | |
| EOP(NOAA) 93 R 03 | 1 | 0.1 | | | | | |
| SLR | | | | | | | |
| EOP(CSR) 91 L 01 | 3 | 3 | | | | | |

Table 1- GPS, VLBI and SLR Universal Time available at IERS/CB as of 15 March 1993

Differences between the "UT1" series for each GPS center and an external reference like the IERS combined solution (EOP (IERS) C 04) show a wide range of errors (Fig. 1) mainly linked to inaccuracy in the celestial frame defined in orbit computation. Fig.2 shows the geometrical configuration of the satellite orbit relatively to the various reference frames implied. Due to mismodeling in the even zonal harmonics of the gravity field, to ocean tides and also to atmospheric gravitational effects linked to pressure variations, the node longitude and consequently UT1 (hour angle, reckoned from the prime meridian, of a point on the celestial equator) [3] are affected by long-term errors. This prevents the satellite technique to accurately determine long-term UT1 variation. Some analysis centers like CSR have solved this problem by using external a-priori VLBI values in their computations[4].

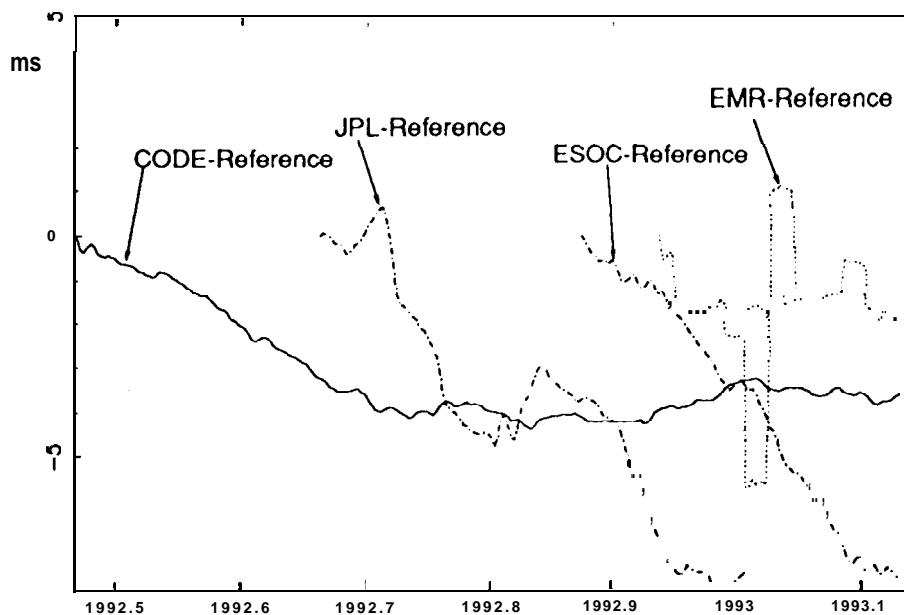


Fig. 1 - Raw "UT1" (or integrated values of LOD for JPL and ESOC) derived from GPS analysis present large systematic low-frequency errors relative to external series (IERS combined solution) which prevents their direct use in current analyses. The plotted differences are arbitrarily set to zero at the start of the time series.

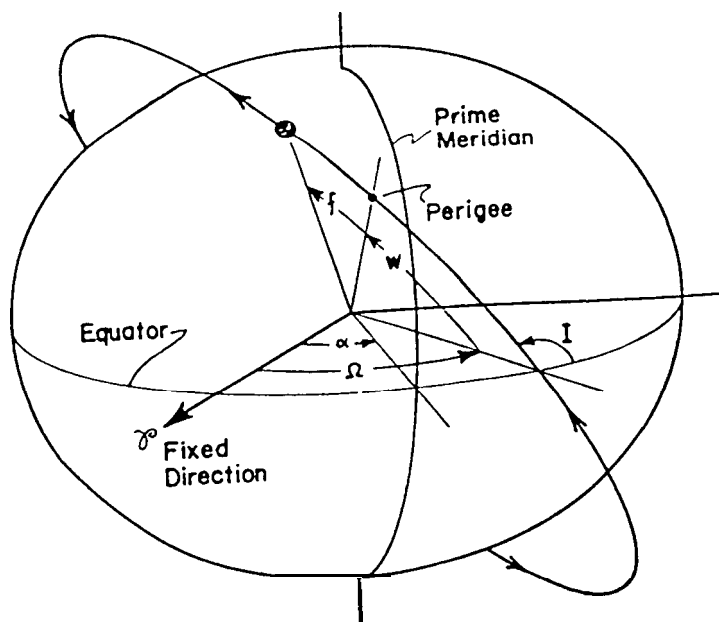


Fig. 2 - Representation of the orbit configuration relative to various reference frames. α : angle proportional to UT1 is obviously correlated to Ω , longitude of the ascending node of the satellite orbit; its determination suffers from mismodeling of Q .

CONSTRUCTION OF A UT1 SERIES BASED ON GPS AND VLBI SOLUTIONS

We want to set up a procedure of constructing a mixed UT1 series involving long-term VLBI variations of EOP(NOAA) 93 R 01 associated to high-frequency variations given by GPS analysis *e.g.* UT1(VLBI+GPS) the most simple possible for clarity of the process. High frequency terms are removed in VLBI series while they are kept for internal GPS "UT1" series. The critical point concerns the threshold determination within which the high-frequency information contained in the GPS series is valuable. The criteria we have chosen is the following:

Parallel **periodograms** are made for CODE, JPL and the VLBI solutions. Depending on the analysis center (CODE or JPL) the agreement is fair until a specific period (respectively about 80 and 30 days) which is the threshold corresponding to the optimal filtering (Fig.3). This analysis could not be done for ESOC and EMR because of the relatively short data interval available.

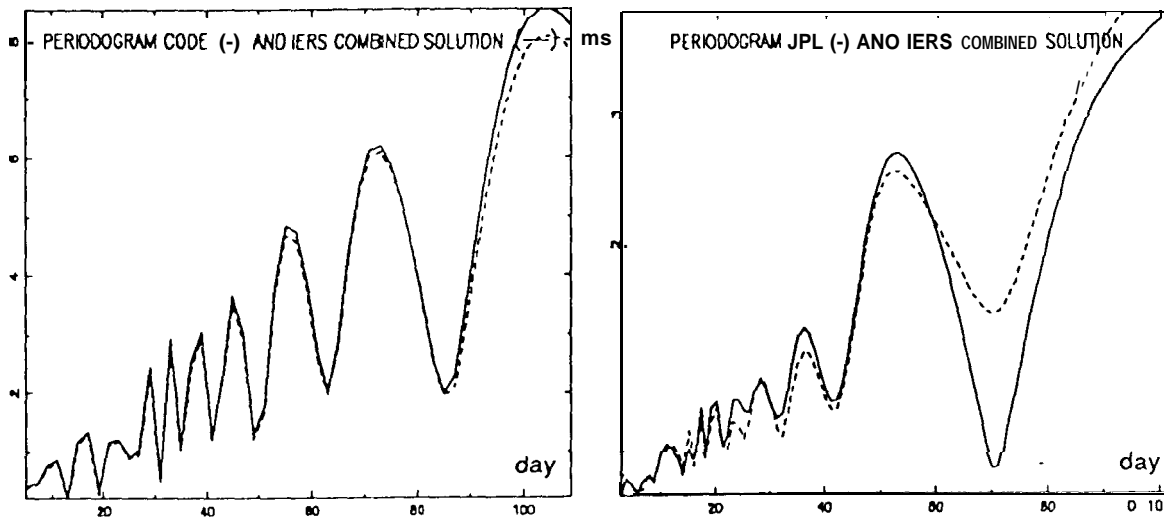


Fig. 3- Periodograms of raw "UT1" GPS series compared to those of EOP(NOAA) 93 R 01. This analysis gives the threshold for smoothing characteristics determination

COMPARISONS OF UT1(VLBI+GPS) WITH VLBI AND SLR SERIES

In order to estimate the precision of the obtained mixed UT1 (VLBI+GPS) solution comparisons with various series have been made. Fig. 4 shows its difference with NOAA and CSR solution; the rms differences of the three series are of the same order. Fig. 5 shows the differences between the mixed UT1 (VLBI+GPS) solution and VLBI (EOP(NOAA) 93 R 01) and SLR (EOP(CSR) 91 L 01).

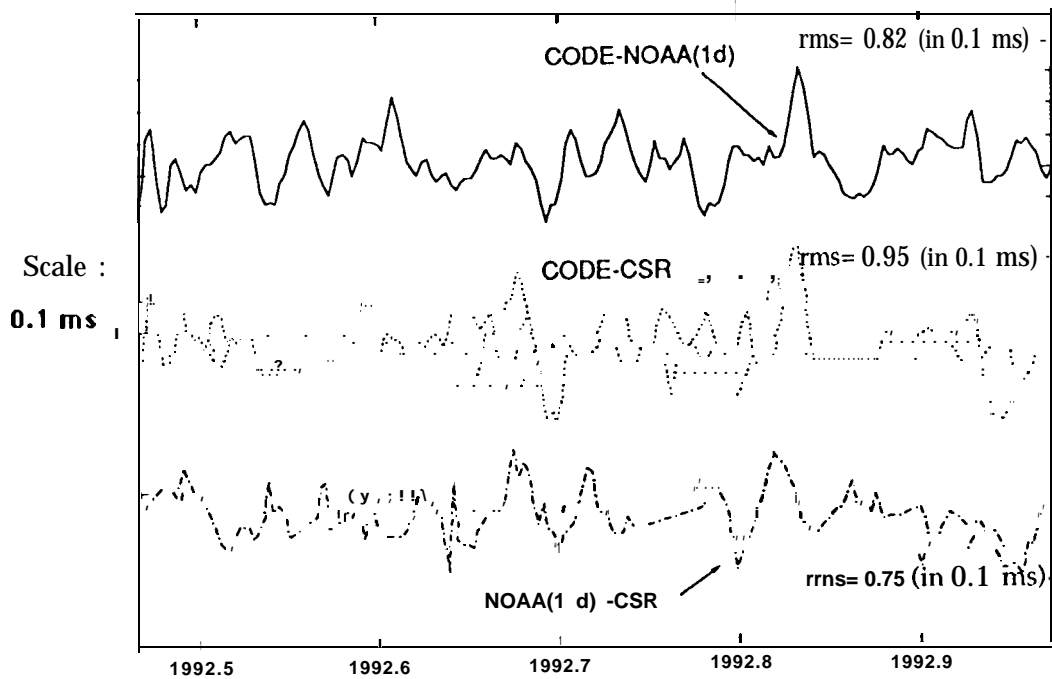


Fig. 4 - Differences between *UT1(NOAA+CODE)* solution with respectively *EOP(NOAA) 93 R 01* and *EOP(CSR) 91 L 01*. RMS of the three series give estimation of the precision.

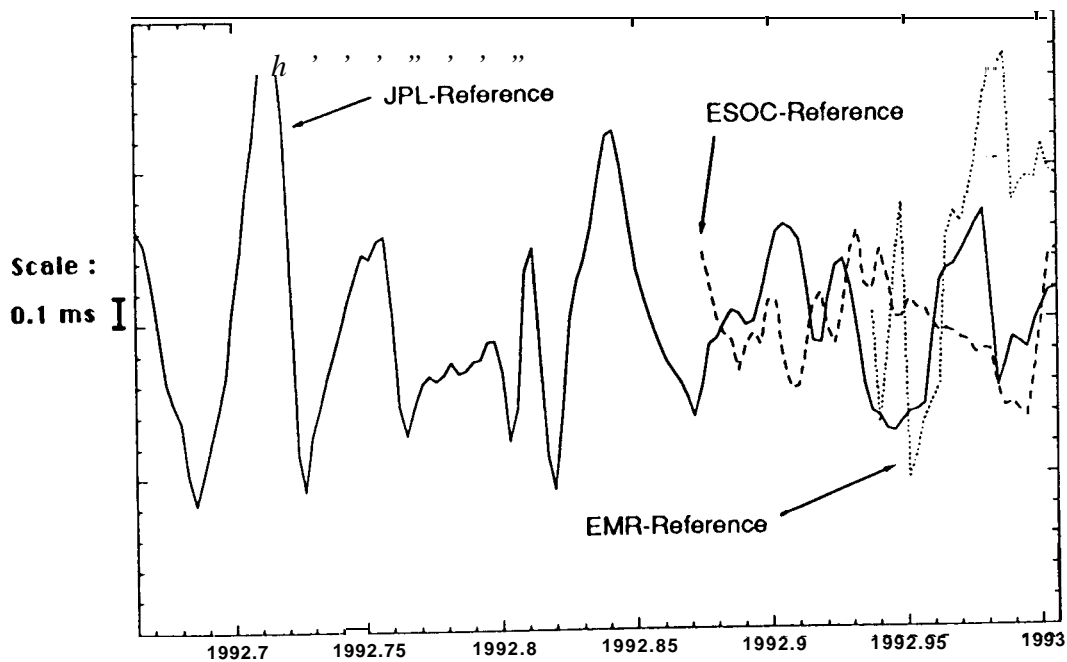


Fig. 5- Differences between *UT1(GPS+NOAA)* solutions with an external reference (here *EOP(IERS) 90 C 04*).

Table 2 gives an estimation of the precision of each series by comparison to **EOP(IERS) 90 C 04**. These values are only indicative, the **combined IERS** solution being dependant on VLBI and SLR series.

| Series | UT1 (0,0001s) |
|-------------------|---------------|
| GPS | |
| UT1(NOAA+CODE) | 0.81 |
| UT1(NOAA+JPL) | 2.80 |
| UT1(NOAA+ESOC) | 1.47 |
| UT1(NOAA+EMR) | 3.87 |
| VLBI | |
| EOP(NOAA) 93 R 02 | 0.41 |
| EOP(NOAA) 93 R 03 | 0.64 |
| SLR | |
| EOP(CSR) 91 L 01 | 0.73 |

Table 2- RMS differences of various series with **EOP(IERS) 90 C 04**.

CONCLUSIONS

Although the internal UT1 series derived from GPS determinations are not directly usable for Earth Orientation monitoring, its high-frequency information can be used together with an external long-term calibration to derive a combined **UT1(VLBI+GPS)** solution which may be used both for scientific and operational purposes. Outside its high accuracy comparable to other series (NOAA, CSR) the advantage is its high sampling contribution (sub-diurnal) and also, what is not negligible its low production price due only to an additional effort in analyses. Moreover, monthly VLBI contribution seems sufficient to ensure long-term stability of the solution. Refinements of the data analyses are assumed to improve the results in a near future.

REFERENCES

- [1]- Annual Report for 1991.
- [2]- **IGS'92** campaign, IERS Reports.
- [3]- IERS Technical note 8
- [4]- Aoki S.,Guinot B., Kaplan K.H.,Kinoshita H.,McCarthy D.D. and P.K. Seidelman, 1982, *Astron. Astrophys.*,105,359 -361.

IGS Orbit Comparison

Clyde Goad *

One of the responsibilities of the IGS Analysis Center Coordinator is to provide the user community and especially the analysis centers with an assessment of the qualities of the orbital products being generated on a weekly basis by the analysis centers. The analysis centers who participated in the generation of orbits for the IGS campaign are as follows:

CODE Center for Orbit Determination in Europe, Bern, Switzerland

EMR Energy, Mines, and Resources, Ottawa, Canada

ESA European Space Agency, Darmstadt, Germany

GFZ Zentralinstitut für Physik der Erde, Potsdam, Germany

JPL Jet Propulsion laboratory, Pasadena, California

SIO Scripps Institute of Oceanography, La Jolla, California

UTX University of Texas, Austin, Texas

On a weekly basis these institutes provided their determinations of GPS orbits to the scientific community in the S1'3 format as defined by Dr. Benjamin Remondi of the US National Geodetic Survey. The older SP 1 format was used by two of the participants.

These orbital products were delivered to IGS global data centers for deposit. Afterward, those who choose to compare derived orbital products with data collected either within the framework of the IGS or otherwise, are able to download these products for such comparisons. The data center used by OSU in the comparisons was the CDDIS located at Goddard Space Flight Center, Greenbelt, Maryland, USA. As with delivery of all products within the IGS, the user should have a connection capability via the Internet electronic mail facility.

Early into the IGS campaign, comparisons were made by plotting the actual differences between Earth centered fixed Cartesian coordinates between the different centers' orbits. This proved to be very helpful in discovering a few problems which were easily corrected by the analysis centers. However after the first few weeks, the orbital products were without problems and the process of generating plots of orbital differences was stopped.

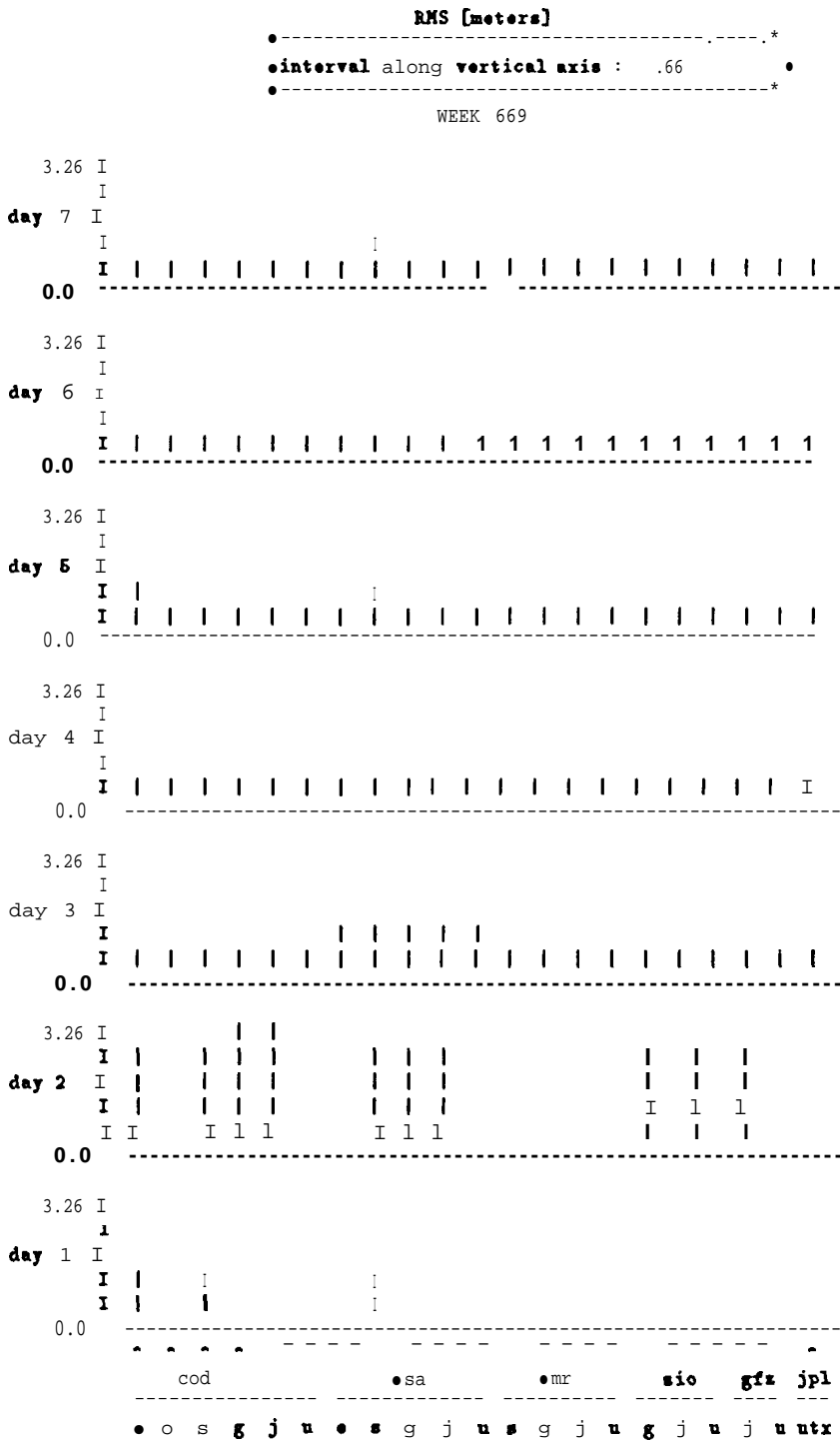
Rather another approach was taken which was far less demanding in terms of required computer and manpower support and provided a needed compaction of information. Using initially software provided to the Analysis Center Coordinator by Gerhard Beutler of the University of Bern, comparisons were made in terms of least-squares determinations of Helmert transformations (seven parameter) between any two centers' orbits. The resulting root mean square (rms) values from the derived models then were a measure of the closeness of

* The Ohio State University, Department of Geodetic Science and Surveying, 1958 Neil Avenue, Columbus, Ohio 43210, USA

any two orbits. This technique removes any differences due to different coordinate system realizations. The contributed software was modified so that it could be run more automatically each week to perform the required comparisons. These comparisons are generated for daily orbital products. Although in some cases a different number of weeks of comparisons were provided, the usual procedure evolved into providing three weeks of results with the latest week's comparison having a latency of two weeks. Not all analysis centers provided orbital products within the two weeks required to be included in the first opportunity for comparisons. However only rarely would an orbital product not make the third opportunity. Table 1. contains the comparisons for GPS week 659. The reference point on the satellite is the center of mass. In the early part of the IGS Campaign, JPL reported the phase center of the antenna as its reference point rather than the center of mass which explains the large scale difference between JPL orbits in table 1. Later JPL switched to the center of mass. In studying this example, one will notice large differences between the different days' results. One also notices the absence of orbital products during some days. This usually was due to one of three sources: eclipsing satellites, orbital maneuvers (thrusts), or the presence of Selective Availability (SA). During some of the IGS campaign SA was turned off. However if SA had been turned on then it was being tested during the weekend (Saturday through Monday morning). Thus orbital dropouts were common on these days. Large RMS values were also indicative of the presence of SA during weekends. For example one can see a significant difference between RMS values on Monday, August 24 and Tuesday, August 25. Thirty-six contiguous weeks of the IGS orbit determinations have been summarized in table 2. Here the orbital comparisons have been scanned for the largest and smallest rms of differences between any two centers for any day. These maximum and minimum differences are then listed for GPS weeks 650-685. A definite trend toward improvement is easily seen. The open question is whether this trend will continue or even stabilize into the future. Since SA was off toward the end of the 36-week period, the potential for degradation once SA returns is still present. We should know soon; the US Department of Defense (DoD) has returned to testing SA at the writing of this article -sometimes up to five days in a week. Some suggested or nominal mathematical models were distributed to each analysis center prior to the beginning of the IGS campaign. Table 3. contains a summary of these nominal models. Each analysis center had much latitude in the way its orbits were to be determined. Data sampling, choice of which fiducial stations to use, whether or not to attempt an improvement of Earth rotation parameters (ERP's), whether or not to include pseudorange along with phases, use of nondifferenced data versus (say) double differences, etc were to be decided by each center. A tremendous amount of work went into the generation of these orbital products. Data cleansing for literally hundreds of thousands of phase measurements had to be performed. Sometimes this could be done using automatic techniques; often not. Also the financial support of those agencies which felt that GPS is truly now competitive among the techniques which will lead us to a better understanding of this Earth is greatly acknowledged. The Analysis Center Coordinator has only praise for the smooth operation that he witnessed during the official campaign and after it ended. Although the future service has to contend with SA, with the improved tracking hardware which we either now have or anticipate being available in the near future, orbits approaching 50cm or better with a latency of a few days to one week are indeed close by. Without the commitment of the data collectors, the data archive centers, the data analyzers, and the funding agencies on an international scale, it is

difficult to imagine how the scientific community could have reached this point any other way. All who contributed to this effort should take pride in a job well done.

Table i .
Comparison of Contributed Orbits for GPS Week 669



a m i f p t m i f p t i f p t f p t p t
a r o z l x r o z l x o z l x x l x l x

(R + scale*I)*X1 + Translation --> x2
I is 3x3 identity matrix R= $\begin{pmatrix} 1 & 1 & RZ \\ -RZ & 1 & RX \\ RY & -RX & 1 \end{pmatrix}$

ORBIT COMPARISON FOR DAY 1 OF GPS WEEK 669 (day 1 is Sunday)

| MODIFIED JULIAN DATE | DAY | MONTH | YEAR | Translations, RMS - meters |
|----------------------|-----|-------|------|----------------------------|
| 48867 | 23 | 8 | 1992 | Scale - ppb |

| DX | DY | DZ | RX | RY | RZ | SCALE | RMS | |
|--------|--------|--------|------|------|-------|-------|------|--------------------|
| 0.0230 | 0.0140 | 0.082 | 1.0 | -2.2 | -1.7 | -1.1 | 0.66 | cod0659-->esa0659 |
| 0.102 | 0.013 | 0.092 | -0.6 | 2.8 | 10. S | -2.2 | 0.72 | cod0659-->sio0659 |
| 0.061 | 0.024 | -0.089 | 1.3 | 6.2 | 11.6 | -1.0 | 0.79 | ● sa0669-->sio0669 |

ORBIT COMPARISON FOR DAY 2 OF GPS WEEK 669 (day 1 is Sunday)

| MODIFIED JULIAN DATE | DAY | MONTH | YEAR | Translations, RMS - meters |
|----------------------|-----|-------|------|----------------------------|
| 48868 | 24 | 8 | 1992 | Scale - ppb |

| DX | OY | DZ | RX | RY | RZ | SCALE | RMS | |
|--------|---------|--------|------|------|------|-------|------|--------------------|
| -0.668 | -0.381 | 0.296 | 6.3 | -6.6 | -2.4 | -6.8 | 2.04 | cod0659-->esa0659 |
| 0.201 | 0.132 | 0.387 | -0.4 | 7.2 | 10.4 | 6.0 | 2.68 | cod0659-->sio0659 |
| -0.622 | -0.0680 | 0.317 | -4.2 | 4.8 | 11.6 | -12.8 | 3.26 | cod0659-->gfs0659 |
| 0.3100 | 0.262 | 0.099 | 18.1 | 4.1 | -3.3 | -27.6 | 2.82 | cod0659-->jpl0659 |
| 0.693 | 0.466 | -0.162 | 7.4 | 8.3 | 13.8 | 4.3 | 2.11 | ● aa06S9-->sio0669 |
| 0.4400 | 0.386 | -0.426 | 7.7 | 4.9 | 2.3 | 1.4 | 2.00 | ● na06S9-->@a0669 |
| 0.600 | 0.441 | -0.379 | 11.7 | 7.6 | 0.2 | -27.9 | 2.07 | ● aa0869-->jpl0669 |

| | | | | | | | | |
|--------|--------|--------|------|------|-------|-------|------|-------------------|
| -0.441 | -0.411 | -0.160 | -4.4 | 1.9 | -3.6 | -16.9 | 2.21 | sio0659-->gfs0659 |
| 0.039 | 0.139 | -0.263 | 18.8 | -4.2 | 13.7 | -32.2 | 2.27 | sio0659-->jpl0659 |
| 0.4930 | 0.288 | -0.381 | 17.9 | 0.1 | -10.9 | -16.8 | 2.68 | gfs0659-->jpl0659 |

ORBIT COMPARISON FOR DAY 3 OF GPS WEEK 669 (day 1 is Sunday)

| MODIFIED JULIAN DATE | DAY | MONTH | YEAR | Translations, RMS - meters |
|----------------------|-----|-------|------|----------------------------|
| 48869 | 26 | 6 | 1992 | Scale - ppb |

| DX | DY | DZ | RX | RY | RZ | SCALE | RMS | |
|--------|-------|--------|------|-----|------|-------|------|-------------------|
| -0.094 | 0.068 | 0.109 | -1.6 | 1.0 | -2.1 | 0.6 | 0.62 | cod0659-->esa0659 |
| 0.0680 | 0.031 | 0.061 | -2.1 | 1.6 | -1.2 | 0.1 | 0.49 | cod0659-->emr0659 |
| 0.0200 | 0.019 | -0.029 | -1.0 | 2.1 | 3.9 | 0.1 | 0.48 | cod0659-->utr0659 |

```

0.0820-0.023 0.033 -1.6 2.1 11.7 -1.2 0.64 cod0669-->si0669
-0.038-0.001-0.009 -3.7 -1.1 0.8 -3.9 0.69 cod0669-->gfr0669
0.028 0.026-0.073 0.8 2.8 -0.8 -34.2 0.42 cod0669-->jpl0669

0.161-0.026-0.069 -0.6 0.6 0.8 -0.6 0.74 ● sa0669-->omr0669
0.113-0.038-0.139 0.6 1.1 -1.6 -0.6 0.67 ● esa0669-->utr0669
0.172-0.034-0.076 0.0 1.1 13.8 -1.8 0.76 ● sa0669-->si0669
0.066-0.069-0.118 -2.2 -2.1 2.9 -4.6 0.78 ● sa0669-->@0669
0.122-0.032-0.180 2.3 1.9 1.3 -34.8 0.68 ● sa0669-->jpl0669

-0.039-0.012-0.060 1.1 0.6 -2.7 0.0 0.49 ● mr0669-->utr0669
0.016-0.006-0.020 0.6 0.4 13.0 -1.3 0.66 ● mr0669-->si0669
-0.100-0.030-0.061 -1.6 -2.7 2.0 -4.0 0.60 ● mr0669-->gfr0669
-0.034-0.002-0.125 2.9 1.2 0.4 -34.3 0.38 ● r0669-->jpl0669

0.060 0.002 0.063 -0.6 0.0 16.6 -1.4 0.41 utr0669-->si0669
-0.069-0.0200.020 -2.7 -3.2 4.7 -4.1 0.66 utr0669-->gfr0669
0.0080.006-0.043 1.7 0.8 3.1 -34.3 0.36 utr0669-->jpl0669

-0.118-0.022-0.047 -2.2 -3.2 -10.9 -2.6 0.62 si0669-->gfr0669
-0.061 0.003-0.106 2.2 0.8 -12.6 -33.0 0.42 si0669-->jpl0669

0.0660.028-0.061 4.4 4.0 -1.6 -30.3 0.60 gfr0669-->jpl0669

```

ORBIT COMPARISON FOR DAY 4 OF GPS WEEK 669 (day 1 is Sunday)

| MODIFIED JULIAN DATE | DAY | MONTH | YEAR | Translations, RI(S` meters |
|----------------------|-----|-------|------|-------------------------------|
| 48860 | 26 | 8 | 1992 | Rotations - mas Scale` ppb |

```

DI  DY  DZ  RX  RY  RZ  SCALE  RMS
0.022 0.032 0.114 0.7 -2.0 -1.0 0.3 0.67 cod0669-->esa0669
0.008 0.013 0.007 -1.0 -2.3 -2.3 -0.4 0.66 cod0669-->emr0669
0.004-0.046-0.070 -0.1 0.4 -3.7 0.1 0.36 cod0669-->utr0669
0.0360.017 0.021 -0.1 2.8 11.6 -0.7 0.49 cod0669-->si0669
-0.089 0.021-0.093 -2.2 -0.9 1.4 -3.8 0.66 cod0669-->gfr0669
0.016 0.006-0.069 2.0 2.1 -0.3 -34.8 0.41 cod0669-->jpl0669

-0.014-0.020-0.107 -1.8 -0.3 -1.3 -0.7 0.66 esa0669-->emr0669
-0.002-0.071-0.191 -0.7 2.6 -2.6 0.3 0.60 ● sn0669-->utr0669
0.010-0.013-0.086 -0.8 4.8 12.6 -0.9 0.66 ● aa0669-->si0669
-0.111-0.012-0.207 -3.0 1.1 2.4 -4.1 0.63 esa0669-->gfr0669
0.012-0.018-0.190 1.3 4.2 0.8 -34.6 0.64 ● sa0669-->jpl0669

0.016-0.066-0.062 1.1 2.8 -0.8 1.2 0.46 ● mr0669-->utr0669
0.026 0.007 0.016 1.0 6.0 13.9 -0.3 0.46 ● mr0669-->si0669
-0.097 0.008-0.099 -1.2 1.4 3.7 -3.4 0.66 ● mr0669-->@0669
0.029 -0.003-0.061 3.1 4.6 2.6 -33.7 0.44 ● mr0669-->jpl0669

0.0160.046 0.093 -0.2 2.2 14.6 -1.4 0.42 utr0669-->si0669
-0.114 0.064-0.027 -2.4 -1.6 4.7 -4.6 0.64 utr0669-->gfr0669
0.0130.061 0.001 2.0 1.7 3.3 -34.0 0.33 utr0669-->jpl0669

-0.122 0.003-0.118 -2.2 -3.6 -10.2 -3.0 0.66 si0669-->gfr0669
-0.002 0.004-0.093 2.3 -0.6 -11.4 -33.6 0.40 si0669-->jpl0669

0.127-0.001 0.028 4.4 3.2 -1.4 -30.4 0.47 gfr0669-->jpl0669

```

ORBIT COMPARISON FOR DAY 6 OF GPS WEEK 669 (day 1 is Sunday)

| MODIFIED JULIAN DATE | DAY | MONTH | YEAR | Translations, RMS - meters |
|----------------------|-----|-------|------|--------------------------------|
| 46661 | 27 | 8 | 1992 | Rotations - mas Scale - ppb |

| DX | DY | DZ | RX | RY | RZ | SCALE | RMS | |
|--------|--------|--------|------|-------|--------|-------|------|-------------------|
| 0.051 | 0.067 | 0.133 | 0.4 | -2.3 | -1.9 | -0.8 | 0.74 | cod0659-->esa0659 |
| 0.060 | 0.021 | 0.012 | -2.0 | -0.1 | -1.8 | -0.5 | 0.45 | cod0659-->emr0659 |
| -0.010 | 0.026 | -0.094 | -0.4 | -0.1 | -4.7 | 0.4 | 0.37 | cod0659-->utr0659 |
| 0.009 | 0.047 | 0.038 | -7.8 | -14.8 | -188.4 | -1.3 | 0.48 | cod0659-->sio0659 |
| -0.086 | 0.085 | -0.073 | -2.4 | -1.3 | -0.1 | -4.2 | 0.69 | cod0659-->gfr0659 |
| 0.024 | 0.036 | -0.087 | 2.4 | 2.4 | -1.0 | -36.2 | 0.46 | cod0659-->jpl0659 |
| -0.001 | -0.046 | -0.121 | -2.4 | 2.2 | 0.1 | 0.3 | 0.68 | esa0659-->emr0659 |
| -0.060 | -0.041 | -0.227 | -0.8 | 2.2 | -2.8 | 1.2 | 0.61 | sa0669-->utr0659 |
| -0.026 | -0.038 | -0.080 | -7.8 | -12.6 | -183.3 | -0.3 | 0.73 | sa0869-->sio0659 |
| -0.136 | -0.001 | -0.206 | -2.6 | 1.0 | 1.8 | -3.4 | 0.61 | sa0659-->@0669 |
| -0.016 | -0.007 | -0.220 | 2.0 | 6.0 | 0.6 | -33.8 | 0.66 | esa0659-->jpl0659 |
| -0.060 | 0.004 | -0.106 | 1.6 | 0.0 | -2.9 | 0.9 | 0.38 | mr0669-->utr0669 |
| -0.041 | 0.014 | 0.026 | -6.8 | -14.7 | -184.8 | -1.2 | 0.47 | emr0659-->sio0659 |
| -0.136 | 0.044 | -0.086 | -0.4 | -1.2 | 1.8 | -3.7 | 0.60 | r0659-->gfa0669 |
| -0.021 | 0.022 | -0.098 | 4.3 | 2.6 | 0.9 | -34.3 | 0.36 | r0669-->jpl0659 |
| 0.036 | 0.016 | 0.137 | -7.3 | -14.6 | -181.6 | -1.8 | 0.43 | utr0659-->sio0659 |
| -0.076 | 0.040 | 0.021 | -2.0 | -1.2 | 4.6 | -4.6 | 0.61 | utr0659-->gfr0659 |
| 0.036 | 0.014 | 0.000 | 2.8 | 2.6 | 3.6 | -36.4 | 0.33 | utr0659-->jpl0659 |
| -0.116 | 0.036 | -0.102 | 6.4 | 13.6 | 186.4 | -2.8 | 0.61 | sio0659-->gfr0659 |
| -0.036 | 0.016 | -0.138 | 10.1 | 17.3 | 186.6 | -33.6 | 0.46 | sio0659-->jpl0659 |
| 0.119 | -0.018 | -0.016 | 4.9 | 3.8 | -0.9 | -30.6 | 0.49 | gfr0659-->jpl0659 |

ORBIT COMPARISON FOR DAY 6 OF GPS WEEK 669 (day 1 is Sunday)

| MODIFIED JULIAN DATE | DAY | MONTH | YEAR | Translations, Rotations | RMS meters |
|----------------------|-----|-------|------|-------------------------|------------|
| 46862 | 28 | 8 | 1992 | Seal. ppb | |

| DX | DY | DZ | RX | RY | RZ | SCALE | RMS | |
|--------|--------|--------|------|------|-------|-------|------|-------------------|
| 0.068 | 0.036 | 0.040 | 0.1 | -0.8 | -1.3 | 0.4 | 0.64 | cod0659-->esa0659 |
| 0.062 | 0.002 | -0.021 | -0.1 | -1.7 | -1.6 | -0.9 | 0.41 | cod0659-->emr0659 |
| -0.036 | -0.016 | -0.112 | 0.6 | 0.1 | -4.4 | 0.1 | 0.39 | cod0659-->utr0659 |
| 0.034 | 0.001 | -0.066 | 1.5 | 3.8 | 12.0 | -1.1 | 0.41 | cod0659-->sio0659 |
| -0.042 | -0.023 | -0.123 | -1.7 | -1.8 | -0.4 | -4.0 | 0.62 | cod0659-->gfr0659 |
| -0.006 | 0.018 | -0.078 | 3.6 | 3.0 | -0.8 | -34.8 | 0.37 | cod0659-->jpl0659 |
| -0.016 | -0.033 | -0.081 | -0.2 | -0.6 | -0.2 | -1.3 | 0.64 | sa0669-->emr0669 |
| 0.103 | 0.061 | -0.162 | 0.6 | 0.9 | -3.1 | -0.3 | 0.63 | sa0669-->utr0669 |
| -0.039 | -0.033 | -0.086 | 1.4 | 4.6 | 13.3 | -1.6 | 0.64 | x.a0669-->sio0669 |
| -0.111 | -0.068 | -0.163 | -1.8 | -0.9 | 0.6 | -4.4 | 0.68 | sa0669-->gfr0669 |
| -0.066 | -0.031 | -0.123 | 3.3 | 3.8 | 0.0 | -36.1 | 0.62 | esa0659-->jpl0659 |
| -0.087 | -0.017 | -0.080 | 0.7 | 1.7 | -2.9 | 1.0 | 0.43 | mr0669-->ut x0669 |
| -0.019 | 0.003 | -0.033 | 1.6 | 6.4 | 13.6 | -0.2 | 0.60 | mr0669-->sio0669 |
| -0.096 | -0.026 | -0.102 | -1.6 | -0.1 | 1.0 | -3.1 | 0.61 | r0669-->gfa0669 |
| -0.067 | 0.009 | -0.067 | 3.6 | 4.6 | 0.3 | -33.7 | 0.36 | mr0669-->jpl0669 |
| 0.070 | 0.016 | 0.067 | 0.9 | 3.7 | 16.4 | -1.2 | 0.42 | utr0659-->sio0659 |
| -0.008 | -0.007 | -0.011 | -2.3 | -1.8 | 4.0 | -4.1 | 0.63 | utr0659-->gfr0659 |
| 0.036 | 0.028 | 0.026 | 2.8 | 2.9 | 3.4 | -34.8 | 0.38 | utr0659-->jpl0659 |
| -0.076 | -0.026 | -0.070 | -3.3 | -6.6 | -12.6 | -2.6 | 0.66 | sio0659-->gfr0659 |
| -0.032 | 0.006 | -0.032 | 1.9 | -0.8 | -12.9 | -33.6 | 0.43 | sio0659-->jpl0659 |
| 0.047 | 0.036 | 0.042 | 6.2 | 4.7 | -0.7 | -30.6 | 0.48 | gfr0659-->jpl0659 |

 ORBIT COMPARISON FOR DAY 7 OF GPS WEEK 669 (day 1 is Sunday)

| MODIFIED JULIAN DATE | | | DAY | MONTH | YEAR | Translations, RMS - meters | | Rotations - mas | Scale - ppb |
|---------------------------|-----------|--------------|-----------|-------------|-----------|----------------------------|------------|-----------------------------|-------------|
| 48863 | | | 29 | 8 | 1992 | SCALE | RMS | | |
| DX | DY | DZ | RX | RY | RZ | SCALE | RMS | | |
| 0.0230 | 0.046 | 0.034 | 0.0 | -1.8 | -0.6 | -0.2 | 0.46 | cod0659-->sa0659 | |
| 0.0540 | 0.013 | -0.061 | -0.9 | 1.6 | -1.0 | -0.3 | 0.38 | cod0659-->emr0659 | |
| 0.042 | -0.039 | -0.089 | 0.7 | 0.1 | -4.3 | -0.3 | 0.36 | cod0659-->utx0659 | |
| 0.0230 | 0.049 | 0.004 | -4.9 | -12.7 | 13.6 | 0.0 | 0.64 | cod0659-->sio0659 | |
| -0.011 | 0.024 | -0.063 | -1.9 | -1.3 | -0.3 | -4.0 | 0.62 | cod0659-->gfx0659 | |
| 0.0370 | 0.036 | -0.076 | 4.9 | 3.6 | -0.6 | -36.0 | 0.38 | cod0659-->jpl0659 | |
| 0.031-0.033-0.116 | | | -0.9 | 0.2 | -0.6 | -0.1 | 0.48 | sa0669-->omr0669 | |
| 0.019-0.086-0.133 | | | 0.7 | 1.9 | -3.8 | -0.1 | 0.60 | sa0669-->utx0669 | |
| -0.001 0.006-0.031 | | | -4.9 | -10.9 | 13.9 | 0.2 | 0.70 | sa0669-->sio0669 | |
| -0.034-0.022-0.087 | | | -1.9 | 0.6 | 0.2 | -3.8 | 0.69 | sa0669-->gfx0669 | |
| 0.034-0.036-0.139 | | | 4.8 | 6.4 | -0.6 | -34.8 | 0.47 | sa0669-->jpl0669 | |
| -0.012 | -0.062 | -0.018 | 1.6 | 1.7 | -3.2 | 0.0 | 0.34 | mr0669-->utx0669 | |
| -0.0320 | 0.037 | 0.086 | -4.0 | -11.1 | 14.6 | 0.3 | 0.63 | mr0669-->aio0869 | |
| -0.066 | 0.011 | 0.016 | -1.0 | 0.3 | 0.8 | -3.7 | 0.62 | mr0669-->x0669 | |
| -0.0130 | 0.021 | -0.003 | 6.8 | 6.0 | 0.2 | -34.6 | 0.28 | emr0659-->jpl0659 | |
| -0.020 | 0.090 | 0.101 | -6.6 | -12.6 | 17.7 | 0.3 | 0.64 | utx0659-->sio0659 | |
| -0.0630 | 0.0630 | 0.036 | -2.6 | -1.4 | 4.0 | -3.7 | 0.66 | utx0659-->gfx0659 | |
| 0.004 | 0.072 | 0.021 | 4.2 | 3.4 | 3.6 | -34.6 | 0.34 | utx0659-->jpl0659 | |
| -0.030 | -0.026 | -0.086 | 3.0 | 11.4 | -13.7 | -3.9 | 0.61 | sio0659-->gfx0659 | |
| 0.021 | 0.000 | -0.088 | 9.9 | 16.2 | -14.0 | -34.7 | 0.49 | sio0659-->jpl0659 | |
| 0.064 | 0.016 | -0.012 | 6.9 | 4.8 | -0.7 | -30.6 | 0.60 | gfx0659-->jpl0659 | |

Table 2. Minimum and Maximum RMS Differences
For a 36-Week Period During and After the
 IGS Campaign

| Begin Day | Week | Minimum RMS | Day Centers | Maximum RMS | Day Centers |
|-----------------|------------|-------------|------------------|-------------|------------------|
| M-D-Y | | (m) | | (m) | |
| 02-21-93 | 686 | 0.36 | 4 COD-EMR | 1.37 | 6 ESA-EMR |
| 02-14-93 | 684 | 0.23 | 4 EMR-JPL | 1.99 | 7 EMR-JPL |
| 02-07-93 | 683 | 0.23 | 6 EMR-JPL | 0.82 | 4 ESA-SIO |
| 01-31-93 | 682 | 0.21 | 2 EMR-JPL | 1.03 | 6 COD-ESA |
| 01-24-93 | 681 | 0.20 | 4 EMR-JPL | 0.76 | 6 ESA-SIO |
| 01-17-93 | 680 | 0.19 | 7 EMR-JPL | 1.41 | 1 COD-JPL |
| 01-10-93 | 679 | 0.26 | 6 COD-EMR | 1.07 | 7 COD-ESA |
| 01-03-93 | 678 | 0.26 | 1 EMR-JPL | 1.38 | 3 ESA-JPL |
| 12-27-92 | 677 | 0.21 | 6 EMR-JPL | 1.14 | 3 COD-ESA |
| 12-20-92 | 676 | 0.18 | 7 EMR-JPL | 1.01 | 6 COD-ESA |
| 12-13-92 | 675 | 0.24 | 7 EMR-JPL | 1.36 | 1 ESA-JPL |
| 12-06-92 | 674 | 0.27 | 6 EMR-JPL | 1.73 | 2 COD-ESA |
| 11-29-92 | 673 | 0.31 | 4 EMR-JPL | 3.16 | 6 COD-ESA |
| 11-22-92 | 672 | 0.20 | 3 EMR-JPL | 1.48 | 7 COD-ESA |
| 11-16-92 | 671 | 0.19 | 2 EMR-JPL | 1.14 | 7 COD-ESA |
| 11-08-92 | 670 | 0.18 | 4 EMR-JPL | 1.68 | 2 COD-SIO |
| 11-01-92 | 669 | 0.18 | 7 EMR-JPL | 1.34 | 2 ESA-JPL |

| | | | | | | | |
|----------|-----|------|---|---------|------|---|---------|
| 10-26-92 | 668 | 0.20 | 6 | EMR-JPL | 1.67 | 2 | ESA-JPL |
| 10-18-92 | 687 | 0.23 | 3 | EMR-JPL | 2.96 | 1 | ESA-SIO |
| 10-11-92 | 666 | 0.21 | 3 | EMR-JPL | 6.37 | 6 | SIO-JPL |
| 10-04-92 | 666 | 0.31 | 6 | EMR-JPL | 2.47 | 1 | ESA-SIO |
| 09-27-92 | 664 | 0.34 | 4 | EMR-JPL | 2.31 | 2 | SIO-JPL |
| 09-20-92 | 663 | 0.32 | 4 | EMR-JPL | 2.71 | 2 | SIO-JPL |
| 09-13-92 | 662 | 0.38 | 6 | EMR-JPL | 6.83 | 1 | ESA-SIO |
| 09-06-92 | 661 | 0.32 | 2 | EMR-JPL | 1.72 | 3 | ESA-GFZ |
| 08-30-92 | 660 | 0.29 | 6 | UTX-JPL | 0.71 | 7 | ESA-JPL |
| 08-23-92 | 669 | 0.28 | 7 | EMR-JPL | 3.26 | 2 | COD-GFZ |
| 08-16-92 | 668 | 0.36 | 4 | GFZ-JPL | 4.38 | 7 | COD-SIO |
| 08-09-92 | 667 | 0.31 | 4 | COD-JPL | 4.76 | 1 | COD-SIO |
| 08-02-92 | 666 | 0.34 | 4 | UTX-JPL | 4.67 | 1 | UTX-SIO |
| 07-26-92 | 666 | 0.32 | 2 | GFZ-JPL | 3.32 | 7 | UTX-SIO |
| 07-19-92 | 664 | 0.36 | 1 | UTX-JPL | 1.69 | 1 | COD-UTX |
| 07-12-92 | 663 | 0.37 | 1 | COD-SIO | 2.13 | 3 | SIO-GFZ |
| 07-06-92 | 662 | 0.39 | 3 | COD-UTX | 2.63 | 6 | ESA-GFZ |
| 06-28-92 | 661 | 0.46 | 6 | COD-JPL | 1.36 | 1 | ESA-GFZ |
| 06-21-92 | 660 | 0.68 | 3 | COD-SIO | 2.70 | 1 | ESA-UTX |

Table 3. Nominal Models To Be Used In Analysis Center or Orbit Determinations

Gravity Model: GEM-T3 through **degree** and order 8 with **C(2,1)** and **s(2,1)** replaced

Ae=6378137

GII=3.988004416 x10¹⁴ (m³/s²)

Solid and Ocean Tides

Third Body Perturbations of the Sun and Moon

ROCK 4, ROCK 42 Solar Radiation Models according to **Fliegel, Gallini, Swift**

formalized **C(2,1), S(2,1)** -> **-0.17 x 10⁻⁹, 1.19 x 10⁻⁹**

Earth Rotation Parameters to be obtained from **IERS Rapid Service Values**

SHORT - TERM POLAR MOTION AND UT1 VARIATIONS OBSERVED BY IGS

Jan Hefty*

The GPS polar motion and UT1 series available from the IGS'92 Campaign and its continuation are compared with the geodetic IERS combined series and the modelled atmospheric series based on effective atmospheric angular momentum functions. The short-term oscillations are obtained by removing the long periodical variations of the individual series. Polar motion variations in range from days to months are observed by GPS and significant correlation with both IERS combined and atmospheric series is found. The correlation of GPS UT1R with geodetic combined and atmospheric series reaches maximum for weekly variations. The monthly GPS UT1 oscillations exhibit discrepancies with other series.

ANALYZED DATA

The daily GPS series from 3 processing centers CODE, JPL and SIO are available for almost whole period 1992.5-1993.0. They give polar motion and the CODE series also UT1. The daily IERS series based on combination of VLBI, SLR and LLR observations [1] gives x , y , UT1 and covers the whole IGS Campaign. For the UT comparisons we use also the daily VLBI series from Westford - Wettzell baseline. The complete Yoder et. al [2] model for periodic variations due to zonal tides is removed from all UT1 series. In Table 1 we summarize the data used in further comparison studies.

The EOP variations caused by meteorological excitations have been obtained from time series of atmospheric angular momentum X-functions at 12-hour intervals computed from pressure and wind fields generated at the Japan Meteorological Agency [3]. The motions of Celestial Ephemeris Pole $\mathbf{p}(t)=\mathbf{p}_1+i\mathbf{p}_2$ induced by atmospheric fluctuations $\boldsymbol{\chi}=\boldsymbol{\chi}_1+i\boldsymbol{\chi}_2$ are computed from linearized Liouville equation [4]

* observatory of the Slovak Technical University, Department of Theoretical Geodesy, Radlinskeho 11, 81368 Bratislava, Slovak Republic

$$\mathbf{p}(t) + \frac{i}{\sigma_0} \frac{d\mathbf{p}(t)}{dt} = \boldsymbol{\chi}(t) , \quad (1)$$

where σ_0 is frequency of Chandler wobble. Let $\mathbf{P}(\omega)$ denote the Fourier transform of $\mathbf{p}(t)$ and $\mathbf{X}(\omega)$ the Fourier transform of $\boldsymbol{\chi}(t)$. Then eq. (1) transformed into frequency domain becomes

$$\mathbf{P}(\omega) = \frac{\sigma}{\sigma - \omega} \mathbf{X}(\omega) . \quad (2)$$

The procedure used to compute the **AAM** induced polar motion consist in Fast Fourier Transform (**FFT**) Of $\boldsymbol{\chi}(t)$, multiplication with transfer function (2) and recovering $\mathbf{p}(t)$ by inverse FFT. Two alternatives of $\mathbf{p}(t)$ from X-functions have been obtained according to the pressure term used - with and without the inverted barometer (**IB**) approximation.

The atmosphere induced UT is inferred from $\boldsymbol{\chi}_3$ component (wind term and pressure term with **IB**) by numerical integration.

Table 1
Analyzed series

| Technique | Series | Period | EOP |
|-----------|--------------------------------------|------------------------------------------------------------------|--------------------------------------------------------------------------------|
| GPS | EOP(CODE) 92 P 04 | 1992 Jun. 19 - 1993 Jan. 26 | x, y, UT1 |
| GPS | EOP(JPL) 92 P 02 EOP(JPL) 92 P 03 | 1992 Jul. 17 - 1992 Nov. 14 1992 Nov. 15 - 1993 Jan. 16 | x, y |
| GPS | EOP(SIO) 92 P 03 | 1992 Jun. 7 - 1993 Nov. 12 | x, y |
| Combined | EOP(IERS) 90 C 04 | 1992 Jan. 1 - 1993 Jan, 31 | x, y, UT1 |
| VLBI | EOP(NOAA) 92 R 02 | 1992 Jan. 1 - 1992 Dec. 31 | UT1 |
| AAM | AAM(JMA) 92 * 01 | 1992 Jan. 1 - 1992 Dec. 31 | $\boldsymbol{\chi}_1, \boldsymbol{\chi}_2, \boldsymbol{\chi}_3$ -> x, y, UT |

HIGH FREQUENCY VARIATIONS OF EARTH ROTATION PARAMETERS

The short-term oscillations of x , y and UTIR as well as of the AAM induced series are obtained by removing the long periodical variations of the individual series. Three types of residuals according to degree of Vondrak [5] smoothing are analysed. Fig.1 shows transfer functions of the used filters, The cut-off periods 9 days (filter I), 30 days (filter II) and 90 days (filter III) correspond roughly to daily, weekly and monthly variations of residuals,

Fig.2 and Fig.3 show the high pass filtered monthly and daily oscillations of the three GPS polar motion solutions and the AAM induced polar motion based on JMA pressure term without IB approximation for the period 1992.5-1993.0. Mean formal uncertainties of GPS series are 0.11 mas for CODE, 0.18 mas for JPL and 0.20 mas for S10. The upper graphs show that the individual GPS series follow the same pattern which is sporadically identical with AAM variations. The daily variations in lower graphs have significantly larger scatter for CODE and S10 series when compared with JPL polar motion and significantly exceed the formal uncertainties.

Fig.4 shows the UTIR residuals of GPS CODE series, combined IERS series as well as the UT AAM series. The monthly GPS variations differ from IERS and AAM in the beginning of IGS campaign, the daily variations of the three series have similar behaviour.

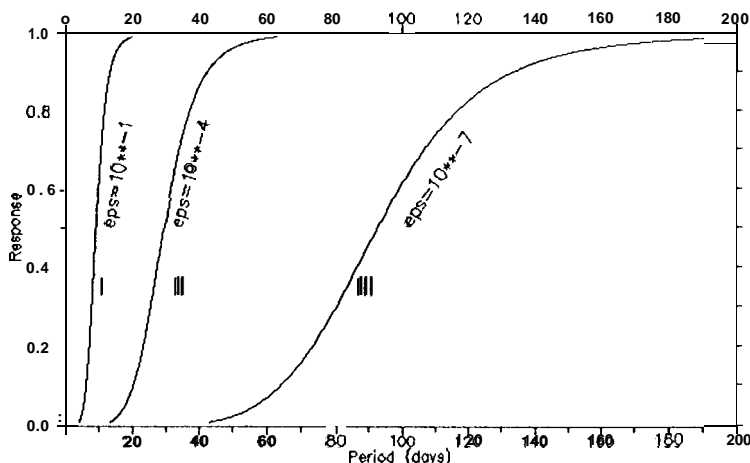


Fig.1 Transfer functions of Vondrak smoothing

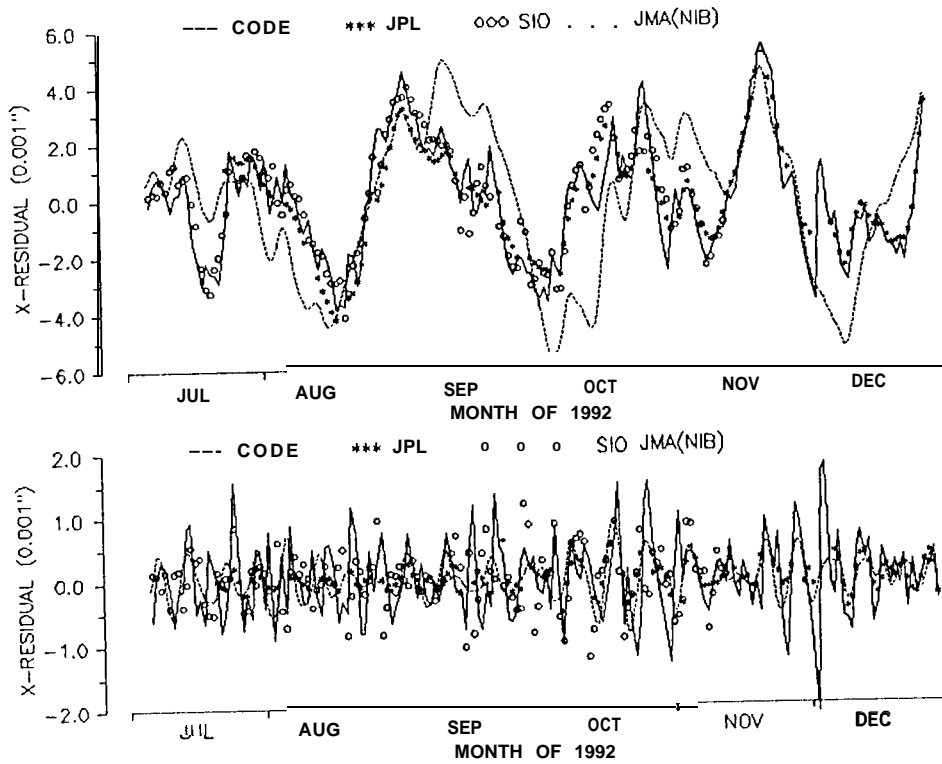


Fig.2 x-coordinate residuals from smoothing III (upper graph) and from smoothing I (lower graph)

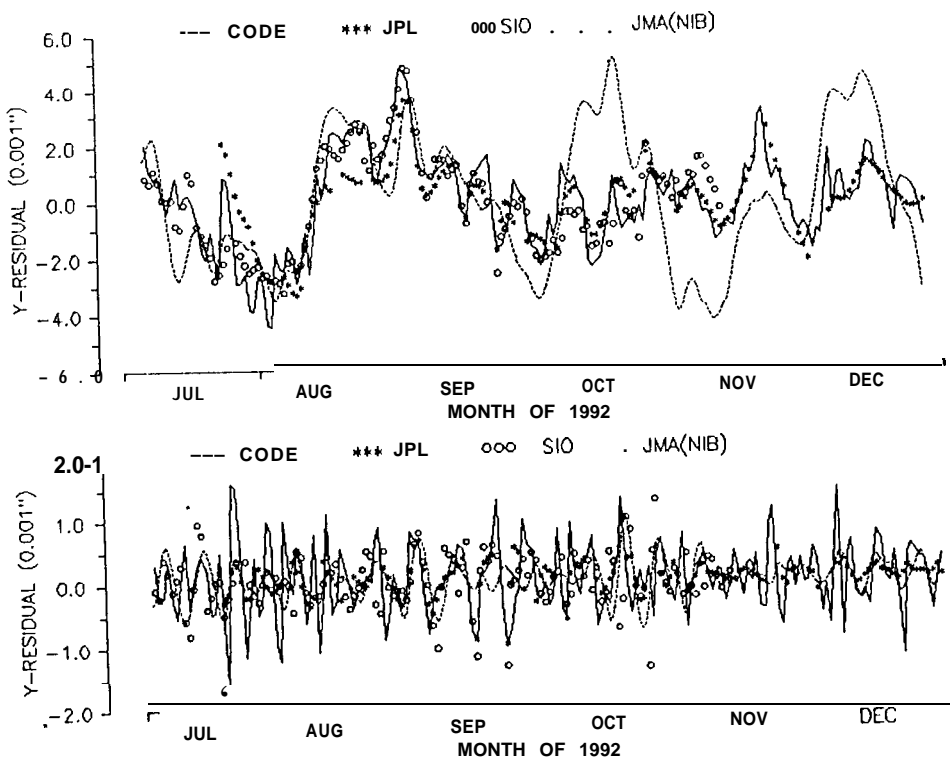


Fig.3 y-coordinate residuals from smoothing III (upper graph) and from smoothing I (lower graph)

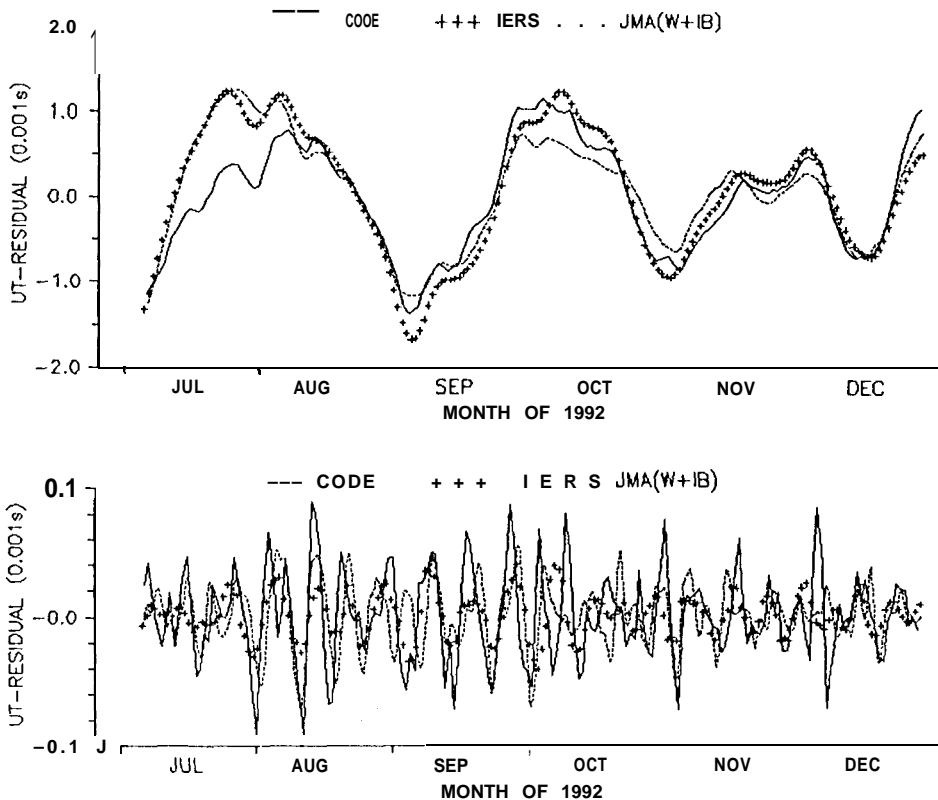


Fig.4 UTIR residuals from smoothing III (upper graph) and from smoothing I (lower graph)

DIFFERENCES OF EOP SERIES - UNCERTAINTIES AND CORRELATIONS

The residuals of GPS solutions, combined series and AAM series (with IB and without IB) representing the monthly, weekly and daily variations are compared pair by pair. Table 2 gives the estimates of rms differences after removing bias. As we are analyzing the residuals, bias of their differences is close to zero. For pairs of GPS series also the corresponding formal uncertainties based on information from processing centers are shown. Fig.5 is a plot of rms differences between GPS solutions. Displayed are also rms differences between JPL GPS series and IRES combined solution - two series with the best mutual agreement.

Table 3 summarizes correlation coefficients for pairs considered in Table 2. Correlation exceeding critical values at 0.01 significance level is found for each pair of geodetic series except the difference between S10 and CODE daily variations (0.05 level). Correlation coefficients between GPS series and between JPL and combined series are shown in Fig.6.

Table 2
 Rms differences of various pole coordinates series
 (units 0.001"). Uric. means the formal uncertainty of GPS
 series differences.

| Series | Filter | JPL | IERS | SIO | AAM (NIB) | AAM (IB) |
|----------|--------|------|------|------|--------------|-------------|
| CODE | 111 x | 0.89 | 0.95 | 1.09 | 2.23 | 1.75 |
| | Y | 1.00 | 0.85 | 0.98 | 2.14 | 1.53 |
| | 11 x | 0.70 | 0.80 | 0.95 | 1.03 | 1.11 |
| | Y | 0.71 | 0.79 | 0.91 | 1.07 | 0.95 |
| | I x | 0.48 | 0.59 | 0.70 | 0.57 | 0.58 |
| | Y | 0.51 | 0.56 | 0.66 | 0.61 | 0.58 |
| Unc. | | 0.20 | | 0.23 | | |
| AAM(IB) | 111 x | 1.40 | 1.42 | 1.48 | | |
| | Y | 1.07 | 1.23 | 1.48 | | |
| | 11 x | 0.67 | 0.80 | 0.75 | | |
| | Y | 0.63 | 0.53 | 0.74 | | |
| | 1 x | 0.17 | 0.14 | 0.39 | | |
| | Y | 0.23 | 0.13 | 0.42 | | |
| Unc. | | | | | | |
| AAM(NIB) | 111 x | 2.04 | 1.98 | 2.26 | | |
| | Y | 2.18 | 1.98 | 2.07 | | |
| | II x | 0.71 | 0.75 | 0.82 | | |
| | Y | 0.74 | 0.72 | 0.89 | | |
| | I x | 0.25 | 0.21 | 0.46 | | |
| | Y | 0.31 | 0.23 | 0.42 | | |
| Unc. | | ~ | | | | |
| SIO | 111 x | 0.89 | 0.77 | | | |
| | Y | 0.87 | 0.71 | | | |
| | 11 x | 0.58 | 0.64 | | | |
| | Y | 0.43 | 0.53 | | | |
| | 1 x | 0.35 | 0.42 | | | |
| | Y | 0.31 | 0.38 | | | |
| Unc. | | 0.26 | | | | |
| IERS | 111 x | 0.82 | | | | |
| | Y | 0.69 | | | | |
| | 11 X | 0.48 | | | | |
| | Y | 0.39 | | | | |
| | 1 x | 0.18 | | | | |
| | Y | 0.23 | | | | |
| Unc. | | | | | | |

Table 3
Correlation coefficients for x and y pole coordinates
Crit. means the critical value for $\alpha=0.01$.

| Series | Filter | JPL | IERS | SIO | AAM (NIB) | AAM (IB) |
|----------|--------------|-------------|-------------|-------------|--------------|-------------|
| COOE | 111 x | 0.97 | 0.89 | 0.82 | 0.57 | 0.54 |
| | y | 0.81 | 0.86 | 0.84 | 0.4B | 0.37 |
| | 11 x | 0.78 | 0.74 | 0.55 | 0.54 | 0.38 |
| | y | 0.68 | 0.73 | 0.53 | 0.40 | 0.40 |
| | Ix | 0.44 | 0.36 | 0.15 | 0.42 | 0.48 |
| | y | 0.37 | 0.30 | 0.20 | 0.16 | 0.18 |
| | Crit. | 0.22 | 0.18 | 0.21 | 0.22 | 0.22 |
| AAM(IB) | III x | 0.65 | 0.65 | 0.60 | | |
| | y | 0.51 | 0.45 | 0.44 | | |
| | 11 x | 0.43 | 0.51 | 0.60 | | |
| | y | 0.45 | 0.60 | 0.22 | | |
| | 1 x | 0.34 | 0.61 | 0.35 | | |
| | y | 0.33 | 0.49 | 0.34 | | |
| | Crit. | 0.22 | 0.18 | 0.21 | | |
| AAM(NIB) | 111 x | 0.65 | 0.66 | 0.50 | | |
| | y | 0.51 | 0.55 | 0.49 | | |
| | II X | 0.57 | 0.65 | 0.55 | | |
| | y | 0.61 | 0.63 | 0.47 | | |
| | 1 x | 0.49 | 0.68 | 0.28 | | |
| | y | 0.34 | 0.61 | 0.34 | | |
| | Crit. | 0.22 | 0.18 | 0.21 | | |
| SIO | 111 X | 0.91 | 0.91 | | | |
| | y | 0.89 | 0.91 | | | |
| | 11 x | 0.71 | 0.73 | | | |
| | y | 0.84 | 0.72 | | | |
| | 1 x | 0.49 | 0.31 | | | |
| | y | 0.64 | 0.39 | | | |
| | Crit. | 0.26 | 0.21 | | | |
| IERS | 111 X | 0.91 | | | | |
| | y | 0.88 | | | | |
| | 11 x | 0.85 | | | | |
| | y | 0.83 | | | | |
| | Ix | 0.50 | | | | |
| | y | 0.43 | | | | |
| | Crit. | 0.18 | | | | |

Standard deviations and correlations for pairs of UTIR series GPS, combined, daily VLBI and AAM are given in Table 4 and Table 5. The statistics obtained for weekly variations and daily variations have similar value for all compared series. This proves that GPS observed variations are reliable for periods shorter than one month.

Table 4
Rms differences between GPS, daily VLBI, IERS combined and atmospheric UT series (units 0.001 ms)

| Series | Filter | IERS | VLBI | AAM |
|--------|--------|-------|-------|-------|
| COOE | 111 | 0.507 | 0.527 | 0.522 |
| | II | 0.103 | 0.096 | 0.093 |
| | I | 0.034 | 0.048 | 0.037 |
| AAM | 111 | 0.229 | 0.298 | |
| | II | 0.108 | 0.093 | |
| | I | 0.021 | 0.041 | |
| VLBI | 111 | 0.261 | | |
| | 11 | 0.093 | | |
| | 1 | 0.036 | | |

Table 5
Correlation coefficients between GPS, daily VLBI, IERS combined and atmospheric UT series.
Crit. means the critical value-at significance level $\alpha=0.01$.

| Series | Filter | IERS | VLBI | AAM |
|--------|--------|------|------|------|
| COOE | 111 | 0.77 | 0.71 | 0.71 |
| | 11 | 0.80 | 0.80 | 0.79 |
| | I | 0.39 | 0.17 | 0.37 |
| | Crit. | 0.18 | 0.24 | 0.18 |
| AAM | III | 0.96 | 0.91 | |
| | II | 0.78 | 0.80 | |
| | I | 0.50 | 0.14 | |
| | Crit. | 0.18 | 0.24 | |
| VLBI | III | 0.94 | | |
| | 11 | 0.84 | | |
| | I | 0.23 | | |
| | Crit. | 0.24 | | |

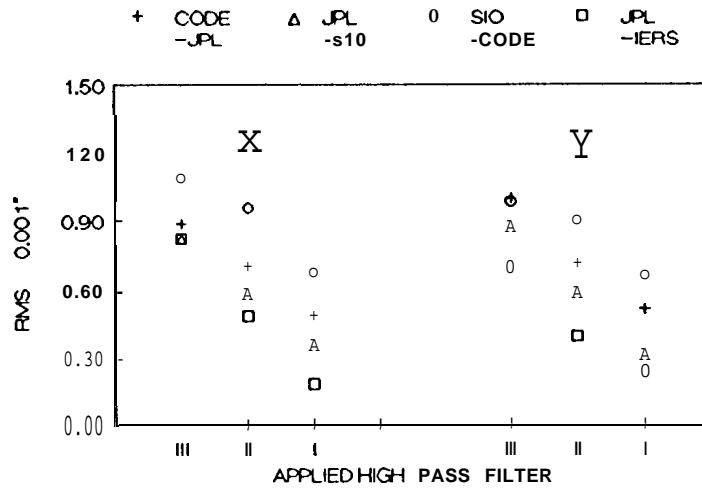


Fig.5 Rms differences of polar motion series

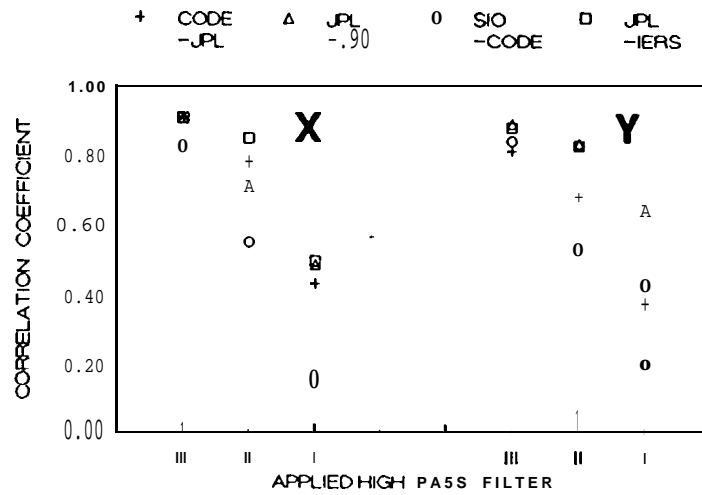


Fig.6 Correlation coefficients between polar motion series

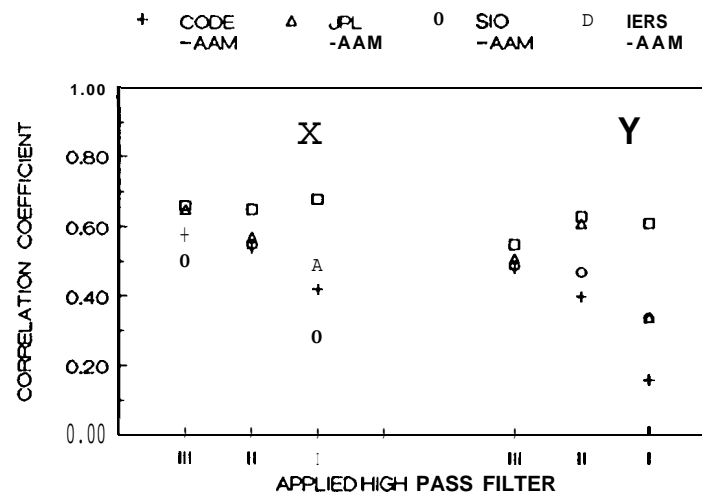


Fig.7 Correlation coefficients between geodetic and AAM polar motion

CONCLUSIONS

The short-term polar motion variations in range from days to months observed by GPS are at 0.5 - 5 mas level according to used high pass filtering and significantly exceed the formal uncertainties. Rms differences for pairs of geodetic series (GPS and combined) are below 1 mas and gradually decrease towards high frequencies. Correlations between geodetic series is also decreasing but remains significant for daily variations except the SIO-CODE pair. Significant correlation 0.4 - 0.6 results from comparison of GPS polar motion series with both IB and without IB approximation atmospheric models.

Monthly, weekly and daily non-tidal UT variations are well observed by GPS CODE series. The monthly GPS oscillations exhibit the most significant discrepancies with other geodetic series, especially in the beginning of IGS campaign. The atmospheric driving of short-term Earth's rotation is recognized by GPS at the time scales from days to months.

ACKNOWLEDGEMENT

Author thanks N. Essaifi from IERS/CB for providing the GPS EOP series and I. Naito and Y. Tamura from NAO Mizusawa for granting the atmospheric angular momentum data.

REFERENCES

- [1] IERS, "1991 IERS Annual Report", Central Bureau of IERS, Observatoire de Paris, 1992
- [2] Yoder, C.F., Williams, J.G., Parke, M.E., "Tidal Variations of Earth Rotation", J. Geophys. Res., 86, 881-891, 1981.
- [3] Ozaki, T., Kuma, K., Kikuchi, N., Naito, I., "Effective Atmospheric Angular Momentum Functions Computed from the Japan Meteorological Agency Data", Priv. Comm., 1993.
- [4] Gross R.S., Lindqwister U., "Comparison of GIG'92 Polar Motion Results with Atmospheric Angular Momentum CHI Functions", JPL Geodesy and Geophysics Preprint No. 222, 1992.
- [5] Vondrak, J., "A Contribution to the Problem of Smoothing Observational Data", Bull. Astron. Inst. Czechosl. 20, 349-355, 1969.

THE USE OF GPS EARTH ORIENTATION DATA BY THE INTERNATIONAL EARTH ROTATION SERVICE SUB-BUREAU FOR RAPID SERVICE AND PREDICTIONS

Dennis D. McCarthy
U. S. Naval Observatory
Washington, DC 20392 USA

The International GPS Service provides polar motion data which have become an important contribution to the operation of the International Earth Rotation Service (IERS) Sub-bureau for Rapid Service and Predictions. Comparison with other techniques shows that these data provide estimates of the position of the rotational pole with an accuracy of approximately ± 0.5 milliseconds of arc. This accuracy along with the fact that the daily data are available soon after observation could make this source of data a valuable addition to the contributors to the IERS.

INTRODUCTION

Analyses of the orbits of the satellites of the Global Positioning System (GPS) by participants in the International GPS Service (IGS) (Mueller and Beutler, 1992) have provided daily observations of high-accuracy polar motion described by the pole coordinates, x along the Greenwich meridian, and y along the meridian of ninety degrees west. These data are used routinely by the IERS Sub-bureau for Rapid Service and Prediction in its normal operations. The GPS data have also been analyzed by some centers to produce estimates of UT 1 -UTC. Because of unresolved apparent systematic error in these data, however, they are not being used operationally by the Sub-bureau. Also, a longer series of GPS Earth orientation information is required to assess the value of the data in maintaining a reference system over a long period of time. The purpose of this paper is to provide an assessment of these observations and show how this information is used currently.

The National Earth Orientation Service (NEOS) serves as the IERS Sub-bureau for Rapid Service and Predictions. It is comprised of the U. S. Naval Observatory and the National Ocean Services of the National Oceanic and Atmospheric Administration of the United States. Each week NEOS publishes, in IERS Bulletin A, information for approximately 350 users regarding the orientation of the Earth with respect to a celestial reference frame. These data are near real-time estimates of the orientation of the Earth as well as their predictions. This information is obtained from contributors who provide data obtained from very long baseline radio interferometry, laser ranging to satellites and the Moon, and now, from the analyses of GPS orbits.

SOURCES OF DATA

Daily estimates of pole positions have been provided by contributors to the IGS. These contributors include the Department of Energy, Mines, and Resources (EMR), the European Space Agency (ESOC), the GeoForschungsZentrum (GFZ), Jet Propulsion Laboratory (JPL), Scripps Institute of Oceanography, the University of Berne, and the University of Texas Center for Space Research. Estimates of UT1-UTC are contributed by EMR and the University of Berne.

ANALYSIS OF GPS DATA

The time series contributed by each of the institutions mentioned above were analyzed by comparing them with the National Earth Orientation Service (NEOS) combination series produced for the International Earth Rotation Service (IERS) Bulletin A. The data used to produce this series are derived from Very Long Baseline Interferometry (VLBI), Satellite Laser Ranging (SLR) and Lunar Laser Ranging (LLR). Figures 1 and 2 show plots of recent differences in polar motion after the removal of biases. Table 1 shows the statistical analysis of the polar motion data.

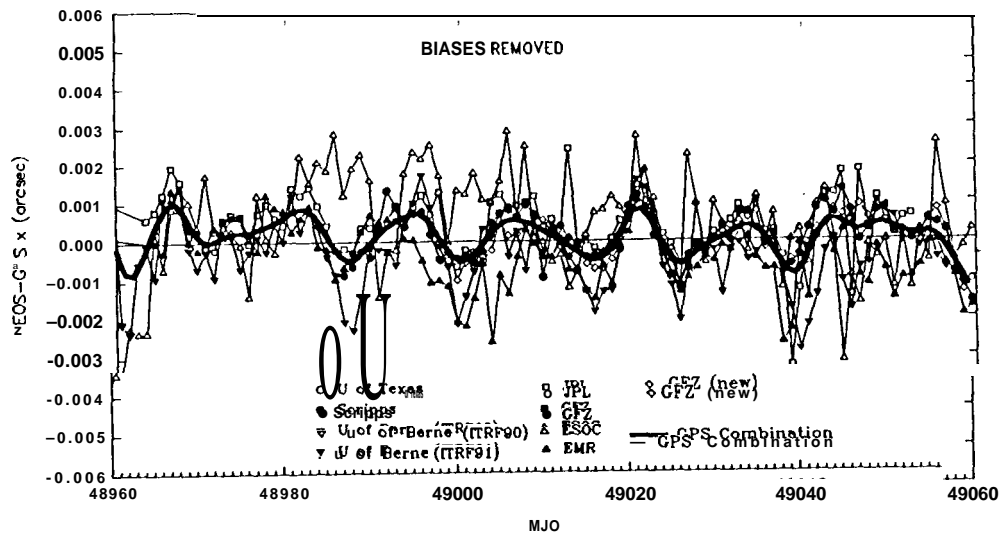


Figure 1. GPS data in x.

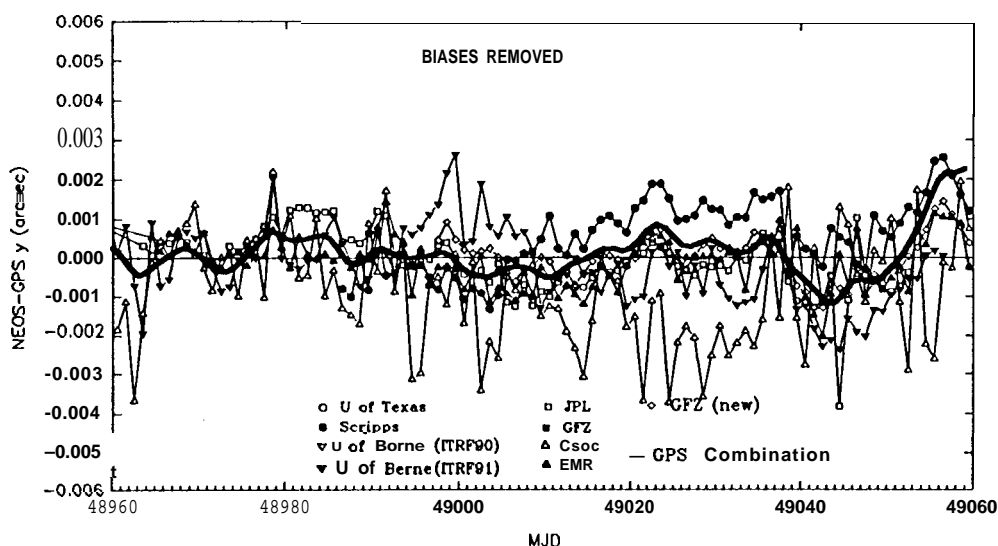


Figure 2. GPS data in y.

Table 1. Comparison of GPS data with NEOS. Units are milliseconds of arc.

| Contributor | Data Span (MJD) | Points | Mean (NEOS - GPS) | | Standard Deviation | |
|-------------------------|--------------------|--------|----------------------|-------|--------------------|------|
| | | | x | y | x | y |
| U. of Texas | 48794.5-48880.5 | 76 | -1.89 | -3.11 | 0.82 | 0.63 |
| Scripps | 48780.5-49052.5 | 236 | -1.56 | -0.81 | 0.65 | 0.67 |
| U. of Berne (ITRF90) | 48792.5-48799.5 | 8 | -0.89 | 1.21 | 1.52 | 1.88 |
| U. of Berne (ITRF91) | 48800.5-49056.5 | 257 | -0.51 | -0.19 | 0.95 | 0.89 |
| JPL | 48794.5-49045.5 | 220 | -0.79 | 0.01 | 0.82 | 0.74 |
| GFZ | 48795.0-48925.5 | 107 | -2.33 | -1.99 | 1.13 | 1.12 |
| ESOC | 48794.5-49052.5 | 259 | -1.17 | -0.89 | 1.42 | 1.85 |
| EMR | 48838.5-49059.5 | 176 | -1.06 | 0.32 | 1.07 | 0.74 |
| GFZ (New Series) | 48997.0-49059.5 | 63 | 1.89 | -1.48 | 0.57 | 0.58 |

USE OF GPS DATA IN IERS BULLETIN A

The NEOS now makes use of GPS data contributed to the IERS in its combination series. This is done by smoothing the contributed data separately using algorithms similar to that used in the procedure to combine the VLBI, SLR and LLR data now (McCarthy and

Luzum, 1991). The smoothed fit is shown in Figures 1 and 2 as a thick solid line. Statistical weights are assigned to each of the contributors based on their past agreement with the NEOS combination series. Figures 3 and 4 show the agreement between the smoothed GPS estimates and those derived using data from other techniques for recent times.

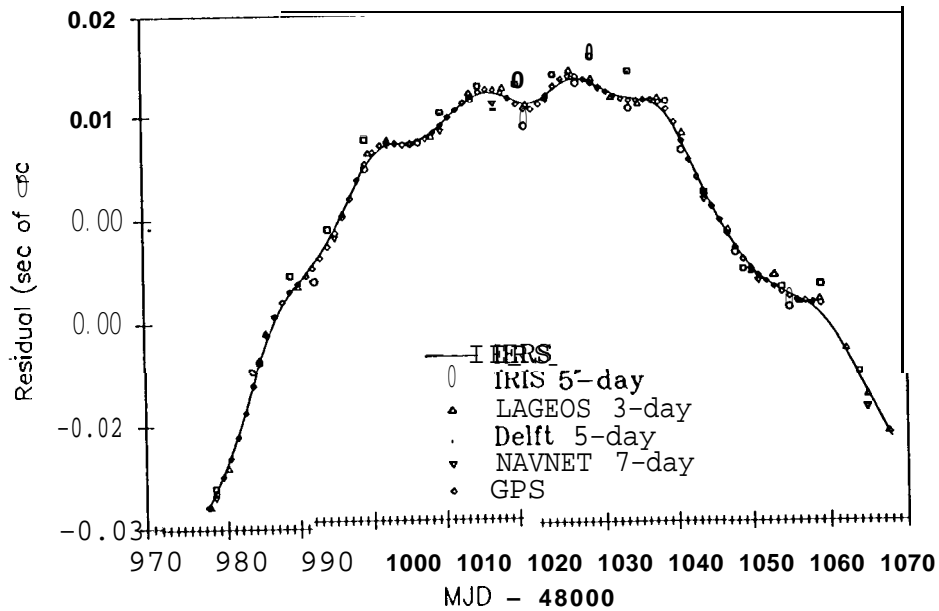


Figure 3. x minus a linear fit.

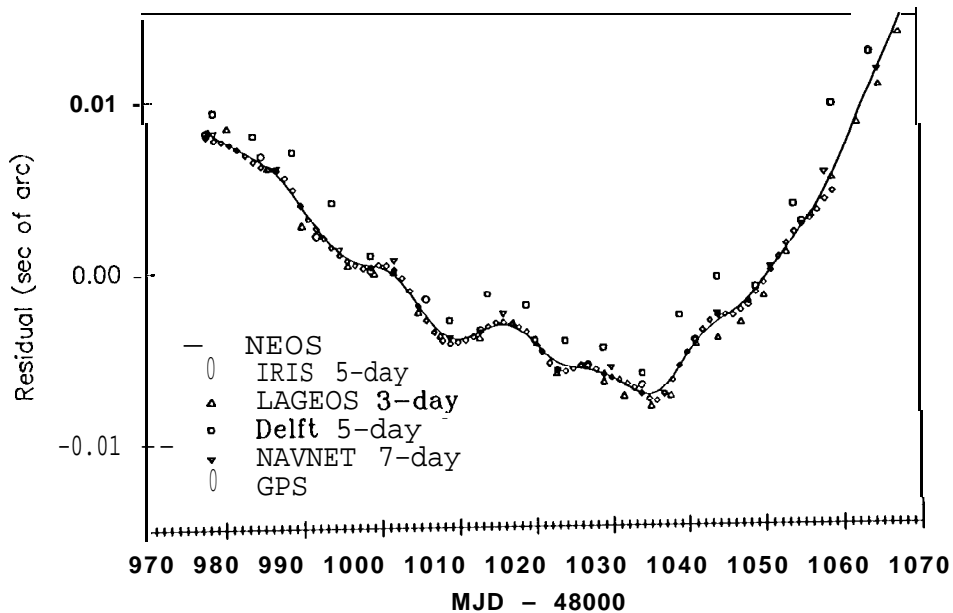


Figure 4. y minus a linear fit.

ACCURACY

Comparison with the other techniques shows that the combined GPS series has an accuracy of ± 0.55 msec of arc in x and ± 0.48 msec of arc in y. Figures 1 and 2 show that serious systematic differences between the contributors remain which must be resolved to obtain further improvement.

CONTRIBUTION TO RAPID SERVICE AND PREDICTIONS

The contribution to the rapid service estimates of polar motion and prediction are shown graphically in Figure 5. The term "contribution" is estimated by taking into account the frequency with which the data are reported, the adopted *a priori* accuracy of each contributor, and the time delay between the epoch of the last available data point and the date of the weekly publication. It is a measure of the overall weight of the data in the weekly solution.

The contribution of the GPS data to the long-term maintenance of the reference frame remains unclear. A longer series of data is required to assess the value of the information in preserving a reference system over an extended period.

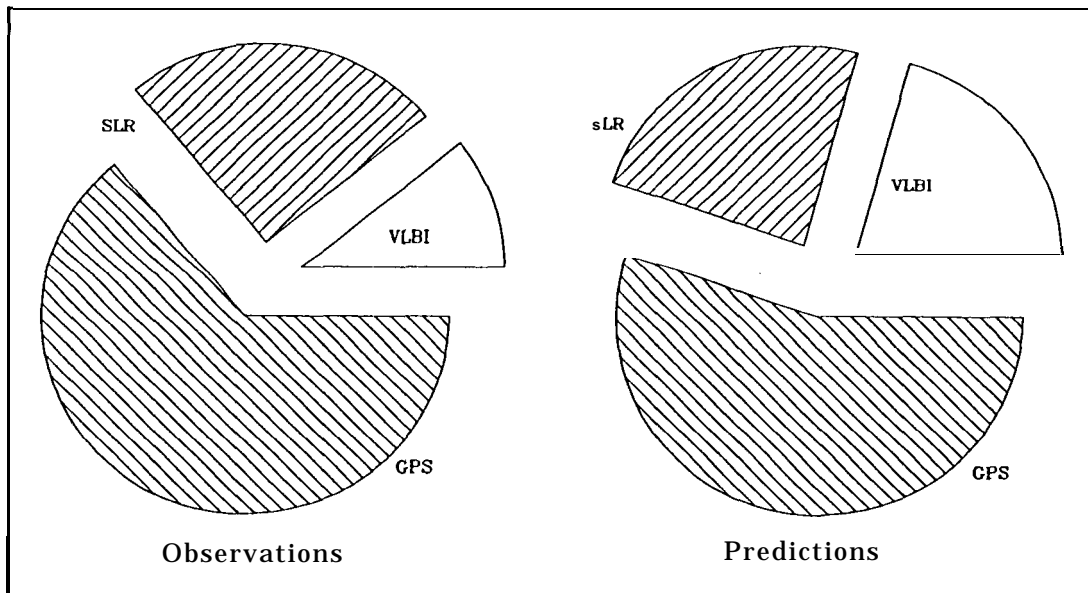


Figure 5. Contribution to rapid service and prediction.

REFERENCES

- McCarthy, D. D. and Luzum, B. J. (1991). Combination of precise observations of the orientation of the Earth, *Bulletin Géodésique*, 65, 22-27.
- Mueller, I. I., and Beutler, G. (1992). The International GPS Service for Geodynamics - Development and Current Structure, *Proceedings of the Sixth International Geodetic Symposium on Satellite Positioning*.

TOWARDS AN OFFICIAL IGS ORBIT BY COMBINING THE RESULTS OF ALL IGS PROCESSING CENTERS

Springer T. A., Beutler G.”

In the near future it will be necessary for the International GPS Geodynamics Service (IGS) to supply the user community with one official orbit instead of all the separate orbits from the different processing centers. This orbit should be a weighted combination based on all the orbit results submitted to the IGS. A good example for such a procedure is the International Earth Rotation Service (IERS) where all the available pole results are combined to yield one official pole.

Here we will present the first experiences made when combining the orbits of different IGS processing centers. The orbits are first compared in both the earth fixed and the inertial reference frame. The results show that the best solution is to combine the orbits in a Earth Fixed (EF) reference frame. We will develop the ideas how to compute the combined solution and we will present the first results.

INTRODUCTION

IGS orbits refer to the (earth fixed) International Terrestrial Reference Frame (ITRF) (Boucher e.a.,1992) and they are distributed in the NGS SP1 or SP3 format (Remondi, 1989). It can be shown however that comparisons between the orbit systems of two different processing centers show significant rotations. These rotations are mainly due to the different pole estimates from the different IGS processing centers. The estimates of the pole coordinates from two centers may differ up to three milliarc seconds (mas), the same differences are found in the orientation of the two orbit systems. Figure 1a illustrates that the difference between the x-coordinates of the pole, as determined by two IGS processing centers, is very closely related to the rotation about the y-axis of the orbit systems of the same two IGS processing centers (rotation parameter about the y-axis of a seven parameter Helmert transformation between the two orbit systems). Figure 1 b shows that an analogous statement holds for the difference between the estimates of the y-coordinates of the pole and the rotation about the x-axis of the two orbit systems. Other reference frame differences may be caused by using different coordinates for the fiducial stations, different software, different force models and many more.

“Both at the Astronomical Institute, University of Bern, Sidlerstrasse 5, CH-3012 Bern, Switzerland

Figures 1a and 1b show that before combining the orbits in a EF system they must be rotated around the x- and y-axis in order to refer to one and the same reference frame. This procedure is quite simple in principle. First we define or select a “true” IGS pole. This could be a weighted mean of the pole estimates of the IGS centers, but we also might select the IERS pole estimates (Bulletin A or B) for that purpose. Then each individual orbit system has to be rotated by the differences $(x_{igs}-x_{center})$ around the y-axis and $(y_{igs}-y_{center})$ around the x-axis in order to actually refer to the same system.

Figures 1a and 1b also tell us that there are no significant rotations between the different IGS orbits in the inertial system. Therefore another possibility would be to use the pole of each processing center to transform their orbits into the inertial system. This would also remove the reference frame differences caused by differences in the x- and y-coordinate estimates of the pole. This transformation is somewhat difficult due to the different ways the processing centers are submitting their results of the LOD estimation. Due to this problem and due to the fact that the rms values of the orbit comparisons were not significantly smaller in the inertial system compared to the comparisons in the earth fixed system we decided to combine the orbits in the earth fixed system.

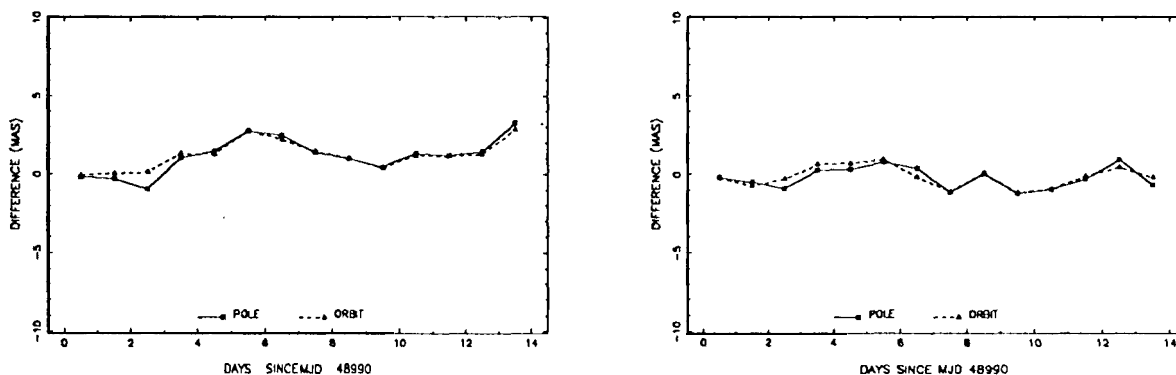


Figure 1a: Difference in x-coordinate of the pole and y-rotation of the orbit system between EMR & COD (left) and JPL & COD (right)

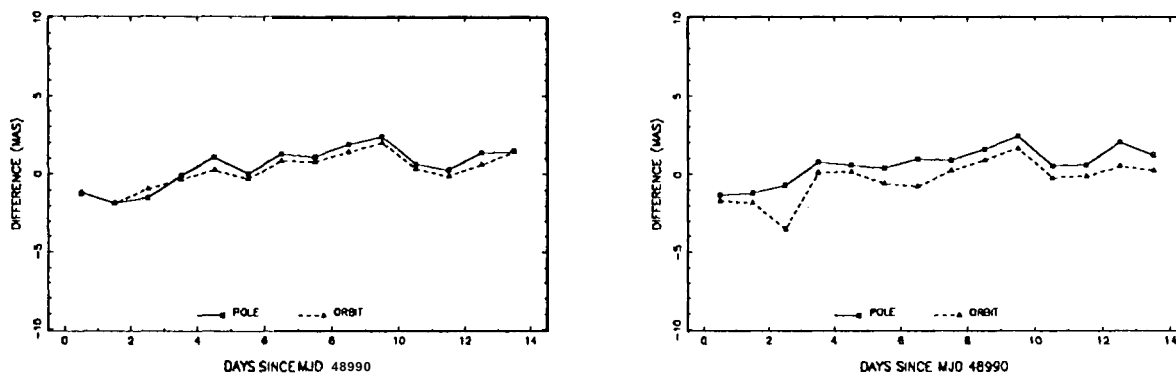


Figure 1b: Difference in y-coordinate of the pole and x-rotation of the orbit system between EMR & COD (left) and JPL & COD (right)

Another interesting fact following from Figures 1 is that there is almost no correlation between the estimation of the orbits in the inertial system and the estimation of the pole. We made a small test in which we corrupted the pole by tens of mas followed by a parameter estimation in which the pole was not estimated but fixed to these corrupted values. The comparison of the resulting inertial orbit with the “true” inertial orbit showed no significant differences. This characteristic is only true if we use sampling intervals if an integer number of days.

ORBIT COMBINATION

Principle

We want to create **one** combined orbit ephemerides file for each day. The ephemerides will be given in the NGS SP3 format and will refer to the ITRF system. As “true” pole we adopt the IERS pole (Bulletin A or B) and each individual orbit system is rotated by the differences $(x_{iers}-x_{center})$ around the y-axis and $(y_{iers}-y_{center})$ around the x-axis.

Significant differences in achieved accuracies exist between the IGS processing centers. Also the accuracies of individual centers show noticeable differences from day to day. To be able to use the orbit estimates from **all** processing centers the combined orbit will have to be represented by a weighted mean of the orbit estimates from all processing centers. These weights will have to be determined prior to the orbit combination and for every day new weights for all processing centers have to be determined.

Reference frame differences between two centers might exist even after applying the rotations described above. We solve this problem by estimating the parameters of a seven parameter Helmert transformation for each day and each IGS processing center. From the analysis of a long series of orbit estimates a systematic difference between two centers may be determined. The orbit systems can then be corrected a priori in the same way as they are corrected for the pole differences. The seven parameter Helmert transformation would become obsolete in the long run.

Problems exist in the modelling of eclipsing GPS satellites. This will show up as different accuracies for different satellites. Other satellite specific problems might arise because of manoeuvres and for new satellites (e.g. due to warming effects). To avoid any influence of badly modelled satellites on the determination of the Helmert transformation parameters it will be necessary to use satellite specific weights in the estimation scheme. These weights have to be determined before the Helmert estimation.

Different spacing between data points are used in the ephemeris files produced by different centers. Most centers use a 15 minute interval for the ephemerides but some use other intervals. To insure that the combined orbit is based on the results from all processing centers only those epochs common to all centers are used. Another problem is the absence of satellites in one or more of the ephemerides files. At present we get around that problem by leaving out satellites in the combined orbit which are missing in one or more of the ephemerides files. This seems an acceptable ad hoc solution because missing satellites are either new satellites or satellites which experienced a manoeuvre on that specific day.

Thus the principle of our orbit combination can be summarized as follows. The orbits will be combined in the ITRF system and therefore the combined orbit will refer to the same system, The orbit estimates of all IGS processing centers will be used but center specific weights will be applied to reduce the effect of less precise orbit estimates. To remove reference frame differences between the different processing centers a seven parameter **Helmert** transformation is estimated for each day and center. In this estimation satellite specific weights are used in order reduce the influence of bad modelled satellites.

Parameter Estimation

In a first step the ephemerides files of each processing center are rotated into the ITRF as described above. Comparisons between the orbit system of the different processing centers show rotations around the z-axis in the order of several mas. Therefore it was decided to use one center as reference and rotate the orbit systems of the remaining centers with respect to this reference center using the value of the estimated z-axis rotation between this reference center and each individual processing centers.

In a second step we have to determine the a priori center specific and satellite specific weights. We therefore compute the unweighed mean value for every satellite position. Let us call the result of this procedure the first combined orbit system. Then we perform a seven parameter **Helmert** transformation between this first combined orbit system and the orbit system of each individual IGS center. From the rms errors of the transformed satellite position the center specific and satellite specific weights are determined. The center specific weights are used to compute the weighted mean value for every satellite position, see Eq. 1.

$$\bar{x} = \frac{\sum_{i=1}^n \frac{\bar{x}_i}{\sigma_i^2}}{\sum_{i=1}^n \frac{1}{\sigma_i^2}} \quad (1)$$

Where: \bar{x}_i satellite coordinate vector as estimated by center i,
 σ_i rms for center i as established in the first **Helmert** transformation.

Let us call the result of this procedure the second combined orbit system. Then, in a third step, a seven parameter **Helmert** transformation is performed between this second combined orbit system and the orbit system of each individual IGS processing center using the satellite specific weights in the least squares estimation. After the last iteration of this least squares estimation the IGS orbit is formed using the estimated **Helmert** parameters and the center specific weights, see Eq.(2)

$$\bar{x} = \frac{\sum_{i=1}^n \frac{R_{i_{kellm}} (\bar{x}_i + \Delta \bar{x}_{i_{kellm}})}{\sigma_i^2}}{\sum_{i=1}^n \frac{1}{\sigma_i^2}} \quad (2)$$

Where: \bar{x}_i satellite coordinate vector as estimated by center i,
 σ_i rms for center i as established in the first Helmert transformation,
 $R_{i_{kellm}}$ rotation matrix containing the three estimated rotations and the estimated scale factor for center i,
 $\Delta \bar{x}_{i_{kellm}}$ vector containing the three estimated transformations for center i.

RESULTS

We have analyzed orbits from four different weeks. Namely the two weeks of Epoch'92 and the first **two** full weeks of 1993. The time frame of Epoch'92 was chosen since it is most likely that for this period the need for an IGS orbit will soon arise. The first two weeks of January were chosen to analyze a more recent dataset because the number of GPS satellites has increased from 18 during Epoch'92 to 21 in January 1993 and because several processing centers have improved their processing strategies. Furthermore it should be noted that for Epoch'92 the processing centers CODE, JPL and S10 have reanalyzed the data and the orbit ephemerides from these **new** analyses were used,

A first problem that showed up was the fact that the pole coordinate differences of S10 did not correlate with the estimated orbit rotations for the first two weeks of January as can be seen in Figure 2, they should be correlated as in Figures 1. Therefore in the case of S10 we have corrected all three rotation using the estimated rotations with respect to the same reference center used for the z-axis rotations. The reference center chosen to was CODE.

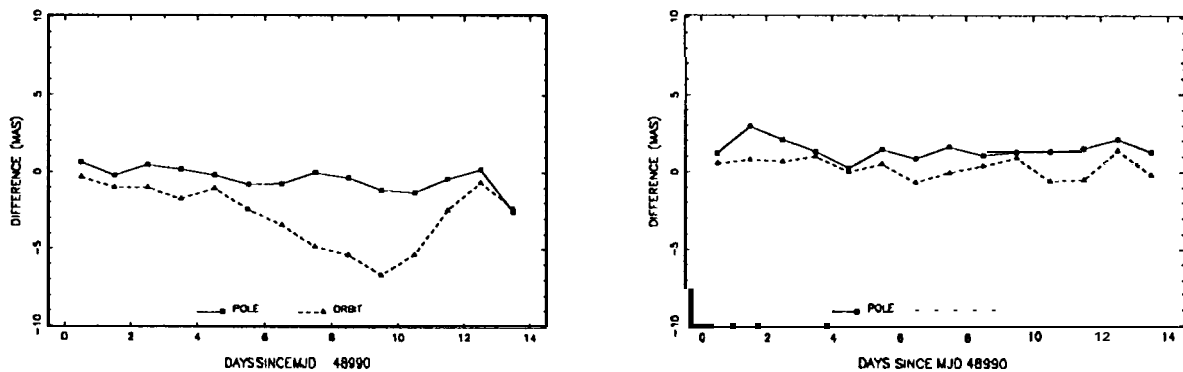


Figure 2: Difference in x-coordinate of the pole and y-rotation of the orbit system (left) and y-coordinate of the pole and x-rotation of the orbit system (right) between S10 & EMR

Table 1 shows the center specific rms values as determined in the first step of the orbit combination. Here one can see the relatively large day to day variations in the achieved accuracies for each center.

Table 1
RMS PER CENTER FOR ORBIT COMBINATION

| DAY " (MJD) | RMS COD | (m) for EMR | center ESA | GFZ | J PL | S10 | UTX |
|----------------|-------------|----------------|---------------|-------------|-------------|-------------|-------------|
| 48829 | 0.26 | | 0.83 | 0.39 | 0.18 | 0.26 | 0.50 |
| 48830 | 0.28 | | 0.73 | 0.27 | 0.13 | 0.19 | 0.39 |
| 48831 | 0.26 | | 1.18 | 0.37 | 0.19 | 0.19 | 0.43 |
| 48832 | 2.13 | | 0.75 | 0.41 | 0.15 | 0.29 | 0.59 |
| 48833 | 0.20 | | 1.85 | 0.41 | 0.18 | 0.24 | 0.30 |
| 48834 | 0.24 | | 0.78 | 0.36 | 0.14 | 0.16 | 0.34 |
| 48838 | 0.22 | | 0.74 | 0.33 | 0.15 | 0.14 | 0.25 |
| 48839 | 0.12 | | 0.73 | 0.33 | 0.12 | 0.19 | 0.33 |
| 48840 | 0.17 | | 0.88 | 0.31 | 0.12 | 0.23 | 0.22 |
| 48841 | 0.28 | | 0.94 | 0.48 | 0.12 | 0.19 | 0.18 |
| 48990 | 0.26 | 0.18 | 0.90 | | 0.15 | 0.20 | |
| 48991 | 0.33 | 0.2.3 | 0.86 | | 0.13 | 0.29 | |
| 48992 | 0.51 | 0.28 | 0.67 | | 1.09 | 0.50 | |
| 48993 | 0.13 | 0.23 | 0.77 | | 0.38 | 0.27 | |
| 48994 | 0.14 | 0.17 | 1.15 | | 0.54 | 0.27 | |
| 48995 | 0.21 | 0.15 | 0.79 | | 0.25 | 0.26 | |
| 48996 | 0.27 | 0.16 | 0.74 | | 0.49 | 0.18 | |
| 48997 | 0.24 | 0.11 | 0.70 | | 0.36 | 0.20 | |
| 48998 | 0.22 | 0.11 | 0.76 | | 0.24 | 0.20 | |
| 48999 | 0.22 | 0.17 | 0.62 | | 0.26 | 0.26 | |
| 49000 | 0.22 | 0.15 | 0.73 | | 0.23 | 0.22 | |
| 49001 | 0.17 | 0.13 | 0.73 | | 0.31 | 0.21 | |
| 49002 | 0.17 | 0.16 | 0.84 | | 0.89 | 0.28 | |
| 49003 | 0.19 | 0.23 | 0.96 | | 0.18 | 0.24 | |

• Days influenced by AS are excluded

In order to verify that the orbit resulting from the combination is closely related to a solution of the equations of motions we used the orbit in our processing software, the Bernese GPS software version 3.4 (Rothacher, 1991), to create a so called standard orbit. This standard orbit is created by an integration of the equations of motion and by making the best fit, in the least square sense, of the given ephemerides. The rms errors per coordinate of this fit gives an indication of how well the ephemerides comply with the equations of motion. Table 2 lists the results for one of the satellites for all processing centers and for the combined orbit for the first two full weeks of 1993. The results are similar for all satellites. Note that for the individual processing centers the orbits were first rotated into the ITRF and rotated around the z-axis with respect to the reference center as described above.

The rms values of CODE are of course very low because here the same program, and therefore the same modelling, is used to reconstruct the orbit as was used in creating them. That the rms values are not exactly equal to zero is caused by second order pole effects (e.g. pole drift) because a slightly different pole is used. Here we used the IERS pole (EOP90C04) and the CODE precise orbits are created using our own pole estimates. Other centers will use

other modelling methods (e.g. stochastic) and/or different reference frames which will cause disagreements with our orbit modelling and therefore larger rrns values. Nevertheless we can conclude that the combined orbit may very well be approximated by a particular solution of the equations of motion.

Table 2
RMS OF ORBIT FIT FOR SATELLITE 2

| DAY (MJD) | RMS IGS | (m) for COD | center EMR | ESA | J PL., | S10 |
|--------------|------------|----------------|---------------|------|--------|------|
| 48990 | 0.06 | 0.02 | 0.10 | 0.04 | 0.09 | 0.05 |
| 48991 | 0.12 | 0.01 | 0.21 | 0.04 | 0.17 | 0.05 |
| 48992 | 0.06 | 0.02 | 0.13 | 0.03 | 0.14 | 0.05 |
| 48993 | 0.03 | 0.02 | 0.08 | 0.05 | 0.08 | 0.04 |
| 48994 | 0.02 | 0.01 | 0.04 | 0.06 | 0.11 | 0.06 |
| 48995 | 0.03 | 0.02 | 0.06 | 0.05 | 0.10 | 0.05 |
| 48996 | 0.05 | 0.01 | 0.11 | 0.08 | 0.12 | 0.04 |
| 48997 | 0.03 | 0.01 | 0.06 | 0.04 | 0.29 | 0.03 |
| 48998 | 0.03 | 0.01 | 0.05 | 0.06 | 0.08 | 0.04 |
| 48999 | 0.04 | 0.01 | 0.07 | 0.04 | 0.12 | 0.04 |
| 49000 | 0.03 | 0.01 | 0.03 | 0.07 | 0.12 | 0.05 |
| 49001 | 0.05 | 0.01 | 0.10 | 0.05 | 0.11 | 0.07 |
| 49002 | 0.02 | 0.01 | 0.05 | 0.03 | 0.11 | 0.05 |
| 49003 | 0.04 | 0.01 | 0.08 | 0.05 | 0.10 | 0.06 |

DISCUSSION

We will have to modify the program to include satellites missing in one or more of the files. Also it will be necessary to use all data points and not only the simultaneous epochs in the files. The best solution would be to specify a standard time interval to be used by all processing centers.

Although it will always be necessary to correct the orbits for the pole coordinate differences it should be possible in the future to combine the orbits without estimating any remaining transformations and rotations. This can be achieved by determining a constant set of seven Helmert transformation parameters for each center based on the analysis of a long series of orbits, comparable with the constant pole offsets the IERS is using for each center submitting pole estimates. Table 3 lists the mean and rms of the seven Helmert parameters estimation over the 14 day period in January 1993. Of course this time period is too short to serve as a reliable source for adopting a constant set of Helmert transformation parameters. It is shown here to give the reader an impression of the size of the transformation parameters. The rms value could also be determined from such an analysis although this might be somewhat troublesome due to the satellite problems that occur from time to time and the large day to day variations of the individual processing centers.

Table 3
MEAN AND RMS OF THE HELMERT TRANSFORMATIONS OVER A 14
DAY PERIOD

| CENTER | | DX (m) | DY (m) | DZ (m) | RX (mas) | RY (mas) | RZ (mas) | SCALE |
|--------|------|-----------|-----------|-----------|-------------|--------------|-------------|---------|
| CODE | MEAN | -0.007 | 0.009 | -0.027 | -0.31 | -0.05 | 0.14 | -0.0002 |
| | RMS | 0.003 | 0.003 | 0.008 | 0.04 | 0.03 | 0.10 | 0.0000 |
| EMR | MEAN | 0.012 | 0.001 | 0.007 | 0.02 | -0.01 | -0.13 | 0.0003 |
| | RMS | 0.003 | 0.005 | 0.006 | 0.06 | 0.06 | 0.09 | 0.0001 |
| ESA | MEAN | 0.006 | -0.030 | 0.009 | 0.70 | -0.12 | 0.57 | -0.0004 |
| | RMS | 0.022 | 0.012 | 0.011 | 0.15 | 0.13 | 0.17 | 0.0002 |
| JPL | MEAN | 0.026 | -0.066 | -0.021 | 0.64 | -0.14 | 0.22 | -0.0004 |
| | RMS | 0.006 | 0.007 | 0.006 | 0.06 | 0.05 | 0.26 | 0.0001 |
| S10 | MEAN | -0.039 | 0.046 | 0.019 | -0.20 | 0.13 | 0.05 | 0.0000 |
| | RMS | 0.006 | 0.008 | 0.005 | 0.11 | 0.05 | 0.11 | 0.0001 |

ACKNOWLEDGMENTS

We would like to thank Jan Kouba (EMR), Joachim Feltens (ESA), James F. Zumberge (JPL), Yehuda Bock (S10) and Bob Schutz (UTX) for supplying us with the detailed pole information for the orbits used in our analysis. These contributions were essential for our understanding of the procedures applied at the individual IGS processing centers.

REFERENCES

Boucher, C., Z. Altamimi, L. Duhem; ITRF 91 and its associated velocity field; IERS Technical note 12; Observatoire de Paris; October 1992.

Remondi, Benjamin W.; Extending the National Geodetic Survey Standard GPS Orbit Formats; NOAA Technical Report NOS 133 NGS46; November 1989.

Rothacher, M.; Bernese GPS software version 3.3; Berne; May 1991.

Chapter 5

Epoch '92

Solutions using European GPS Observations produced at the “Center for Orbit Determination in Europe” (CODE) during the 1992 IGS Campaign

E. Brockmann, G. Beutler, W. Gurtner
M. Rothacher, T. Springer *
L. Mervart †

During the 1992 IGS test campaign the IGS Processing Center CODE (Center for Orbit Determination in Europe) performed solutions using data of 12 European sites (in addition to the routine “global solutions”). The goal of these regional solutions was the estimation of station coordinates of the European stations involved in IGS and a comparison of the accuracy level of the “European orbits” with respect to the orbits determined using the worldwide IGS Core Network. During the three months data processing (21 June - 23 September 1992) more than 100 overlapping 3-day solutions were computed. With the beginning of the *IGS Pilot Service* this processing mode was modified by introducing all European stations as “free” stations (see below) into the Global network. The paper will show that the European station coordinates agree with the ITRF coordinates on the 1-2 cm level. The European orbits differ significantly (2 m rms level) from the global orbits. Problems arise for the orbit determination with European stations on AS (anti spoofing) days. Nevertheless the European orbits are of similar quality as the globally determined ones for regional surveying tasks.

INTRODUCTION

The Astronomical Institute, University of Berne (AIUB), the Federal Institute of Topography (L+ T), the Institut Géographique National (IGN), the Institute of Applied Geodesy (IfAG) are part of the CODE (Center for Orbit Determination in Europe) processing center of IGS. In order to be able to collect, preprocess, and process data of some 30 stations every day a highly automated data processing scheme had to be set up at CODE. This covers the data collection of the receivers through the IGS distribution system (see [3, *Gurtner W. 1992*]) and the *Bernese GPS Software* (see [8, *Rothacher M. 1993*]) for the data processing.

THE EUROPEAN STATION NETWORK

The 12 sites in the European network (plus Zimmerwald, Switzerland (Trimble) and Bar Gyora, Israel) are listed in Table 1.

*all at the Astronomical Institute, University of Berne

†Institut of Geodesy, Technical university of Prague

Table 1: European Sites: Core Stations and fiducial sites

| Site | Site number | VLBI /SLR Receiver | % data available during campaign |
|----------------------|-----------------|--------------------|----------------------------------|
| Graz Lustbühl | GRAZ 11 001M002 | SLR | Rogue 94.8 |
| Herstmonceux | HERS 13212M007 | SLR | Rogue 80.0 |
| Kootwijk | KOSG 13504M003 | SLR | Rogue 97.4 |
| Madrid | MADR 13407S012 | VLBI | Rogue 87.0 |
| Mat era | MATE 12734M008 | VLBI | Rogue 94.0 |
| Metsahovi | METS 10503S011 | SLR | Rogue 90.4 |
| Onsala | ONSA 10402M004 | VLBI | Rogue 98.3 |
| Tromsø | TROM 10302M003 | VLBI | Rogue 95.6 |
| Wettzell | WETT 14201S020 | VLBI/SLR | Rogue 87.0 |
| Mas Palomas | MASP 31303M001 | -- | Rogue 93.0 |
| Ny-Alesund | NYAL 10317M001 | -- | Rogue 92.2 |
| Zimmerwald | ZIMM 14001M004 | SLR | Ashtech 48.7 |
| Bar Gyyora *) | BARG 20702M002 | -- | Trimble 3.5 |
| Zimmerwald **) | ZIMM 14001M002 | SLR | Trimble 60.0 |

*) only during Epoch '92 Campaign

**) processed independently for orbit checks

The data of the IGS core stations were available very reliably during the entire campaign. The average availability was about 90%. The same is true for the fiducial stations Mas Palomas and Ny-Alesund. A Trimble receiver was in Zimmerwald during the entire campaign. It was used for test purposes and orbit quality checks only. For this receiver we encountered problems with elevation dependent phase center variations [6, Rocken, C. 1992]. From 27 July to 5 October 1992 an Ashtech receiver could be used in Zimmerwald. These data were included in our daily analyses.

PROCESSING STRATEGY

Data flow

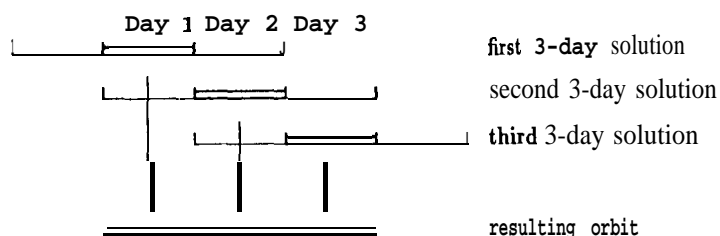
The IGS core data were sent to CODE through Internet (FTP) by the *Network Datacenter* IGN (Institut Géographique National, Paris, France) and the *Regional Datacenter* at IfAG (Institut für Angewandte Geodäsie, Frankfurt). The data transfer automatically starts every day at 00:00 local time and ends at about 7:00 in the morning. On 4-5 out of 7 days no manual interactions were and are necessary.

Processing

After datafile decompression, data screening, code processing, orbit preparation, etc. which are common for the global and the European solutions, daily solutions are performed. We use them only for the data check. Afterwards overlapping 3-day solutions are computed using ITRF91 coordinates as fixed coordinates for orbit estimation. Then we produced so-called free network solutions. We solve for station coordinates, orbital elements plus direct

radiation pressure and y-bias for each satellite, about four troposphere zenith delays per day and site, and for ambiguity parameters. Daily values of the x and y coordinates of the pole and the UT1-UTC drift (equivalent to the length of day) are only determined in the global network solution.

We use double difference phase observations forming the ionosphere free linear combination of the phase observations. The models in our analyses follow as closely as possible the IGS Standards. We are using the ITRF91 velocity model for the station coordinates, 20 degree elevation cut-off angles, and 3 minute data sampling. We produce overlapping 3-days solutions modelling the satellite orbits with 3-day arcs:



The processing was severely handicapped by AS, the so-called “Anti-Spoofing”, which was turned on for a varying number of satellites on most of the weekends following August 1. Unfortunately the principal receiver of the core network did not handle the L_2 phases properly under AS. In spite of the limited amount of available observations during AS days CODE delivered orbits for all days of the campaign. If only European sites were used the orbit accuracy was drastically reduced. Since end of February 1992 most of the receivers got an upgraded receiver firmware which should no longer show problems under AS.

Two types of European solutions were produced:

- “free” network solutions
- regional orbit determination (using ITRF91 coordinates of the stations Kootwijk, Madrid, Matera, Tromsø, Wettzell and Onsala as fixed)

EUROPEAN SOLUTIONS

Free Solutions during the IGS 1992 Test Campaign

The a priori constraints of the “free” solutions are:

| Constraint on | East and North-Coordinates | Up-Coordinate |
|---------------------|----------------------------|---------------|
| Wettzell: | 0.02 m | 0.05 m |
| all other Stations: | 0.05 m | 0.10 m |

These constraints are introduced through quasi observations with a priori weights in the normal equation system. In view of the resulting variance-covariance matrix the relative network geometry is not affected by these constraints.

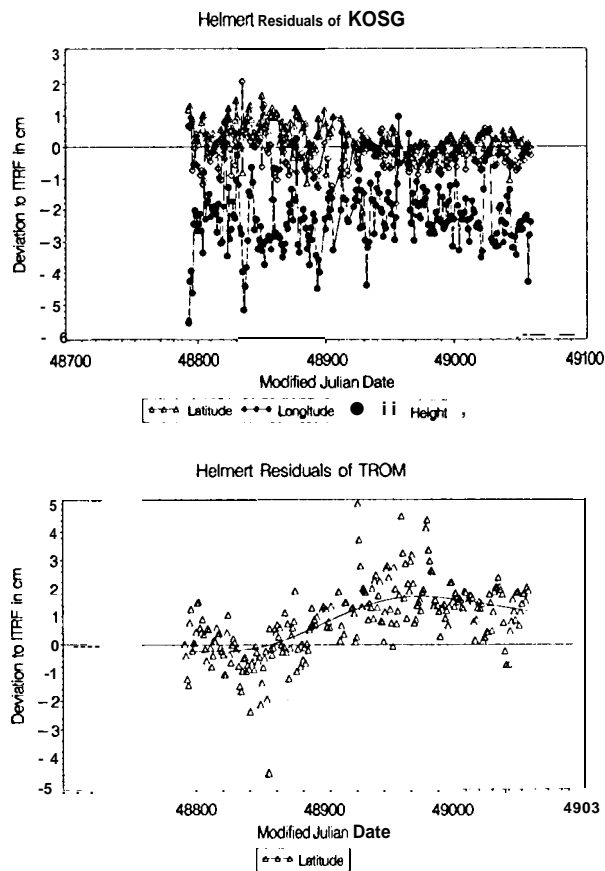


Figure 1: Timeseries of the residuals of the stations Kootwijk and Tromsø after a Helmert transformation of each free solution with respect to the ITRF91 coordinates, all AS days included.

For 115 3-day solutions (overlapping, days 171 to 285) the residuals of all European sites with respect to the ITRF coordinates were analysed (after 6 parameter Helmert transformation (3 rotations, 3 translations)). These residuals are in some cases significantly different from zero. The GPS derived height in Kootwijk e.g. differs by -2.5 cm from the ITRF91 coordinates (see Figure 1). The day to day variations are larger by a factor of 3-4 in the height than in the horizontal coordinates. The offset of -2.5 cm seems to be real however. In Figure 1 the results of the “AS - weekends” are included too. Larger residuals are mostly due to that circumstance.

After the end of the IGS 1992 Campaign we changed the processing mode. With the beginning of the *IGS Pilot Service* on November 1, 1992 the “free European solutions” are performed with all global sites included, some of them as fixed sites. This improved the daily repeatability by a factor of 2-3 (see Figure 2) and reduced the scatter in Figure 1 after November 1 (MJD 48927) significantly.

A coordinate set (EU-92) was computed with the following properties:

- The sum of the residuals (after 6 parameter Helmert transformation (no scale para-

meter) of each 3-day solution to EU-92) over all days of each coordinate is zero.

- Scale, translation and orientation of EU-92 is the same as ITRF.

This coordinate set was submitted to IERS and was used for an improvement of the ITRF91 coordinates (see [2, *Boucher C. 1993*]) together with the coordinate estimation of other *IGS Processing Centers*.

In Table 2 the Helmert transformation of EU-92 to ITRF91 is given.

Table 2: Residuals of a Helrnert transformation between the mean GPS coordinates EU-92 (days 171-285, only European stations) with ITRF91. rms error of the transformed coordinates: 1.1 cm, no translation and rotation between both coordinate sets.

| Station name | VLBI / SLR | Residuals in Meter | | |
|-------------------------|------------|--------------------|---------|---------|
| | | North | East | up |
| Graz Lustbühl | SLR | 0.0047 | -0.0192 | 0.0041 |
| Herstmonceux | SLR | -0.0013 | -0.0097 | 0.0039 |
| Kootwijk | SLR | 0.0057 | -0.0019 | -0.0249 |
| Madrid | VLBI | 0.0007 | 0.0174 | 0.0105 |
| Mat era | SLR | -0.0096 | -0.0031 | 0.0092 |
| Troms o e | V L B I | -0.0009 | 0.0077 | 0.0070 |
| Wetzell | VLBI | 0.0153 | 0.0076 | -0.0065 |
| Onsala | VLBI | 0.0062 | -0.0007 | 0.0068 |
| Metsahovi | VLBI | -0.0167 | 0.0053 | 0.0030 |
| Zimmerwald | SLR | -0.0039 | -0.0032 | -0.0130 |
| _ rms of transformation | | 0.0111 | | |

In most cases the EU-92 coordinates agree with ITRF91 on the 1 cm level. Discrepancies are the mentioned height difference in Koot wijk and some smaller deviations in Graz, Madrid, Metsahovi, and Wetzell.

Ambiguities fixed Solutions

In addition to the above routine solutions we made a few three 3-day solutions (mean days 191, 243, and 254) with fixed ambiguities. After fixing the widelane ambiguities using the Melbourne/ Wiibbena linear combination of phase and code ([5, *Melbourne 1985*], [9, *Wübbena 1985*]) an iterative algorithm was used to solve for the narrowlane ambiguities on baselines up to 1000 km (see [4, *Mervart 1993*]). 80% of the ambiguities could be fixed with this procedure.

The residuals of the Helmert transformation between the mean coordinate set of the ambiguity fixed solutions and of the corresponding coordinate set without ambiguities fixing with respect to the mean set of the entire campaign (EU-92, without ambiguity fixing) are given in Table 3. The consistency of the two GPS derived coordinate sets in case (a) using different processing strategies is impressive.

Ambiguities fixed solutions using only data of 9 days of data (three 3-day solutions) are comparable with the results of averaging more than 100 solutions without ambiguity fixing!

We conclude that ambiguity resolution really improves the solution quality. It will interesting to see the corresponding improvement in the other parameters (e.g. orbital elements, earth rotation parameters).

Table 3: Residuals of the Helmert transformations between the mean GPS coordinate set EU-92 (days 171-285, only European stations) with a) the mean coordinate set of three 3-day solutions with 80 % ambiguities fixed. b) the mean coordinate set of three 3-day solutions without ambiguity fixing.

| Station name | VLBI / SLR | a) Residuals in meters | | | b) Residuals in meters | | |
|-----------------------|------------|------------------------|---------|---------|------------------------|---------|---------|
| | | North | East | up | North | East | up |
| Graz Lustbühl | SLR | 0.0015 | -0.0014 | 0.0061 | -0.0099 | -0.0243 | -0.0320 |
| Kootwijk | SLR | -0.0021 | -0.0030 | -0.0008 | 0.0007 | 0.0195 | -0.0029 |
| Madrid | VLBI | -0.0040 | 0.0025 | -0.0017 | -0.0405 | 0.0396 | 0.0158 |
| Mat era | SLR | 0.0013 | 0.0059 | 0.0080 | -0.0286 | -0.0058 | -0.0030 |
| Troms o e | VLBI | 0.0027 | 0.0017 | 0.0190 | 0.0423 | -0.0118 | -0.0333 |
| Wettzell | VLBI | 0.0020 | -0.0011 | 0.0016 | -0.0077 | 0.0034 | -0.0048 |
| Onsala | VLBI | -0.0013 | -0.0061 | -0.0163 | 0.0149 | 0.0078 | -0.0010 |
| Metsahovi | VLBI | 0.0000 | 0.0015 | -0.0159 | 0.0288 | -0.0284 | 0.0611 |
| rms of transformation | | 0.0081 | | | 0.0291 | | |

Solutions during the IGS Pilot Service

To check the accuracy of the European coordinate set EU-92 a third coordinate set was estimated. This set was derived from a global station network with data since the beginning of the *IGS Pilot Service*. In these solutions all European stations were included into the global network. Wettzell was kept fix together with seven other VLBI/SLR sites outside Europe. All other European stations were completely free.

Our coordinate set "EU-92-2" is a result of the combination of 119 3-day solutions (7 November 1992-4 March 1993) using the full variance-covariance matrix of each solution. No Helmert transformation is necessary in this procedure. This result is identical with a rigorous least-squares adjustment of the entire 119 3-day solutions in one adjustment step!

Table 4: Residuals of the Helmert transformation of coordinate set EU-92 (days 171-285, only European stations) with coordinate set EU-92-2 (days 312-063(1993), global network, Wettzell and 7 other sites outside Europe fixed)

| Station name | VLBI / SLR | Residuals in Meter | | |
|-----------------------|------------|--------------------|---------|---------|
| | | North | East | up |
| Graz Lustbühl | SLR | -0.0023 | 0.0065 | 0.0009 |
| Herstmonceux | SLR | -0.0054 | -0.0012 | -0.0040 |
| Kootwijk | SLR | -0.0044 | 0.0002 | 0.0057 |
| Madrid | VLBI | 0.0002 | -0.0066 | -0.0002 |
| Hat era | SLR | -0.0029 | -0.0013 | -0.0043 |
| Troms oe | VLBI | 0.0164 | -0.0087 | 0.0008 |
| Wettzell | VLBI | -0.0065 | 0.0060 | 0.0108 |
| Onsala | VLBI | 0.0009 | 0.0042 | -0.0030 |
| Metsahovi | VLBI | 0.0038 | 0.0009 | -0.0068 |
| rms of transformation | | 0.0064 | | |

The GPS derived coordinate sets "EU-92" and "EU-92-2" were estimated in a different way due to the used data (only European data - global station supported data) and due to the computation (analysis of residuals after Helmert transformation – least-squares adjustment with full variance- covariance matrix). Table 4 shows the Helmert transformation between the two solutions "EU-92" and "EU-92-2". With the exception of Tromsø (north component, see Figure 1) and Wet t zell (height) all residuals are below the 1 cm level.

Figure 2 compares the baseline length repeatabilities for the two different processing strategies. A direct comparison is correct even for free solutions because the baseline length is an invariant under rotations and translations. During the IGS 1992 Campaign a repeatability of 13 ppb (part per billion) could be achieved, whereas with the global station support the European baselines are consistent within 4 ppb (improvement by a factor of about 3).

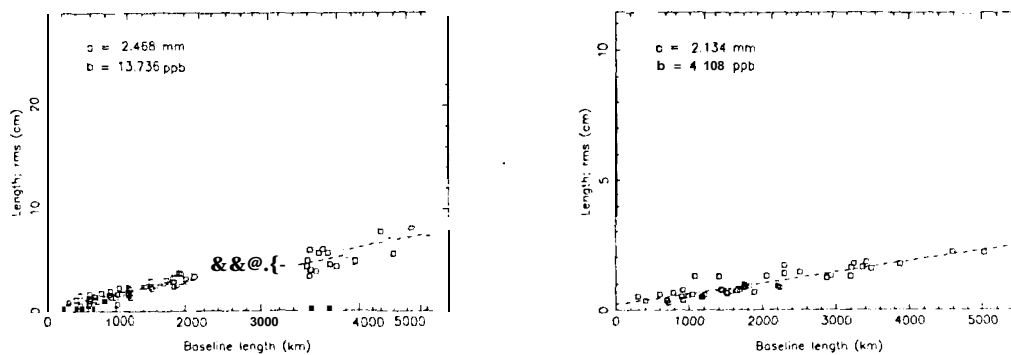


Figure 2: Baseline length repeatability y of the European solutions a) days 171-285 only with European stations, b) days 312-063(1993) with global stations support

ORBIT DETERMINATION USING ONLY EUROPEAN STATIONS

For the time interval 23 June -11 October we determined GPS orbits using the observations from the stations in Table 1 only. All coordinates of the VLBI/SLR stations were fixed on the ITRF values in these solutions. No earth rotation parameters were estimated in this regional analysis. Apart from that the processing strategy was identical with the one used in the global analysis.

A direct comparison between our European and global orbits may give a first impression of the differences. Figure 3 shows these differences for one satellite. Due to problems in orbit determination on "AS - days" with European stations only non-AS-days are compared.

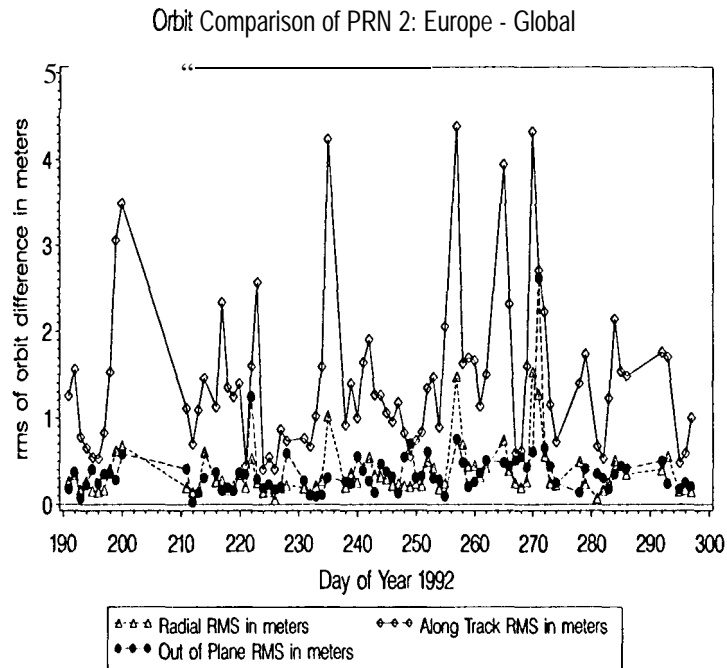


Figure 3: Orbit Comparison over the area of Europe of PRN 2

A better test of the orbit quality consists of the processing of an independent baseline and of comparing the repeatability of the coordinate estimates using different orbits. Figure gives the baseline repeatability of the baseline Wettzell (Rogue) - Zimmerwald (Trimble) (475 km) using (a) Broadcast orbits, (b) European orbits and (c) Global orbits. The data of the Zimmerwald Trimble receiver were not included in the orbit determination. It can be concluded that

- our CODE orbits (Global and European) are superior by a factor of 5-10 with respect to broadcast orbits
- For regional (European) analyses the global and European orbits give results of comparable quality.

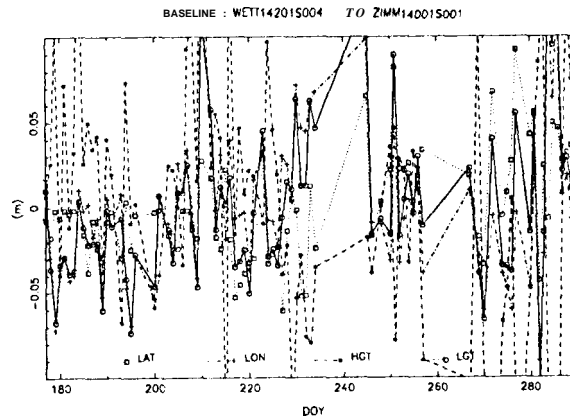


Figure 4a): Baseline repeatability using broadcast orbits

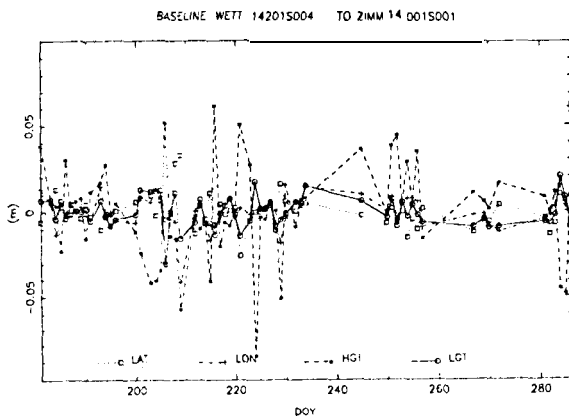


Figure 4b): Repeatability using European orbits

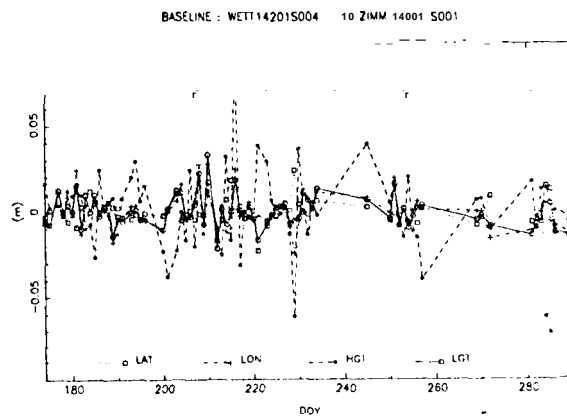


Figure 4c): Repeatability using Global orbits

CONCLUSION

The GPS results show a strong inner consistency. All coordinate sets estimated at CODE during the last 9 months of GPS data (free European solutions, globally supported European solutions (Wettzell fixed), and ambiguities freed solutions) agree on a level below 1 cm. The agreement of the GPS solutions with the ITRF coordinates of the VLBI and SLR stations is of same order of magnitude (exceptions mentioned). The reasons for some of the differences to ITRF may be due to incorrect local ties or antenna height inconsistencies. In two cases (Graz and Metsahovi) we detected such problems on the 3-4 cm level. These GPS derived differences could be removed after a new measurement of the local ties. On such a low level of discrepancies it becomes more and more difficult to detect problems either in the reference frames (VLBI / SLR / GPS - system) or in the local ties. It is only a question of time that errors in the used velocity model will be detected. For this issue totally free solutions will give the best information. At present we are preparing the necessary software

tools to produce solutions of this kind.

We could show that a regional orbit determination service would be able to produce orbits of a similar quality as the global CODE orbits (of course only over the region of the tracking stations).

References

- [1] Beutler, G.: The 1992 Activities of the International GPS Geodynamics Service (IGS), IAG-Symposium No. 112, Potsdam 1992
- [2] Boucher, C.: The Contribution of IGS '92 to the International reference frame, this volume
- [3] Gurtner, W.: Automated Data Flow and Processing at the "Center for Orbit Determination in Europe" (CODE) during the 1992 IGS Campaign, IAG-Symposium No. 112, Potsdam 1992
- [4] Mervart, L.: Ambiguity resolution strategies using the orbit results of the International GPS Geodynamics Service (IGS), this volume
- [5] Melbourne, W.G. : The case for ranging in GPS based geodetic system. First International Symposium on Precise Positioning with GPS, Rockville, 1985
- [6] Rocken, C.: UNAVCO Memo, November 12, 1992
- [7] Rothacher, M.: Results of the "Center for Orbit Determination in Europe" (CODE) during the IGS 1992 Campaign, IAG-Symposium No, 112, Potsdam 1992
- [8] Rothacher, M.: Documentation of the Bernese GPS Software Version 3.4, April 1993, Astronomical Institute, University of Berne (in print)
- [9] Wübbena, G.: Software Developments for Geodetic Positioning with GPS Using TI 4100 Code and Carrier Measurements. First International Symposium on Precise Positioning with GPS, Rockville, 1985

Precise Ephemeris and geodetic campaigns in Sweden 1992

by Gunnar Hedling
National Land Survey of Sweden
S-801 82 Gävle, Sweden

INTRODUCTION

During 1992 the implementation of the SWEPOS Network began. Six stations are already (March 1993) in operation, see figure 1.

The SWEPOS Network has been designed by **Onsala** Space Observatory and the National Land Survey of Sweden to be a multi-purpose network. The stations should have good enough monumentation to be used in **geodynamic** applications. This will be needed in an investigation, supported by the NASA DOSE project, studying postglacial rebound in Fennoscandia. At the same time the rawdata from the stations should be usable for geodetic and photogrammetric production work. Some of the stations will also generate **pseudorange** corrections for DGPS applications.

IGS CAMPAIGN

One of the SWEPOS stations, **Onsala** was a **CORE** station during the IGS 1992 campaign, three of the stations; **Mårtsbo**, **Furuögrund** and **Esränge (Kiruna)** were reported as **FIDUCIAL** stations. During the processing of the Epoch '92 data (see Johansson et al (1992)), **Lovö** close to Stockholm was also treated as a **FIDUCIAL** station.

| Day | 2 | 2 | 2 | 2 | 2 | 2 | 2 | 2 | 2 | 2 | 2 | 2 | 2 | 2 | 2 | 2 |
|---------|------|---|----|---|----|-----|----|---|---|-----|---|---|---|---|---|-----|
| | 0001 | 1 | 1 | 1 | 1 | 1 | 1 | 1 | 1 | 1 | 1 | 1 | 1 | 1 | 1 | 122 |
| Station | 7 | 8 | 9 | 0 | 1 | 234 | 5 | 6 | 7 | 890 | 1 | | | | | |
| MART | X | X | X | X | X | X | X | A | S | X | X | X | X | X | X | XAS |
| LOVO | X | X | X | X | X | X | X | - | - | - | - | - | - | - | - | - |
| FURU | X | X | XX | X | XX | X | XX | - | - | X | X | X | X | X | X | " |
| KIRU | X | X | X | X | X | X | X | - | - | X | X | X | X | X | X | " |

Table. Observation data from the Swedish fiducial stations during Epoch '92.

EPOCH '92 RELATED CAMPAIGNS

During August 1992 several delayed geodetic campaigns took place in Scandinavia and around the Baltic Sea. One reason for the delay was that we have had bad satellite configurations in northern Europe for several years. Another reason is that we used squaring L2-receivers in Scandinavia a couple of years ago. This fact together with a *very* turbulent ionosphere over the North Pole around **1989** made many of the observed datasets a nightmare to process.

In the summer 1992 the ionosphere had calmed down and we had many p-code receivers available. The IGS campaign provided us with quick access to high-precision ephemerides. The time was right to do some long postponed GPS campaigns, see figure 2.

SWET 92

The SWET 92 campaign (Scandinavian West-East Traverse 1992) was carried out 17-25 August using 17 P-code Ashtech receivers (7 with P-code on L1 and L2, 10 with P-code only on L2).

The traverse consists of 34 stations with an interstation distance of about 50 km's. Six stations were permanently equipped with GPS receivers during the campaign. The other stations were observed for at least two days. This campaign was a cooperation between five agencies in four Nordic countries:

Geodettinen Laitos, Finland
Lantmäteriverket, Sweden
SjUfartsverket, Sweden
Statens Kartverk, Norway
Kort- og Matrikelstyrelsen, Denmark

The purposes of the traverse are to check and improve the NKG Nordic Standard Geoid (see Forsberg (1989)).

EUREF-BAL

The EUREF-BAL campaign was observed directly after SWET 92 from August 29 to September 4. As the name implies it is an extension of the EUREF Network.

The same agencies as above where cooperating with:

Riiklik Ehilusuuringute Instituut, Estonia
Department of Geology, Geodesy and Cartography, Latvia
Department of Geodesy, Vilnius Technical University,
Lithuania

The Gotland GPS campaign finally was observed between August 31 and September 3 at the same time as the EUREF-BAL. The purpose of this campaign was to connect the island of Gotland with the Swedish mainland and the Baltic states.

REFERENCES

Forsberg, R.: NKG Nordic Standard Geoid 1989, Proc. of the 11th General Meeting of the Nordic Geodetic commission, pp. 75-89, Copenhagen, 1990.

Johansson, J.M., J.L. Davis, J.X. Mitrovica, I.I. Shapiro, R.T.K. Jaldehag, G. Elgered, B.O. Rönnäng, B. Jonsson, G. Hedling and M. Ekman, Initial GPS measurements of Fennoscandian uplift (abstract), Eos Trans. AGU, 73 (43), Fall Meeting Suppl., 123, 1992.

SWEPOS

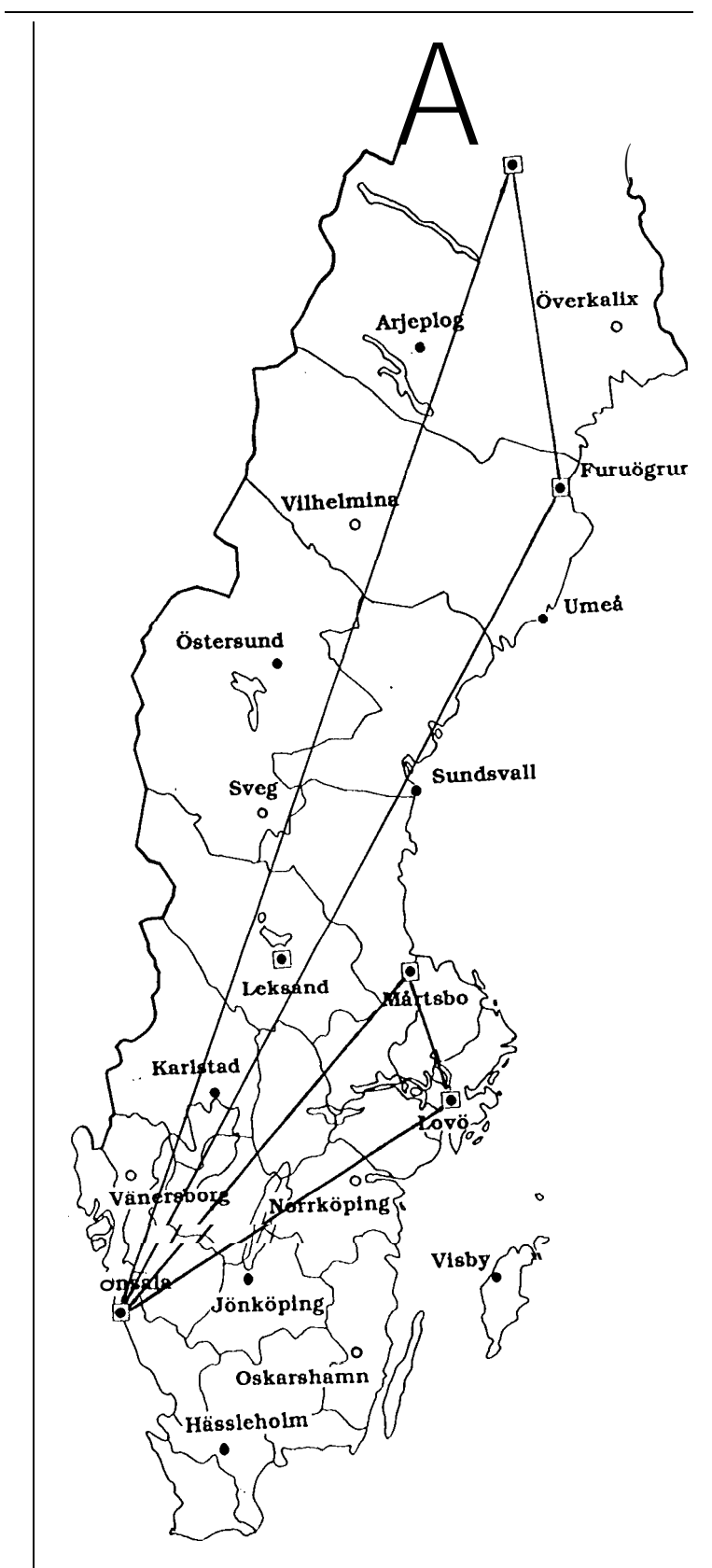
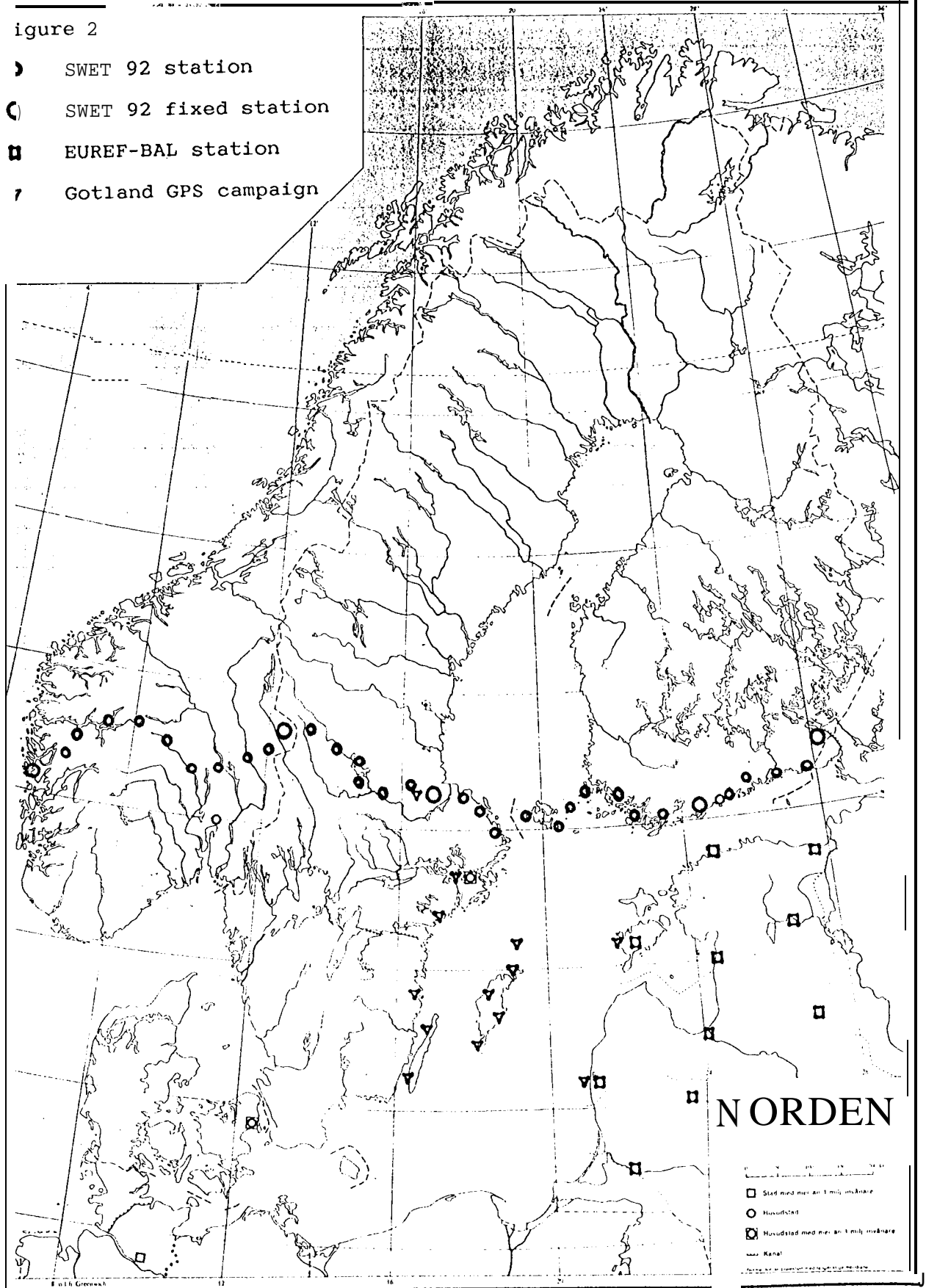


Figure 1

- Planned station
- Monumented station
- ◻ SWEPOS station equipped with GPS receiver (March 1993)
- Epoch '92 baseline loop

Figure 2

- ▷ SWET 92 station
- SWET 92 fixed station
- EUREF-BAL station
- 7 Gotland GPS campaign



SCIENTIFIC CONTRIBUTIONS OF THE SWEDISH IGS ACTIVITIES

J.M. Johansson¹, R.T.K. Jaldehag², J.L. Davis¹, M. Ekman³,
G. Elgered², G. Hedling³, J.X. Mitrovica⁴, B. Jonsson³,
B.O. Rönnäng², and I.I. Shapiro¹

Preliminary measurements of a subnet of the "Fennoscandian GPS network" are presented. Three epochs of data have been analyzed, ranging from July 1992 (Epoch '92) to February 1993, including IGS Core sites and IGS Fiducial sites. About 20 stations have been used in the data analysis where data from the global network were used for satellite orbit determination. Short term repeatabilities on the order of 3-20 ppb in baseline length, and a factor of 4 worse in the vertical component, were obtained. GIPSY II has been used for this analysis. Test cases using the Bernese software version 3.2 and IGS precise ephemerides have been performed. The repeatability obtained in this study implies that the rate uncertainties, after about five years of daily observations, will be 0.3 mm/yr horizontal and 1.2 mm/yr vertical, to be compared to an expected maximum land uplift in Scandinavia due to the post glacial rebound of about 10 mm/yr vertical and a horizontal motion of about 1-2 mm/yr.

INTRODUCTION

The last million years or so of the Earth's history has been characterized by a series of glacial cycles, each with a duration of approximately 100 kyr [1]. In turn, each cycle has been characterized by a slow glaciation (or growth) phase, followed by a much more rapid deglaciation. The last growth phase ended with a glacial maximum about 20 kyr ago, with much of the ice subsequently dissipating in just 10-15 kyr [2]. At the time of the last glacial maximum, ice sheets of approximately 2-3 km in thickness covered most of present-day Canada, Siberia, the Barents and Kara Seas, and Scandinavia [2,3].

The last deglaciation was so recent (ending just 5-10 kyr ago) and so massive (raising ocean levels by about 120 m) that the Earth presently remains in a state of isostatic disequilibrium. The adjustment which characterizes the Earth's return to a state of equilibrium is termed "glacial isostatic adjustment." When regions previously covered by ice are being considered, the term "postglacial rebound" is more common.

In a project funded, in the U. S., by NASA (the DOSE project), in Canada by the Natural Sciences and Engineering Research Council (NSERC), and in Sweden by the Natural Science Research Council (NFR), and in cooperation with the National Land Survey of Sweden (Lantmäteriverket or LMV), we will be using the Global Positioning System (GPS) and Very Long Baseline Interferometry (VLBI) to measure the present-day three-dimensional crustal deformation in Fennoscandia (Scandinavia and Finland) associated with glacial isostatic adjustment. In this paper, we will first describe the geodetic network to be used, then discuss geophysical applications of this study, and finally present some preliminary measurements.

¹ Harvard-Smithsonian Center for Astrophysics, 60 Garden St., Cambridge, Massachusetts 02138, USA

² Onsala Space Observatory, Chalmers University of Technology, S-439 92 Onsala, Sweden

³ National Land Survey of Sweden

⁴ Department of Physics, University of Toronto, 60 St. George Street, Toronto, Ontario, Canada, M5S 1A7

THE GEODETIC NETWORK

In Fig. 1, we show the positions of (both planned and existing) GPS and VLBI sites in Fennoscandia. Data obtained from these sites will be used for this study. The first occupation of all sites is planned for the summer 1993. The full network is comprised of three independent networks, each run by the host country: Norway, Sweden or Finland. The Norwegian network, implemented and operated by the Norwegian Mapping Authority (Statens **Kartverk**) consists of ten permanently operating TurboRogue receivers. The Finnish GPS network has not been fully monumented; monumentation will begin in early Spring, 1993. The Finnish sites will be occupied with receivers owned by NASA, the **Onsala Space Observatory (OSO)** and the Harvard-Smithsonian Center for Astrophysics (**CfA**). The NASA, CfA, and OSO receivers are TurboRogue GPS receivers. The design and implementation of the Swedish GPS network has been a collaborative effort between researchers at the Swedish National Land Survey, the **Onsala Space Observatory**, the Harvard-Smithsonian Center for Astrophysics, and (as of January 1993) the University of Toronto. Six of the Swedish sites already have permanently operating **GPS** receivers (see **CURRENT WORK**). The monuments for the Swedish GPS network have been designed by the Swedish National Land Survey. (See Fig. 2.) Each site consists of two 3-m high pillars, atop which the GPS antenna mounts directly onto a 3-in bolt set into the monument. Surrounding the pillars, at a distance of 10 m or so, are six standard reference marks. These marks may be sighted directly by a **theodolite** which may be mounted on the pillar instead of a GPS antenna. At regular intervals, the **theodolite** is used to measure the horizontal angle between the reference marks and the vertical angle from the horizon to the mark. In this way, motion of the pillar itself may be detected and, if present, corrected for. The design of the monument obviates the need for a tripod and adaptor to be carried to the site, and for antenna height measurements to be obtained. The status of network monumentation is shown in Fig. 1. The stations will be equipped with un-interruptible power supplies, telephone and modem connections, and a PC.

Onsala Space Observatory frequently participates in VLBI observations involving European, American, and other **VLBI** sites around the world. (OSO also has a permanently operating Rogue GPS receiver.) In particular, the velocity vector between **Onsala Space Observatory** and the **Wetzell** site in Germany is known with an uncertainty of less than 1 **mm/yr** horizontal and 2 **mm/yr** vertical [4]. These and other VLBI determinations within Fennoscandia will help to fix the "absolute" motion of the entire **Fennoscandian** GPS network, as well as the internal calibration.

GEOPHYSICAL APPLICATIONS OF DETERMINATIONS OF INTERSITE VELOCITY

There are two geophysical areas in which we intend to apply the geodetic measurements: inferences of mantle viscosity and correction of tide-gauge records for the contamination due to glacial **isostatic** adjustment.

Inferences of mantle viscosity

The inference of mantle viscosity from the analysis of postglacial rebound data is a classic problem of geophysics, beginning in earnest with **Haskell** [5] and continuing up to today [6-12]. In nearly all previous works, forward calculations only have been used to derive viscosity inferences. References [7] and [12] consider the inverse problem, and it is possible to use their methodologies to assess the uncertainty of the inferences and to consider the resolving power of the data used to obtain it. Our analysis will be based on the method of references [12] and [13] and will use the three-dimensional intersite velocities as input.



Fig. 1 "Fennoscandian GPS network", comprised of the Norwegian, Swedish, and Finnish GPS networks (see text). Filled squares: Monumentation complete. Hollow squares: Monumentation will be completed during spring '93. Big circles: Planned and existing VLBI sites.

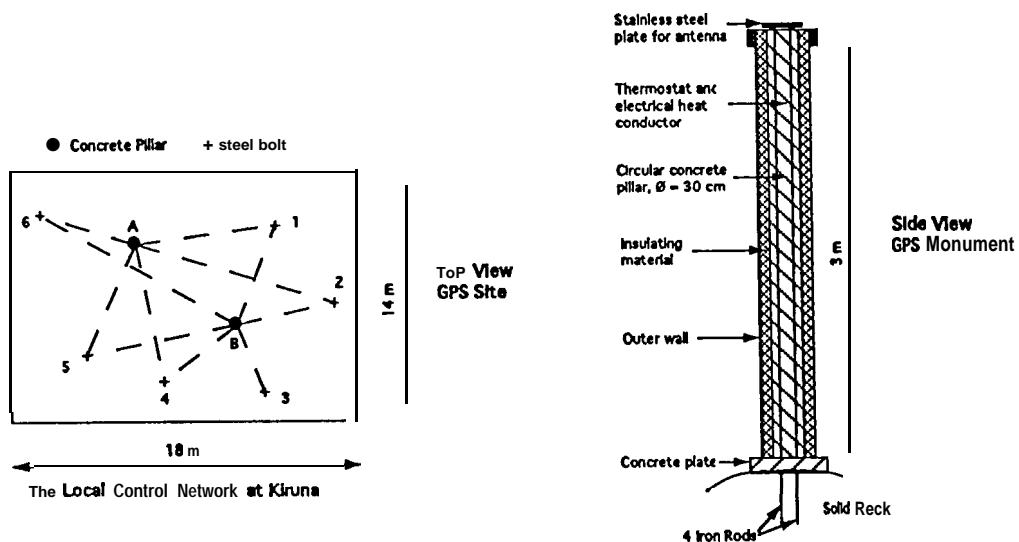


Fig. 2 Layout of Kiruna site in the Swedish GPS network (left). A,B: Pillars. 1-6: Reference marks. Schematic of pillar used in the Swedish GPS network (right).

The previous analyses have provided some insight into the radial profile of mantle rheology, but certain problems remain. The most obvious of these problems is the fact that different inferences of mantle viscosity based upon relative sea level data vary by an order of magnitude or more at all depths [8-10,11]. As mentioned above, almost all analyses of the glacial isostatic adjustment data set have been based on solutions of a forward problem, and hence estimates of the non-uniqueness (resolving power) or uncertainty of any “preferred” model have not been assessed. The inverse-technique analysis of reference [12] has, for example, indicated two areas of non-uniqueness in inversions for the mantle viscosity profile below Fennoscandia based upon the relaxation spectrum [6] for the region. First, an increase or decrease in the **aesthenospheric** viscosity (that is, the region below the lithosphere and down to 400 km depth) can be compensated by, respectively, an increase or decrease in the assumed **lithospheric** thickness in fitting the central uplift data. (This trade-off was also apparent in the forward solutions of references [6] and [8].) Furthermore, a trade-off exists between the viscosity of the transition zone (400-670 km depth) and the viscosity of the shallowest regions of the lower mantle (670-1200 km depth) such that the average viscosity across the entire region must be near 10^{21} Pa s.

We intend to use the unique capabilities of space geodesy to resolve these problems. Using space geodesy, we obtain not only estimates of uplift for the various sites, but the **three-dimensional** intersite velocity vectors. Using this fact, we can estimate the radial length scale over which the viscosity profile can be resolved, as a function of depth, given a forward theory for predicting three-dimensional motions due to post-glacial rebound [14], and having specified both the late Pleistocene **deglaciation** model for Fennoscandia and the geographic location of GPS sites. We have performed a preliminary resolving power analysis based on a simplified model of the surface load history in the vicinity of Fennoscandia using only the Swedish GPS network. This analysis suggests that incorporating horizontal motions in the inference of mantle viscosity will improve the resolving power by -20% at the base of the upper mantle, and by 60% at the base of the lithosphere, over that which is obtainable using uplift rates only.

Correction of tide-gauge data

The numerical modelling of the glacial isostatic adjustment process has been used to correct tide-gauge observations which measure the total present day rate of sea level (bathymetry) change at particular geographic sites [15,16]. At a site (θ, ϕ) , the present day rate of sea level change V_S due to the adjustment process may be written as the difference between the rate of geoid or ocean-surface change, V_G , and the rate of solid surface change, V_R :

$$V_S(\theta, \phi, t) = V_G(\theta, \phi, t) - V_R(\theta, \phi, t)$$

Previous corrections to the tide-gauge observations for the signature due to glacial isostatic adjustment have removed an approximation to $V_S(\theta, \phi, t)$, numerically derived using a specific spherically symmetric linear **visco-elastic** Earth model [15,16]. While these studies represent an important first step, they suffer a potentially serious limitation. The model of the visco-elastic structure of the Earth used in these studies is chosen on the basis of an argument that it “best fits” a global data base of relative sea level (**RSL**) curves in forward analyses [15]. It is not at all clear that this viscosity model yields numerical predictions of present day solid surface uplift rates which are consistent with the true deformation (V_R) occurring in any specific region. Numerical corrections to tide-gauge records in Fennoscandia are potentially susceptible to this error source since the global RSL data set used to infer the viscosity model includes only a small fraction of the available Fennoscandian data, and the model may therefore be unrepresentative of this region. Of course, precise solid surface deformation rates are not generally known in most regions of the globe. If they were known in a specific area, they could be used in one of two ways. First, to “fine tune” the viscosity model in order that it yields, in numerical predictions, deformation rates consistent with the observed; and then to

use the same viscosity model to compute the numerical correction to tide-gauges in the same region for the glacial **isostatic** adjustment signal. Alternately, the uplift rates may be used directly to correct nearby tide-gauge records. In central regions of previously glaciated areas, such as **Fennoscandia**, \mathbf{V}_S is dominated by V_R [17]. For such regions a more reliable tide-gauge correction would be based on the removal of the observed, rather than the numerically predicted value of \mathbf{V}_R . This procedure may be augmented by removing from the tide-gauge observations the smaller, numerically derived contribution for \mathbf{V}_G . Recent technical advances [17] have made extremely high spatial resolution numerical predictions of V_G possible. The correction of tide-gauge data can also benefit from an analysis involving horizontal as well as vertical motions. Contributions to sea-level change from the glacial **isostatic** adjustment process can be numerically determined using viscosity profiles obtained (as described above) from the three-dimensional space-geodetic velocity estimates. Because data from an entire network are used to determine corrections, this method is statistically more robust, and corrections can be computed for tide-gauge sites that are not near to space-geodetic sites. Using this method, one may determine tide-gauge corrections consistent with the entire pattern of adjustment determined from the regional network.

Using either of the above correction procedures for tide-gauge data from **Fennoscandia** should result in a record which more accurately reflects present-day sea level variations from sources other than the last major **deglaciation** event of the current ice age. The estimates of sea-level rates determined from tide-gauge records acquired over a wide region can then be examined to determine if the corrections for rebound significantly improve the consistency of the estimates [16]. If so, then the trend in sea-level could be used to constrain present-day global sea-level rise due to the combined contributions of the **steric** effect of ocean thermal expansion and present-day variations in the ocean-ice mass balance potentially caused by global warming.

CURRENT WORK

Preliminary GPS measurements have been obtained since July 1992 on a subset of the Swedish network for the purpose of gaining experience in setting up data flow routines and analysis strategies, detecting problems, and developing an intuition for the accuracies that can be expected once the full network is operational. During one of the observation epochs we also studied the influence of "receiver mixing," i.e., **having more than one type of GPS receiver/antenna used to acquire GPS data** [18]. All receivers used were dual-frequency P-code receivers. Data were obtained during July 25-27, during October 6-9, 1992, and during January 11 to February 3, 1993, at **Kootwijk, Metsähovi, Onsala, Tromsø, Wettzell (IGS Core sites); Furuögrund, Kiruna, Mårtsbo (IGS Fiducial sites); and Lovö (Swedish Network)**. Data from the global GPS network were used for satellite orbit determination. The regional sites involved, as well as the type of GPS receiver located at the different sites, are shown in Table 1. All the data have been processed with **GIPSY II**. In addition all data from 1992 has been processed, with similar results [18], using the **Bernese** version 3.2 software and the precise ephemerides obtained from the **IGS** processing centers. Examples of estimates of baseline length and the vertical component are shown shown in Fig. 3. The separation of the stations used for Fig. 3 varies from 140 km up to 1000 km. For these data we obtained short term (i.e., day-to-day) repeatabilities on the order of 3-20 ppb in baseline length and about a factor 4 worse for the vertical component. A detailed examination of Fig. 3 reveals the presence of a few "**outliers.**" A close inspection of the raw data in these cases indicated that either there were considerably less data from the specific station, on that particular day, or cycle-slips remained in the **pre-processed** data leading to **outlier** detection in the postfit residuals and deletion of many data. The cause **being** that the automatic editing in **GIPSY II** sometimes failed for data obtained from the **Ashtech** receivers. A possible explanation for this failure might be that Ashtech data seem to be "clean" in the **widelane** combination but not in the ionospheric combination, a problem not incurred with the edited Rogue data. We are presently investigating the difference between the two receiver types in this aspect and the possible implication on the editing algorithms in **GIPSY II**. This problem was not encountered editing the single- and

double-differenced data within the **Bernese Software**. We also observed that the phase residuals for the baselines between the far Northern sites (**Furuögrund** and **Kiruna**) was worse than for the other sites. As a result many data had to be deleted and the elevation cut-off had to be set to 20 degrees. Presumably this effect is due to higher ionospheric activity at those latitudes. The long term repeatabilities, shown in Fig. 4, were on the order of 4 mm + 2.5 ppm and 10 mm + 4.6 ppb for the baseline length and the vertical component, respectively.

Our experience with this preliminary data set has shown us that mixing receivers and antennas introduces many practical problems in the analysis of the data. One of the most vexing problems was that with different antennas within the network, antenna heights are measured differently for each site. This problem will be minimized by having permanent installations in the network. In order to be able to process the data in a timely manner, routines for automatic data flow and processing have been set up at **Onsala Space Observatory**. The full network consisting of more than 15 permanent stations in Sweden will be operational by summer 1993.

Implications for scientific goals

The above results imply that the accuracy of the estimates of relative position will be about 3 mm for the horizontal component and 13 mm for the vertical, ignoring baseline-length dependence. Since the network is operating continuously, in principal we will obtain daily estimates of relative position. The difference between short- and long-term scatter, though, implies that day-to-day results are not independent. If we assume that **decorrelation** occurs over 30 days, then after 5 years of observations our rate uncertainties will be **0.3 mm/yr** horizontal and **1.2 mm/yr** vertical. It should be considered, however, that at this stage both mixed receivers and not permanently monumented receivers have been used. Also, no attempt has been done to solve for the phase ambiguities. The rate uncertainties above can be compared with Fig. 5, which provides predictions, based on a standard Earth model and ice history, of the horizontal and vertical deformation rates due to glacial isostatic adjustment along a profile from **Luleå**, Sweden, to **Wetzell**, Germany [14]. The detection of **crustal** deformation rates in this region implies a constraint on parameters influencing the adjustment process, namely the radial profile of mantle viscosity. In particular, calculations indicate [14] that this sensitivity to viscosity is strongest in the radial region extending from the surface down to approximately **1200 km** depth below Fennoscandia.

ACKNOWLEDGEMENT

This work is supported by NASA grant **NAG5-1930**, the Smithsonian Institution, the Swedish Natural Science Research Council (**NFR**), and the Swedish Council for Planning and Coordination of Research (**FRN**), and the Natural Sciences and Engineering Research Council (**NSERC**) of Canada. The processing software used in this study are developed at Jet Propulsion Laboratory (**GIPSY H**) and the Astronomical Institute, University of Bern (**Bernese Software v 3.2**).

REFERENCES

- [1] Shackleton, N. J., Oxygen isotope analyses and Pleistocene temperatures re-assessed, *Nature*, **215**, 15-17, 1967.
- [2] Denton, G.H., and I.J. Hughes (Eds.), *The Last Great Ice Sheets*, Wiley, New York, 1981.
- [3] Tushingham, A.M., and W.R. Peltier, **ICE-3G**: A new global model of late Pleistocene deglaciation based upon geophysical predictions of post-glacial relative sea-level change, *J. Geophys. Res.*, **96**, 4497-4523, 1991.

- [4] Ma, C., J.W. Ryan, and D.S. Caprette, *Crustal Dynamics Project Data Analysis-1991*, NASA Tech. Mere. 104552, 424 pp., 1992.
- [5] Haskell, N. A., The motions of a viscous fluid under a surface load, 1, *Physics*, 6, 265-269, 1935.
- [6] McConnell, R. K., Viscosity of the mantle from relaxation time spectra of isostatic adjustment, *J. Geophys. Z/es.*, 73, 7089-7 105, 1968.
- [7] Parsons, B. E., *Changes in the Earth's shape*, Ph.D. Thesis, Cambridge University, 1972.
- [8] Cathles, L.M. III, *The Viscosity of the Earth's Mantle*, Princeton University Press, Princeton, 1975.
- [9] Peltier, W.R., and J.T. Andrews, Glacial isostatic adjustment, I, The forward problem, *Geophys. J. R. Astron. Soc.*, 46, 605-646, 1976.
- [10] Nakada, M., and K. Lambeck, Late Pleistocene and Holocene sea-level change in the Australian region and mantle rheology, *J. Geophys.*, 96, 497-517, 1989.
- [11] Tushingham, A. M., and W.R. Peltier, Validation of the ICE-3G model of Würm-Wisconsin deglaciation using a global data base of relative sea level histories, *J. Geophys. Res.*, 97, 3285-3304, 1992.
- [12] Mitrovica, J. X., and W.R. Peltier, The inference of mantle viscosity from an inversion of the Fennoscandian relaxation spectrum, in press, *Geophys. J. Int.*, 1993.
- [13] Mitrovica, J.X., and W.R. Peltier, Present-day secular variations in the zonal harmonics of the Earth's geopotential, in press, *J. Geophys. Res.*, 98, 4509-4526, 1993.
- [14] Mitrovica, J.X., J.L. Davis, and I.I. Shapiro, A spectral formalism for computing three-dimensional deformation due to surface load, 2. Present-day glacial isostatic adjustment, in preparation, 1993.
- [15] Peltier, W. R., and A.M. Tushingham, Global sea level rise and the greenhouse effect: Might they be connected? *Science*, 244, 806-810, 1989.
- [16] Douglas, B. C., Global sea level rise, *J. Geophys. Res.*, 96, 6981-6992, 1991.
- [17] Mitrovica, J. X., and W.R. Peltier, On post-glacial geoid subsidence over the equatorial oceans, *J. Geophys. Res.*, 96, 20,053-20,071, 1991.
- [18] Johansson, J. M., J.L. Davis, J.X. Mitrovica, I.I. Shapiro, R.T.K. Jaldehag, G. Elgered, B.O. Rönnäng, B. Jonsson, G. Hedling, and M. Ekman, Initial GPS measurements of Fennoscandian uplift (abstract), *Eos Trans. AGU*, 73 (43), Fall Meeting Suppl., 123, 1992.

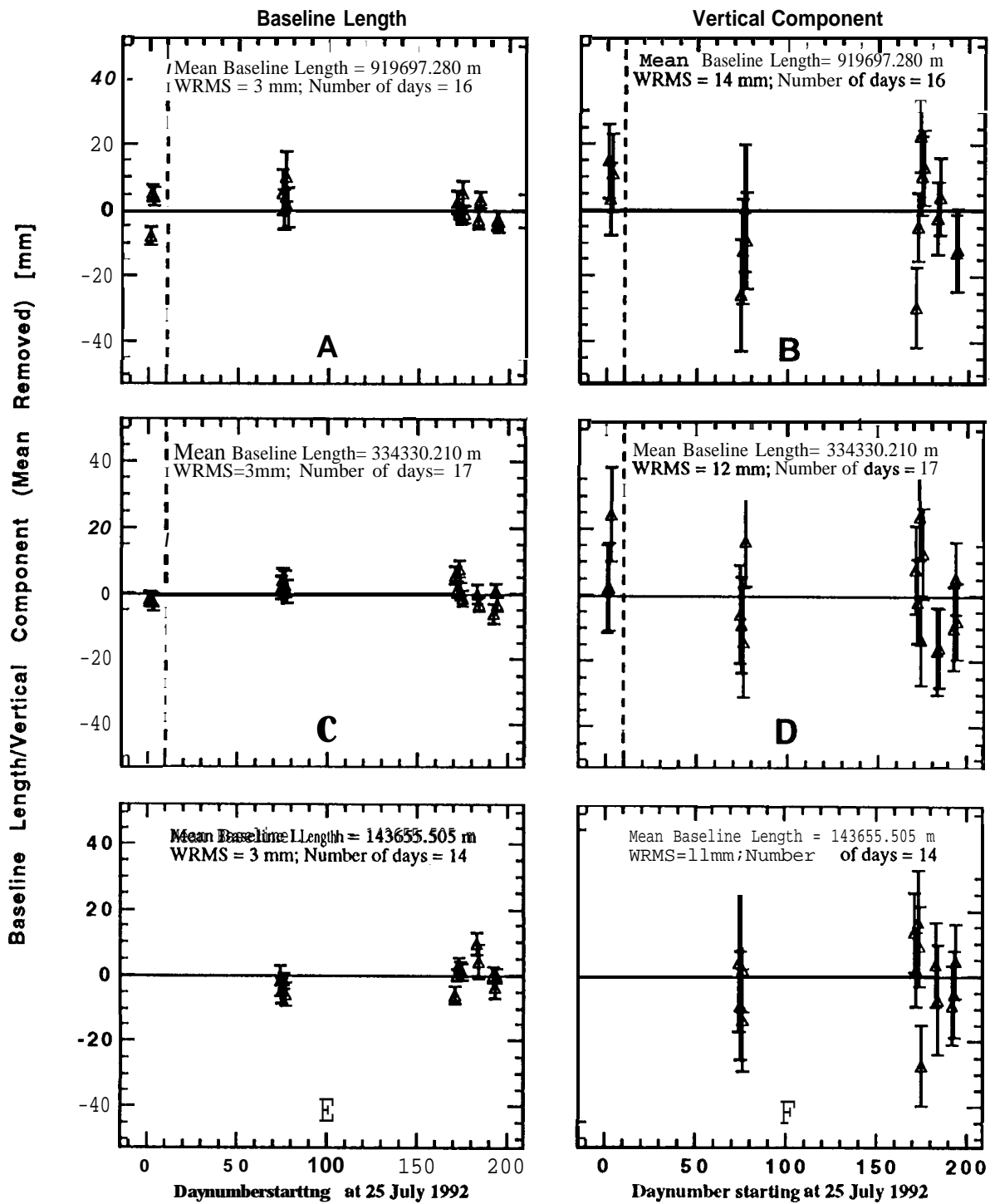


Fig. 3 Estimates of the baseline length and the vertical component for three station pairs, namely *Onsala to Wettzell (A,B)*, *Kiruna to Furuögrund (C,D)*, and *Mårtsbo to Lovö (E,F)*. The mean baseline lengths and the weighted RMS values are given in the figure. The dashed vertical line indicates a change in the global GPS tracking network used for this study.

Table 1.

SITES AND GPS RECEIVERS USED IN THE MEASUREMENTS

| | Rogue | Mini-Rogue | Turbo-Rogue | Ashtech |
|------------|-------|------------|-------------|---------|
| Onsala | X | | | x |
| Lovö | | x | | X |
| Mårtsbo | | | x | X |
| Furuögrund | | | | X |
| Kiruna | | | | X |
| Wetzell | X | | | |
| Metsähovi | X | | | |
| Tromsø | X | | | |

X: Permanent receiver. x: Additional receiver installed for the campaign October 6-9, 1992.

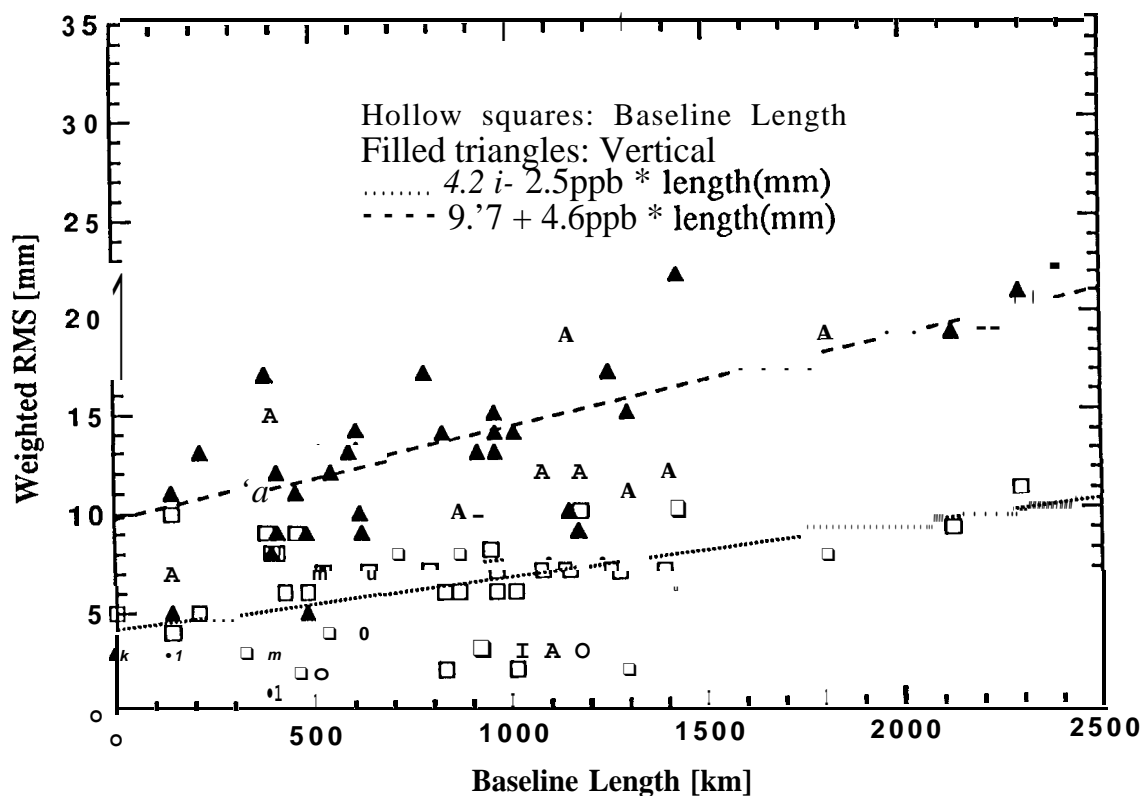


Fig. 4 Weighted RMS for the baseline length and the vertical component as a function of baseline length.

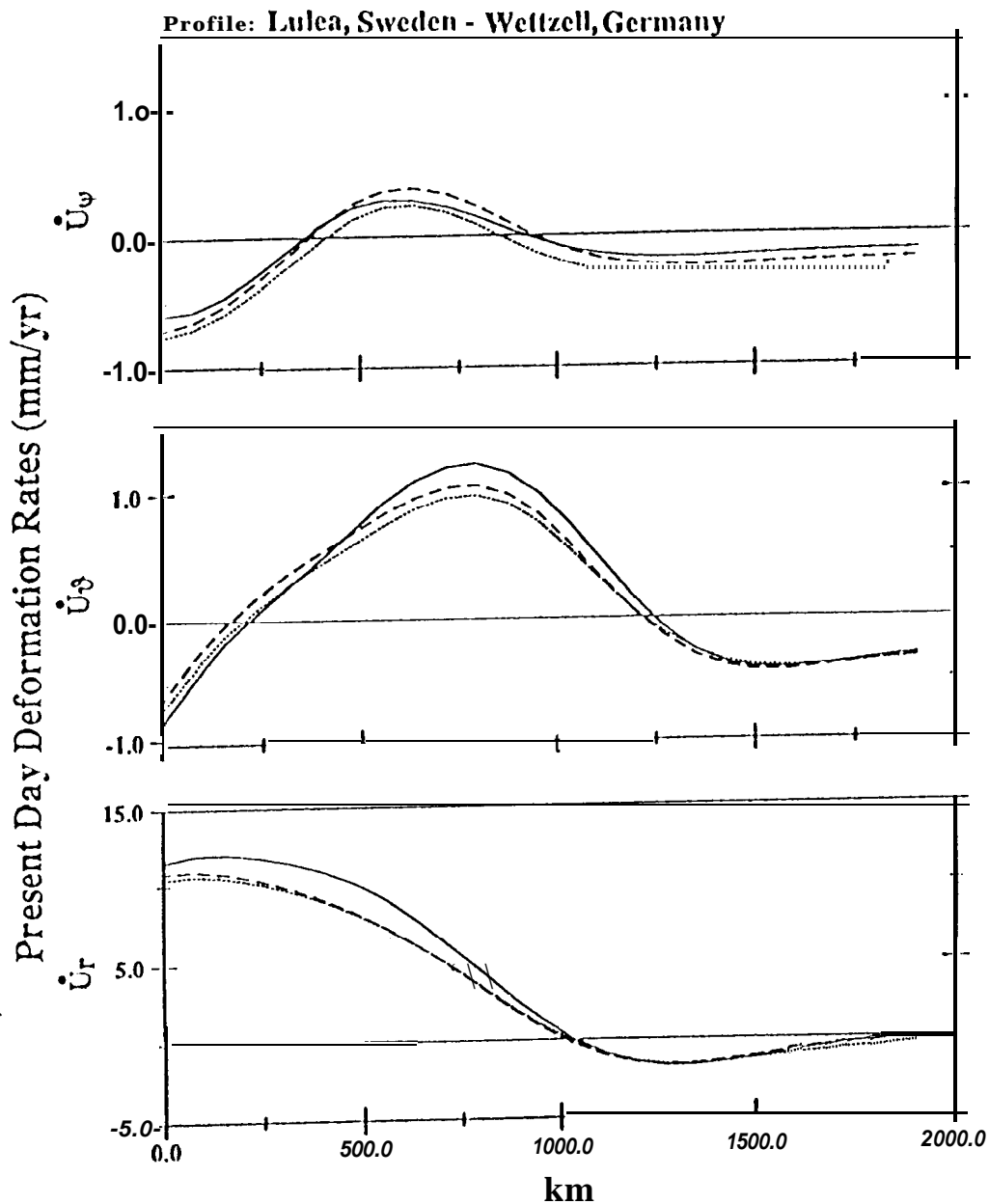


Fig. 5 The present day three-dimensional velocity computed along a great circle profile from Luleå (about 10 km north of Furuögrund), Sweden to Wettzell, Germany. The top, middle and bottom frames of the figure refer to the three components of velocity in the local cartesian reference frame. These are, respectively, \dot{U}_ψ (local east), \dot{U}_θ (local south), and \dot{U}_r (local up, or radial). All calculations were performed using the standard Earth model, and the Pleistocene ice loading history adapted from ICE-3G deglaciation chronology. The different lines on each frame are distinguished on the basis of the representation of the ocean load component of the surface mass load adopted in the calculations. From [14].

ESOC STATION COORDINATE SOLUTIONS FOR THE IGS'92 CAMPAIGN, INCLUDING EPOCH'92

T.J. Martin Mur^a, J.M. Dow^b, J. Feltens^c, C. Garcia Martinez^a

ESOC has been participating in the IGS service from June of 1992, providing daily solutions for the earth orientation parameters (cop's) and orbits. Now a multiarc solution for the station coordinates has been developed and it has been sent to the IERS Central Bureau as a part of ESOC contribution to the 1992 IERS Annual Report. This solution and others obtained by ESOC are compared with those derived by other analysis centres and by IERS.

INTRODUCTION

Initial GPS station coordinates were derived from well known positions of collocated VLBI, LLR, or SLR instruments. Coordinates for receivers not collocated with other instruments were derived by making GPS station coordinates solutions using the receivers with better known positions as fiducial stations. An example of this approach was the solution SSC (JPL) 92 P 011, which used VLBI stations as fiducial sites. Other solutions have been developed since then by several analysis centres, but the position of some critical (because isolated) stations is still not known with the accuracy needed to use them for the IGS service. ESOC has developed various GPS solutions, testing different sets of constraints, to obtain a solution for station coordinates that is:

1. Complete, including all the stations that are being used by ESOC for the daily processing.
2. Self-consistent, deriving all the coordinates from only one solution and not from a combination of different solutions.
3. Close to the ITRF91 system.

-
- a. GMV S.A. Technical Department, C/ Isaac Newton, s/n, PTM - Tres Cantos, E-28760 Madrid, Spain
Currently based at ESOC.
 - b. Orbit Attitude Division, ESA, European Space Operations Centre, Robert-Bosch-Str. 5, D-6100 Darmstadt, Germany
 - c. mbp Software&Systems GmbH, Lyoner Straße 30, D-6000 Frankfurt a. M. 71, Germany. Currently based at ESOC.

ESTIMATION STRATEGY

Preprocessing

Data from a total of 30 stations, listed in Table 1, were used to obtain the ESOC station coordinate **solutions**. We use double difference ionospheric free phase observable for GPS processing. These observable are computed from L1 and L2 phase observable contained in the RINEX observation files by using the preprocessing program GPSOBS. Propagated orbits obtained after the fit of the previous day are used to calculate simulated measurements at the same sampling rate as in the RINEX file (30 s). These simulated measurements are compared with the real measurements to identify cycle slips and to do a coarse ambiguity correction to the measurements, that are output every 6 minutes. Only those double-difference links that span more than 72 minutes without cycle slips are selected. Figure 1 shows the station combinations that were formed in week 687.

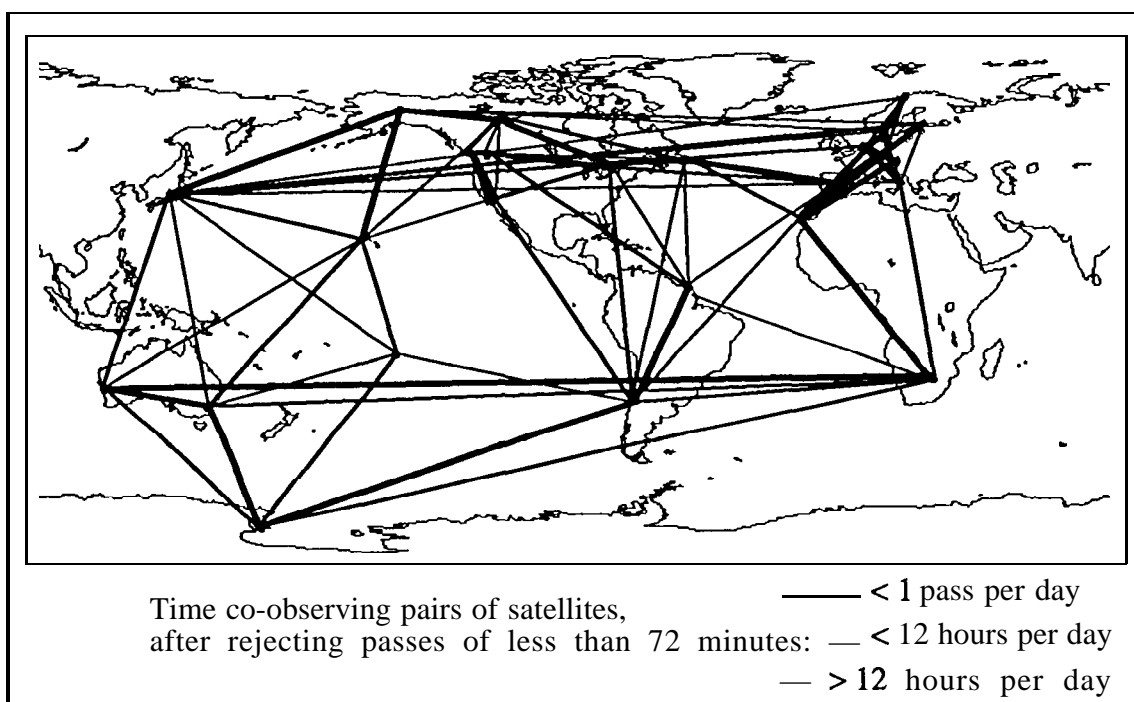


Fig. 1 Baselines used for IGS processing at ESOC for GPS week 687.

Obtaining the observation equations

After obtaining the observation file for an arc of 24 hours we run BAHN, the standard orbit determination and geodetic parameter estimation program of ESOC². The models and values we use for orbit determination are those recommended in the IERS Standards (1992) for GPS³, except the following: no station position ocean loading correction is

made, no relativistic corrections are applied, and for all the stations the **Nuvel-1** NNR velocity field is **used**. In every 24 hour BAHN run the following parameters are estimated:

- Satellite state vectors (position and velocity at the beginning of the arc, CR, Y-bias)
- Ambiguity parameters, one every 2 stations and 2 satellites link, with a new value estimated after **every** cycle slip. They are estimated as real parameters.
- Station zenith delays as linear functions of time, with intervals of 3 hours.

The eop values from IERS Bulletin A are used, including celestial pole offsets. Observation equations are obtained for the estimated parameters and additional considered parameters, including station coordinates.

Observation equations were obtained for a total of 33 non A/S days, including 10 days of Epoch'92 and 23 additional days from November 15, 1992 to December 19, 1992.

Multiarc parameter estimation

These observation equations are processed to eliminate the parameters not relevant for the station coordinate solution and to fix others, like the cop's, to the initial values (IERS Bulletin A). The elimination is needed because of the huge number of parameters that need to be taken into account (about 1000 parameters per day) and the fact that the actual value of these parameters is of little or no interest once it is obtained (for example ambiguity parameters). The parameters that are left to be estimated are station coordinates, CR'S, and Y- biases. CR'S and Y biases are included to check the validity of the solution for every arc. The output of this processing is a set of normal equations for every one day arc. The program used to obtain the **multiarc** solutions is called MULTIARC. Additional observation equations can be created to constrain the solution. Solutions were obtained using 1992.5 as epoch for the station coordinates.

FREE NETWORK SOLUTIONS

A solution without any station coordinate constraints was obtained to evaluate what constraints are needed in the final solution. The fact that the cop's were fixed to the IERS Bulletin A and that a dynamic approach was used allowed for a non-singular system. Solutions were obtained for three periods of 10 to 12 days of data and for the total 33 days. Table 2 shows the comparison of these solutions with the initial coordinates, i.e. those of the IGS Mail 90⁴.

As can be seen in Table 2, the **centre** of mass position is not determined with the required accuracy (**3cm**) with this approach, specially the Z component. X and Y components are determined with the same accuracy as a typical GPS satellite orbit, but Z is less observable because the spatial distribution of the observations. The rotation about **the Z axis is also**

Table 1
LIST OF STATIONS INCLUDED IN THE ESOC SOLUTIONS

| Name | Dome | Listed in ITRF91 | Location | Epoch'92 | Nov 15- Dec 19 | Notes |
|----------------|------------------|---------------------|--------------------|----------|-------------------|--------------------------|
| Albert Head | 40129MO03 | | B. Columbia | included | included | fiducial station |
| Algonquin | 401 04MO02 | yes | Ontario | included | included | fiducial station |
| Penticton | 401 05MO02 | | B. Columbia | included | included | |
| Fairbanks | 40408MO01 | yes | Alaska | included | included | fiducial station |
| Goldstone | 40405s031 | | California | included | included | fiducial station |
| Graz | 11 001MO02 | | Austria | included | included | |
| Hartebeesthoek | 30302MO02 | yes | South-Africa | included | included | |
| Hobart | 50116S004 | | Tasmania | included | included | |
| Pasadena | 40400MO07 | | California | included | | |
| Pasadena | 40400" | | California | | included | antenna was moved |
| Kokee Park | 40424MO04 | yes | Hawaii | included | included | |
| Kootwijk | 13504MO03 | yes | Netherlands | included | included | fiducial station |
| Kourou | 97301" | | French Guyana | | included | operated by ESOC |
| Madrid | 13407S012 | yes ^b | Spain | included | included | fiducial station |
| Maspalomas | 31303MO01 | | Canary Is. | included | included | operated by ESOC |
| Matera | 12734MO08 | | Italy | included | included | fiducial station |
| Mc Murdo | 66001M001 | | Antarctica | included | included | |
| Metsahovi | 10503s011 | | Finland | included | included | fiducial station |
| Ny Alesund | 10317MO01 | yCS | Spitsbergen | included | | antenna was hit |
| Onsala | 10402MO04 | | Sweden | included | included | fiducial station |
| Pamate | 92201MO03 | | Tahiti | included | included | |
| Pinyon Flat | 40407MO03 | | California | included | | |
| Richmond A | 40499MO02 | | Florida | included | | |
| Richmond B | 40499" | | Florida | | included | antenna was moved |
| Santiago | 41705MO03 | | Chile | included | included | |
| St. Johns | 40101M001 | | Newfoundland | included | included | |
| Tidbinbilla | 50103" | | East Australia | included | included | |
| Tromso | 10302MO03 | yes | Norway | included | included | fiducial station |
| Usuda | 21729" | | Japan | included | | |
| Usuda | 21729' | | Japan | | included | antenna was moved |
| Wetzell | 14201S020 | | Germany | included | included | fiducial station |
| Yarragadee | 501 07MO04 | yes | West Australia | included | included | |
| Yellowknife | 40127MO03 | yes | N.W.T., Canada | included | included | fiducial station |

a. No monument number available for GPS marker.

b. 13407S012 is the same as 13407S013, that is listed in **ITRF91**, but with the coordinates reduced to the bottom of the choke ring, since the initial coordinates were referred to the top of the choke ring.

Table 2
TRANSFORMATION PARAMETERS AND RESIDUALS AFTER THE TRANSFORMATION
FROM THE IERS/IGS SET OF COORDINATES TO THE ESOC FREE NETWORK
SOLUTIONS

| Time span | T1 (cm) | T2 (cm) | T3 (cm) | D (10⁻⁶) | RI .001" | R2 .001" | R3 .001" | rms Ion. (cm) | rms lat. (cm) | rms hei. (cm) |
|---------------|--------------------------|--------------------------|--------------------------|--------------------------------------|---------------------------|---------------------------|---------------------------|------------------------------------------|------------------------------------------|------------------------------------------|
| Epoch '92 | -23.27 | 24.28 | -273.06 | 0.010 | -0.052 | -5.148 | -57.042 | 9.0 | 9.1 | 14.3 |
| Nov 15 -Dec 2 | -2.96 | 14.11 | -187.71 | 0.006 | -2.190 | -4.387 | -87.769 | 7.5 | 8.2 | 13.5 |
| Dec 8 -Dec 19 | -13.48 | 5.91 | -131.54 | 0.004 | -2.938 | -3.778 | -6.871 | 7.4 | 7.7 | 13.9 |
| All days | -12.48 | 14.07 | -183.77 | 0.005 | -1.379 | -4.002 | 2.911 | 8.3 | 8.8 | 13.1 |

more than we would like to have. A posterior uncertainties in station longitude are from 5 meters for McMurdo and Ny-Alesund to 28 meters for Kourou, representing an uncertainty of about 0.9" in the rotation about the Z axis. Uncertainties in latitude and height are in the order of 6 to 22 cm and give confidence ellipses for the station position in the meridian plane that have the **semimajor** axis in the direction of the Z axis.

SOLUTION SSC (ESOC) 93 P 01

For the solution SSC (ESOC) 93 P 01 we selected 12 stations in Europe and North America (those listed in Table 1 as fiducial stations) with well known coordinates and we gave to the initial latitude and longitude of these stations a weight of 5 cm. Initial coordinates were obtained from the IGS Mail 90⁴. All these sites are listed in the ITRF91 datum, but not all of them as the current GPS monument. We use this constraint to make our solution consistent with ITRF91 in origin and rotation about the Z axis, thus overcoming the weakness of the Free Network solution. No constrain in height was applied since it can be seen that in the Free Network solution the scale factor has an acceptable value without applying this constraint. Table 3 lists the comparison between the ESOC 93 P 01 solution and the original coordinates. Table 4 lists the actual coordinates obtained and their uncertainties. Table 5 lists the differences between the ESOC coordinates and the IERS/IGS datum, as shifts in X, Y, and Z from one to the other and as discrepancies in **topocentric** frame after a seven parameter transformation. Stations at Usuda, Pasadena, and Richmond were considered as different during Epoch '92 and the other arcs because their antennas were moved in the meantime.

The level of agreement for the fiducial stations after a seven parameter transformation is up to 2.2 cm, significantly lower than the a priori weight used to constraint the longitude and latitude of these stations.

Table 3
TRANSFORMATION PARAMETERS AND RESIDUALS AFTER THE TRANSFORMATION
FROM THE IERS/IGS SET OF COORDINATES TO THE SSC (ESOC) 93 P 01 SOLUTION

| Set of stations | T1 (cm) | T2 (cm) | T3 (cm) | (1%) | RI .001" | R2 .001" | R3 .001" | rms lon. (cm) | rms lat. (cm) | rms hei. (cm) |
|------------------------|-------------|-------------|--------------|-------|--------------|---------------|---------------|---------------------|---------------------|---------------------|
| Att the stations | 7.48 | -1.89 | -5.93 | 0.008 | -0.902 | -3.121 | 0.336 | 7.7 | 6.6 | 9.7 |
| Fiducial stations only | 0.08 | 1.82 | -1.31 | 0.001 | 0.402 | -0.248 | -0.124 | 1.7 | 2.2 | 2.2 |

COMPARISON OF SOLUTIONS

We now inter-compare different GPS station coordinate solutions, including the ESOC solutions. The solutions to be compared are:

- . The **IERS/IGS** set of station coordinates, as described in the IGS Mail 90⁴. This is a combination of station coordinates obtained from the **ITRF91** datum and brought to 1992.5 with coordinates calculated from local ties to other well know markers and also coordinates calculated by other analysis centres and transformed to ITRF91.
- The ESOC Free Network solution, described above.
- The SSC (**ESOC**) 93 P 01 solution, **described** above.
- . The SSC (**CSR**) 92 P 02 solution, described in the IGS Mail 1425. For this solution the coordinates of **Kokee** Park, Fairbanks, and **Wetzell** were fixed to a combination of laser and VLBI solutions translated to the GPS marker. Only the coordinates of other GPS stations were estimated.
- The GPS station coordinate solution obtained by PGGGA at Scrips, as described in IGS Mail 168⁶, based in 16 months of data.

Not all of these solutions include the same number of stations, and sometimes they list different locations for the same station. Table 6 shows the result of the comparison of these sets. The biggest contributors to the rrns of residuals are listed in Table 7. Discrepancy vectors with respect to the **IERS/IGS** datum for these stations are listed in Table 8.

CONCLUSION

In order to obtain a GPS solution for station coordinates it is necessary to constrain the rotation about the Z axis and the position of the centre of mass, as seen in the ESOC Free Network solution. Solutions obtained without these constraints show a high disagreement with the conventional centre of mass and origin of latitudes. A solution constraining latitude and longitude shifts for a set of well known stations has been obtained by ESOC. The agreement of this solution with other GPS solutions is in the order of 4 to 9 cm horizontal and 8 to 14 cm vertical RMS, but this result would be greatly improved if isolated stations were not included in the comparison. Table 9 shows the comparison between different solutions when four of these isolated stations are excluded. When all the stations are

Table 4
SOLUTION SSC (ESOC) 93 P 01
Epoch for the coordinates Is 1992.5

| DOME | | x | Y | z | SX | SY | SZ | Ant. | |
|---------------|-----------------|-------------------------|-----------------------|------------------------|-----------------------|-----------|-----------|-------------|-----------------|
| NUMBER | NAME | m | m | m | m | m | m | Hei. | Receiver |
| 10302MOO3 | Tromso | 2102940.414 | 721569.372 | 5958192.0870.021 | 0.0180.0362.473 | | | | Rogue |
| 103 17M001 | Ny-Alesund | 1202430.675 | 252626.646 | 6237767.4320.0520.046 | 0.0855.203 | | | | Rogue |
| 10402MOO4 | Onsala | 3370658.737 | 711876.985 | 5349786.7910.0230.016 | 0.0320.995 | | | | Rogue |
| 10503S011 | Metsahovi | 2892571.035 | 1311843.326 | 5512634.0360.0220.018 | 0.0330.000 | | | | Rogue |
| 11 001MOO2 | Graz | 4194424.030 | 1162702.513 | 4647245.2570.0290.019 | 0.0312.068 | | | | Rogue |
| 12734MO08 | Matera | 4641949.803 | 1393045.217 | 4)33287.243 | 0.0330.0210.0300.135 | | | | Rogue |
| 13407S012 | Madrid | 4849202.512 | -360329.195 | 4114912.9720.0290.018 | 0.0260.000 | | | | Rogue |
| 13504MO03 | Kootwijk | 3899225.300 | 396731.770 | 5015078.2860.0260.01 | 70.0320.105 | | | | Rogue |
| 14201S020 | Wetzell | 4075578.677 | 931852.631 | 4801569.9700.0250.016 | 0.0290.000 | | | | Rogue |
| 21729S003 | Usuda (E'92) | -3855262.636 | 3427432.257 | 3741020.9270.0990.103 | 0.0690.000 | | | | Rogue |
| 21729? | Usuda (N-D) | -3855263.111 | 3427432.539 | 3741020.4930.0580.061 | 0.0420.000 | | | | Rogue |
| 30302MO02 | Hartebeesthoek | 5084625.761 | 2670366.643 | -2768494.17 | 10.0560.0700.0449.754 | | | | Rogue |
| 31303M001 | Maspalomas | 5439189.211 | -1522054.891 | 2953464.1470.0340.027 | 0.0250.122 | | | | Rogue |
| 401 01MOO1 | St, Johns | 2612631.344 | -3426807.060 | 4686757.7470.0240.023 | 0.0240.162 | | | | Rogue |
| 401 04MOW | Algonquin | 918129.627 | -4346071.238 | 4561977.7800.0210.024 | 0.0250.114 | | | | Rogue |
| 401 05MOO2 | Penticton | -20591 64.592 | -3621108.370 | 4814432.3950.021 | 0.0250.0290.118 | | | | Rogue |
| 40127MO03 | Yellowknife | -1224452.385 | -2689216.046 | 5633638.2800.0180.021 | 0.031 0.117 | | | | Rogue |
| 40129MO03 | Albert Head | -2341332.827 | -3539049.497 | 4745791.391 | 0.0220.0250.0290.118 | | | | Rogue |
| 40400MO07 | Pasadena (E'92) | -2493304.086 | -4655215.549 | 3565497.2960.0270.037 | 0.031 0.093 | | | | Rogue |
| 40400? | Pasadena (N-D) | -2493304.4394655215.346 | 3565497.2610.0300.034 | 0.0280.093 | | | | | Rogue |
| 40405S031 | Goldstone | -2353614.067 | -4641385.389 | 3676976.4090.0260.034 | 0.0290.000 | | | | Rogue |
| 40407MO03 | Pinyon Flats | -2369510.494 | -4761207.099 | 3511396.0560.0290.037 | 0.0301.844 | | | | Rogue |
| 40408M001 | Fairbanks | -2281621.317 | -1453595.706 | 5756961.9430.0230.021 | 0.0340.116 | | | | Rogue |
| 40424MO04 | Kokee Park | -5543838.151 | -2054587.563 | 2387809.5730.0450.042 | 0.0320.093 | | | | Rogue |
| 40499MO02 | Richmond (E'92) | 961319.007 | -5674091.016 | 2740489.5360.0500.061 | 0.0380.094 | | | | Rogue |
| 40499? | Richmond (N-D) | 961319.198 | -5674091.001 | 2740489.5210.0370.038 | 0.0280.094 | | | | Rogue |
| 41705MO03 | Santiago | 1769693.466 | -5044574.311 | -3468321.3340.0520.046 | 0.0440.094 | | | | Rogue |
| 50103S017 | Canberra | -4460995.871 | 2682557.113 | -3674444.054 | 0.0520.0570.0450.000 | | | | Rogue |
| 501 07MOO4 | Yarragadee | -2389025.165 | 5043316.986 | -3078531.098 | 0.0620.0520.0420.073 | | | | Rogue |
| 501 16S004 | Hobart | -3950183.833 | 2522364.489 | -4311588.582 | 0.0520.0580.0470.000 | | | | Minimac |
| 66001M001 | Mc Murdo | -1310695.009 | 310468.824 | -6213363.679 | 0.0590.0610.0424.990 | | | | Rogue |
| 92201MO03 | Pamatai | -5245194.962 | -3080472.495 | -1912825.6150.0700.071 | 0.0428.420 | | | | Rogue |
| 97301? | Kourou | 3839591.506 | -5059567.648 | 579956.7610.0510.049 | 0.0310.132 | | | | Rogue |

Table 5
SHIFTS AND RESIDUALS PER SITE OF THE COMPARISON BETWEEN
THE IERS/IGS AND THE SSC (ESOC) 93 P 01 SOLUTION

| DOME NUMBER NAME | Before 7-par. DX m | Before 7-par. DY m | Before 7-par. DZ m | After 7-par. RE m | After 7-par. RN m | After 7-par. RU m |
|---------------------------|-----------------------------|-----------------------------|-----------------------------|----------------------------|----------------------------|----------------------------|
| 10302MOO3 Tromso | -0.037 | -0.007 | 0.015 | -0.011 | 0.044 | -0.006 |
| 103 17M001 Ny-Alesund | -0.072 | 0.008 | -0.060 | 0.009 | 0.049 | -0.067 |
| 10402MOO4 Onsala | -0.020 | -0.004 | -0.021 | -0.011 | 0.007 | -0.057 |
| 10503S011 Metsahovi | 0.018 | 0.026 | 0.017 | 0.004 | -0.009 | 0.009 |
| 11 001MOO2 Graz | -0.066 | 0.057 | -0.042 | 0.063 | 0.019 | -0.100 |
| 12734MO08 Matera | -0.011 | 0.014 | -0.023 | 0.014 | -0.010 | -0.072 |
| 13407S012 Madrid | 0.006 | -0.016 | -0.031 | -0.024 | -0.032 | -0.074 |
| 13504MO03 Kootwijk | -0.047 | 0.011 | -0.010 | 0.005 | 0.025 | -0.074 |
| 14201S020 Wettzell | -0.006 | -0.003 | -0.010 | -0.008 | 0.002 | -0.053 |
| 21729S003 Usuda (E'92) | -0.055 | -0.159 | 0.104 | 0.158 | 0.225 | 0.059 |
| 21729? Usuda (N-D) | n/a | n/a | n/a | n/a | n/a | n/a |
| 30302MO02 Hartebeesthoek | 0.357 | 0.144 | -0.132 | 0.032 | 0.006 | 0.284 |
| 31303MO01 Maspalomas | 0.095 | 0.030 | 0.094 | 0.046 | 0.034 | 0.037 |
| 401 OIMOO1 St. Johns | -0.010 | -0.066 | -0.006 | -0.061 | -0.030 | -0.010 |
| 401 O4MOO2 Algonquin | 0.009 | -0.014 | -0.020 | -0.008 | -0.007 | -0.024 |
| 401 O5MOO2 Penticton | 0.015 | 0.050 | -0.068 | -0.015 | 0.042 | -0.067 |
| 40127MO03 Yellowknife | -0.016 | 0.002 | -0.006 | -0.007 | 0.028 | 0.016 |
| 40129MO03 Albert Head | 0.003 | 0.001 | 0.000 | -0.009 | 0.053 | 0.020 |
| 40400MO07 Pasadena (E'92) | -0.023 | 0.000 | -0.043 | -0.050 | 0.020 | 0.086 |
| 40400? Pasadena (N-D) | n/a | n/a | n/a | n/a | n/a | n/a |
| 40405S031 Goldstone | 0.016 | 0.017 | -0.062 | -0.021 | 0.017 | -0.046 |
| 40407MO03 Pinyon Flats | -0.136 | 0.101 | -0.079 | -0.198 | 0.009 | -0.062 |
| 40408MO01 Fairbanks | 0.010 | 0.069 | -0.033 | -0.046 | 0.067 | -0.013 |
| 40424MO04 Kokee Park | -0.071 | -0.041 | 0.003 | -0.012 | 0.081 | 0.118 |
| 40499MO02 Richmond (E'92) | 0.002 | -0.050 | -0.011 | -0.032 | -0.046 | -0.028 |
| 40499? Richmond (N-D) | n/a | n/a | n/a | n/a | n/a | n/a |
| 41705MO03 Santiago | 0.238 | -0.208 | -0.196 | 0.036 | -0.051 | 0.229 |
| 50103S017 Canberra | 0.230 | -0.068 | -0.049 | -0.027 | -0.022 | -0.169 |
| 501 O7MOO4 Yarragadee | 0.166 | 0.156 | -0.172 | -0.132 | 0.027 | 0.119 |
| 501 16S004 Hobart | 0.210 | 0.059 | 0.066 | -0.013 | 0.068 | -0.132 |
| 66001M001 Mc Murdo | 0.241 | -0.056 | -0.230 | -0.010 | -0.102 | 0.091 |
| 92201MO03 Pamatai | 0.186 | -0.294 | 0.028 | 0.265 | 0.165 | -0.025 |
| 97301? Kourou | n/a | n/a | n/a | n/a | n/a | n/a |

Table 6
COMPARISON OF GPS STATION COORDINATE SOLUTIONS
When all the common stations are included

| First System | Second System | Nsta | T1 | T2 | T3 | D | RI | R2 | R3 | rms Ion. | rms lat. | rms hei. |
|--------------|---------------|------|-----------------|-------------|-------------------|---------------------|--------------|--------------|------------|------------|----------|----------|
| | | | (cm) | (cm) | (cm) | (10 ⁻⁶) | .001" | .001" | .001" | (cm) | (cm) | (cm) |
| IERS/IGS | ESOC 93 P01 | 29 | 7.48 | -1.89 | -5.93 | 0.008 | -0.902 | -3.121 | 0.336 | 7.7 | 6.6 | 9.7 |
| IERS/IGS | CSR 92 P02 | 24 | 0.91 | 6.58 | 0.59 | 0.008 | 3.069 | 0.161 | 3.986 | 6.6 | 5.8 | 6.4 |
| IERS/IGS | PGGA/SIO | 38 | -4.00 | 4.91 | -1.44 | 0.006 | 1.531 | 1.300 | 0.975 | 5.1 | 7.3 | 5.9 |
| ESOC 93 P01 | ESOC F/N | 33 | -19.67 | 15.61 | -177.48 | -0.003 | -0.480 | -0.854 | 2.619 | 1.6 | 3.3 | 5.0 |
| ESOC 93 P01 | CSR 92 P02 | 20 | -7.79 | 7.45 | 5.83 | -0.003 | 3.256 | 2.977 | 3.443 | 4.6 | 3.6 | 7.9 |
| ESOC 93 P01 | PGGA/SIO | | 26-14.50 | 6.82 | 4.56-0.001 | 2.52 | 4.758 | 0.494 | 6.4 | 8.9 | | 14.4 |
| CSR 92 P02 | PGGA/SIO | 24 | -5.37 | -1.92 | -2.03 | -0.001 | -1.254 | 1.273 | -2.613 | 5.5 | 8.7 | 11.4 |

Table 7
COMPARISON OF GPS STATION COORDINATES
Stations with higher discrepancies when different solutions are compared

| First System | Second System | Station with discrepancies higher than 20 cm in any component | Station with discrepancies higher than 10 cm in any component |
|--------------|---------------|---------------------------------------------------------------|---------------------------------------------------------------------------------|
| IERS/IGS | ESOC 93 P01 | Santiago, Hartebeesthoek, Pamatai, Usuda | Graz, Hobart, Kokee Park, Mc Murdo, Pinyon Fiats, Canberra, Yarragadee |
| IERS/IGS | CSR 92 P02 | - | Santiago, Hartebeesthoek, Pamatai, Usuda |
| IERS/IGS | PGGA/SIO | Santiago | Hartebeesthoek, Usuda, Mc Murdo, Yarragadee, Darwin, Taiwan |
| ESOC 93 P01 | CSR 92 P02 | - | Santiago, Hartebeesthoek, Pamatai, Hobart, Kokee Park |
| ESOC 93 P01 | PGGA/SIO | Santiago, Hartebeesthoek | Pamatai, Hobart, Kokee Park, Madrid, Richmond, Canberra, Yarragadee, Ny-Alesund |
| CSR 92 P02 | PGGA/SIO | Santiago, Hartebeesthoek | Pamatai, Hobart, Mc Murdo, St. Johns, Canberra, Townsville, Yarragadee |

compared, the biggest contribution to the differences between the ESOC solution and the IERS/IGS datum comes from the height of stations like Hartebeesthoek, Hobart, Santiago and Canberra. Further efforts are needed to obtain a better station coordinate solution for these stations.

REFERENCES

- [1] C. Boucher, Z. Altamimi, L. Duhem, "ITRF 91 and its associated velocity field", IERS Technical Note 12, October 1992.

Table 8
COMPARISON OF GPS STATION SOLUTIONS
Discrepancies with IERS/IGS after seven parameter transformation

| Station | ESOC | | | CSR | | | SIO | | |
|----------------|--------------|--------------|--------------|--------------|--------------|--------------|--------------|--------------|--------------|
| | Lat. (cm) | Len. (cm) | Hei. (cm) | Lat. (cm) | Len. (cm) | Hei. (cm) | Lat. (cm) | Len. (cm) | Hei. (cm) |
| Graz | 6.3 | 1.9 | -10.0 | n/a | n/a | n/a | 3.2 | 1.3 | -3.9 |
| Usuda | 15.8 | 22.5 | 5.9 | 19.6 | 17.8 | -1.0 | 17.8 | 17.8 | -1.6 |
| Hartebeesthoek | 3.2 | 0.6 | 28.4 | -9.0 | 2.9 | 12.5 | 8.5 | -19.9 | -14.4 |
| Hobart | -2.7 | 6.8 | -12.2 | 1.3 | 5.7 | -3.1 | -0.6 | -6.7 | 5.5 |
| Kokee Park | -1.2 | 8.1 | 11.8 | -1.2 | -1.8 | -5.3 | 2.2 | -2.2 | -4.2 |
| Mc Murdo | -1.0 | -10.2 | 9.1 | 2.2 | -6.5 | 2.3 | -4.0 | 3.4 | 12.7 |
| Pamatai | 26.5 | 16.5 | -2.5 | 16.8 | 12.5 | 5.1 | 5.4 | 2.6 | -6.6 |
| Santiago | 3.6 | -5.1 | 22.9 | -4.5 | 5.7 | -4.6 | -8.7 | -23.4 | -20.1 |
| Canberra | -2.7 | 2.2 | -16.9 | -1.0 | 0.1 | -9.5 | -0.1 | -9.8 | 0.6 |
| Yarragadee | -13.2 | 2.7 | 11.9 | -3.7 | -3.4 | 1.5 | 5.0 | -14.4 | 3.2 |

Table 9
COMPARISON OF GPS STATION COORDINATE SOLUTIONS
When Santiago, Hartebeesthoek, Pamatai, and Usuda are not included in the comparison

| First System | Second System | N | s | t | a | T1 T2 T3 | | | R1 | R2 | R3 | rms | rms | rms |
|--------------|---------------|-----------|--------------|--------------|--------------|--------------|---------------|--------------|---------------|------------|------------|------------|-------|-------|
| | | | | | | (cm) | (cm) | (cm) | | | | (1%) | .001" | .001" |
| IERS/IGS | ESOC 93 P01 | 25 | 6.54 | -0.70 | -5.23 | 0.004 | -1.096 | -2.997 | -0.915 | 4.5 | 4.1 | 7.1 | | |
| IERS/IGS | CSR 92 P02 | 21 | 0.40 | 9.09 | 0.35 | 0.006 | 3.115 | 0.057 | 3.570 | 3.0 | 4.1 | 5.1 | | |
| IERS/IGS | PGGA/SIO | 34 | -1.47 | 4.15 | -2.20 | 0.009 | 0.821 | 0.444 | 0.490 | 3.7 | 3.8 | 4.1 | | |
| ESOC 93 P01 | CSR 92 P02 | 16 | -6.32 | 8.39 | 5.01 | 0.001 | 3.687 | 2.68 | 4.58 | 3.1 | 3.6 | 7.0 | | |
| ESOC 93 P01 | PGGA/SIO | 22 | -10.85 | 3.94 | 2.13 | 0.007 | 1.647 | 3.636 | 1.123 | 5.6 | 5.7 | 7.4 | | |
| CSR 92 P02 | IERS/IGS | 20 | -1.95 | -5.40 | -2.26 | 0.005 | -2.209 | 0.435 | -2.824 | 3.9 | 4.9 | 6.1 | | |

- [2] J.M. Dow et al., "Satellite determination of earth orientation with emphasis on GPS", World Space Congress, August-September 1992.
- [3] Dennis.D. McCarthy (ed.), "IERS Standards (1992)", IERS Technical Note 13, July 1992.
- [4] C. Boucher and Z. Altamimi, "IGS site information and coordinates", IGS Electronic Mail Number 90, September 9, 1992.
- [5] M.M. Watkins, B.E. Schutz, and P.A.M. Abusali, "GPS Site Positions from CSR92P02", IGS Electronic Mail Number 142, December 1, 1992.
- [6] Yehuda Bock, "List of coordinates based on 16 months of PGGA analysis", IGS Electronic Mail 168, January 11, 1993.

AMBIGUITY RESOLUTION STRATEGIES USING THE RESULTS OF THE INTERNATIONAL GPS GEODYNAMICS SERVICE

**Leoš Mervart¹, Gerhard Beutler¹,
Markus Rothacher¹, Urs Wild²**

Resolving the initial phase ambiguities of GPS carrier phase observations was always considered an important aspect of GPS processing techniques. Resolution of the so-called wide-lane ambiguities using a special linear combination of the L_1 and L_2 carrier and code observations has become standard. New aspects have to be considered today: (1) Soon AS, the so-called Anti-Spoofing, will be turned on for all Block 11 spacecraft. This means that precise code observations will be no longer available, which in turn means that the mentioned approach to resolve the wide-lane ambiguities will fail. (2) Most encouraging is the establishment of the new International GPS Geodynamics Service (IGS), from where high quality orbits, earth rotation parameters, and eventually also ionospheric models will be available. We are reviewing the ambiguity resolution problem under these new aspects: We look for methods to resolve the initial phase ambiguities without using code observations but using high quality orbits and ionospheric models from IGS, and we study the resolution of the "narrow-lane ambiguities" (after wide-lane ambiguity resolution) using IGS orbits.

INTRODUCTION

The Observation Equations

We consider dual-band GPS receivers and we use a notation similar to (Goad, 1985) or (Blewitt, 1989). All observables have the dimension of length, terms due to noise and multipath are not explicitly shown, and higher-order ionospheric terms are ignored:

$$\begin{aligned} L_{1k}^i &= \varrho_k^i - I_k^i \frac{f_2^2}{f_1^2 - f_2^2} + \lambda_1 b_{1k}^i \\ L_{2k}^i &= \varrho_k^i - I_k^i \frac{f_1^2}{f_1^2 - f_2^2} + \lambda_2 b_{2k}^i - \Delta \varrho_k^i \\ P_{1k}^i &= \varrho_k^i + I_k^i \frac{f_2^2}{f_1^2 - f_2^2} \\ P_{2k}^i &= \varrho_k^i + I_k^i \frac{f_1^2}{f_1^2 - f_2^2} - \Delta \varrho_k^i \end{aligned} \quad (1)$$

where k is the receiver index, i the satellite index, L_{1k}^i and L_{2k}^i are the carrier-phase pseudoranges, P_{1k}^i and P_{2k}^i the P-code pseudoranges, f_1, f_2 the frequencies of the L_1 and L_2 carriers,

¹ Astronomical Institute, University of Berne, Sidlerstrasse 5, CH-3012 Berne, Switzerland

² Federal Office of Topography, Seftigenstrasse 264, CH-3084 Wabern, Switzerland

and λ_1, λ_2 the corresponding wavelengths. By our definition the term I_k^i is the difference in ionospheric delay between the L_1 and L_2 carriers. The term ϱ_k^i is the non-dispersive delay, lumping together the effects of geometric delay, tropospheric delay, clock signatures, and any other delays which affect all four observables identically. $\Delta\varrho_k^i$ is the differential delay between the L_1 and L_2 antenna phase centers. The phase biases b_{1k}^i and b_{2k}^i are composed of three terms:

$$\begin{aligned} b_{1k}^i &= n_{1k}^i + \delta\Phi_{1k} - \delta\Phi_1^i \\ b_{2k}^i &= n_{2k}^i + \delta\Phi_{2k} - \delta\Phi_2^i \end{aligned} \quad (2)$$

The integer numbers n_{1k}^i and n_{2k}^i are the initial phase ambiguities or briefly ambiguities, the terms $\delta\Phi_{1k}$ and $\delta\Phi_{2k}$ are uncalibrated components of phase delay originating from the receiver (assumed to be common for all satellite channels); the terms $\delta\Phi_1^i$ and $\delta\Phi_2^i$ originate from the satellite transmitter (assumed to be common for all receivers). Most software systems providing the highest accuracies (e.g. the Bernese GPS Software - see (Rothacher, 1991)) process double differenced data so that the double difference phase biases are integer numbers (Goad, 1985):

$$b_{f_k}^{ij} = (b_{f_k}^i - b_{f_k}^j) - (b_{f_i}^i - b_{f_i}^j) = n_{f_k}^{ij} \quad , \quad f = 1, 2 \quad (3)$$

Linear Combinations of Observable

With equations (1) we can form e.g. the following two linear combinations:

$$L_{3k}^i = \frac{1}{f_1^2 - f_2^2} (f_1^2 L_{1k}^i - f_2^2 L_{2k}^i) = \varrho_k^i - \Delta\varrho_k^i \frac{f_2^2}{f_1^2 - f_2^2} + B_{3k}^i \quad , \quad (4)$$

where

$$B_{3k}^i = \frac{1}{f_1^2 - f_2^2} (f_1^2 \lambda_1 b_{1k}^i - f_2^2 \lambda_2 b_{2k}^i) \quad (5)$$

and

$$L_{5k}^i = \frac{1}{f_1 - f_2} (f_1 L_{1k}^i - f_2 L_{2k}^i) = \varrho_k^i + I_k^i \frac{f_1 f_2}{f_1^2 - f_2^2} + \Delta\varrho_k^i \frac{f_2}{f_1 - f_2} + \lambda_5 b_{5k}^i \quad , \quad (6)$$

where

$$b_{5k}^i = b_{1k}^i - b_{2k}^i \quad \text{and} \quad \lambda_5 = \frac{c}{f_1 - f_2} \quad . \quad (7)$$

Equation (4) represents the so-called ionosphere-free combination, equation (6) is often called the wide-lane combination because of the relatively large wavelength of $\lambda_5 \approx 86 \text{ cm}$. These two linear combinations play a fundamental role in all ambiguity resolution strategies for baselines longer than about 10 km.

OUR AMBIGUITY RESOLUTION APPROACH

We have to distinguish between the strategy used for ambiguity resolution and the algorithm implemented to reach that goal.

Strategy

As many ambiguity resolution strategies we resolve first the wide-lane ambiguity parameter b_5 . For this purpose the direct approach suggested by (Melbourne, 1985) and (Wübbena, 1965) can be used if the P-code is available on both frequencies. In the opposite case we can use some alternative approaches e.g. (Blewitt, 1989). It should be mentioned that ionospheric conditions may reduce the effectiveness of these methods considerably and the estimation of ionosphere parameters may prove to be necessary. Once the wide-lane ambiguity is resolved, a narrow-lane integer search can be performed, see e.g. (Bock, 1986). In this way, both the L_1 and L_2 integer biases can be resolved.

We assume that the International GPS Geodynamics Service (IGS) will provide us with

1. high accuracy orbits (better than 0.5 m),
2. regional ionosphere models.

The first IGS product should allow us to resolve the narrow-lane ambiguities *not* in a network-mode *but* in a baseline-oriented mode. This strategy promises to be much more efficient than usual network-oriented processing schemes, because the computing time grows not linearly but with a much higher power with the number of ambiguities involved (depending somewhat on the algorithm chosen). It also promises to be more reliable, because in our case the search ranges can be opened up in a "generous" way, and more runs can be made.

The second product should allow us to resolve the wide-lane ambiguities without having access to the P-code. This aspect is most important because soon the P-code will no longer be available to the scientific community. Below we will use local single-layer models for the vertical electron content based on the phase measurements of one dual-band receiver in the IGS network. These models are used when processing the wide-lane linear combination of baselines up to 300 km in the "vicinity" of the reference receiver the data of which were used to define the local ionosphere model. Again, the wide-lane ambiguity resolution is done in the baseline-mode. The idea was (and is) to take out the principal ionosphere-induced biases by a model and to hope that the "irregular" part of the ionosphere will be averaged out by using long observation sessions.

The Algorithm

Our algorithm is in principle equivalent to that proposed by (Blewitt, 1989). The implementation is much simpler in the sense that we are not actually forming statistically independent linear combinations of ambiguities. We replace this procedure by an iterative scheme, where in each iteration step we are only resolving "the best" ambiguity. The next iteration step is then based on a solution with all previously resolved ambiguities fixed. This "primitive" and transparent algorithm could be easily implemented into the Bernese GPS software. Let us now present the algorithm in detail: We use the following model for the least squares adjustment:

$$\begin{aligned}
 \hat{L} &= \phi(\hat{X}) \\
 \hat{X} &= X_0 + \hat{x} \\
 \hat{L} &= \underline{L} + \underline{\hat{w}} = \underline{A} \hat{x} + \phi(X_0) \\
 &\quad \underline{\hat{w}} = \underline{A} \hat{x} - \frac{(\underline{L} - \phi(X_0))}{l}
 \end{aligned} \tag{8}$$

where

ϕ is a known operator,

\underline{L} is the array with observed values,

\underline{X}_0 is the array containing the approximate values of the unknown parameters,

\underline{l} contains the so-called reduced observations,

$\hat{\underline{L}}$ is the least-squares estimate of the array \underline{L} ,

$\hat{\underline{X}}$ is the least-squares estimate of the parameters,

$\hat{\underline{w}}$ the least-squares estimate of the corrections to the observations,

$\hat{\underline{x}}$ the least-squares estimate of the corrections to the approximate parameters and

A is the first design matrix.

The stochastic model is defined by the matrix

$$K_{ll} = \sigma_0^2 Q_{ll} = \sigma_0^2 P^{-1} l. \quad (9)$$

According to the least squares method we obtain the following normal equation system:

$$\underbrace{A^T P A}_{N=Q_{xx}^{-1}} \hat{\underline{x}} = \underbrace{A^T P l}_{\underline{b}} \quad (10)$$

and the following expression for the a posterior variance of unit weight:

$$m_0^2 = \frac{\hat{\underline{w}}^T P \hat{\underline{w}}}{n - u} = \frac{\underline{l}^T P \underline{l} - \hat{\underline{x}}^T N \hat{\underline{x}}}{n - u}. \quad (11)$$

The variance-covariance matrix is known to be:

$$K_{xx} = m_0^2 Q_{xx}. \quad (12)$$

This matrix determines which biases are to be solved first. Because we process double difference data, we choose a priori one single difference (between receivers) bias $b_{f_{kl}}^j$ as reference and our unknown ambiguity parameters are

$$n_{f_{kl}}^{ij} = b_{f_{kl}}^i - b_{f_{kl}}^j. \quad (13)$$

The index j stands for the frequency, k and l are the two receiver indices, i and j are the two satellite indices. We resolve either $n_{f_{kl}}^{ij}$ directly or the difference between two of these terms

$$n_{f_{kl}}^{i_1 i_2} = n_{f_{kl}}^{i_1 j} - n_{f_{kl}}^{i_2 j}, \quad (14)$$

which, as a matter of fact, is a double difference ambiguity again. (Blewitt, 1989) processes undifferenced data and optimizes the differencing between satellites and the differencing between receivers together. He uses the factorization method for discrete sequential estimation (Bierman, 1977). As opposed to that we initially optimize the differencing between receivers as described in the section 2.2 and we repeat the least squares adjustment for each iteration step. We may choose the maximum number of biases to be resolved per iteration step (SIC).

It should be mentioned that our algorithm allows to correct wide-lane ambiguities during narrow-lane ambiguity resolution. It is important to be aware of the change of the narrow-lane ambiguity (n_1 in eqn. 15 below) due to a change of one (full or half) cycle in the wide-lane ambiguity value (n_5 in eqn. 15). W is the wave length factor ($W = 1$ for full cycle, $W = 2$ for half-cycle ambiguities on L_2).

$$\frac{\partial n_1}{\partial n_5} = \frac{f_2}{f_1 - f_2} \frac{1}{W} \doteq 3.53 \quad (W = 1) \quad \doteq 1.76 \quad (W = 2) \quad (15)$$

TEST DATA SET

Epoch'92

We used the measurements from two different campaigns. The first one was the IGS Epoch'92 campaign. We selected the 10 stations listed in Table 1 and formed the linear independent set of shortest baselines. The map of our network is given in Figure 1. All the

Table 1: Stations and Baselines Used From the IGS Core Network

| Station | Abbreviations | Baseline | Length (km) |
|---------------|---------------|----------------|-------------|
| Graz | GRAZ GZ | GZ-WZ | 300 |
| Kootwijk | K O S G KO | WZ-ZA | 480 |
| Mas Palomas | M A S P M1' | KO-ZA | 600 |
| Madrid | MADR MD | KO-ON | 700 |
| Matera | MATE MT | GZ-MT | 720 |
| Metsahovi | METS MS | MS-ON | 780 |
| Onsala | ONSA ON | MS-TR | 1080 |
| Tromso | TROM TR | MI)- ZA | 1180 |
| Wetzell | WETT WZ | MD-MP | 1740 |
| Zimmerwald | ZIMA ZA | | |

stations were equipped with dual band L1-codes receivers. Since for test purposes we wanted to use P-code measurements we have chosen four sessions without AS. The selected sessions are given in Table 2 (where the session number is identical to the day number of the year 1992).

Euref - CH

The EUREF-CH campaign was organized by the Swiss Federal Office of Topography. The 5 EUREF stations in Switzerland (see Figure 2) were occupied from August 3 until August 8, 1992 with two different receiver types (see Table 3). The campaign took place during EPOCH'92 in order to benefit from the highest possible orbit accuracy. The main goal of the campaign was to improve the geometry of the EUREF stations, which will be the reference frame for the new GPS first order survey in Switzerland.

Table 2: List of Sessions used from Epoch'92

| Session | Date | Time |
|---------|--------------|--------|
| 217 | 4th AUG 1992 | 0 - 24 |
| 218 | 5th AUG 1992 | 0 - 24 |
| 219 | 6th AUG 1992 | 0 - 24 |
| 220 | 7th AUG 1992 | 0 - 24 |

A total of 4 Trimble 4000 SLD and 2 Trimble 4000 SST receivers has been used in the campaign. At the SLR site Zimmerwald (which is at the same time also an IGS station) both receiver types have been operated simultaneously in order to be able to form baselines between the same receiver types. It should be mentioned that the Trimble 4000 SLD are non-P-code receivers. They reconstruct the L_2 carrier using a squaring technique which leads to half-cycle ambiguities for the L_2 phase, the Trimble SST uses a different technique allowing to work with full-cycle ambiguities on L_2 . Both receivers have full-cycle ambiguities on the L_1 carrier, which means, that for the resolution of the narrow-lane ambiguities we may work with full-cycle ambiguities. We processed the 7 sessions of Table 4. Due to

Table 3: Stations and Baselines of the Euref-CH Campaign

| Station | Abbreviations | Receiver | Baseline | Length (km) |
|--------------|---------------|------------------|----------|-------------|
| Zimmerwald 1 | ZIM1 Z1 | Trimble 4000 SLD | Z1-CH | 78 |
| Zimmerwald 2 | ZIM2 Z2 | Trimble 4000 SST | Z1-LG | 114 |
| Chrischona | CHRI CH | Trimble 4000 SLD | Z2-MG | 159 |
| La Givrine | LAGI LG | Trimble 4000 SLD | Z1-PF | 190 |
| Mt. Generoso | MTGE MG | Trimble 4000 SST | | |
| Pfänder | PFAN 11' | Trimble 4000 SLD | | |

technical reasons it was not possible to generate 1 day sessions.

Table 4: List of Sessions used from Euref-CH Campaign

| Session | Date |
|---------|----------------------------------------|
| 2171 | 4th AUG 1992 6:00 - 4th AUG 1992 18:00 |
| 2172 | 4th AUG 1992 18:00 - 5th AUG 1992 6:00 |
| 2181 | 5th AUG 1992 6:00 - 5th AUG 1992 18:00 |
| 2182 | 5th AUG 1992 18:00 - 6th AUG 1992 6:00 |
| 2191 | 6th AUG 1992 6:00 - 6th AUG 1992 18:00 |
| 2192 | 6th AUG 1992 18:00 - 7th AUG 1992 6:00 |
| 2201 | 7th AUG 1992 6:00 - 7th AUG 1992 18:00 |

For both campaigns we have used the orbits computed by the Center for Orbit Determination in Europe (CODE) using the measurements of the IGS stations.

Table 5: The Results of the Wide-lane Ambiguity Resolution

| Baseline | Length (km) | Number of sess. | Number of amb. | Mean square fract. part | | Number of amb. resolved |
|----------|-------------|-----------------|----------------|-------------------------|-----------------|-------------------------|
| | | | | without ion. model | with ion. model | |
| Z1-CH | 78 | 7 | 125 | 0.253 | 0.164 | 116 |
| Z1-LG | 114 | 7 | 122 | 0.274 | 0.172 | 110 |
| Z2-MG | 159 | 7 | 92 | 0.197 | 0.117 | 89 |
| Z1-PF | 190 | 7 | 119 | 0.277 | 0.230 | 97 |

RESULTS

Wide-lane Ambiguity Resolution

For the Epoch'92 data set we used the Melbourne-Wübbena linear combination of the two phase and the two code observations (*Wübbena, 1985*). Their approach based on this linear combination seems to be very reliable but it is not the topic of our interest now. In Table 6 the number of resolved wide-lane ambiguities is shown. For the Euref-CH data we did not have this possibility because I'-code measurements were not available. The most serious problem - ionospheric refraction - was solved by using the ionosphere models produced by program IONEST of the Bernese GPS Software (*Wild, 1989*) using the L_1 and L_2 observations of the Trimble SST receiver located at Zimmerwald. In Figure 3 the distribution of the fractional parts of the wide-lane ambiguities before the first iteration step of our ambiguity resolution scheme (see section 4.2) is shown for all baselines and session (458 ambiguities). The mean square fractional parts of wide-lane ambiguities for all Euref-CH baselines are listed in Table 5. Without using the ionosphere model it was not possible to resolve the ambiguities. With the ionosphere model we resolved about 90 % of all ambiguities. The coordinates were fixed on the values obtained using the ionosphere free linear combination without resolving the ambiguities.

Narrow-lane Ambiguity Resolution

The second step consisted of the narrow-lane ambiguity resolution. In this case the iterative approach is very important because it is necessary to estimate not only the ambiguities but coordinates and troposphere parameters, too. For each baseline we held one station fixed and we estimated the coordinates of the second one. For each station we estimated one troposphere parameter per 6 hours.

In Figure 4 a typical example is shown for the development of the fractional part of the narrow-lane ambiguities during the iteration process (three double difference ambiguities stemming from satellites 13, 14, 23 and 25). In Table 6 the number of resolved ambiguities is shown. The number of ambiguities that may be resolved depends on the confidence level in our statistical tests. We used very conservative confidence level and therefore we could resolve about 85 % of the ambiguities only. In the same table the results using the broadcast

orbits instead of IGS orbits are shown. It is very interesting to inspect the distribution of the fractional part of narrow-lane ambiguities before resolution (Figure 5).

Quality of Results

Below, the daily repeatabilities of our baseline estimations are used as a measure for the success of ambiguity resolution. All the ambiguities previously resolved were fixed and we produced a solution based on the ionosphere-free linear combination. We estimated the troposphere parameters and the coordinates of all the stations (Epoch'92 and Euref-CH) with respect to Zimmerwald. We worked with various observation windows i.e. we used the data from the entire sessions and then from 8, 4, 2 and 1 hour only. The results may be found in Figures 6, 7, 8 and 9. The repeatability of the coordinates proves the stability of the solution. To show the quality of various types of solutions (ambiguities fixed or free and various data intervals) we computed a set of mean coordinates for each type of solution from all sessions. We used the full-session ambiguity fixed solution as a *reference* and computed the Helmert transformation between this solution and the others. The results are given in Figures 10 and 11.

Table 6: The Results of the Narrow-lane Ambiguity Resolution

| Baseline | Length (km) | Number of sess. | Total number of amb. | Number of wide-lane amb. res. | Broadcast orbits | CODE orbits | |
|----------|-------------|-----------------|----------------------|-------------------------------|------------------------|------------------------|---------------------|
| | | | | | mean square frac. part | mean square frac. part | number of amb. res. |
| Z1-CH | 78 | 7 | 125 | 116'' | 0.252 | 0.160 | 103 |
| Z1-LG | 114 | 7 | 122 | 110* | 0.287 | 0.238 | 107 |
| Z2-MG | 159 | 7 | 92 | 89'' | 0.294 | 0.119 | 87 |
| Z1-PF | 190 | 7 | 119 | 97'' | 0.281 | 0.302 | 69 |
| GZ-WZ | 300 | 4 | 103 | 103** | 0.276 | 0.201 | 93 |
| WZ-ZA | 480 | 4 | 101 | 94** | 0.278 | 0.258 | 72 |
| KO-ZA | 600 | 4 | 104 | 95** | 0.311 | 0.217 | 66 |
| KO-ON | 700 | 4 | 109 | 104** | 0.288 | 0.233 | 97 |
| GZ-MT | 720 | 4 | 100 | 100** | 0.292 | 0.214 | 94 |
| MS-ON | 780 | 4 | 126 | 126** | 0.285 | 0.217 | 119 |
| MS-TR | 1080 | 4 | 130 | 127** | 0.280 | 0.226 | 106 |
| MD-ZA | 1180 | 4 | 106 | 95** | 0.277 | 0.222 | 67 |
| MD-MP | 1740 | 4 | 113 | 96** | 0.277 | 0.236 | 64 |

* ionosphere mode' used

** Melbourne-Wübbena approach used

Summary, Conclusions, and Outlook

We processed data from the Epoch'92 campaign and from the Euref-CH campaign using the orbits and the ionosphere models from the CODE processing center of IGS. The ionosphere models were generated using the L_1 and L_2 phase observations of one receiver only (the Trimble SS1 receiver located at the Zimmerwald Observatory).

- With these local ionosphere models it was possible to resolve most of the wide-line ambiguities in the environment (distances and baseline lengths up to 200 km) of the ionosphere reference station without using the P-code. Actually the wide-lane wavelength was about 43 cm on three of the four baselines considered (due to the squaring type receiver), only on one baseline the full wavelength of 86 cm could be used (baseline Z2-MG, Table 3).
- High quality orbits from the CODE processing center of IGS and an iterative ambiguity resolution scheme allowed us then to resolve the narrow-lane ambiguities without major problems in the single baseline mode up to baseline lengths of about 2000 km. Figure 5 proves that IGS orbits are essential to achieve this goal. The broadcast orbit quality was not sufficient for that purpose.
- The resolution of the ambiguities improves considerably the stability of the solution. This is of special importance if the sessions are shorter than about 8 hours.

In a next step we should improve the orbits using the ambiguities fixed by the above procedure. It is planned to set up such a procedure in the near future at the CODE processing center.

References

- [1] Beutler, G.: The Impact of "The International GPS Geodynamics Service (IGS)" on the Surveying and Mapping Community, XVII ISPRS Congress, Washington, 1992a
- [2] Beutler, G.: The 1992 Activities of the International GPS Geodynamics Service (IGS), 7th International Symposium on Geodesy and Physics of the Earth, Potsdam, 1992b
- [3] Bierman, G. J.: Factorization Methods for Discrete Sequential Estimation, Academic, San Diego, 1977
- [4] Blewitt, G.: Carrier Phase Ambiguity Resolution for the Global Positioning System Applied to Geodetic Baselines up to 2000 km. Journal of Geophysical Research. VO1.94 No. B8, 1989
- [5] Bock, Y. et al.: Interferometric analysis of GPS phase observations. Manuscript geodastica, Vol.11, 4/1986
- [6] Bock, Y., Abbot, It. I., Counselman 111, C. C., King, R. W.: A demonstration of one to two parts in 10^7 accuracy using GPS, Bull. Geod., 60, 241-254, 1986
- [7] Feissel, M.: IGS'92 Campaign, Comparison of GPS, SLR, and VLBI Earth Orientation Determinations. IERS Central Bureau, Final Report, November 1992.

- [8] Frei, E., Beutler, G.: Rapid static positioning based on the fast ambiguity resolution approach "FARA": theory and first results. *Manuscripta geodetica*, Vol.15, 6/1990
- [9] Goad, C. C.: Precise relative position determination using Global Positioning System carrier phase measurements in nondifference mode. First International Symposium on Precise Positioning with GPS, Rockville, 1985
- [10] Goad, C. C., Mueller, A.: An automated procedure for generating an optimum set of independent double difference observables using Global Positioning System carrier phase measurements, *Manuscripta geodetica*, Vol.13, 6/1988
- [11] Gurtner, W.: GPS-Papers presented by the Astronomical Institute of the University of Berne in the Year 1985. Bern, **1985**
- [12] McCarthy, D.: Accuracy of high-frequency observations of earth orientation. 7th International Symposium, IAG Symposium No. 112.
- [13] Melbourne, W. G.: The case for ranging in GPS based geodetic system. First International Symposium on Precise Positioning with GPS, Rockville, 1985
- [14] Mueller, I., Beutler, G.: The International GPS Service for Geodynamics - development and current structure. Fifth International Symposium on GPS Positioning, Ohio, 1992
- [15] Remondi, B.: Kinematic and Pseudo-kinematic GPS. Proceedings of the Satellite Division's International Technical Meeting, Colorado Springs, 1988
- [16] Rothacher, M. et al.: Bernese software, version 3.3 Bern, 1991
- [17] Wild, U. et al.: Estimating the Ionosphere Using One or More Dual Frequency GPS Receivers. Proceedings of the 5th International Geodetic Symposium on Satellite Positioning, Las Cruces, New Mexico, 1989
- [18] Wübbena, G.: Software Developments for Geodetic Positioning with GPS Using TI 4100 Code and Carrier Measurements. First International Symposium on Precise Positioning with GPS, Rockville, 1985

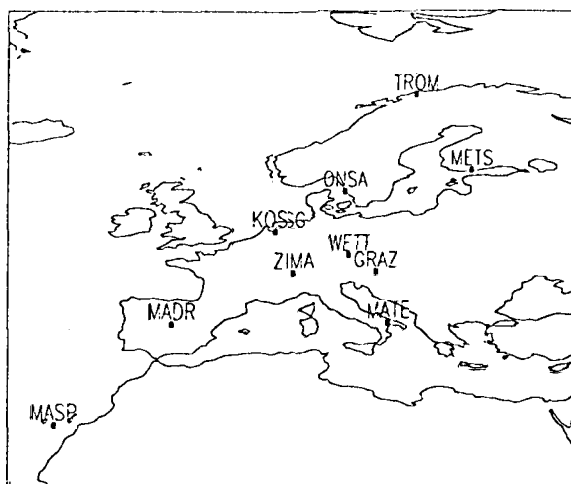


Figure 1: Test Network - Epoch'92

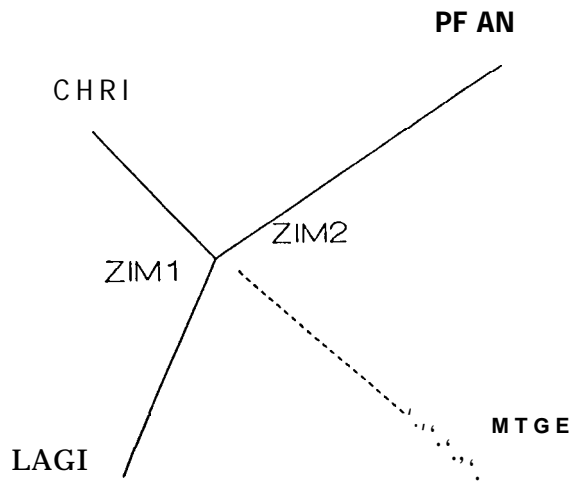


Figure 2: Test Network - Euref-CH Campaign

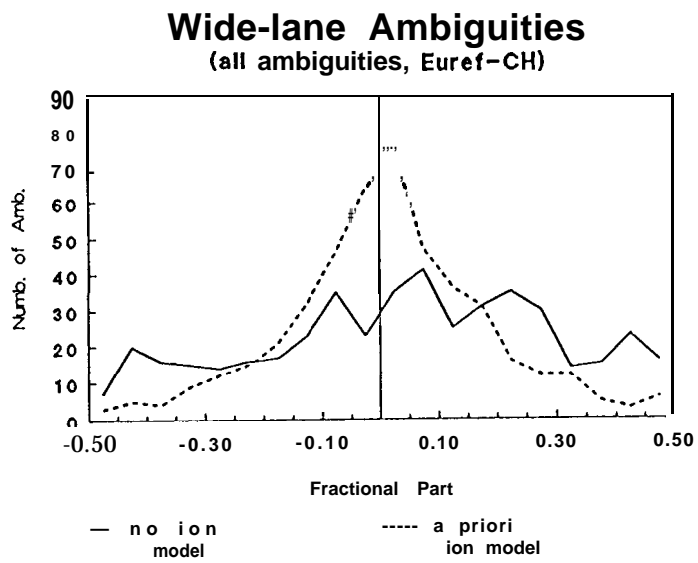


Figure 3: Distribution of the Fractional Parts

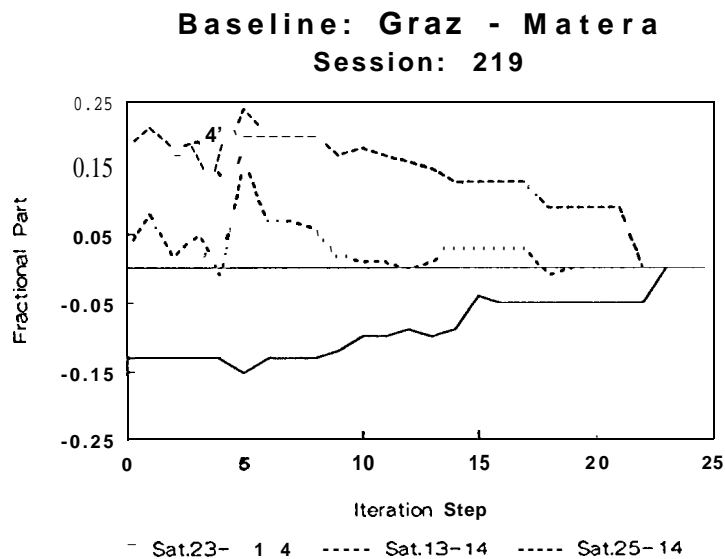


Figure 4: Development of the Fractional Part of the Narrow-lane Ambiguities (double differences 25-14, 13-14 and 23-14)

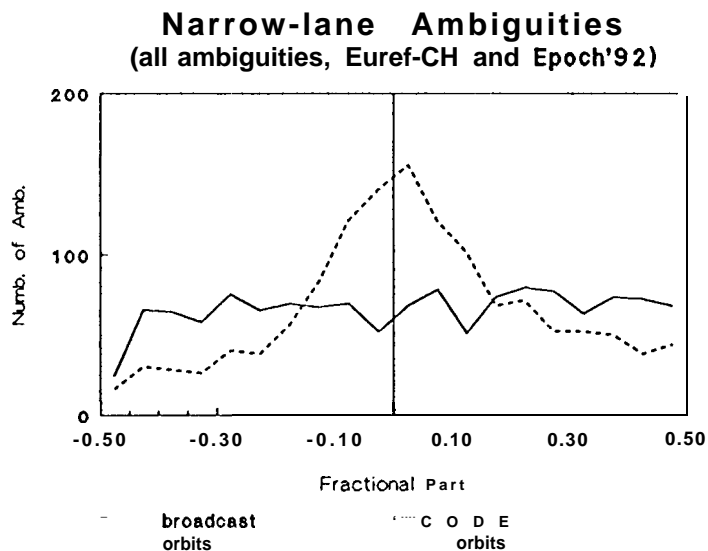


Figure 5: Distribution of the Fractional Parts

Amb. Free

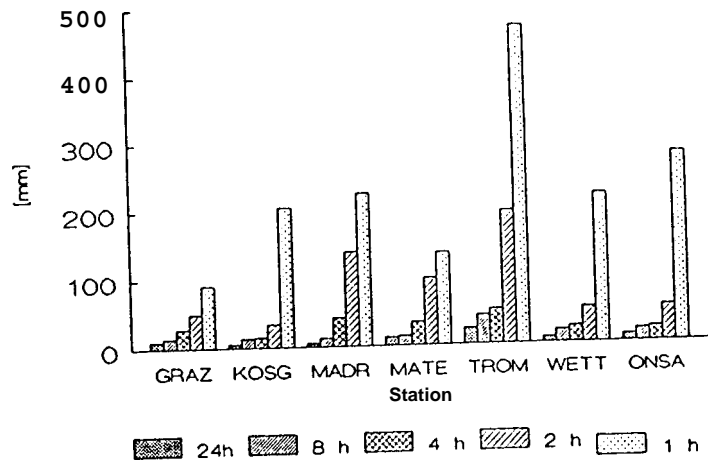


Figure 6: Repeatability of the Horizontal Position for Various Data Intervals

Amb. Fixed

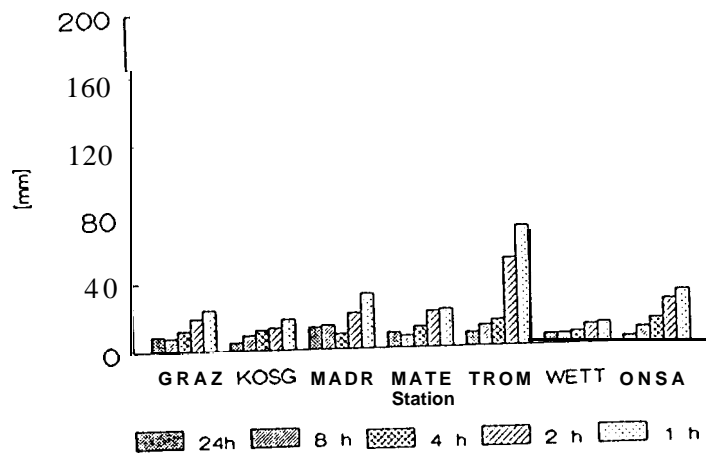


Figure 7: Repeatability of the Horizontal Position for Various Data intervals

Amb. Free

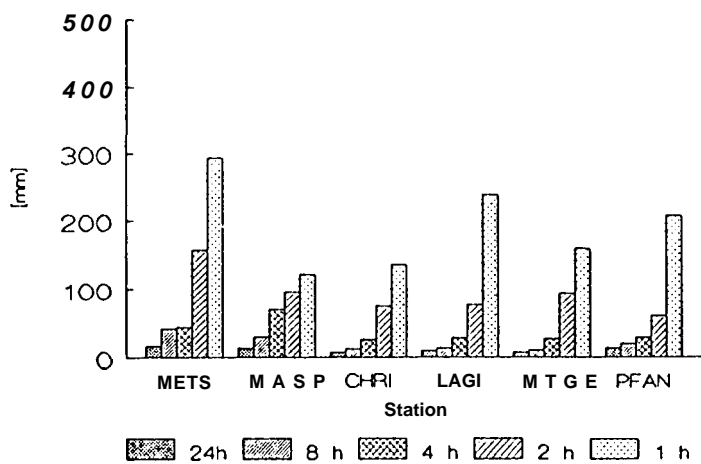


Figure 8: Repeatability of the Horizontal Position for Various Data Intervals

Amb. Fixed

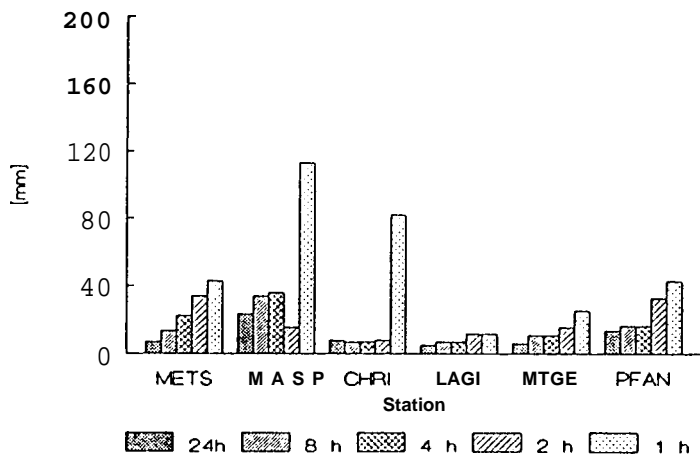


Figure 9: Repeatability of the Horizontal position for Various Data Intervals

Epoch'92

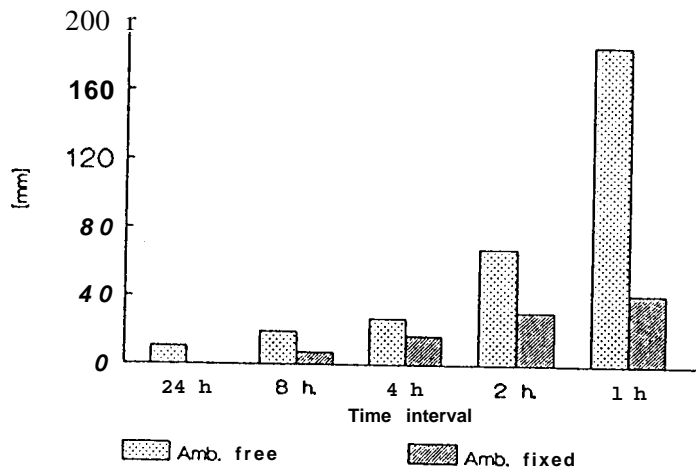


Figure 10: RMS of Residuals in the Horizontal Position After Helmert Transformation

Euref -CH

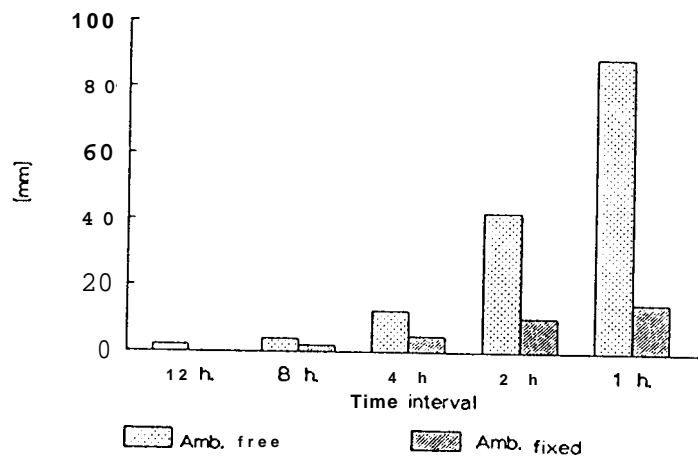


Figure 11: RMS of Residuals in the Horizontal Position After Helmert Transformation

NAL/ERI EPHEMERIDES FOR EPOCH'92

Masaaki Murata*, Toshiaki Tsuji *
Teruyuki Kato[†], and Shigeru Nakao[†]

National Aerospace Laboratory (NAL) and Earthquake Research Institute (ERI) of the University of Tokyo participated in the IGS'92 Campaign as a processing center and a regional data center, respectively. GPS tracking data collected from IGS core sites and archived by ERI through INTERNET were used to determine precise ephemerides of GPS satellites. This paper presents NAL/ERI analysis center results of data collected during the period of IGS Epoch'92 campaign.

INTRODUCTION

National Aerospace Laboratory (NAL) and Earthquake Research Institute (ERI) of the University of Tokyo participated in the IGS'92 Campaign as a processing center and a regional data center, respectively. GPS tracking data archived by ERI through INTERNET were analyzed to determine precise ephemerides of GPS satellites. The purpose of this paper is to summarize results of NAL/ERI orbit products, precise ephemerides and earth rotation parameters, using data collected by IGS core sites during the period of IGS Epoch'92 campaign (July 25- August 8, 1992) (Days 207-221).

On Day 214 (August 1, Sat.) an *Anti-Spoofing* (AS) test began for Block-II satellites. It lasted from Day 214 to 10:00 UTC of Day 216 (August 3, Mon.). AS is a guard against fake transmission of satellite data by encrypting the P-code to form the Y-code. It will be invoked as needed on Block-II satellites, and Block-I satellites do not have AS capability. On and after Day 214 AS has been invoked for most of Block-II satellites and often turned on during weekends. Day 221 (August 8, Sat.) was also anti-spoofed. Although it should be possible to determine orbits of non-AS satellites even during the AS periods, we have not yet attempted to analyze data from AS days so that our orbit files include no ephemerides for these days.

*Systems Division, National Aerospace Laboratory, 7-44-1 Jindaiji-higashi, Chofu, Tokyo 182, JAPAN.

[†] Earthquake Research Institute, The University of Tokyo, 1-1-1 Yayoi, Bunkyo-ku, Tokyo 113, JAPAN.